

# Modulatable Endosomolytic, Intracellularly Biodegradable Vectors for Gene Delivery

Rujikan Nasanit

A thesis submitted to The University of Birmingham for the  
degree of DOCTOR OF PHILOSOPHY

School of Chemistry  
The University of Birmingham  
October 2009

UNIVERSITY OF  
BIRMINGHAM

**University of Birmingham Research Archive**

**e-theses repository**

This unpublished thesis/dissertation is copyright of the author and/or third parties. The intellectual property rights of the author or third parties in respect of this work are as defined by The Copyright Designs and Patents Act 1988 or as modified by any successor legislation.

Any use made of information contained in this thesis/dissertation must be in accordance with that legislation and must be properly acknowledged. Further distribution or reproduction in any format is prohibited without the permission of the copyright holder.

## Abstract

In order to achieve efficient gene delivery, we have designed  $pK_a$  modulatable oligopeptides (2COPs) by combining with lysine, histidine and cysteine residues which will bind DNA extracellularly, internalize *via* endocytosis, provide a tunable endosomal release mechanism, and provide a degradable backbone in order that the DNA can be released once in the cytoplasm. The reducible polycations (RPCs) were synthesized from 2COPs. The sizes, surface charges and the stability of RPC polyplexes under the simulated physiological conditions *extra-* and *intracellularly* suggested that these RPCs are promising vectors. In addition, the transfections revealed that the RPCs can facilitate endosomal buffering and intracellular reduction and are non-toxic to cells.

The nuclear targeting signal (TAT) was incorporated into these vectors. The reducible copolycations (RcPCs) were synthesized *via* oxidative polymerisation between 2COPs and TAT. The RcPC polyplexes are ~100 nm, and are positively charged. Gel shift assay revealed that RcPCs have less potential than RPCs to be used as vectors as they are less stable extracellularly than the RPCs. In addition, chloroquine was required to enhance the transfection of RcPCs. Furthermore, there is no improvement in transfection of RcPC compared to RPCs. Therefore, this suggests that the incorporation of TAT does not improve the transfection.

## Acknowledgements

I would like to express my deepest gratitude and sincere appreciation to Prof Jon Preece, for his supervision and support throughout the last four years. I would also like to thank Prof Leonard Seymour and Prof Cameron Alexander for their support and guidance during my study. I would also like to extend my gratitude to Dr. Mark Stevenson and Dr. Simon Briggs for their assistance while I was doing experiments in the University of Oxford (department of clinical pharmacology).

I would also like to thank Dr. Parvez Iqbal, post-doctoral student in Jon's group, for his help with NMR and NMR titration studies and his helpful advice and suggestions. I would like to convey my deepest thanks to members of staff in the HPLC, Mass spectroscopy, and NMR department, especially Graham Burns (HPLC) who has given generous assistance and been very welcoming through my work in his lab. I would also like to thank Mahmoud Soliman (school of pharmacy, the University of Nottingham) for his help with AFM and MALLS studies.

A huge thank you to all the members of Jon's and Len's group, both past and present, who have helped make throughout the duration of my PhD.

I would like to thank the Royal Thai Government for giving me the funding throughout my study.

Finally, I would also like to dedicate this opportunity to thank my parents and all members in my family also Kevin Maskell for their love and support.

# CONTENTS

<b>CHAPTER 1</b>	<b>1</b>
<b>1 INTRODUCTION</b>	
<b>1.1 Introduction to gene delivery</b>	<b>7</b>
1.1.1 Vectors for gene delivery	9
1.1.1.1 Viral vectors	9
1.1.1.2 Non-viral vectors or synthetic vectors	12
1.1.1.2a. Cationic lipids	12
1.1.1.2b. Cationic polymers	16
1.1.2 Cellular barriers to gene delivery	22
1.1.2.1 Extracellular barriers	24
1.1.2.1a. Biodistribution and interaction in bloodstream	24
1.1.2.1b. Cell targeting	25
1.1.2.1c. Cell uptake	25
1.1.2.2 Intracellular barriers	27
1.1.2.2a. Endosomal escape	27
1.1.2.2b. Nuclear localization	29
<b>1.2 Non-viral gene delivery based on synthetic peptides</b>	<b>33</b>
1.2.1 Lysine-based peptides: Extracellular binding of DNA	33
1.2.2 Histidine-based peptides: Endosomal escape of DNA	35
1.2.3 Lysine and histidine-based peptides: Extracellular binding and endosomal escape of DNA	36
1.2.4 Cysteine-based peptides: Intracellular release of DNA	38
1.2.5 Arginine-based peptides: Nuclear localization of DNA	39
<b>1.3 Essential vector features for efficient non-viral gene delivery</b>	<b>40</b>
<b>1.4 Can we extend the design of non-viral peptide vectors?</b>	<b>41</b>
1.4.1 Lysine: extracellular stabilization (Vector feature <b>I</b> )	41
1.4.2 Cysteine: extracellular stabilization (Vector feature <b>I</b> )	42
1.4.3 Lysine: endocytosis (Vector feature <b>III</b> )	42
1.4.4 Histidine: endosomal release (Vector feature <b>IV</b> )	43
1.4.5 Cysteine: intracellularly degradable (Vector feature <b>V</b> )	44
1.4.6 Nuclear targeting signal (Vector feature <b>VI</b> )	45

<b>1.5</b>	<b>Design of new vectors</b>	<b>45</b>
<b>1.6</b>	<b>Hypothesis behind the vector design</b>	<b>48</b>
1.6.1	New strategies	48
1.6.1.1	$pK_a$ modulation	48
1.6.1.2	Cross-linking disulfide bonds	49
1.6.2	Known strategies	51
1.6.2.1	Electrostatic binding with DNA	51
1.6.2.2	Disulfide bond backbone	51
1.6.2.3	NLS incorporation	52
<b>1.7</b>	<b>Overview of thesis</b>	<b>54</b>
<b>1.8</b>	<b>References</b>	<b>56</b>
<b>CHAPTER 2</b>		<b>74</b>
<b>2</b>	<b>MATERIALS AND METHODS</b>	
<b>2.1</b>	<b>Suppliers of materials</b>	<b>79</b>
<b>2.2</b>	<b>Source of nucleic acids, oligopeptides and cell lines</b>	<b>79</b>
2.2.1	Source of nucleic acids	79
2.2.2	Source of oligopeptides	80
2.2.3	Source of cell lines	80
<b>2.3</b>	<b>Oligopeptide purification and characterization</b>	<b>81</b>
<b>2.4</b>	<b><math>pK_a</math> determination of oligopeptides</b>	<b>86</b>
<b>2.5</b>	<b>Reducible polycations (RPCs) formation</b>	<b>87</b>
2.5.1	Oxidative polymerisation to form RPCs	87
2.5.2	Formation of <i>cross-linked</i> RPCs	88
2.5.3	Formation of reducible <i>copolypeptides</i> (RcPCs) and reducible polyTAT (RP-TAT)	89
2.5.4	Gel Permeation Chromatography (GPC)	90
2.5.5	Polymer purification	90
2.5.6	Polydispersity index (PDI) of polycations	91
<b>2.6</b>	<b>Amino acid analysis of RcPCs</b>	<b>92</b>
<b>2.7</b>	<b>Formation of polyplexes</b>	<b>93</b>
2.7.1	Calculation of charge ratio	93
2.7.2	Formation of polyplexes	94

<b>2.8 Physicochemical characterisation of polyplexes</b>	<b>94</b>
2.8.1 Analysis of polyplex diameter by photon correlation spectroscopy (PCS)	94
2.8.2 Analysis of polyplex surface charge by zeta potential	95
2.8.3 Atomic force microscopy	95
2.8.4 Agarose gel electrophoresis of DNA	96
2.8.5 Gel shift assay	96
2.8.5.1 Polyaspartic acid assay	96
2.8.5.2 Glutathione and NaCl assay	97
<b>2.9 Cell culture</b>	<b>97</b>
2.9.1 Maintenance of established cell lines	98
2.9.2 Determination of viable cell number	98
<b>2.10 Biological studies of polyplexes</b>	<b>99</b>
2.10.1 Cell transfection <i>in vitro</i>	99
2.10.2 Luciferase assay	100
2.10.3 Advanced protein assay	100
2.10.4 MTS cell proliferation assay	101
2.10.5 Intracellular glutathione analysis	102
<b>2.11 Expression of data</b>	<b>103</b>
<b>CHAPTER 3</b>	<b>104</b>
<b>3 SYNTHESIS AND CHARACTERIZATION OF OLIGOPEPTIDES, REDUCIBLE POLYCATIONS (RPCs) AND POLYPLEXES</b>	
<b>3.1 Introduction</b>	<b>109</b>
<b>3.2 Objectives</b>	<b>111</b>
<b>3.3 Methodology</b>	<b>112</b>
<b>3.4 Results and discussion</b>	<b>116</b>
3.4.1 Oligopeptide purification and characterization	116
3.4.2 Determination of the $pK_a$ of the oligopeptides	117
3.4.3 Formation and characterization of reducible polycations (RPCs)	121
3.4.3.1 Polymerization as a function of oligopeptide concentration	122
3.4.3.2 Polymerization as a function of temperature for 2COP 1	125
3.4.3.3 Polymer stability in HEPES buffer	126
3.4.4 Formation and characterization of polyplexes	126

3.4.4.1	Weight per charge and N:P ratio calculation	126
3.4.4.2	RPCs polyplexes formation and characterization	129
3.4.4.2a	Diameter and zeta potential of polyplexes	129
3.4.4.2b	Shape of polyplexes	131
3.4.4.2c	Extracellular stability studies of polyplexes	133
3.4.4.2d	Intracellular reduction studies of polyplexes	134
3.4.4.3	Formation of polyplexes with low molecular weight RPCs	144
3.4.4.3a	Diameter and zeta potential of polyplexes	144
3.4.4.3b	Extracellular stability studies of polyplexes	145
3.4.4.3c	Intracellular reduction studies of polyplexes	146
3.4.4.4	Oligopeptide polyplexes formation and characterization	149
3.4.5	Formation and characterization of <i>cross-linked RPCs</i>	151
<b>3.5</b>	<b>Conclusions</b>	<b>155</b>
<b>3.6</b>	<b>References</b>	<b>160</b>
<b>CHAPTER 4</b>		<b>164</b>
<b>4</b>	<b>DELIVERY OF NUCLEIC ACID USING LYSINE, HISTIDINE AND CYSTEINE BASED OLIGOPEPTIDES AND REDUCIBLE POLYCATIONS (RPCs)</b>	
<b>4.1</b>	<b>Introduction</b>	<b>168</b>
<b>4.2</b>	<b>Objectives</b>	<b>170</b>
<b>4.3</b>	<b>Methodology</b>	<b>171</b>
<b>4.4</b>	<b>Results and discussion</b>	<b>175</b>
4.4.1	Cytotoxicity of RPC polyplexes	176
4.4.2	Cell transfection of RPCs polyplexes	181
4.4.2.1	Cell transfection of RPCs polyplexes based on endosomolytic buffering: effect of CQ	182
4.4.2.2	Cell transfection of RPCs polyplexes based on intracellularly reducible property: effect of GSH-MEE/BSO	187
4.4.2.2a	Artificially increase the intracellular GSH level: effect of GSH-MEE	188
4.4.2.2b	Artificially depleting the intracellular GSH level: effect of BSO	191



4.4.2.2c	Assessing intracellular GSH level in A549 and bEND3 cells treated with GSH-MEE and BSO	192
4.4.2.3	Cell transfection of RPCs polyplexes based on the combination of endosomolytic and intracellularly reducible properties	195
4.4.2.4	Cell transfection of RPCs polyplexes as a function of RPCs molecular weight	198
4.4.3	Cell transfection of oligopeptide polyplexes	197
<b>4.5</b>	<b>Conclusions</b>	<b>199</b>
<b>4.6</b>	<b>References</b>	<b>211</b>
<b>CHAPTER 5</b>		<b>214</b>
<b>5</b>	<b>SYNTHESIS AND CHARACTERIZATION OF REDUCIBLE COPOLYCATIONS (RcPCs) CONTAINING LYSINE, HISTIDINE AND CYSTEINE BASED SEQUENCES AND TAT PEPTIDE</b>	
<b>5.1</b>	<b>Introduction</b>	<b>219</b>
<b>5.2</b>	<b>Objectives</b>	<b>221</b>
<b>5.3</b>	<b>Methodology</b>	<b>222</b>
<b>5.4</b>	<b>Results and discussion</b>	<b>225</b>
5.4.1	TAT oligopeptide purification and characterization	225
5.4.2	Formation and characterization of reducible copolycations (RcPCs)	226
5.4.3	2COP and TAT sequence ratio analysis	228
5.4.4	Formation and characterization of TAT and RcPC polyplexes	231
5.4.4.1	Weight per charge and N:P ratio calculation	231
5.4.4.2	TAT and RcPCs polyplex formation and characterization	234
5.4.4.2a	Diameter and zeta potential of polyplexes	234
5.4.4.2b	Extracellular stability studies of polyplexes	236
5.4.4.2c	Intracellular reduction studies of polyplexes	238
<b>5.5</b>	<b>Conclusions</b>	<b>241</b>
<b>5.6</b>	<b>References</b>	<b>244</b>

## 6 DELIVERY OF NUCLEIC ACID USING REDUCIBLE COPOLYCATION (RcPC) CONTAINING LYSINE, HISTIDINE AND CYSTEINE BASED SEQUENCES AND TAT PEPTIDE

<b>6.1 Introduction</b>	<b>251</b>
<b>6.2 Objectives</b>	<b>256</b>
<b>6.3 Methodology</b>	<b>256</b>
<b>6.4 Results and discussion</b>	<b>258</b>
6.4.1 Cytotoxicity of polyplexes	258
6.4.1.1 Cytotoxicity of RP-TAT and RcPCs polyplexes	258
6.4.1.2 Cytotoxicity of RcPCs polyplexes as a function of RcPC molecular weight and 2COP:TAT ratio	261
6.4.1.2a Cytotoxicity of RcPCs polyplexes as a function of RcPC molecular weight	261
6.4.1.2b Cytotoxicity of RcPCs polyplexes as a function of 2COP:TAT ratio	263
6.4.2 Cell transfection of polyplexes	263
6.4.2.1 Cell transfection of RP-TAT and RcPC polyplexes based on the endosomolytic buffering: effect of CQ	265
6.4.2.2 Cell transfection of RP-TAT and RcPCs polyplexes based on intracellularly reducible property: effect of BSO/GSH-MEE	267
6.4.2.2a Artificially increase the intracellular GSH level: effect of GSH-MEE	267
6.4.2.2b Artificially depleting the intracellular GSH level: Effect of BSO	268
6.4.2.3 Cell transfection of RP-TAT and RcPCs polyplexes based on the combination of endosomolytic and intracellularly reducible properties	269
6.4.2.4 Cell transfection of RcPC polyplexes compared to RPCs	270
6.4.2.5 Cell transfection of RcPC polyplexes as a function of RcPC molecular weight and 2COP:TAT ratio	272

6.4.2.5a	Cell transfection of RcPC polyplexes as a function of RcPC molecular weight	272
6.4.2.5b	Cell transfection of RcPC polyplexes as a function of 2COP:TAT ratio	274
<b>6.5</b>	<b>Conclusions</b>	<b>274</b>
<b>6.6</b>	<b>References</b>	<b>277</b>
 <b>CHAPTER 7</b>		 <b>279</b>
<b>7.</b>	<b>CONCLUSIONS</b>	
<b>7.1</b>	<b>Conclusions</b>	<b>283</b>
7.1.1	$pK_a$ modulation of 2COPs	285
7.1.2	Diameter and zeta potential of polyplexes	285
7.1.3	Extracellular stability of polyplexes	286
7.1.4	Intracellular reduction of polyplexes	287
7.1.5	Transfection efficiency of polyplexes	288
7.1.5.1	Transfection in endothelial (bEND3) and epithelial (A549) cells	288
7.1.5.2	Transfection efficiency of RPC and RcPC polyplexes	289
7.1.5.3	Relative transfection enhancement by CQ of RPC and RcPC polyplexes	291
7.1.6	2COPs conclusion	292
7.1.7	Cross-linked RPC conclusions	292
<b>7.2</b>	<b>Limitations and future work</b>	<b>292</b>
7.2.1	Improve cell targeting	292
7.2.2	Improve nuclear localization	293
<b>7.3</b>	<b>References</b>	<b>294</b>
 <b>CHAPTER 8</b>		 <b>298</b>
<b>8.</b>	<b>APPENDIX</b>	
<b>8.1</b>	<b>Preparative HPLC chromatograms of crude oligopeptides and analytical HPLC chromatograms of purified oligopeptides</b>	<b>302</b>
8.1.1	Preparative HPLC and analytical HPLC of 2COP 1	302
8.1.2	Preparative HPLC and analytical HPLC of 2COP 2	303

8.1.3	Preparative HPLC and analytical HPLC of 2COP 3	304
8.1.4	Preparative HPLC and analytical HPLC of 2COP 4	305
8.1.5	Preparative HPLC and analytical HPLC of 2COP 5	306
8.1.6	Preparative HPLC and analytical HPLC of 2COP 6	308
8.1.7	Preparative HPLC and analytical HPLC of 3COP 7	309
8.1.8	Preparative HPLC and analytical HPLC of TAT	310
<b>8.2</b>	<b><sup>1</sup>H NMR of purified oligopeptides</b>	<b>311</b>
8.2.1	<sup>1</sup> H NMR of purified 2COP 1	311
8.2.2	<sup>1</sup> H NMR of purified 2COP 2	312
8.2.3	<sup>1</sup> H NMR of purified 2COP 3	313
8.2.4	<sup>1</sup> H NMR of purified 2COP 4	314
8.2.5	<sup>1</sup> H NMR of purified 2COP 5	315
8.2.6	<sup>1</sup> H NMR of purified 2COP 6	316
8.2.7	<sup>1</sup> H NMR of purified 3COP 7	317
8.2.8	<sup>1</sup> H NMR of purified TAT	318
<b>8.3</b>	<b>Samples of <sup>1</sup>H NMR spectra at different pH in NMR titration experiments of 2COPs</b>	<b>319</b>
<b>8.4</b>	<b>Samples of GPC chromatograms in oxidative polymerization experiments</b>	<b>321</b>
<b>8.5</b>	<b>Publication</b>	<b>323</b>

## Abbreviations

$\lambda$	Wavelength (in nm)
$\lambda_{em}$	Excitation wavelength
$\lambda_{ex}$	Emission wavelength
$\mu$	Micro
<sup>1</sup> H NMR	Proton nuclear magnetic resonance
2COP	Bis-cysteine containing oligopeptide
3COP	Tris-cysteine containing oligopeptide
AAV	Adeno-associated virus
AET	Aminoethanethiol
AFM	Atomic force microscopy
APAR	Advanced protein assay reagent
BSA	Bovine serum albumin
BSO	Buthionine sulfoximine
CMV	Human cytomegalovirus
CPP	Cell penetrating peptide
CQ	Chloroquine
Cys (C)	Cysteine
Da	Dalton
DC-Chol	3 $\beta$ [ <i>N</i> -( <i>N,N'</i> -dimethylaminoethane)-carbamoyl] cholesterol
DLS	Dynamic light scattering
DMEM	Dulbecco's modified Eagles medium
DMSO	Dimethyl sulfoxide
DNA	2-Deoxyribonucleic acid
DOGS	Diocetadecyl amino glycil spermine
DOTAP	1,2-bis(oleoyloxy)-3-(trimethylammonio)propane
DOTMA	<i>N</i> -[1-(2,3-dioleyloxy)propyl]- <i>N,N,N</i> -trimethylammonium chloride
DTBP	Dimethyl-3,3'-dithiobispropionimidate•2HCl
DTT	Dithiothreitol
EDTA	Ethylenediamine tetra-acetic acid
ESI	Electrospray ionisation
FCS	Foetal calf serum

<b>Fmoc</b>	9-Fluorenylmethoxycarbonyl
<b>GC</b>	Gas chromatography
<b>GPC</b>	Gel permeation chromatography
<b>GSH</b>	Glutathione
<b>GSH-MEE</b>	Glutathione monoethyl ester
<b>GSSG</b>	Oxidized glutathione
<b>HCl</b>	Hydrochloric acid
<b>HEPES</b>	N-[2-hydroxyethyl]-piperazine-N'-[2-ethanosulphonic acid]
<b>HGP</b>	Human genome project
<b>HGT</b>	Human gene therapy
<b>HIV</b>	Human immunodeficiency virus
<b>His (H)</b>	Histidine
<b>HMW</b>	High molecular weight
<b>HPLC</b>	High performance liquid chromatography
<b>HSPG</b>	Heparan sulfate proteoglycan
<b>HSV</b>	Herpes simplex virus
<b>HTLV</b>	Human T cell leukemia virus type 1
<b>kb</b>	Kilobase
<b>kDa</b>	Kilodalton
<b>l</b>	Litre
<b>LMW</b>	Low molecular weight
<b>Lys (K)</b>	Lysine
<b>M</b>	Molar
<b>MALLS</b>	Multi-angle laser light scattering
<b>mBCl</b>	Monochlorobimane
<b>MeCN</b>	Acetonitrile
<b>min</b>	Minute(s)
<b>ml</b>	Millilitre
<b>mM</b>	Millimolar
<b>MS</b>	Mass spectrometry
<b>MTS</b>	[3-(4,5-dimethylthiazol-2-yl)-5-(3-carboxymethoxyphenyl)-2-(4-sulphophenyl-2H-tetrazolium]

<b>MW</b>	Molecular weight
<b>NaCl</b>	Sodium chloride
<b>NaOD</b>	Deuterated sodium hydroxide
<b>ng</b>	Nanogram
<b>NLS</b>	Nuclear localisation sequence
<b>nm</b>	Nanometre
<b>NMR</b>	Nuclear magnetic resonance
<b>NPC</b>	Nuclear pore complex
<b>PBS</b>	Phosphate saline buffer
<b>PAA</b>	Polyaspartic acid
<b>PAMAM</b>	Polyamidoamine
<b>PCS</b>	Photo correlation spectroscopy
<b>PDI</b>	Polydispersity index
<b>PEG</b>	Poly (ethylene glycol)
<b>PEI</b>	Polyethylenimine
<b>PLH-g-PLL</b>	N-Ac-poly(L-histidine)-graft-poly-(L-lysine)
<b>PLL</b>	Polylysine
<b>PTD</b>	Protein transduction domains
<b>RCL</b>	Reducible cationic lipid
<b>RcPC</b>	Reducible copolycation
<b>RCPP</b>	Reducible copolypeptide
<b>RLU</b>	Relative light units
<b>RNA</b>	Ribonucleic acid
<b>RPC</b>	Reducible polycation
<b>RP-HPLC</b>	Reverse phase high performance liquid chromatography
<b>rpm</b>	Revolutions per minute
<b>RP-TAT</b>	Reducible polyTAT
<b>RT</b>	Room temperature
<b>s</b>	Seconds
<b>SEC</b>	Size exclusion chromatography
<b>SV40</b>	Simian virus 40
<b>TFA</b>	Trifluoroacetic acid

<b>Tris</b>	2-amino 2-(hydroxymethyl) propan-1,3 diol
<b>UV</b>	Ultraviolet
<b>V</b>	Volts
<b>wpc</b>	Weight per charges
<b>WSLP</b>	Water soluble cationic lipopolymer
<b>Z<sub>av</sub></b>	Average diameter



# **CHAPTER 1**

## **Introduction**

# CONTENTS

## List of Figures

## List of Tables

### 1 INTRODUCTION

<b>1.1 Introduction to gene delivery</b>	<b>7</b>
1.1.1 Vectors for gene delivery	9
1.1.1.1 Viral vectors	9
1.1.1.2 Non-viral vectors or synthetic vectors	12
1.1.1.2a. Cationic lipids	12
1.1.1.2b. Cationic polymers	16
1.1.2 Cellular barriers to gene delivery	22
1.1.2.1 Extracellular barriers	24
1.1.2.1a. Biodistribution and interaction in bloodstream	24
1.1.2.1b. Cell targeting	25
1.1.2.1c. Cell uptake	25
1.1.2.2 Intracellular barriers	27
1.1.2.2a. Endosomal escape	27
1.1.2.2b. Nuclear localization	29
<b>1.2 Non-viral gene delivery based on synthetic peptides</b>	<b>33</b>
1.2.1 Lysine-based peptides: Extracellular binding of DNA	33
1.2.2 Histidine-based peptides: Endosomal escape of DNA	35
1.2.3 Lysine and histidine-based peptides: Extracellular binding and endosomal escape of DNA	36
1.2.4 Cysteine-based peptides: Intracellular release of DNA	38
1.2.5 Arginine-based peptides: Nuclear localization of DNA	39
<b>1.3 Essential vector features for efficient non-viral gene delivery</b>	<b>40</b>
<b>1.4 Can we extend the design of non-viral peptide vectors?</b>	<b>41</b>
1.4.1 Lysine: extracellular stabilization (Vector feature <b>I</b> )	41
1.4.2 Cysteine: extracellular stabilization (Vector feature <b>I</b> )	42
1.4.3 Lysine: endocytosis (Vector feature <b>III</b> )	42
1.4.4 Histidine: endosomal release (Vector feature <b>IV</b> )	43
1.4.5 Cysteine: intracellularly degradable (Vector feature <b>V</b> )	44

1.4.6	Nuclear targeting signal (Vector feature <b>VI</b> )	45
<b>1.5</b>	<b>Design of new vectors</b>	<b>45</b>
<b>1.6</b>	<b>Hypothesis behind the vector design</b>	<b>48</b>
1.6.1	New strategies	48
1.6.1.1	p <i>K</i> <sub>a</sub> modulation	48
1.6.1.2	Cross-linking disulfide bonds	49
1.6.2	Known strategies	51
1.6.2.1	Electrostatic binding with DNA	51
1.6.2.2	Disulfide bond backbone	51
1.6.2.3	NLS incorporation	52
<b>1.7</b>	<b>Overview of thesis</b>	<b>54</b>
<b>1.8</b>	<b>References</b>	<b>56</b>

## List of Figures

Figure 1.1.	Number of gene therapy clinical trails approved world wide between years 1989- 2008	8
Figure 1.2.	Cationic lipids	13
Figure 1.3.	Flip-flop mechanism to uptake lipoplexes and subsequently release of DNA	14
Figure 1.4.	Reducible cationic lipids (RCLs) structure	15
Figure 1.5.	Water soluble cationic lipopolymer (WSLP)	16
Figure 1.6.	Polyethyleneimine (PEI) structures	17
Figure 1.7.	Proposed reaction scheme of DTBP (dimethyl-3,3'-dithiobispropionimidate•2HCl) cross-linked PEI	18
Figure 1.8.	Dendrimer synthesis by convergent and divergent routes	19
Figure 1.9.	Structure of polyamidoamine (PAMAM) dendrimer	20
Figure 1.10.	The model of modified PAMAM attached to modified GALA <i>via</i> disulfide bond formation	21
Figure 1.11.	Gene delivery by non-viral vector system	23
Figure 1.12.	Endocytic pathways	27
Figure 1.13.	The proton sponge mechanism	28
Figure 1.14.	Structure of chloroquine	29
Figure 1.15.	Schematic representation of nuclear protein import cycle	32
Figure 1.16.	Chemical structures of amino acids used in peptides for gene delivery	35
Figure 1.17.	The structure of N-Ac-poly(L-Histidine)-graft-poly-(L-Lysine) (PLH-g-PLL)	36
Figure 1.18.	The aminated poly-L-histidine synthesized by Asayama and colleagues	37
Figure 1.19.	The formation of a disulfide bond of two cysteine residues	38
Figure 1.20.	Polyplex formation via electrostatic interaction between nucleic acid and vector	42
Figure 1.21.	Syndecan mediated endocytosis of cationic polyplexes	43
Figure 1.22.	The disulfide bond reduction by glutathione (GSH) catalyzed by glutathione reductase using NADPH to reduce oxidized glutathione	44
Figure 1.23.	Polyplex dissociation by GSH to release DNA intracellularly	44

Figure 1.24.	The proton repulsion of the lysine and histidine based sequences	49
Figure 1.25.	Polyplex formation from reducible polycations (RPCs) and <i>cross-linked</i> RPC	50
Figure 1.26.	Reducible copolycations (RCPCs) synthesised by oxidative polymerisation between 2COPs and Bis-cysteine containing TAT oligopeptides	52
Figure 1.27.	Schematic model of the transfection manner of RPCs and PLL polyplexes based on vector features <b>I</b> and <b>III-VI</b>	53

## List of Tables

Table 1.1.	Properties of viruses used for gene therapy	10
Table 1.2.	Advantages and limitations of viral and non-viral vectors	11
Table 1.3.	The components in nuclear protein import cycle and their functions	30
Table 1.4.	Cysteine containing peptides studied by Mckenzie and colleagues	39
Table 1.5.	Vector features for gene delivery	40
Table 1.6.	The summary of vector features from previous research	41
Table 1.7.	Synthetic oligopeptides used in this study	46
Table 1.8.	Strategies used in vector design and their advantage	47

# 1 INTRODUCTION

## *Abstract*

*This section overviews vectors used in gene delivery. The types of vectors, cellular barriers and the mechanism to overcome gene delivery are described, including a review of the previous research which has studied synthetic vectors, and the biological hurdles these vectors have to overcome to deliver a gene to the cell.*

## 1.1 Introduction to gene delivery

Genes consist of bases that are specific sequences which encode instructions on how to produce proteins.<sup>[1]</sup> When genes are mutated so that the encoded proteins are unable to complete their normal functions genetic disorders can result.<sup>[2]</sup> Gene therapy is a challenging technique which could potentially be used to correct defective genes responsible for disease development. Since the completion of the Human Genome Project (HGP), gene therapy has become an increasingly important technique which many research groups focus on.<sup>[3]</sup> There are two types of gene therapy, somatic gene therapy<sup>[4,5]</sup> and germline gene therapy.<sup>[6]</sup> The correction by the former approach can not be inherited by the offspring, whereas the latter corrects malfunction in eggs and sperm cells, thus these corrections can be passed down to the offspring. It has been claimed that the first clinical trial in gene therapy occurred in the 1960s,<sup>[7-9]</sup> when Shope papilloma virus that encoded an enzyme arginase was injected into two patients which were suffering from hyperargininemia, a hereditary deficiency of enzyme arginase which leads to high level of arginine concentration in blood and cerebrospinal fluid leading to severe mental retardation. There have been increasingly more gene therapy clinical trials since 1989, as can be seen in **Figure 1.1**.

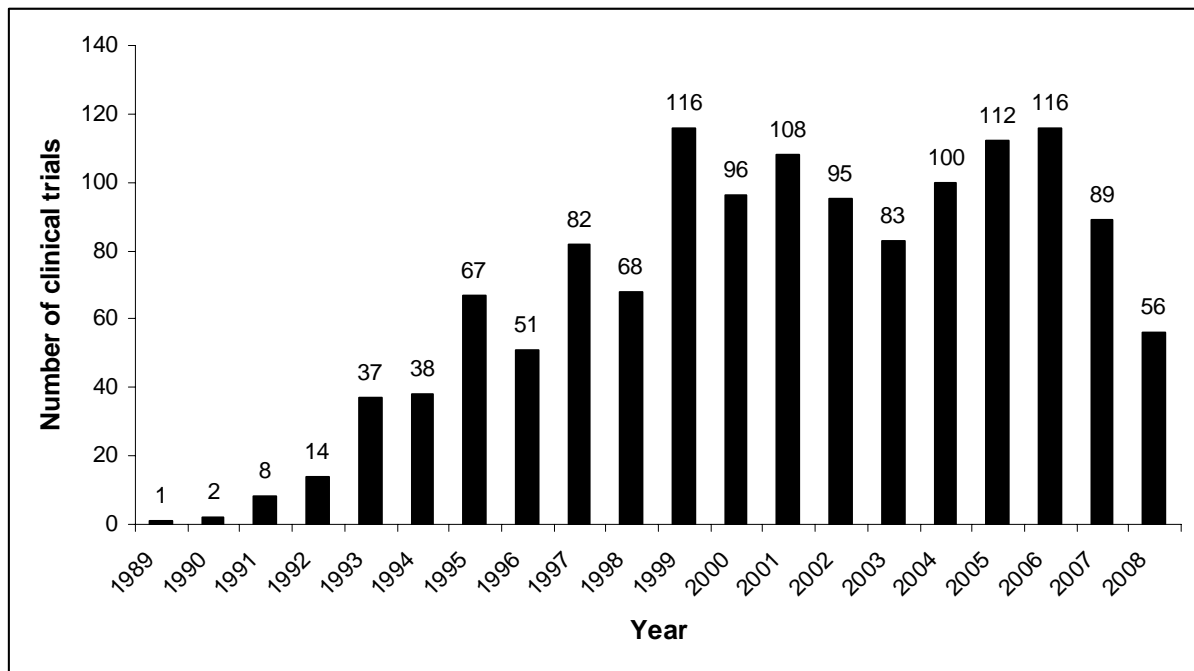


**Figure 1.1. Number of gene therapy clinical trails approved world wide between years 1989 - 2008.**

(Data from [www.wiley.co.uk/genmed/clinical](http://www.wiley.co.uk/genmed/clinical) )

Human gene therapy (HGT) is aimed to correct defective genes by transferring a normal gene to the disease cells of a patient. There are several approaches to correct defective genes<sup>[10]</sup> such as (i) the insertion of a normal gene in nonspecific location within the genome, in order to replace the function of an abnormal gene,<sup>[7,11]</sup> (ii) gene exchange through homologous recombination in order to replace a nonfunctional gene with a normal gene,<sup>[12,13]</sup> (iii) an abnormal gene could be repaired to a normal gene through selective reverse mutation,<sup>[14]</sup> and (iv) a specific gene could be altered in order to regulate a gene to be turned on or off.<sup>[15]</sup>

HGT involves multiple steps<sup>[3]</sup> including delivery to an organ, tissue targeting, cellular trafficking, regulation of gene expression, and modulating the biological activity of therapeutic proteins. In addition, safety<sup>[16]</sup> of the vector and gene product need to be understood. Most of these issues are not completely understood. The gene carrier, which is



called a vector, must be utilized to deliver the normal gene, and is one of the important parts in human gene therapy process.

### **1.1.1 Vectors for gene delivery**

The main objective in gene therapy is successful *in vivo* transfer of genetic materials to target cells of patient. The success or failure of gene therapy depends on the development and efficiency of the transfection of vectors. Vectors that have been developed for gene therapy approaches are divided into two major groups: viral vectors<sup>[17]</sup> and non-viral vectors (so-called synthetic vector).<sup>[17]</sup>

#### *1.1.1.1 Viral vectors*

Viruses have evolved to deliver viral disease-causing genes to specific target cells and utilize the mechanisms of the host cell to multiply the new virus particles in a pathogenic manner.<sup>[18]</sup> In gene therapy, viruses are denatured, the viral gene removed, a therapeutic gene is added, followed by renaturation of the virus.<sup>[17]</sup>

There are several types of viruses that have been used in gene therapy such as retroviruses, adenoviruses, adeno-associated viruses and herpes simplex viruses.<sup>[19]</sup> Retrovirus was the first to be used as a vector.<sup>[20]</sup> Retroviruses are RNA viruses that can be reverse transcribed to double-stranded DNA copies.<sup>[21]</sup> These copies of DNA can then be integrated into the human genome providing long term and heritable expression of the transduced gene. Major limitations of retrovirus are low titre, inability to transfect non-dividing cells and the risk of

insertional mutagenesis.<sup>[19]</sup> A sample of retrovirus is Human Immunodeficiency Virus (HIV). Adenoviruses are double-stranded DNA viruses which normally cause the common cold.<sup>[22]</sup> They can introduce their DNA into the nucleus of the cells. Unlike those of retrovirus, adenovirus DNA is not integrated into human genome, thus they are safer to use than retroviruses and can be produced in high titre. However, using the unintegrated property means adenoviral gene delivery is not permanent, and results in protein production for only a few days to a few weeks. Adeno-associated viruses (AAV) are believed to occur naturally in humans, existing without causing disease or immune response from the body.<sup>[22]</sup> Adeno-associated viruses are small single-stranded DNA viruses that can insert their genetic material at a specific site on chromosome 19. However, this type of vector can only carry less than 5 kb of DNA. Herpes simplex viruses are double-stranded DNA viruses that can infect a particular cell type, neurons.<sup>[22]</sup>

Using viral vectors for gene therapy is efficient. However, there are many hurdles<sup>[23]</sup> such as the limited amount of DNA that viruses can carry (**Table 1.1**).<sup>[24]</sup>

**Table 1.1. Properties of viruses used for gene therapy**<sup>[24]</sup>

Virus	Genetic material	Genome size (kb)	Insert size (kb)
Retrovirus	Linear single-stranded RNA	7-11	4
Adenovirus	Linear double-stranded DNA	36	8-9
AAV	Linear single-stranded DNA	4.7	4.5
HSV-1	Linear double-stranded DNA	152	30
Poxvirus	Linear double-stranded DNA	130-280	30

Moreover, viral vectors can be toxic,<sup>[16]</sup> immune responses,<sup>[16]</sup> are difficult to manufacture at high titres, are expensive to produce and patient compliance is poor. An alternative way to address these drawbacks is with non-viral vectors as a result of (i) the ease of chemical manipulation, which can aid incorporation of essential vector features such as targeting ligands<sup>[25]</sup> and nuclear localization signal,<sup>[26]</sup> (ii) the higher capacity to deliver genetic material, (iii) lower toxicity, (iv) lower cost and easy scale-up processes, and (v) better patient compliance.<sup>[16,17]</sup> The summary of the advantages and limitations of viral and non-viral vectors also show in **Table 1.2**.

**Table 1.2 Advantages and limitations of viral and non-viral vectors**<sup>[16,17,25-29]</sup>

Advantages/Limitations	Viral vectors	Non-viral vector
Advantages	<ul style="list-style-type: none"> <li>- higher transduction efficiency</li> <li>- long-term gene expression as some viruses can facilitate genetic integration into genome (retrovirus, AAV)</li> <li>- broad host range</li> <li>- some viruses are non-pathogenic (AAV)</li> </ul>	<ul style="list-style-type: none"> <li>- ease of manipulation</li> <li>- high flexibility on size of the delivered transgene</li> <li>- safety</li> <li>- low cost</li> <li>- good patient compliance</li> </ul>
Limitations	<ul style="list-style-type: none"> <li>- cytotoxicity</li> <li>- immunogenicity</li> <li>- genetic material capacity limitation (retrovirus, adenovirus, AAV)</li> <li>- Insertional mutagenesis (retrovirus)</li> <li>- difficulty to manufacture at high titres</li> <li>- highly expensive to produce</li> <li>- poor patient compliance</li> </ul>	<ul style="list-style-type: none"> <li>- poor transfection efficiency</li> <li>- transient gene expression</li> <li>- rapid plasma clearance (liposomes)</li> <li>- need targeting ligands for deliver to specific tissue such as transferin</li> <li>- need to escape from endosome</li> <li>- need nuclear localization signal for nuclear import in non-dividing cells</li> </ul>

### 1.1.1.2 Non-viral vectors or synthetic vectors

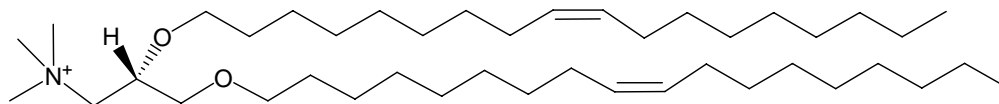
Currently, many researchers are interested in studying non-viral gene delivery systems,<sup>[30]</sup> since synthetic vectors are safer and are able to carry more copies of the gene than viral vectors. Furthermore, they can be manipulated more readily than viral vectors. Synthetic vectors are generally polycationic in nature, therefore, they can form complexes with the polyanionic phosphate backbone of the DNA or RNA. The net charge of these complexes is designed to be positive, which will enable the complexes to interact with the anionic nature of cell membranes, facilitating internalization into cells by syndecan-mediated endocytosis.<sup>[31]</sup> During the last decade efforts to design synthetic vectors have been made by taking advantage of the electrostatic self-assembly of nucleic acids with polycationic materials.<sup>[32]</sup> There are many types of synthetic vectors that have been used such as cationic lipids<sup>[33,34]</sup> and cationic polymers.<sup>[35-42]</sup> Polyamines are among the earliest compounds that were identified as DNA condensing agents.<sup>[43,44]</sup>

#### 1.1.1.2a Cationic lipids

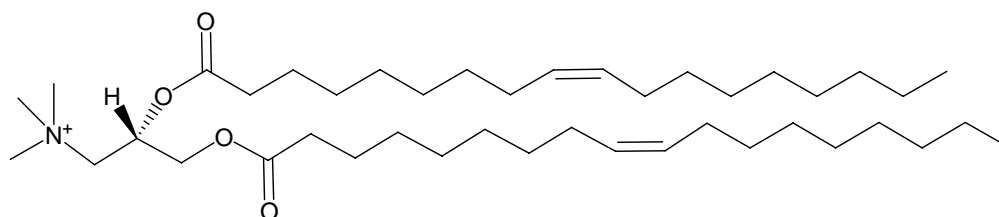
Cationic lipids that form liposomes have become one of the most studied non-viral vectors.<sup>[33,34]</sup> They condense with DNA *via* electrostatic interaction. Cationic liposomes are promising non-viral delivery systems for gene therapy, although the biochemical and biophysical mechanisms of these vectors with respect to gene transfection and expression are not thoroughly understood.<sup>[45]</sup> Most of the cationic lipids used as transfection reagents have three parts: (i) hydrophobic lipid anchor group which can be either a double chain hydrocarbon such as *N*-[1-(2,3-dioleoyloxy)propyl]-*N,N,N*-trimethylammonium chloride (DOTMA),<sup>[46]</sup> 1,2-bis(oleoyloxy)-3-(trimethylammonio)propane (DOTAP),<sup>[47]</sup> and dioctadecyl amino glycol spermine (DOGS, Transfectam®)<sup>[48]</sup> or a cholesterol derivative such as 3β[*N,N'*-dimethylaminoethane)-carbonyl] cholesterol (DC-Chol),<sup>[49]</sup> (ii) linker group such as

an ester, amide or carbamate, and (iii) a positively charge head group which interacts with the nucleic acid backbone (**Figure 1.2**).<sup>[50,51]</sup>

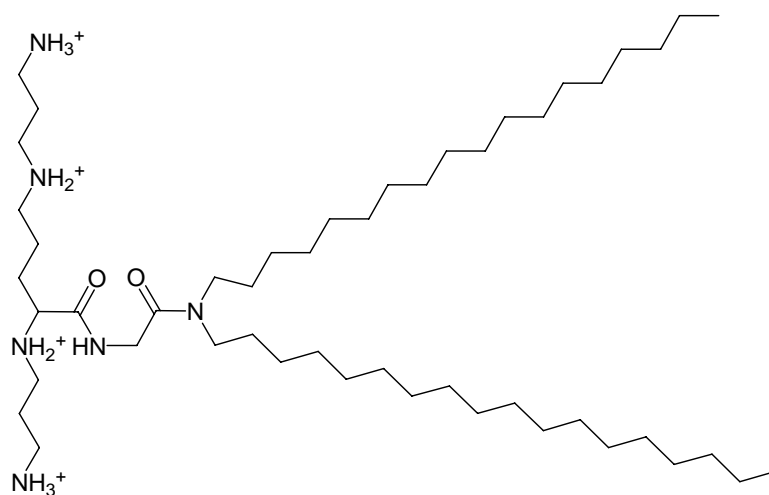
a) DOTMA



b) DOTAP



c) DOGS



d) DC-Chol

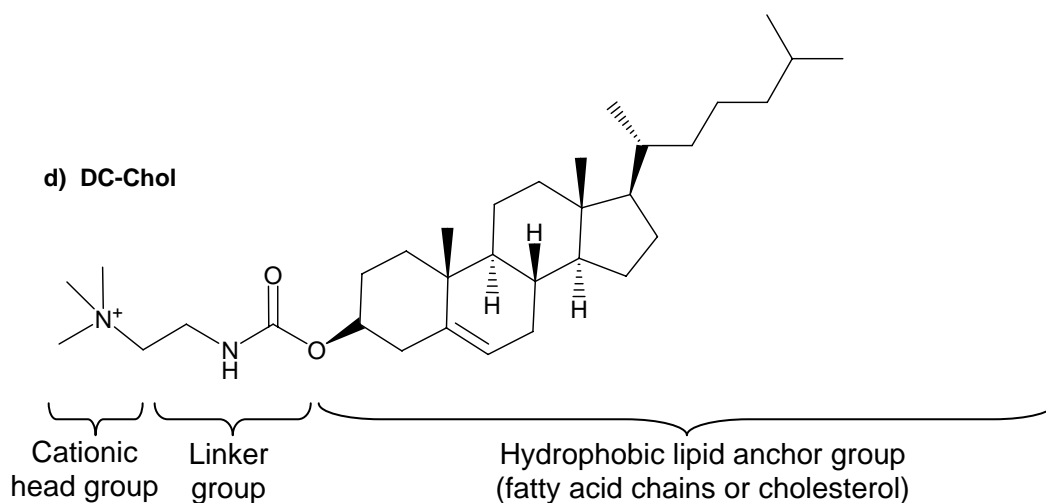


**Figure 1.2. Cationic lipids;** a) *N*-[1-(2,3-dioleoyloxy)propyl]-*N,N,N*-trimethylammonium chloride (DOTMA), b) 1,2-bis(oleoyloxy)-3-(trimethylammonio)propane (DOTAP), c) dioctadecyl amino glycil spermine (DOGS), and d) 3β[*N,N'*-dimethylaminoethane]-carbamoyl] cholesterol (DC-Chol)

The model of DNA release from lipoplexes into the cytoplasm was proposed by Xu and Szoka<sup>[52]</sup> and called the flip-flop mechanism (**Figure 1.3**). The interaction between cationic lipids of lipoplexes and endogenous anionic lipids may promote membrane fusion and transport of DNA across the cell membrane. Thus, the key attribute of lipoplexes may be the ability of the lipid to dissolve into and undergo translational movement within lipid bilayers.

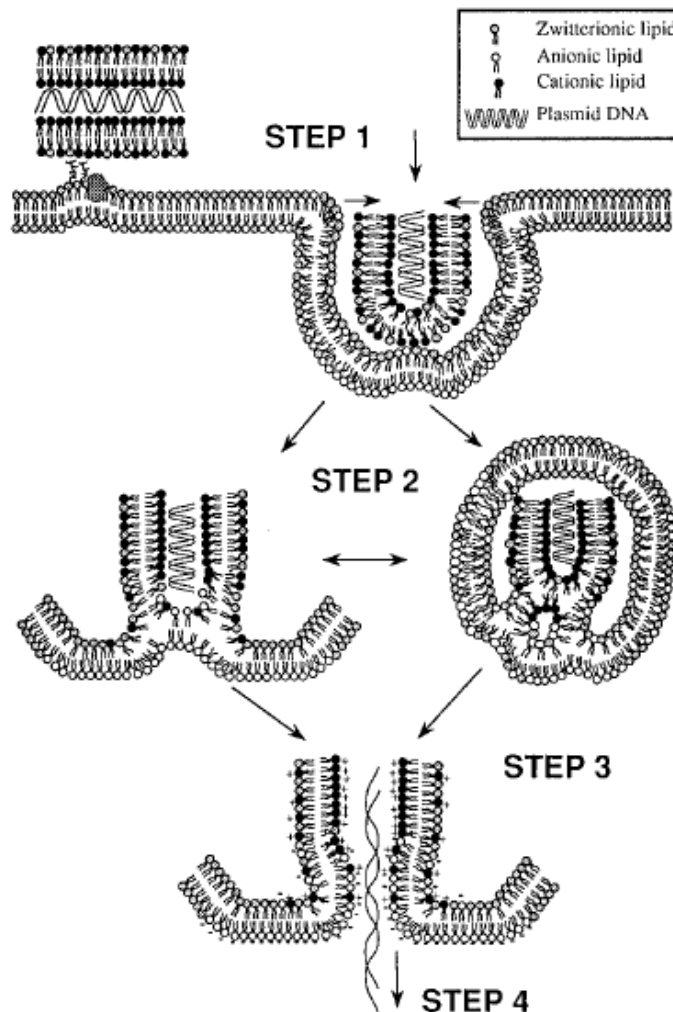
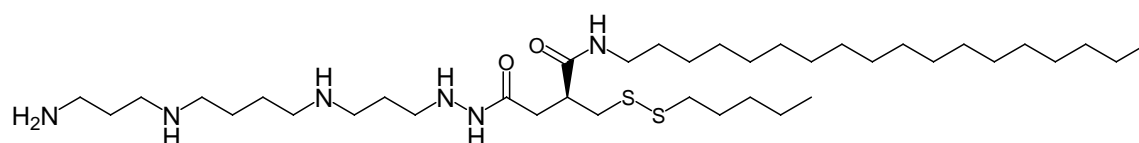


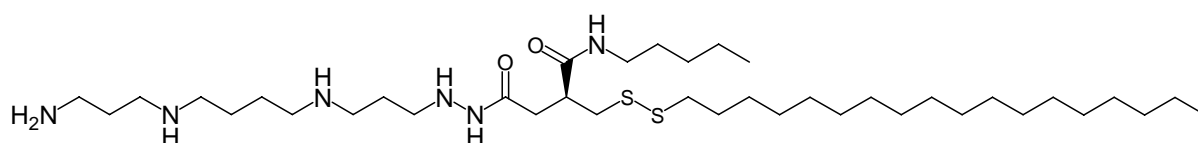
**Figure 1.3. Flip-flop mechanism to uptake lipoplexes and subsequently release of DNA.**<sup>[52]</sup> After electrostatic interaction of cationic lipoplexes with the plasma membrane, lipoplexes are internalized by endocytosis (step 1) followed by the fusion of the lipid bilayers and a vesicle is formed if the membrane pinches off from the cell membrane (step 2). In the early endosome, membrane destabilization results in anionic lipids diffusing into the vesicle and forming a charge neutral ion pair with the cationic lipids (step 3). The DNA dissociates from the vesicle and enters the cytoplasm (step 4).

Reducible cationic lipids (RCLs) (**Figure 1.4**) have also been developed for gene transfer by incorporating disulfide bonds in either the hydrophilic or hydrophobic part of cationic lipids, or within an alkyl chain in order to enhance DNA release from lipoplexes after intracellular reduction.<sup>[34,53]</sup> The transfection by RCLs was 1000-fold greater than their analogues without disulfide bonds.<sup>[53]</sup>

**a) RPR 132775**



**b) RPR 202059**



**c) RPR 203769**

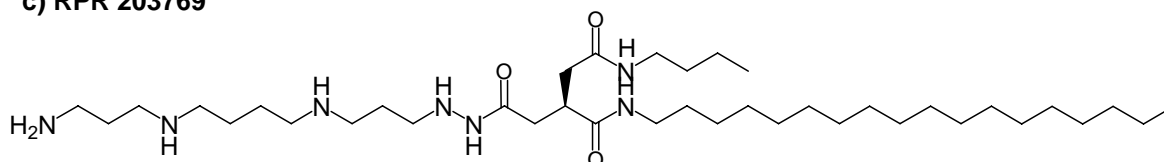


**Figure 1.4. Reducible cationic lipids (RCLs) structures.**<sup>[53]</sup> Lipids with disulfide bond within hydrophobic chain (a,b), and control lipid without disulfide bond (c)

Water soluble cationic lipopolymer (WSLP) (**Figure 1.5**) has been synthesized by conjugating cholesterol choroformate directly to branched PEI 1800 Da.<sup>[54,55]</sup> The cholesterol was used as a lipophilic portion grafted onto branched PEI which serves as a hydrophilic head group. The mean size of WSLP/DNA complexes was approximately 70 nm. The transfection

efficiency of WSLP was higher than PEI 1800 Da, PEI 2500 Da, and naked DNA. Furthermore, WSLP is less toxic than PEI.<sup>[55]</sup>

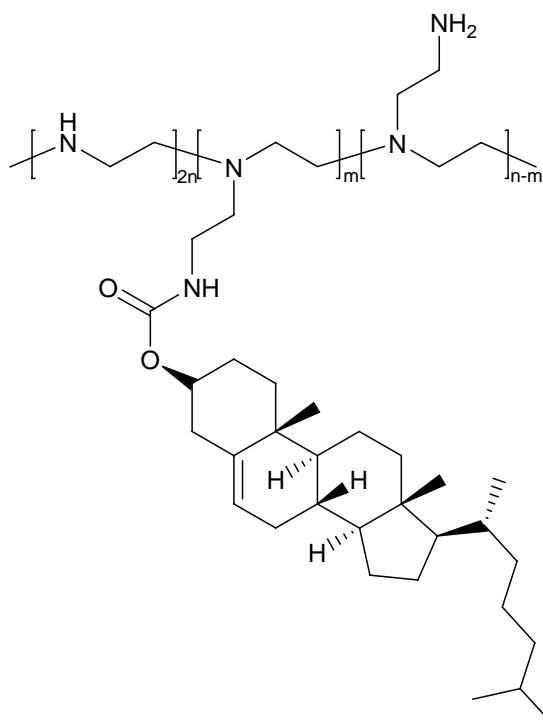


**Figure 1.5.** Water soluble cationic lipopolymer (WSLP)<sup>[54]</sup>

#### 1.1.1.2b Cationic polymers

Cationic polymers have been widely studied as vectors for gene delivery. They include polyethylenimine (PEI)<sup>[35-40]</sup> and amine containing dendrimers<sup>[41,42]</sup> which complex with the gene. The complex is referred to as a polyplex.

##### (i) Polyethylenimine (PEI)

Branched PEI polymers contain primary, secondary and tertiary amino groups (**Figure 1.6**). This polymer has wide range of buffering capacity ( $pK_a$  values of primary, secondary and tertiary amines are 9, 8 and 6-7, respectively) which allows varying degree of protonation of the amine groups in the complex depending on the local pH.<sup>[56]</sup> The overall protonation level increases from 20 to 45% between pH 7 and 5.<sup>[57,58]</sup> This buffering property is very useful in



*in vivo* applications where it can lead to a release process from the endosome (proton sponge hypothesis).<sup>[36,58,59]</sup> PEI is inexpensive, easily available, and its potential use in gene delivery has generated much interest.<sup>[37,56,60,61]</sup>

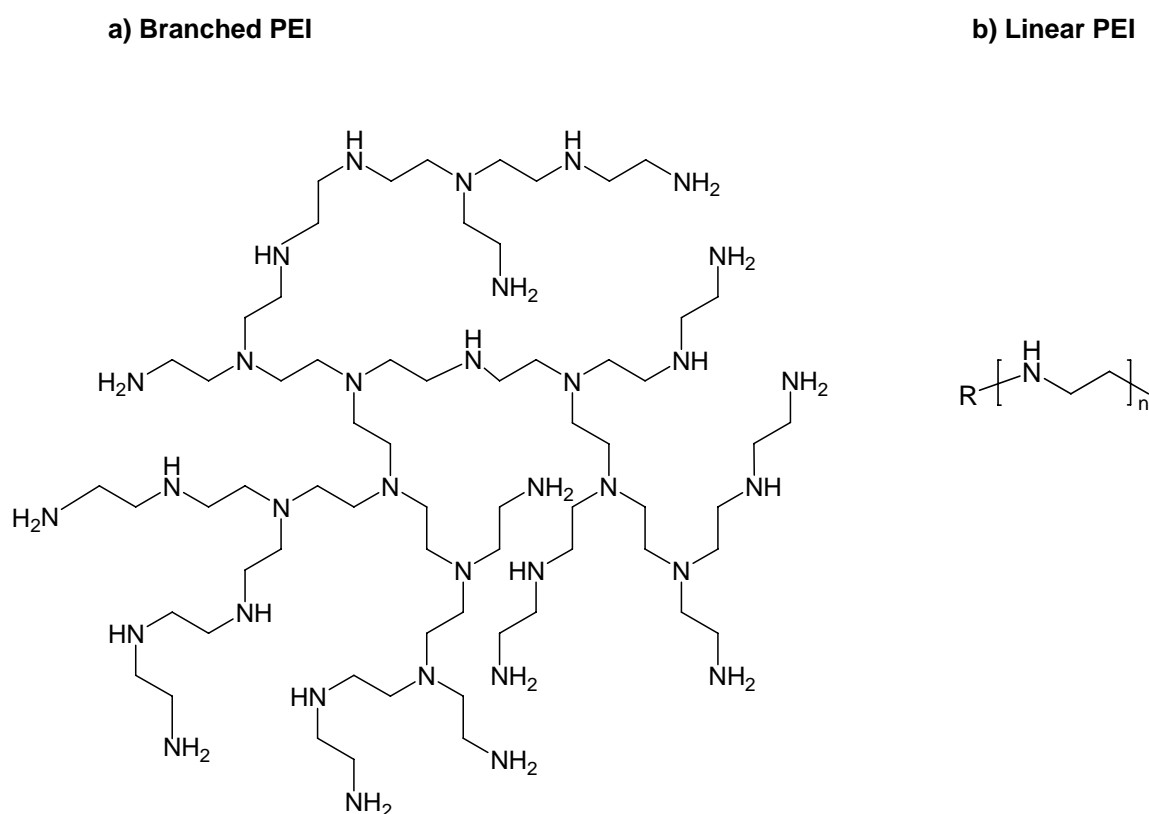


**Figure 1.6. Polyethylenimine (PEI) structures;** a) branched PEI, and b) Linear PEI

The combination of a cell-binding ligand and endosomolytic activity of PEI has been demonstrated which can lead to very efficient gene delivery systems.<sup>[62]</sup> Some of which may be used for condensing and linking plasmid DNA to adenovirus particles.<sup>[63]</sup> However, PEI can cause significant *in vivo* toxicity in cultured cells. PEI is an organic polymer which can not be degraded by cellular enzymes. As a result, total body clearance of high molecular weight PEI is a slow process which leads to the accumulation of PEI *in vivo*.<sup>[38]</sup> To overcome this drawback, the introduction of disulfide bonds into low molecular weight PEI (800 Da)

through dimethyl-3,3'-dithiobispropionimide•2HCl (DTBP) have been designed (**Figure 1.7**) to promote reversion of high molecular weight polyplexes back to their low molecular weight counterparts which should clear more easily from the body.<sup>[35]</sup> PEI (1800 Da) has also been cross-linked with DTBP (CLPEI<sub>50%</sub>, molar ratio of cross-linker reactive group to PEI primary amine was 1:2) and was found that the polyplexes were reduced by GSH at a concentration of 3 mM.<sup>[64]</sup>

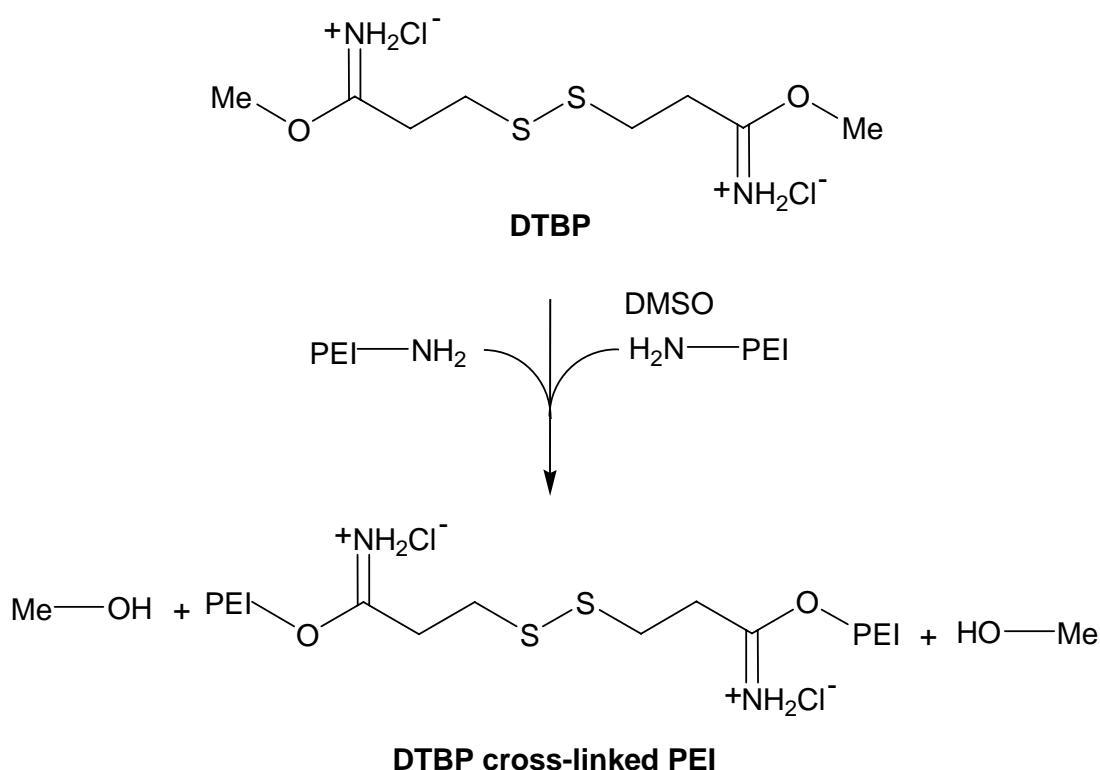


**Figure 1.7. Proposed reaction scheme of DTBP (dimethyl-3,3'-dithiobispropionimide•2HCl) cross-linked PEI<sup>[35]</sup>**

It was found that the cytotoxicity of low molecular weight PEI (LMW-PEI, 5.4 kDa) was reduced by more than one order of magnitude compared with high molecular weight PEI (HMW-PEI, 25 kDa). Moreover, LMW-PEI was shown to increase the transfection efficiency in many types of cell lines.<sup>[37]</sup> The incorporation of the fusogenic peptide (KALA, WEAKLAKALAKALAKHLAKALAKALKACEA) and PEI has also been modulated in

order to combine the endosomal escape and DNA condensation properties of PEI, as well as the cellular entry properties of KALA. The DNA polyplex was produced by condensing DNA with PEI as the core component and the outer layer linked with KALA. This tricomposite showed transfection efficiency better than that by either of KALA or PEI polyplexes alone.<sup>[60]</sup>

### (ii) Dendrimers

Dendrimers are a more recent class of cationic polymers that have been used as vectors for gene delivery.<sup>[41]</sup> A dendrimer<sup>[65]</sup> is a tree-like highly branched monodisperse polymer molecule. Dendrimers can be synthesized by two different routes which are convergent<sup>[66]</sup> and divergent<sup>[67]</sup> routes to form a tree-like architecture (**Figure 1.8**).

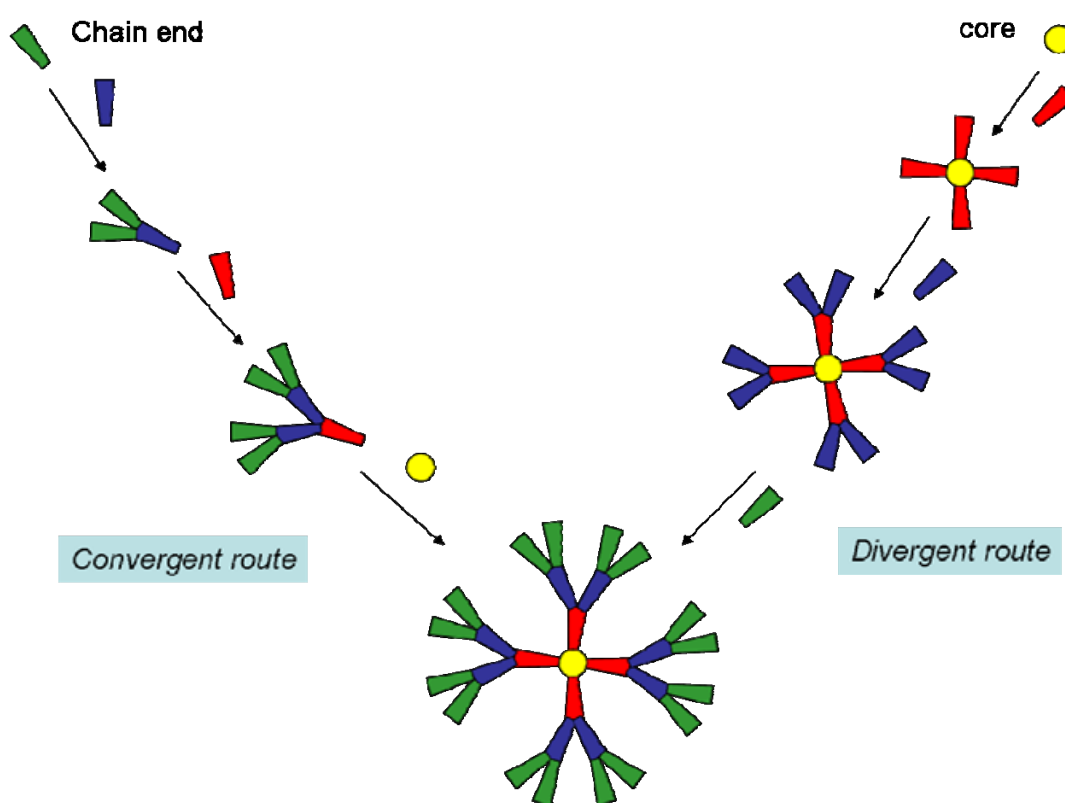


**Figure 1.8. Dendrimer synthesis by convergent and divergent routes**

Several different kinds of dendrimers have been synthesized,<sup>[68-70]</sup> for instance, polyamidoamine (PAMAM) is a dendrimer formed from the amidoamine monomer which is terminated with amine groups (**Figure 1.9**)<sup>[69]</sup> consist of highly ordered, three dimensional, hyperbranched arrays of dendrons. They are synthesized by iterative reaction sequences with methylacrylate and ethylenediamine.<sup>[65]</sup>

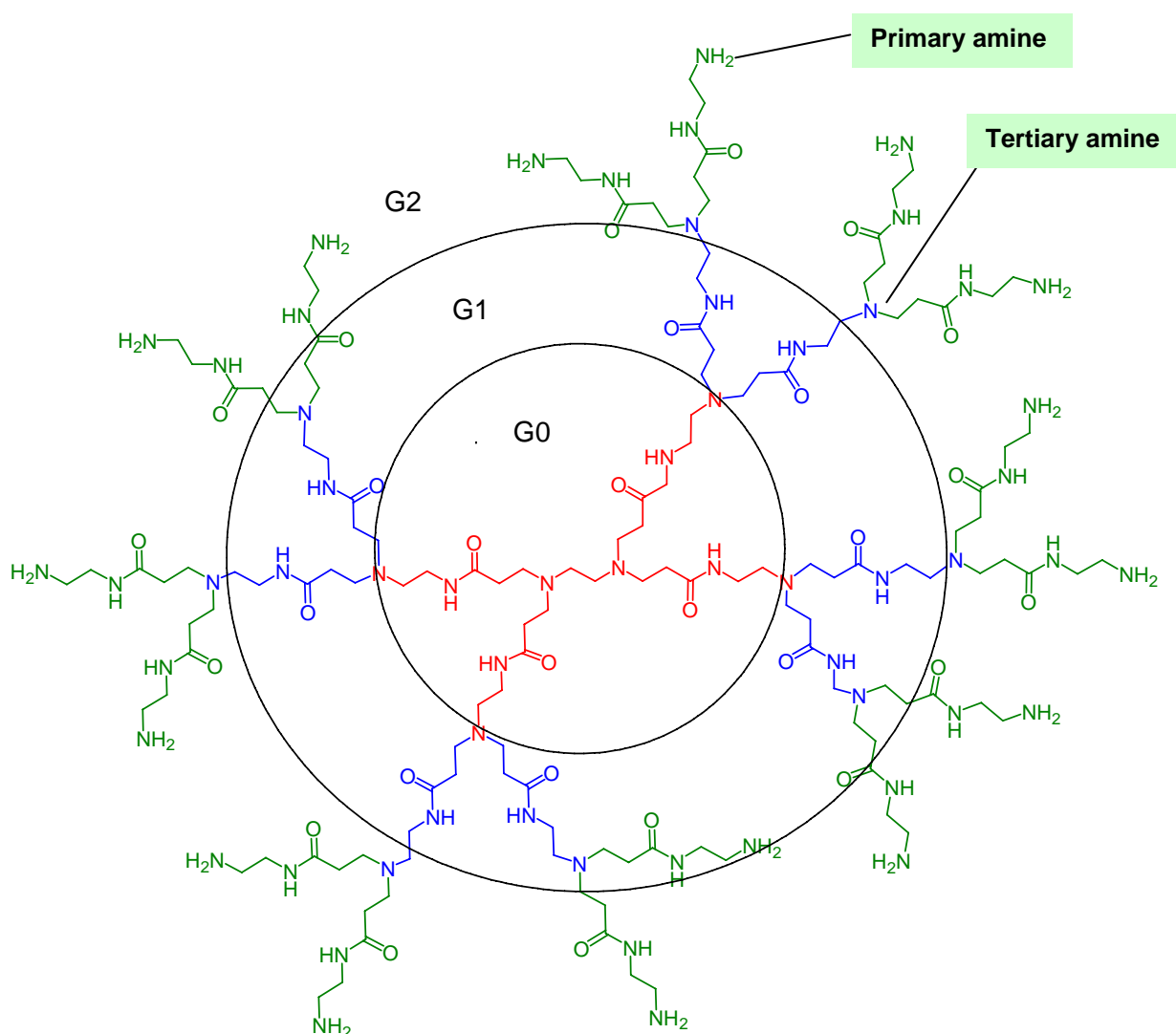


**Figure 1.9. Structure of polyamidoamine (PAMAM) dendrimer.** (The core is shown in red (G0). Primary (G1) and secondary (G2) generations are shown in blue and green, respectively)

Dendrimer size is designated by a generation number. After one reaction iteration on the initiator core, the dendrimer is a generation 0 dendrimer (G0), and with each subsequent reaction iteration, the generational number increases by one. PAMAM dendrimers have multiple terminal primary amine groups with  $pK_a$  of approximately 9, thus at physiological pH these amine groups are protonated which gives a spheroidal polycation character and their tertiary amines have a  $pK_a$  of 5.5.<sup>[71,72]</sup> The tertiary amines are able to buffer the endosome and prevent plasmid degradation. The capability of dendrimers in cell transfection depends on their size, structure and number of amino group on the surface.<sup>[41]</sup> PAMAM dendrimers from G2-G10 were used to study their gene transfer properties *in vitro*. The G6 dendrimer at charge ratio of 1:6 (-/+) produced maximal transfection levels at 1000-fold greater gene expression in CV-1 cells than that from PLL and 100-fold greater than that from DOTMA-based lipoplexes.<sup>[71]</sup> A fusogenic peptide, GALA (WEAALAEALAEALAEHLAEALAEAL EAL(C)AA), was modified by replacing leucine (L) at position 28 with cysteine (C) and attaching it to a modified PAMAM (G5) dendrimer by disulfide bond formation (**Figure 1.10**).<sup>[71]</sup> The combination of a fusogenic peptide and a dendrimer resulted in improving the transfection efficiency because GALA catalyzed the endosomal lysis leading the free dendriplex escaped to the cytoplasm.

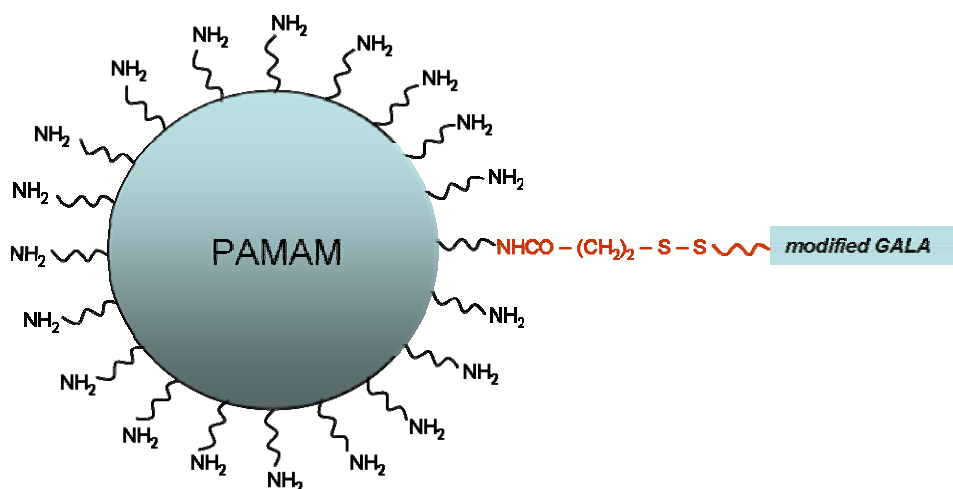


**Figure 1.10.** The model of modified PAMAM attached to GALA *via* disulfide bond formation<sup>[71]</sup>

The investigation of *in vitro* transfection efficiencies of dendrimer complexes has also been studied by Tomlinson and colleagues.<sup>[73]</sup> The mean size of the complexes were shown to be monodisperse and below 200 nm at charge ratios of 1:0.25 to 1:6 (-/+). The maximum transfection efficiency was also observed with G5 and G6 dendrimer complexes at a charge ratio of 1:6 (-/+). The larger dendrimers resulted in significant cell toxicity.

Polypeptides are also used as vector as will be described later.

### 1.1.2 Cellular barriers to gene delivery

There are several cellular barriers that need to be overcome in order for a gene to be delivered to the nucleus.<sup>[74,75]</sup> The polyplexes have to protect the nucleic acids from degradation by nucleases<sup>[74]</sup> and the interactions with blood components extracellularly, which would result in the clearance of the polyplexes. Cells must be able to internalize the vector/DNA or RNA polyplexes in the form of an endosome by endocytosis.<sup>[76]</sup> When internalized into the cytoplasm the polyplexes must be able to escape from the endosomal compartment by the proton sponge mechanism.<sup>[58]</sup> Once released to the cytoplasm, the polyplexes have to unpack and release the nucleic acid.<sup>[75]</sup> If the polyplexes were formed with RNA, then it can be expressed transiently by the cell. If the polyplexes were formed with DNA, the transportation of DNA to the nucleus is essential. In the nucleus, the normal DNA replaces the abnormal DNA or is transcribed to mRNA which is exported to the cytoplasm, where it is translated to the therapeutic protein (**Figure 1.11**). Thus, the design of a vector carrying DNA needs to have several factors (i) gene binding, (ii) cell targeting, (iii) cell uptake, (iv) endosomal escape, (v) DNA release and (vi) nuclear localization.

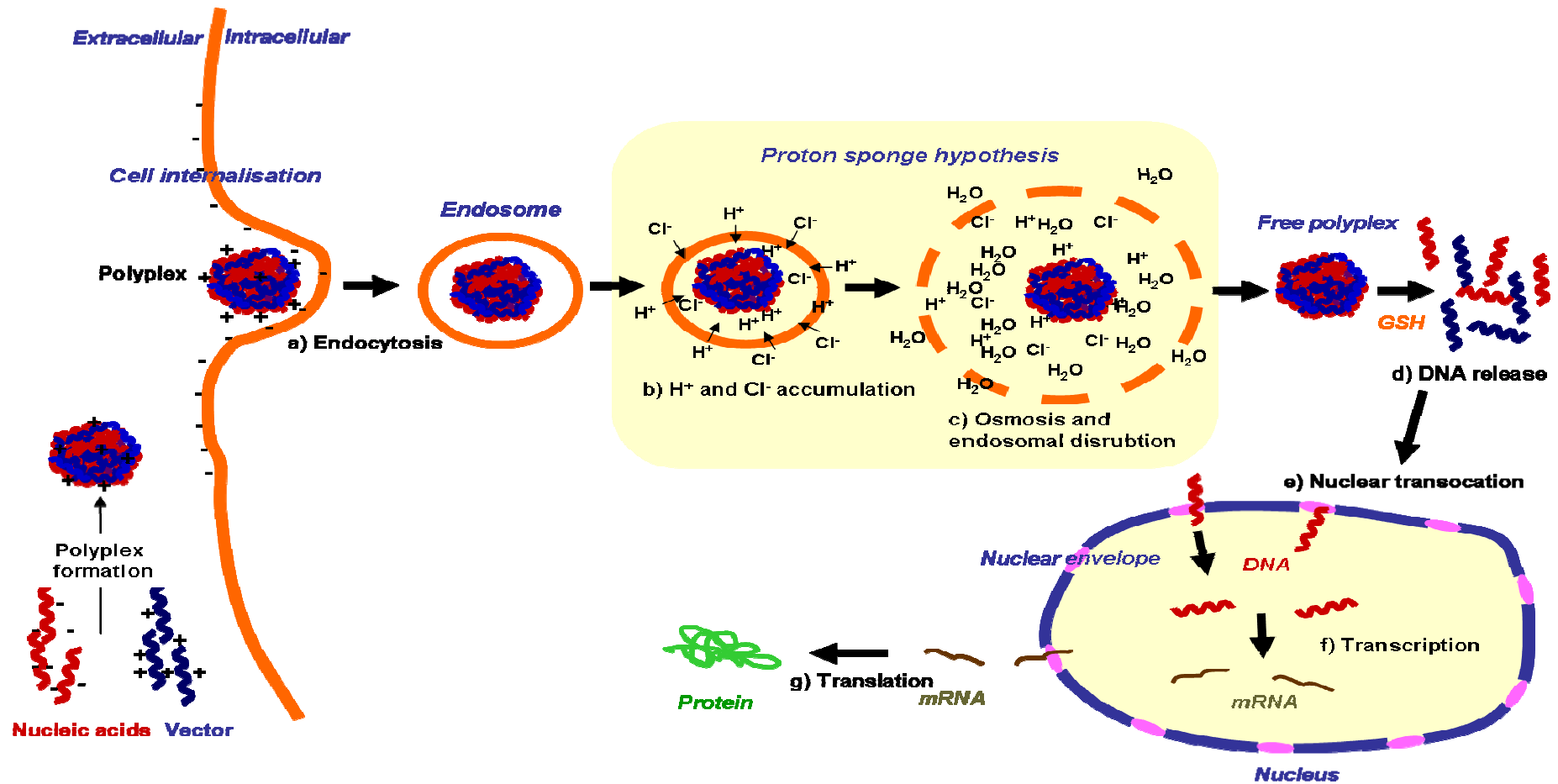


**Figure 1.11. Gene delivery by non-viral vector system.** Cationic polyplex interacts with anionic cell membrane then enters into cell by endocytosis (a). pH in endosome drop from 7 to 5 by proton and chloride ions accumulation (b) which cause water influx since the increasing of the osmolarity in the endosome, and result endosomal disruption eventually (c) The free polyplex in cytosol then has to unpack and release free nucleic acid (d) then DNA translocates to nucleus (e) for further DNA transcription (f) and mRNA translation (g).

In this section, *extra-* and *intracellular* barriers for gene delivery will be described.

### 1.1.2.1 Extracellular barriers

#### 1.1.2.1a Biodistribution and interaction in bloodstream

In general, opsonization occurs in the bloodstream when foreign particles are coated by specific plasma proteins (opsonins), which allows macrophages to recognize and remove foreign particles from the bloodstream.<sup>[77]</sup> The opsonization of hydrophobic particles has been shown to occur more quickly than hydrophilic particles due to the higher adsorbability of plasma proteins on the surfaces.<sup>[78]</sup> A study of liposome clearance from blood circulation by opsonization,<sup>[79]</sup> showed that hydrophobic particles are opsonized and taken up by fixed macrophages of liver and spleen with 80-90% efficiency within a few minutes of intravenous administration. Therefore, non-viral delivery systems must have a hydrophilic surface in order not to be opsonized.<sup>[80, 81]</sup>

Particle size is also significant for survival in bloodstream. Particle diameters that are greater than 7  $\mu\text{m}$  cause capillary blockage, regardless of their surface properties.<sup>[79]</sup> Whilst particle diameter less than 1  $\mu\text{m}$  may circulate longer in the bloodstream if there are no interactions with blood components or fixed macrophages.<sup>[79]</sup> Normally, a single plasmid could be condensed to approximately 25 nm in diameter.<sup>[82]</sup> However, the polyplexes mostly contain several plasmids which lead to sizes of 100-150 nm in diameter.<sup>[83]</sup> At physiological salt concentration ( $\sim 0.1\text{M}$ ),<sup>[84]</sup> however, the polyplexes tend to aggregate,<sup>[85]</sup> and they are bound with negative serum proteins resulting in larger sizes (200-1000 nm in diameter).<sup>[86,87]</sup> This aggregation results in mobility retardation of the polyplexes to the target cells.<sup>[81]</sup>



### 1.1.2.1b Cell targeting

Synthetic vectors that are non-specific are able to transfer a gene *in vitro*, however, these vectors are unable to transfer genes *in vivo*, since they are non-specific to the target cells.<sup>[88, 89]</sup> In order to target the specific cells, the vector needs to be coupled with a ligand which is able to bind to a receptor on the cell surface.<sup>[25]</sup> The most widely used preexisting targeting ligands are based on endogenous molecules which are already present in the body such as folic acid<sup>[90]</sup> and transferrin.<sup>[91-95]</sup> The receptor of folic acid is overexpressed on a number of human tumors *via* folate receptor-mediated endocytosis.<sup>[90]</sup> Transferrin is a serum iron transport protein which delivers Fe(III) into cells *via* receptor-mediated endocytosis, and has become one of the most widely used ligands for targeting the synthetic vectors. For example, Wagner and colleagues<sup>[93]</sup> used conjugates of PLL-transferrin to bind and condense DNA and deliver it to the transferrin receptor, where upon it enters the cell *via* endocytosis *in vitro*. A galactose-terminated (asialo-) glycoprotein, asialoorosomuroid (AsOR), is a ligand of asialoglycoprotein receptor of the liver, and was linked to polylysines in order to condense with DNA. This glycosylated-PLL could carry the DNA to the liver *in vivo via* receptor-mediated gene delivery.<sup>[96]</sup>

### 1.1.2.1c Cell uptake

The uptake of most macromolecules or particles into cells by passive diffusion across the plasma membrane is limited by their solubility in the lipid bilayer. Endocytosis<sup>[76]</sup> is the process by which substances are internalized into cell (**Figure 1.12**). When a polyplex binds to the cell an extracellular portion of the plasma membrane is invaginated and pinched off forming a membrane-bounded vesicle called an endosome which encases the polyplex.<sup>[97]</sup> There are several pathways of endocytosis.

a) *Phagocytosis – or cell eating* – is a form of endocytosis which occurs in phagocytes cells such as macrophages, dendritic cells and neutrophils to capture solid particles that are larger than 0.5  $\mu\text{m}$  such as bacteria, pathogens and particulate antigens by pseudopodium (**Figure 1.12a**). The phagosome then fuses with the lysosome to hydrolyse the particles. The sizes of phagosomes vary from 0.5-4  $\mu\text{m}$ .<sup>[98]</sup>

b) *Pinocytosis – or cell drinking* – occurs in almost all cells. Pinocytosis is the process that small particles or extracellular fluid are brought into cell by the invagination of the cell membrane which then pinches off to form endocytic vesicle called a pinosome (**Figure 1.12b**), which subsequently fuses with the lysosome to hydrolyse the particles. The size of micropinosome is 95-100 nm, whilst a macropinosome is 0.5-2  $\mu\text{m}$ .<sup>[99]</sup>

c) *Receptor-mediated endocytosis*, in general, also called clathrin-dependent endocytosis,<sup>[100]</sup> is a major route of most cells to internalize molecules by strong binding of a ligand to a specific cell surface receptor leading to the invagination of coated pits which pinch off from the membrane to form a vesicle called an endosome (**Figure 1.12c**). The coated pit is a region of the membrane that is coated with clathrin for stability and to aid the transport process. Other examples of receptors, such as transferrin receptor and folate receptor, are cell uptake *via* receptor-mediated endocytosis described in section 1.1.2.1b.

d) *Syndecan-mediated endocytosis* is an internalization process of positively charge polyplexes which adhere to the negatively charge heparan sulfate proteoglycans (HSGPs) of transmembrane syndecan expressed on surface of all adherent cells<sup>[101,102]</sup> *via* electrostatic interactions (**Figure 1.12d**).<sup>[103,104]</sup> Cationic polyplexes that enter into cell by this process are, for instance, protonated PEI<sup>[104]</sup> and PLL polyplexes.<sup>[103,104]</sup>

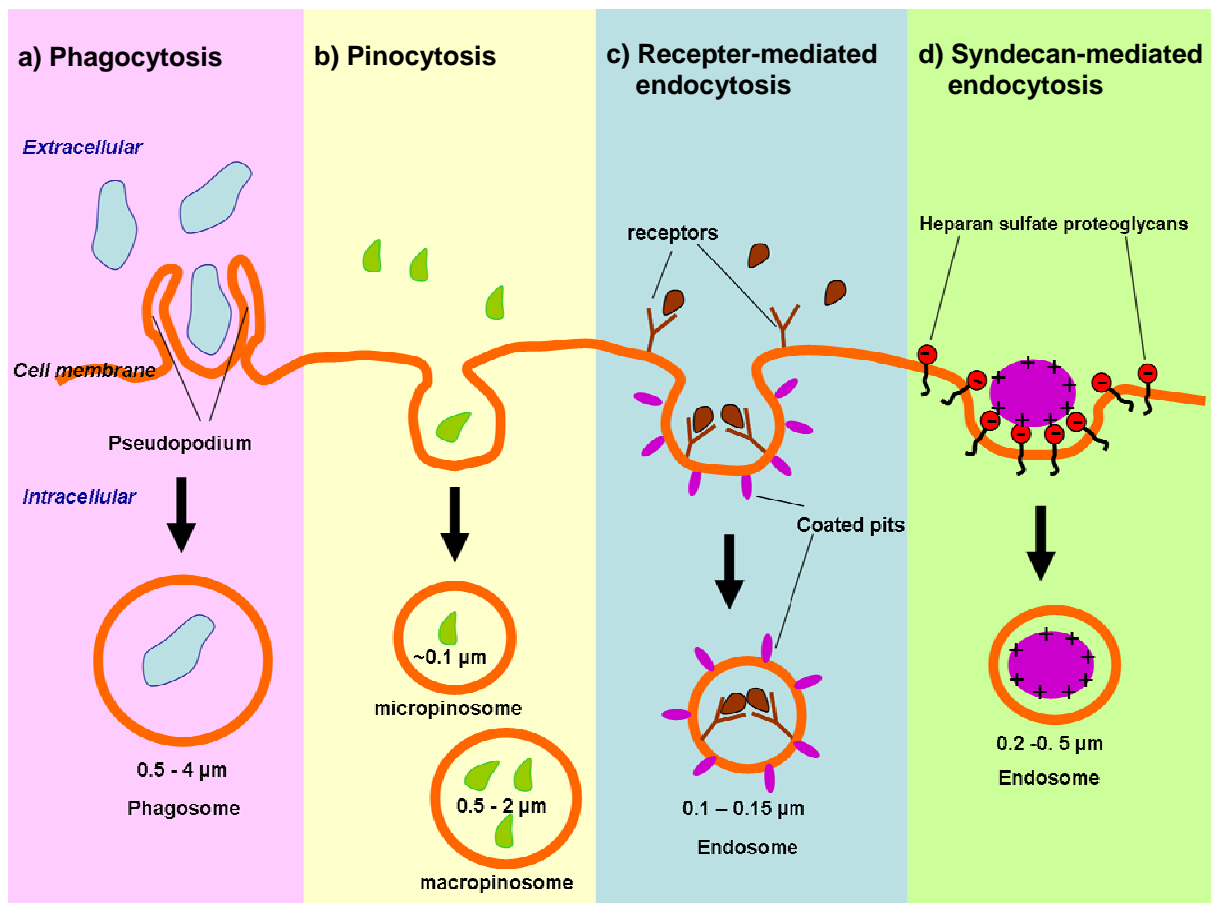


**Figure 1.12. Endocytic pathways;** a) Phagocytosis, b) Pinocytosis, c) Receptor-mediated endocytosis, d) Syndecan-mediated endocytosis

### 1.1.2.2 Intracellular barriers

#### 1.1.2.2a Endosomal escape

As the pH decreases in the endosome from the early (pH ~6) to late (pH ~5-6) endosome, and finally fuses with the lysosomes (pH ~4.5) by the ATPase proton pumps,<sup>[105]</sup> many of the proteins and lipids begin to degrade in the late endosome. Therefore, after internalization into the cell, the polyplex has to be released from the endosome before reaching the late endosome state where it would be degraded.<sup>[97,106]</sup> A mechanism for endosomal polyplex release is based upon proton sponge hypothesis.<sup>[59]</sup> This postulates enhanced transgene delivery by polyplexes containing H<sup>+</sup> buffering polyamines. As the pH in the endosome is buffered by the

polyplexes, the ATPase continues to pump protons into the endosome. This buffering leads to an influx of chloride counterions and increases the osmotic pressure, thus, inducing osmotic swelling by water influx into the vesicle and eventual lysis. The synthetic vectors that are able to release the polyplex by this mechanism are cationic polymers such as PEI,<sup>[36,107]</sup> since they have a capability to buffer the endosomal vesicle. PEI is able to condense DNA at physiological pH, but contains a proportion of tertiary amines that protonate only at lower pH. Thus, PEI becomes protonated in the endosome when the pH drops and causes the endosome disruption.<sup>[40]</sup> **Figure 1.13** shows the mechanism of the proton sponge.

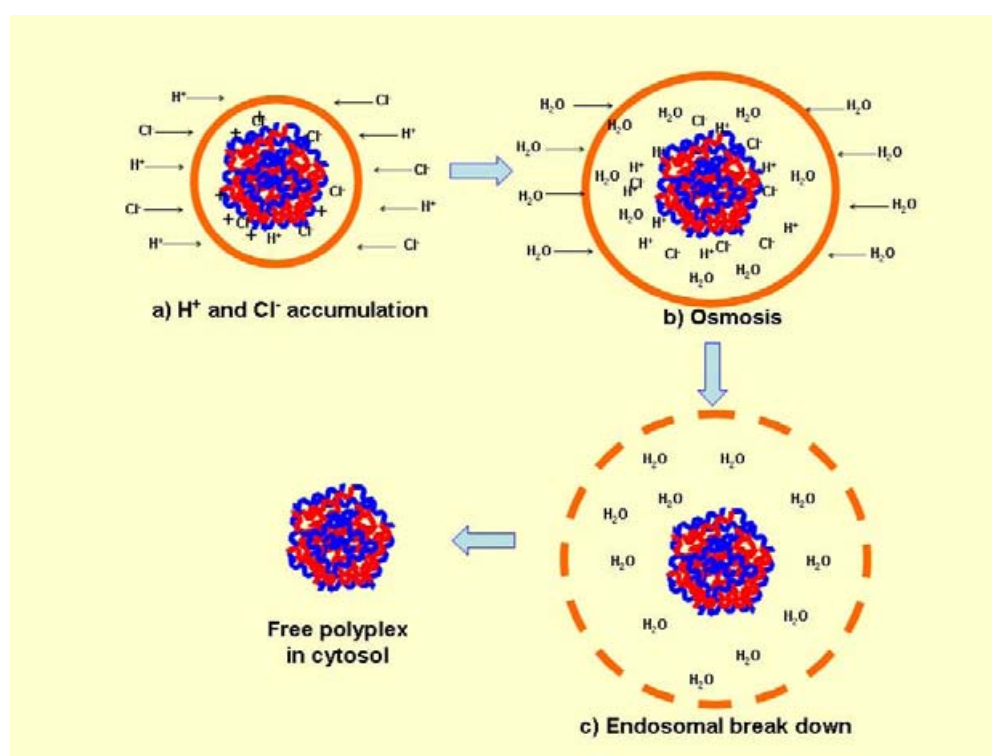


**Figure 1.13. The proton sponge mechanism;** a) Due to the pH buffering in the endosome, the protons are continued to pump in the the vesicle resulting in Cl<sup>-</sup> influx and increase in the osmolarity inside the endosomal vesicle. b) Because of the osmolarity increase, water passes into the endosomal vesicle. (c) The increase of water volume results in the swelling of the endosomal compartment until it ruptures to release the polyplex into the cytoplasm which leads to nuclear uptake of DNA.

- Endosomolytic compound

Chloroquine (**Figure 1.14**), a low molecular weight drug used as a treatment for malaria,<sup>[108]</sup> has been also used in conjunction with the polyplexes.<sup>[107]</sup> Chloroquine is a weak base with  $pK_a$  of 8.1 and 10.2 and is able to diffuse into low-pH compartments, whereupon it is protonated and buffers acidic vesicles, which aids the lysis of the endosome. At approximate concentration 100  $\mu$ M, chloroquine causes substantial improvement in the transfection efficiency. Although cells may be exposed to relative low concentration of chloroquine (100  $\mu$ M) during the transfection, the concentration within cells is found to be much higher and this causes toxicity to cell and further increases in concentration causes substantial loss of cell viability.<sup>[109, 110]</sup>

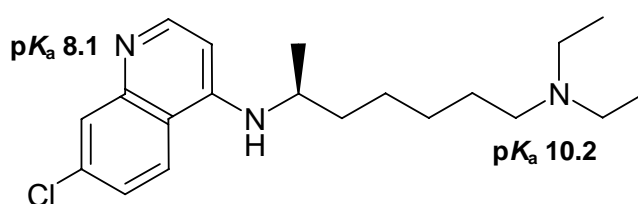


**Figure 1.14.** Structure of chloroquine

There were developments of pH-dependent degradation polymer using polyacetals,<sup>[111,112]</sup> as it is degraded rapidly in endosomal pH (41% MW loss in 25 hours) resulting in non-toxic to cells.

#### 1.1.2.2b Nuclear localization

The DNA must be internalized into the nucleus in order to either replace the non-functional gene or transcribe to mRNA for furthering translation to the therapeutic protein.<sup>[113]</sup> The nuclear membrane is a barrier for most macromolecules that are greater than 40 kDa, unless they are able to interact with the nuclear pore active transport system.<sup>[113]</sup> Nuclear pore

complexes (NPCs) are macromolecular assemblies constructed from multiple copies of approximately 30 different proteins call nucleoporins.<sup>[114]</sup> Importins are the carriers to import protein into nucleus. Importin- $\beta$  is mostly used as an import carrier, while importin- $\alpha$  is used as an adapter protein to import many proteins through NPCs. In order to locate the nucleus, the DNA strand needs to be combined with peptides referred to as nuclear localization signals (NLS) which can be recognized by the import carriers in the cytoplasm.<sup>[115,116]</sup> The mechanism of using the NLS peptides to translocate the DNA into the nucleus is shown in **Figure 1.15**.<sup>[114,117]</sup> Briefly, cargo proteins which contain NLS form complexes with the importin- $\alpha$ : $\beta$  heterodimer (**a, b**). This heterotrimer then binds to the cytoplasmic filaments of NPCs (**c**) and translocate through the NPCs (**d**). Inside nuclearplasmic cargo proteins disassemble from importin complexes (**e, f**) and these importins are then recycled to the cytoplasm (**g**). The components involved in the nuclear protein import cycle shown in **Table 1.3**.

**Table 1.3. The components in nuclear protein import cycle and their functions**

Component	Function
Importin- $\alpha$	Adapter that link NLS-protein cargoes to importin- $\beta$
Importin- $\beta$	Import factor that carriers protein cargoes through NPCs
Ran	GTP binding protein
Ran-GAP	RanGTPase activating protein
NUP50	Nucleoporin 50kDa that displaces protein cargoes bound to importin- $\alpha$
CAS	Nuclear export factor for importin- $\alpha$

Bremner and colleagues<sup>[116]</sup> demonstrated that a peptide derived from human T cell leukemia virus type 1 (HTLV), MPKTRRRPRRSQRKRPTWAHFPFGQGSLC, was able to condense DNA and mediate levels of transgene expression up to 32-fold higher than PLL-based polyplexes.<sup>[116]</sup> The single nuclear localized signal peptide (PKKKRKVEDPYC) modified from the NLS of simian virus 40 large tumor antigen was attached to DNA which was sufficient for translocation through the nuclear pore.<sup>[115]</sup> However, the use of SV40 NLS was the only apparent benefit when used in gene expression for non-dividing cells.<sup>[118]</sup>

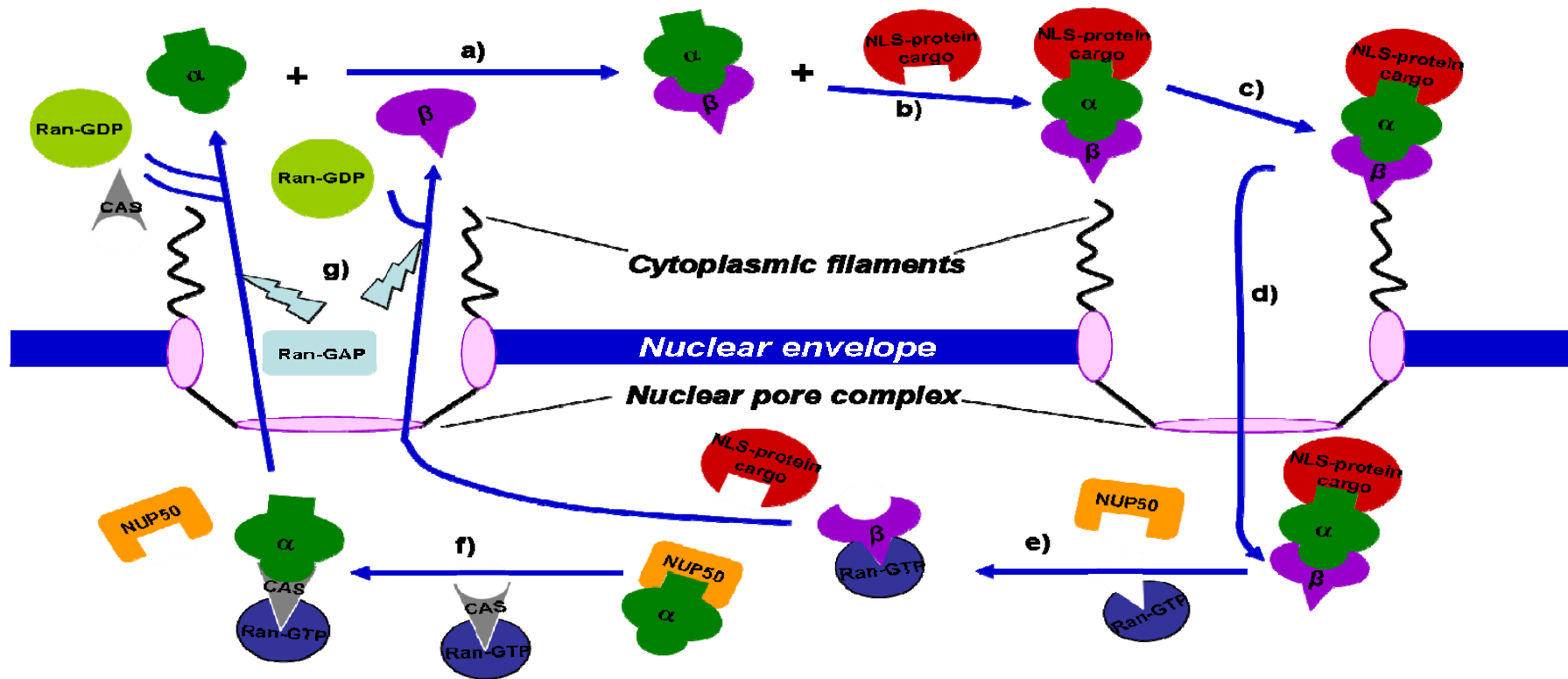


**Figure 1.15. Schematic representation of nuclear protein import cycle.** Importin- $\beta$  form heterodimer with importin- $\alpha$  in cytoplasm (a) which then binds to the protein cargo containing nuclear localization signal (NLS) at the recognition site (b). The heterotrimer then binds to cytoplasmic filaments of the nuclear pore complex (NPC) (c), and subsequently translocate through the nuclear pore into the nucleoplasm (d). The Ran-GTP binds to the complex resulting in dissociation of importin- $\alpha$  complex and NLS-protein cargo is then replaced with NUP50 (e). CAS-RanGTP complex then binds to importin- $\alpha$  to release NUP50 (f) and enables CAS-RanGTP-importin  $\alpha$  complex to transport to the cytoplasm. Importin- $\beta$  and importin- $\alpha$  complex are recycled into the cytoplasm by the activation of RanGAP resulting in dissociation of importins from the complexes (g).



## 1.2 Non-viral gene delivery based on synthetic peptides

A main advantage of a synthetic peptide-based DNA delivery system is its flexibility. For gene delivery, the composition of the polyplex can be easily modified in order to take advantage of specific peptide sequences to overcome *extra-* and *intracellular* barriers. As described previously, vectors need to bind the nucleic acid extracellularly in order to prevent the polyplex degradation. The vectors will then have to promote the endosomal escape after internalization into the cell *via* endocytosis (before it becomes a lysosome where the polyplexes are degraded).<sup>[97,106]</sup> Several peptide sequences are known that can cause pH selective endosomal lysis.<sup>[119]</sup> Furthermore, the intracellular release of DNA from polyplexes is necessary for further gene expression. The nuclear localization signal (NLS) has also shown to be an essential peptide for nuclear translocation to promote gene delivery.<sup>[116,118]</sup>

Below, we review the various amino acids that have been incorporated into peptides for gene delivery and their function.

### 1.2.1 Lysine-based peptides: Extracellular binding of DNA

Lysine is one of the most utilized amino acid in gene delivery studies.<sup>[88,120-122]</sup> The reason being is that the primary amino side chain has a  $pK_a$  of approximately 10.5 (**Figure 1.16**). The high  $pK_a$  means that at physiological pH ( $\sim 7.4$ )<sup>[123]</sup> the amine groups in a polylysine derivative will have a high degree of protonation. Thus, a polycation exists at physiological pH, allowing it to bind to DNA *via* electrostatic interactions. This binding means the polyplex will be stable extracellularly. PLL-Polyplexes are biodegradable, which is an advantage if using the polyplex *in vivo*. PLL is commercially available in various molecular weights ranging from approximately 1 kDa to 300 kDa. However, high molecular weight PLL shows high

levels of toxicity *in vitro*, and PLL-polyplexes without a targeting ligand has poor transfecting ability.<sup>[89, 124]</sup> The immunogenicity study of the D-isomer of PLL showed that it induced the formation of antibodies; thus rendering it unsuitable for use as a vector.<sup>[125]</sup> It is likely that PLL-polyplexes are cleared from the blood as a function of molecular weight. PLL<sub>20</sub> (20 kDa PLL) polyplexes compared to PLL<sub>211</sub> (211 kDa PLL) polyplexes displayed 20 times greater level clearance in blood after 30 minutes.<sup>[126]</sup> Wolfert and colleagues<sup>[127,128]</sup> studied the DNA polyplexes formed from PLL at two different molecular weights (3.9 and 244 kDa) as vectors. The sizes of polyplexes from PLL<sub>3.9</sub> and PLL<sub>244</sub> were in the range from 20-30 nm and 120-300 nm, respectively. However, low molecular weight PLL significantly decreased cytotoxicity. PLL<sub>54</sub> (54 kDa PLL) was used as vector to form polyplex with mRNA and found that it was too stable to release mRNA for further gene expression,<sup>[129]</sup> whereas, using lower molecular weight PLL (3.4 kDa) improved the transfection, but it still required chloroquine.

Fusogenic peptides are also used in order to increase the transfection efficiency of PLL.<sup>[130-132]</sup> For example, Lys based reducible polycations (RPCs) were oxidatively polymerized from CK<sub>16</sub>C and formed a DNA polyplex which contained a fusogenic peptide (GLFEALLELLESLWELLLEA). This polyplex was stable in an extracellular environment and could also release DNA intracellularly for nuclear translocation.<sup>[133]</sup> Targeting ligands, such as transferrin, were also conjugated to PLL to improve the transfection efficiency.<sup>[93]</sup>

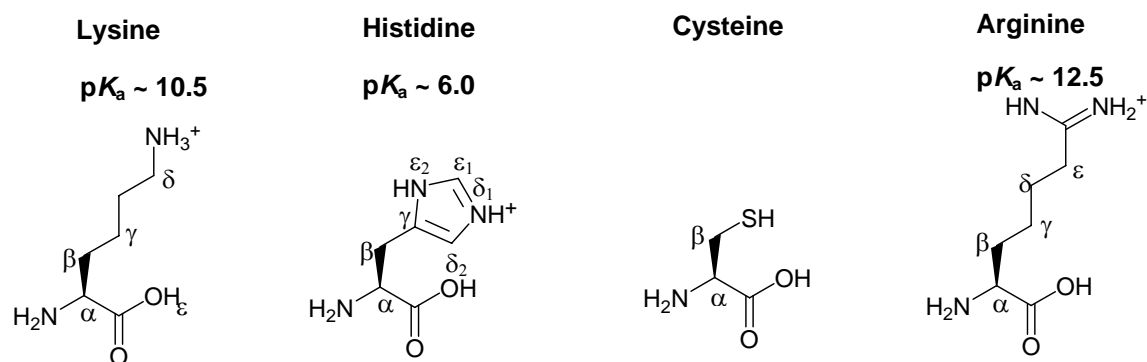


**Figure 1.16.** Chemical structures of amino acids used in peptides for gene delivery

### 1.2.2 Histidine-based peptides: Endosomal escape of DNA

An important barrier to be addressed for *in vivo* gene delivery when using positively charged peptide-DNA polyplexes is that they find it difficult to escape from the endosome before it becomes a lysosome, because there is no proton sponge mechanism. The design of fusogenic peptides in order to make polyplexes that are able to disrupt the endosome was achieved by making use of histidine. Since the  $pK_a$  of an imidazole group in the histidine side chain is approximately 6.0 (**Figure 1.16**),<sup>[134-136]</sup> it promotes buffering of endosomal pH and hence an influx of water, leading to an osmotic pressure in the endosome, leading to the endosome buffering, thus allowing the DNA polyplex to escape from the endosome into the cytoplasm (the proton sponge hypothesis).<sup>[58,137,138]</sup> Midoux and colleagues<sup>[139]</sup> designed a peptide containing several histidine residues (GLFHAI AHFIHGGWHGLIHGWYG). This peptide disrupted the endosomal membrane at a slightly acidic pH (pH 6.4). Subsequently, poly-L-histidine (Mw 11 kDa) has been utilized as a gene vector and was shown to have desirable properties for gene delivery and was nontoxic to cells.<sup>[140]</sup>

### 1.2.3 Lysine and histidine-based peptides: Extracellular binding and endosomal escape of DNA

There are many studies that focus on the combination of extracellular binding of DNA and endosomal escape of polyplexes in order to improve transfection efficiency. For instance, histidylated polylysine polyplexes show enhance transfection levels over PLL-polyplexes in the presence either of chloroquine or the fusogenic peptide.<sup>[130]</sup> N-Ac-poly(L-histidine)-graft-poly-(L-lysine) (PLH-g-PLL) (**Figure 1.17**) was synthesized in order to combine the polyplex formation efficiency of PLL and endosomolytic efficiency of PLH.<sup>[141]</sup> The PLH-g-PLL polyplex enhanced gene expression. However, chloroquine was required for reasonable levels of gene expression.

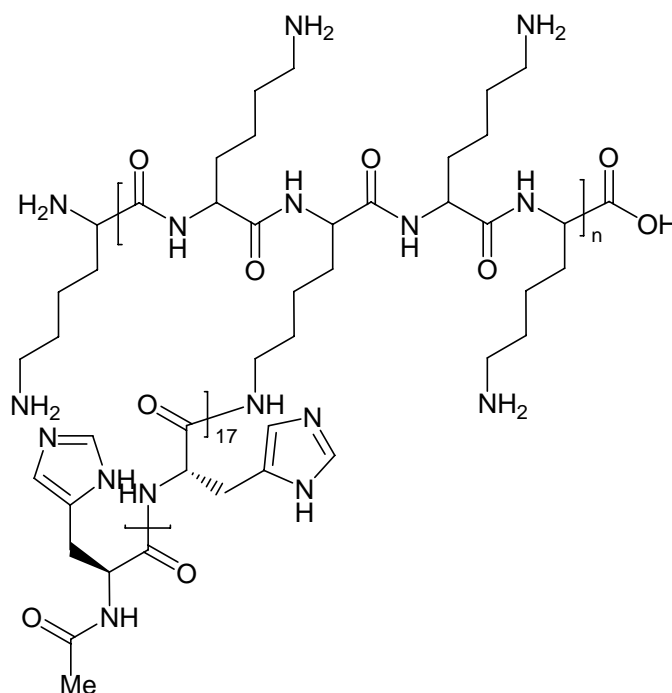


**Figure 1.17.** The structure of N-Ac-poly(L-Histidine)-graft-poly-(L-Lysine) (PLH-g-PLL)<sup>[141]</sup>

The aminated poly-L-histidine (**Figure 1.18**) has been reported to form polyplexes with DNA which led to endosomolysis.<sup>[142]</sup>

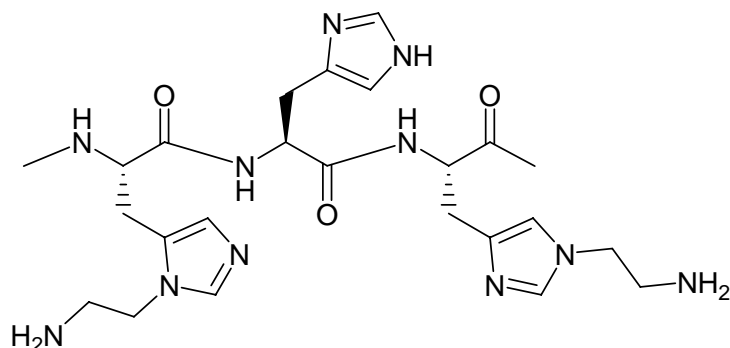


**Figure 1.18.** The aminated poly-L-histidine synthesized by Asayama and colleague.<sup>[142]</sup>

A pH-responsive histidylated oligolysine -K[K(H)KKK]<sub>5</sub>-K(H)KKC- has been designed to incorporate into ligand-liposome polyplex in order to aid in endosomal escape and DNA condensation which improved the transfection efficiency of ligand-liposome polyplex itself.<sup>[143]</sup> The combination of liposomes and branched co-polymers of histidine and lysine as vectors was shown to improve the gene expression 400-fold compared to the liposomes themselves.<sup>[120]</sup> Manickam and Oupicky<sup>[144]</sup> synthesized reducible copolypeptides (RCPPs) from bis-cysteine terminated histidine rich oligopeptide (CKHHHKHHHKC) and bis-cysteine terminated nuclear localization signal (NLS, CGAGPKKKRKVC) *via* oxidative polymerization (see section 1.2.4). These RCPPs had enhanced transfection levels of up to 10 fold over PEI.

### 1.2.4 Cysteine-based peptides: Intracellular release of DNA

The use of cysteine in biological systems has been primarily to bioconjugate molecules together *via* a covalent disulfide bond linkage.<sup>[88]</sup> The disulfide bond arises from the oxidation of two thiol (SH) groups as shown in **Figure 1.19**.

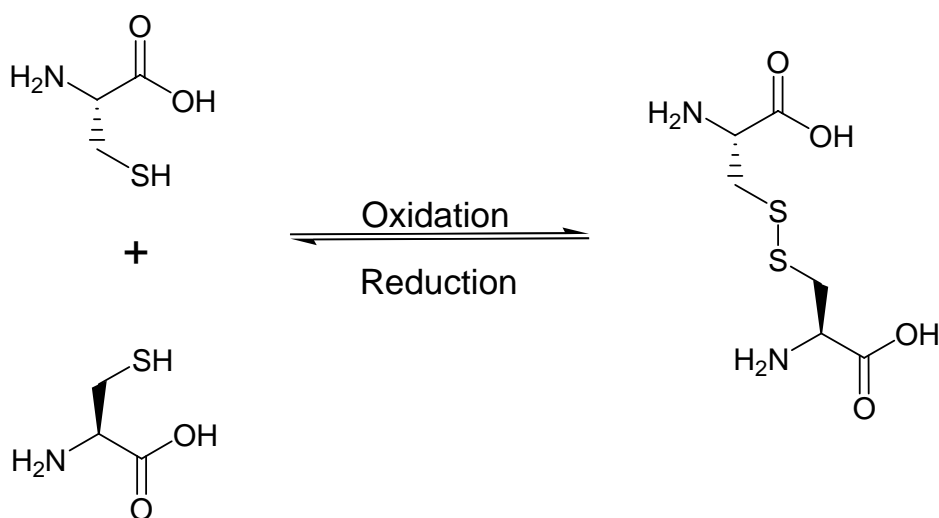


**Figure 1.19.** The formation of a disulfide bond of two cysteine residues

Polyplexes have been formed with disulfide bonds in the polymer backbone which are stabilized in the extracellular matrix, but are cleaved efficiently by high concentrations of intracellular glutathione (GSH), located in both cytoplasmic and nuclear compartments at concentrations of approximately 0.5 – 20 mM, leading to the vector degrading and efficient release of its DNA.<sup>[88,121,144]</sup> Reducible polycations (RPCs) have been synthesized from the Cys-(Lys)<sub>10</sub>-Cys by oxidative polymerization and used to form the polyplexes in combination with DOTAP which result in 187-fold higher transgene expression compared to non-reducible PLL.<sup>[89]</sup> McKenzie and colleagues<sup>[121]</sup> have also developed a reducible polycation by incorporating Lys, His and Cys residues, Cys-His-(Lys)<sub>6</sub>-His-Cys, resulting in improved gene transfection properties.

Cross-linked polymers *via* disulfide bonds were used to form the polyplexes that prevented an early dissociation of polyplexes inside the endosomes.<sup>[88,145]</sup> Thus, cross-linking peptides have been developed by inserting multiple cysteine residues into several 20 amino acid peptides (**Table 1.4**). Increased cross-linking *via* disulfide bond formation increased the stability of polyplexes and decreased the polyplex size.<sup>[88]</sup> However, the gene expression efficiency was inversely proportional to the number of the incorporated cysteine residues. In the study, peptides containing two cysteine residues (II) gave the highest gene expression.

**Table 1.4.** Cysteine containing peptides studied by Mckenzie and colleagues<sup>[88]</sup>

Name	Sequence
CWK <sub>18</sub>	Cys-Trp-Lys <sub>18</sub>
II	Cys-Trp-Lys <sub>17</sub> -Cys
III	Cys-Trp-Lys <sub>8</sub> -Cys-Lys <sub>8</sub> -Cys
IV	Cys-Trp-Lys <sub>5</sub> -Cys-Lys <sub>5</sub> -Cys-Lys <sub>5</sub> -Cys
V	Cys-Trp-Lys <sub>4</sub> -Cys-Lys <sub>3</sub> -Cys-Lys <sub>3</sub> -Cys-Lys <sub>4</sub> -Cys

### 1.2.5 Arginine-based peptides: Nuclear localisation

The study of arginine has been interesting, since the  $pK_a$  of the side chain in the arginine residue is approximately 12.5 (**Figure 1.16**), and is, therefore, fully protonated at physiological pH which promotes the electrostatic interaction with the nucleic acid. Arginine residues also play an important role as protein transduction domains (PTDs) or cell penetrating peptides (CPPs)<sup>[137,146,147]</sup> which can facilitate uptake of the protein into the cells. For example the TAT-peptide 47-57 sequence, RKKRRQRRR, is the transduction domain, or region conveying the cell penetrating properties from HIV-1, and has recently been studied

for its properties as a vector.<sup>[148]</sup> The result revealed that TAT peptides enhanced transfection activity of polyplexes and reduced cytotoxicity. However, they required chloroquine in order for the endosomal vesicles to burst. The condensation between oligomers of TAT peptides and DNA forms nanometric polyplexes. These TAT peptides improved the transfection efficiency 6-7 fold greater than poly-L-arginine.<sup>[149]</sup>

### 1.3 Essential vector features for efficient non-viral gene delivery

As described above, there are many biological barriers for non-viral gene delivery system, which result in less efficient transfection compared to viral vectors (described in **table 1.2** and associated texts). Therefore, the design of a vector needs to have several features in order to achieve an efficient gene delivery system (**Table 1.5**):

**Table 1.5. Vector features for gene delivery**

Vector feature	Function
<b>I</b>	Bind DNA extracellularly
<b>II</b>	Provide a cell targeting ligand
<b>III</b>	Cell uptake <i>via</i> endocytosis
<b>IV</b>	Provide a tunable endosomal release mechanism
<b>V</b>	Provide a degradable backbone in order that the DNA can be released once in the cytoplasm
<b>VI</b>	Provide a nuclear localization signal

As reviewed above, there are several research groups that have focused on the combination of the above features in order to design a promising vector. The summary of those combining vector features are shown in **Table 1.6**.



**Table 1.6. The summary of vector features from previous research**

Vector features	Reference
<b>I + II</b>	[93], [96]
<b>I + III + IV</b>	[60], [71], [130-132], [141-143]
<b>I + III + V</b>	[89]
<b>I + III + VI</b>	[116]
<b>I + II + III + IV</b>	[62]
<b>I + III + IV + V</b>	[88], [121]
<b>I + III + IV + V + VI</b>	[144]

## **1.4 Can we extend the design of non-viral peptide vectors?**

As summarized in **Table 1.6**, the most common vectors that have been studied combined 2-4 vector features. Therefore, a question arises as to how it might be possible to extend the capability of peptide vectors to 5 or more of the features.

In order to examine this question, we should first examine the specific roles that several amino acids adopt in peptide vectors in order that we can rationally design new vectors.

### **1.4.1 Lysine: extracellular stabilization (Vector feature I)**

Lysine has a  $pK_a$  of approximately 10.5, thus at physiological pH (~7.4), it will be almost fully protonated. Thus, this will provide a strong interaction with the phosphate anions of the DNA backbone (**Figure 1.20**) leading to extracellular stability.

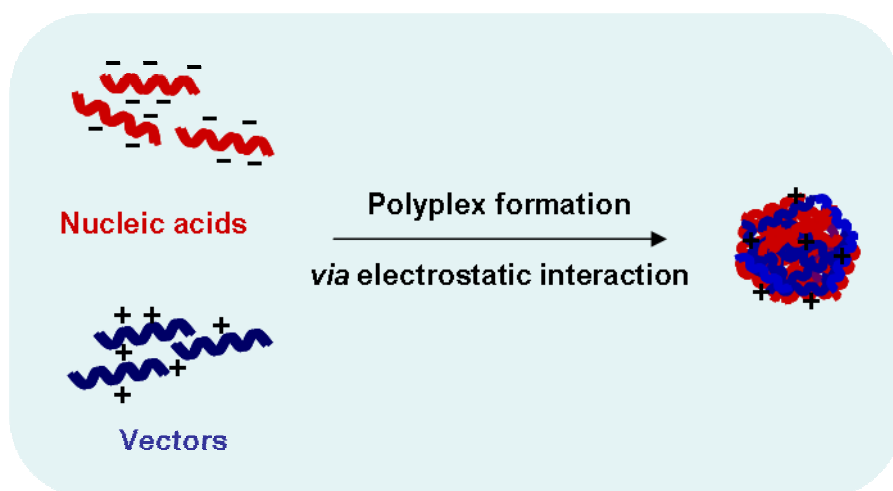


**Figure 1.20** Polyplex formation *via* electrostatic interaction between nucleic acid and vector

#### 1.4.7 Cysteine: extracellular stabilization (Vector feature I)

The terminal cysteine moieties provide functional groups that will allow polymerization of the oligopeptides *via* oxidation of the thiols (R-SH) to disulfides (R-S-S-R) to afford the intracellularly reducible polycations (RPCs). This polymerization will afford RPCs with enhanced binding to the DNA over shorter oligopeptides by virtue of the cooperativity of the extracellular binding.

#### 1.4.3 Lysine: endocytosis (Vector feature III)

The surface charge of the polyplexes formed between the DNA and the RPCs is positive, which promotes electrostatic binding with the negatively charged heparan sulfate proteoglycan of transmembrane syndecan,<sup>[101, 102]</sup> which in turn leads to internalization into cells *via* endocytosis<sup>[103,104]</sup> **Figure 1.21** illustrates the mechanism of polyplexes internalization *via* syndecan-mediated endocytosis : i) the cationic polyplex electrostatically binds to heparan sulfate proteoglycan (HSPGs) on cell surface, ii) then the cluster triggers the phosphorylation of syndecan and linker protein-mediated actin binding to cytoplasmic tail of

the syndecans, which in turn leads to actin binding to linker proteins, and iii) the constant formation of a growing network of cortical actin fibers or of tension fibers is sufficient to pull the polyplexes into cell.

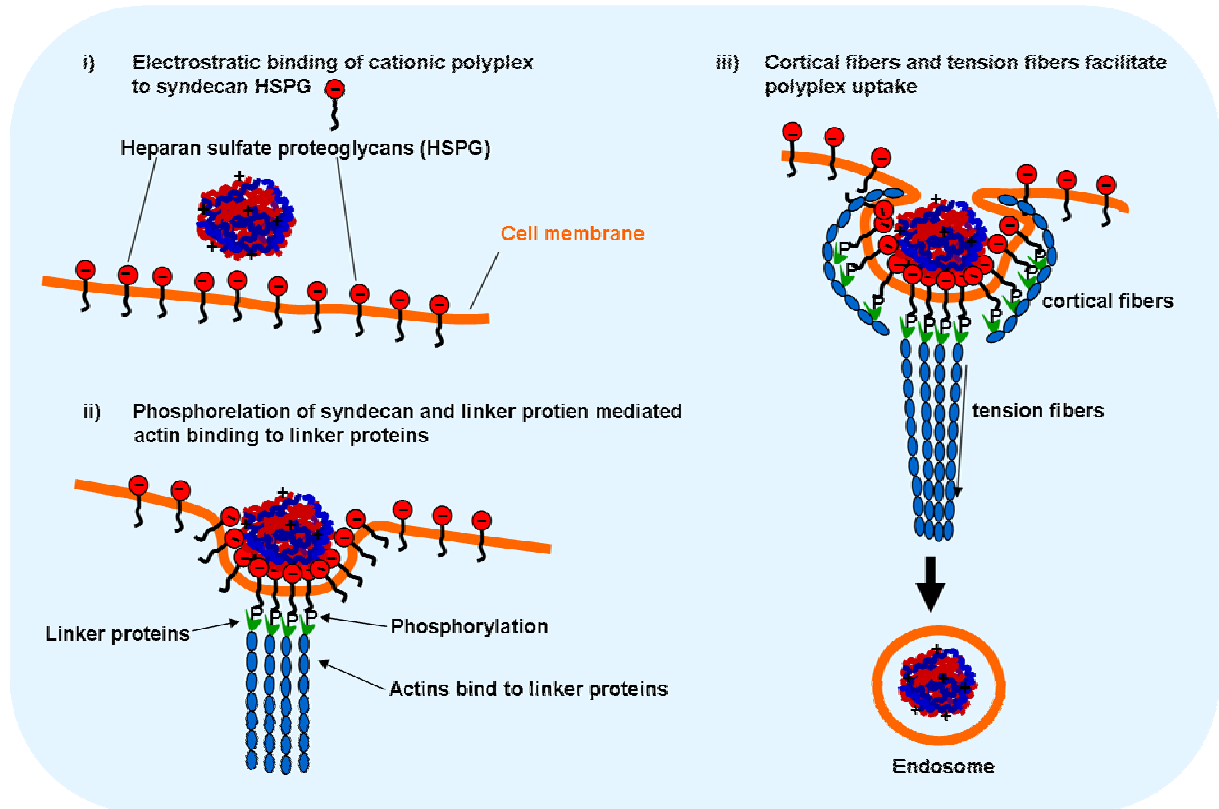


**Figure 1.21. Syndecan mediated endocytosis of cationic polyplexes**

#### **1.4.4 Histidine: endosomal release (Vector feature IV)**

Histidine has an imidazole residue with a  $pK_a$  of approximately 6, thus at physiological cell pH ( $\sim 7.4$ ) it will not be fully protonated and will have a buffering capacity when it is incorporated into the early endosome, whose pH is  $\sim 6$ . This buffering will promote endosomolysis as described earlier under the proton sponge hypothesis in section 1.1.2.2a (page 27)

### 1.4.5 Cysteine: intracellularly degradable (Vector feature V)

The disulfide bonds will be cleaved upon release from the endosome by the relatively high concentration of cytoplasmic glutathione (**Figure 1.22**).<sup>[150]</sup>

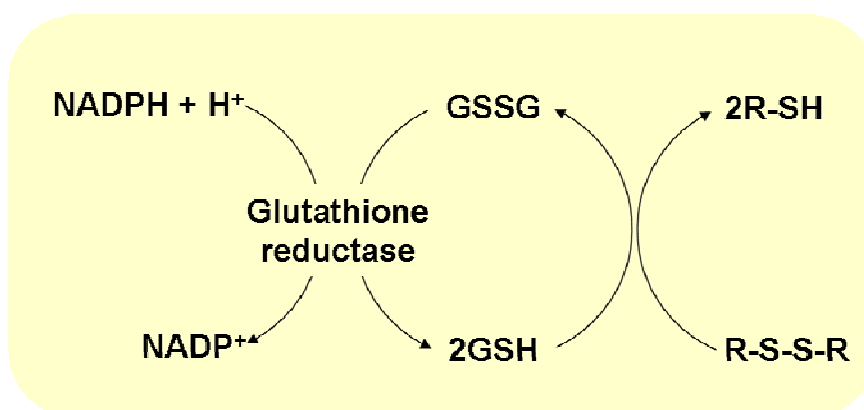


**Figure 1.22.** The disulfide bond reduction by glutathione (GSH) catalyzed by glutathione reductase using NADPH to reduce oxidized glutathione (GSSG)

The cleavage will result in only the oligopeptides binding to the DNA which will dissociate relative easily from the DNA, leaving naked DNA in the cytoplasm (**Figure 1.23**), which is free to be internalized into nucleus.

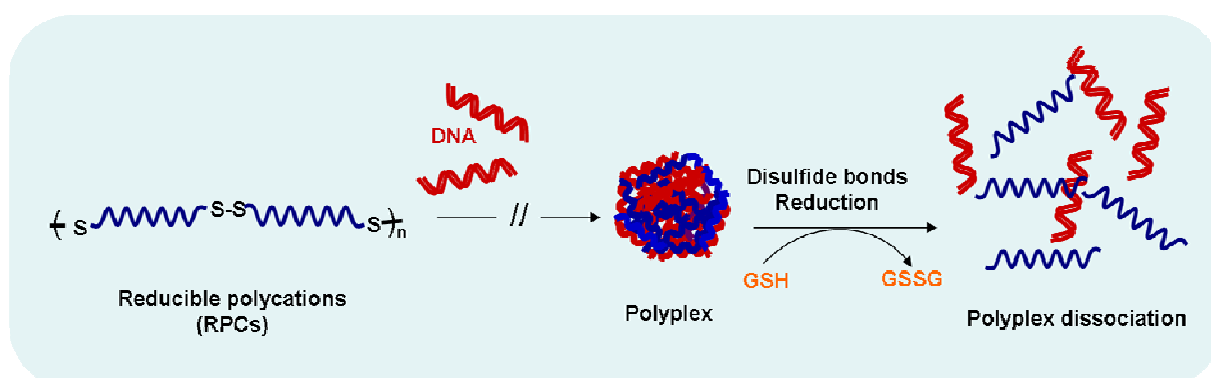


**Figure 1.23.** Polyplex dissociation by GSH to release DNA intracellularly

#### 1.4.6 Nuclear targeting signal (Vector feature VI)

Nuclear targeting signal (NLS) is the peptide that facilitates the nuclear transport through nuclear pore complexes<sup>[114-118]</sup> as described earlier in section 1.1.2.2b (page 29). Therefore, incorporation of NLS into non-viral vectors leads to promote nuclear import of transgene, which could make non-viral vector system more efficient. The most common NLS peptide derived from the simian virus 40 large tumor antigen (PKKKRKV).<sup>[115,116]</sup> In addition, TAT peptide derived from HIV-1 was also investigated as novel type of NLSs,<sup>[147]</sup> and could facilitate nuclear import faster than the SV40 NLS.<sup>[151]</sup>

### 1.5 Design of new vectors

Thus, considering the molecular design elements in the preceding sections (1.41-1.46) and considering the barriers for genes to be delivered to the cell nucleus (**Figure 1.11**), we have designed some new vectors by combining lysine, histidine and cysteine in various constitutional arrangements, and by incorporating TAT such that we could potentially have a vector with up to 5 features.

**Table 1.7** illustrates the oligopeptides which have been designed for the tasks above. They are 10 mers containing lysine (K), histidine (H), and cysteine (C). Each one is terminated by cysteine residues (referred to as bis-cysteine containing oligopeptides (2COPs)) which are 2COPs **1-6**. 2COP **1** has 8 lysine, 2COPs **2-5** have 4 lysine and 4 histidine with an increased degree of “mixing” of the constitution, 2COP **6** has 8 histidine. Peptide **7** is a tris-cysteine containing oligopeptide (3COP) with 4 lysine residues. Bis-cysteine terminating **TAT** peptide was also designed as a vector in the study.

**Table 1.7. Synthetic oligopeptides used in this study**

Oligopeptide	Structure	Oligopeptide	Structure
2COP 1 (CK <sub>8</sub> C)		2COP 5 (CKHKHKHKHC)	
2COP 2 (CK <sub>4</sub> H <sub>4</sub> C)		2COP 6 (CH <sub>8</sub> C)	
2COP 3 (CK <sub>2</sub> H <sub>2</sub> K <sub>2</sub> H <sub>2</sub> C)		3COP 7 (CK <sub>2</sub> CK <sub>2</sub> C)	
2COP 4 (CK <sub>2</sub> HKHKH <sub>2</sub> C)		TAT (CRKKRRQRRRC)	

From the oligopeptides designed in **Table 1.7**, we can synthesize the new vectors by combination of new and known strategies described in **Table 1.8**.

**Table 1.8. Strategies used in vector design and their advantage**

Strategies		Advantage	Vector features	Designed vectors				
New strategies	Chemical unit			PLL	RPC 1	Cross-linked RPCs 2-5	RPCs 2-5	RcPCs 2-5
- pK <sub>a</sub> modulation	2COPs 2-5 (degree dilution of His and Lys)	Proton sponge mechanism for endosomal escape of polyplex	<b>IV</b>	X	X	√	√	√
- Cross-linking disulfides	2COPs/3COP	Extra extracellular stability of polyplex	<b>I</b>	X	X	√	X	X
<b>Known strategies</b>	<b>Chemical unit</b>							
- Electrostatic binding with DNA	Lysine residues	-Electrostatic binding of lysine side chains to DNA to aid extracellular stability -cell uptake <i>via</i> endocytosis	<b>I, III</b>	√	√	√	√	√
- Disulfide bond backbone	Terminated cysteines	-Extracellular stability of polyplex -Intracellular reduction of DNA into cytoplasm	<b>I, V</b>	X	√	√	√	√
-NLS incorporation	TAT incorporation	Nuclear entry of DNA	<b>VI</b>	X	X	X	X	√

Section 1.6 describes in detail of hypothesis behind the strategies in term of how the various chemical molecules will control various processes during gene delivery.

## 1.6 Hypothesis behind the vector design

### 1.6.1 New strategies

#### 1.6.1.1 $pK_a$ modulation

The mixing of the position of the constitution of the amino acid in 2COPs **2-5** will provide a subtle way of modulating the  $pK_a$  of the imidazole residues. The degree of dilution of the histidine residues in the protonated lysine residues will make it increasingly more difficult for the imidazole nitrogen to become protonated, due to charge repulsion of the subphase protons by the protonated lysine residues as can be seen in **Figure 1.24a**. For –His-His-His-His- sequence (**Figure 1.24b**), it is shown that the amino groups on the imidazole ring are more easily protonated due to a lower degree of electrostatic repulsion by the distal protonated lysine residues.

Therefore, the modulation of the  $pK_a$  will provide a way to modulate the buffering capacity in the endosome (vector feature **IV**). RPCs **2-5**, *cross-linked* RPCs **2-5**, and RcPCs **2-5** (see **Table 1.8**) have buffering capacity in the endosome, thus these vectors do not require chloroquine to promote endosomal escape (**Figure 1.27 c,d and e**). On the other hand, PLL and RPC **1** that have no buffering properties and will need chloroquine to promote endosomal disruption. Hence we expect PLL and RPC **1** without CQ not to be released from the



endosome as there is no buffering capacity, and hence transfection will be poor (**Figure 1.27 a and b**).

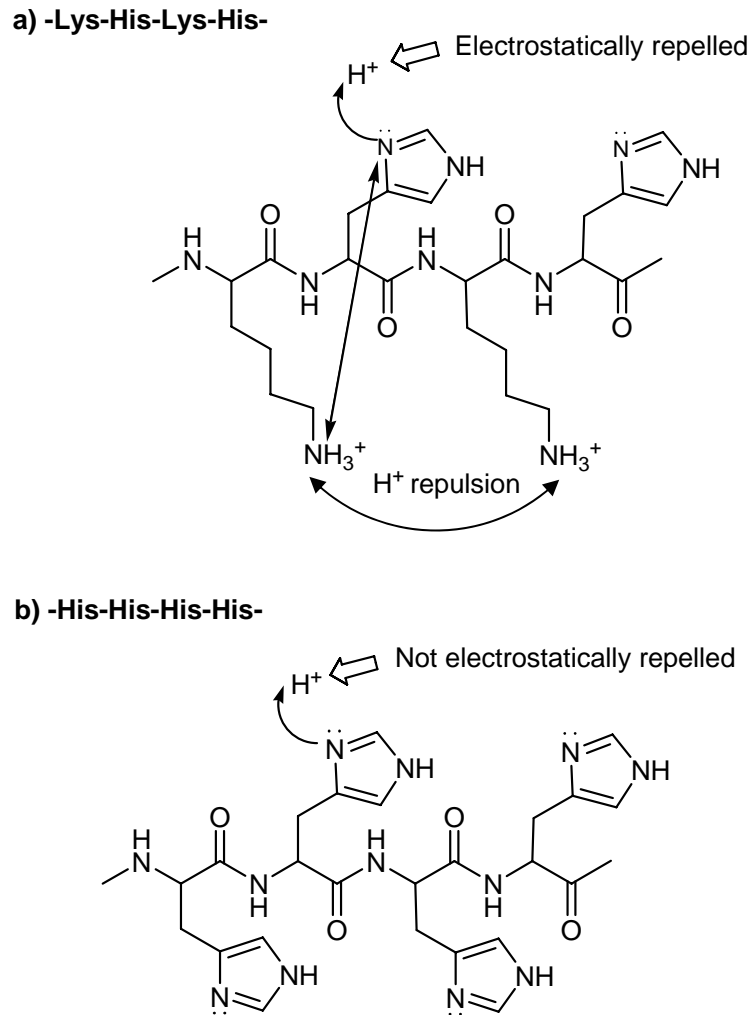


**Figure 1.24.** The proton repulsion of the lysine and histidine based sequences; a) and -Lys-His-Lys-His-  
b) -His-His-His-His-

### 1.6.1.2 Cross-linking disulfide bonds

Mckenzie and colleagues<sup>[88]</sup> developed the low molecular weight peptides (20 amino acids) by incorporating multiple cysteine residues into the peptides. After binding to plasmid DNA thiol groups of cysteine side chains spontaneously oxidize to form cross-linked disulfides

promoting extracellular stability of polyplexes. They also revealed that the cross-linked peptide polyplexes were 5-60 fold more efficient in transfection relative to uncross-linked peptide polyplexes. In addition, McKenzie and colleagues<sup>[121]</sup> revealed that using low molecular weight peptide, CK<sub>2</sub>CK<sub>2</sub>C, to condense with DNA produced large particle (1668 nm), and induced lower transfection level (10-100 fold) relative to CK<sub>8</sub>C polyplexes. However, in none of the previous publications have high molecular weight cross-linked disulfide polypeptides been used. Thus, in our study the tris-cysteine oligopeptide (3COP 7, CK<sub>2</sub>CK<sub>2</sub>C) will be used to form a *cross-linked* RPCs via disulfide bond formation (**Figure 1.25**) with the 2COPs. These cross-linking backbones will provide further extracellular stabilization of the polyplex. Therefore, in combination between cross-linking backbones and pK<sub>a</sub> modulation in *cross-linked* RPCs 2-5 vectors could result with increase efficient transfection (**Figure 1.27c**). In addition, the linear polymer RPCs will also be synthesized by oxidative polymerization of 2COPs in order that the properties of *cross-linked* RPC and linear RPC can be compared.

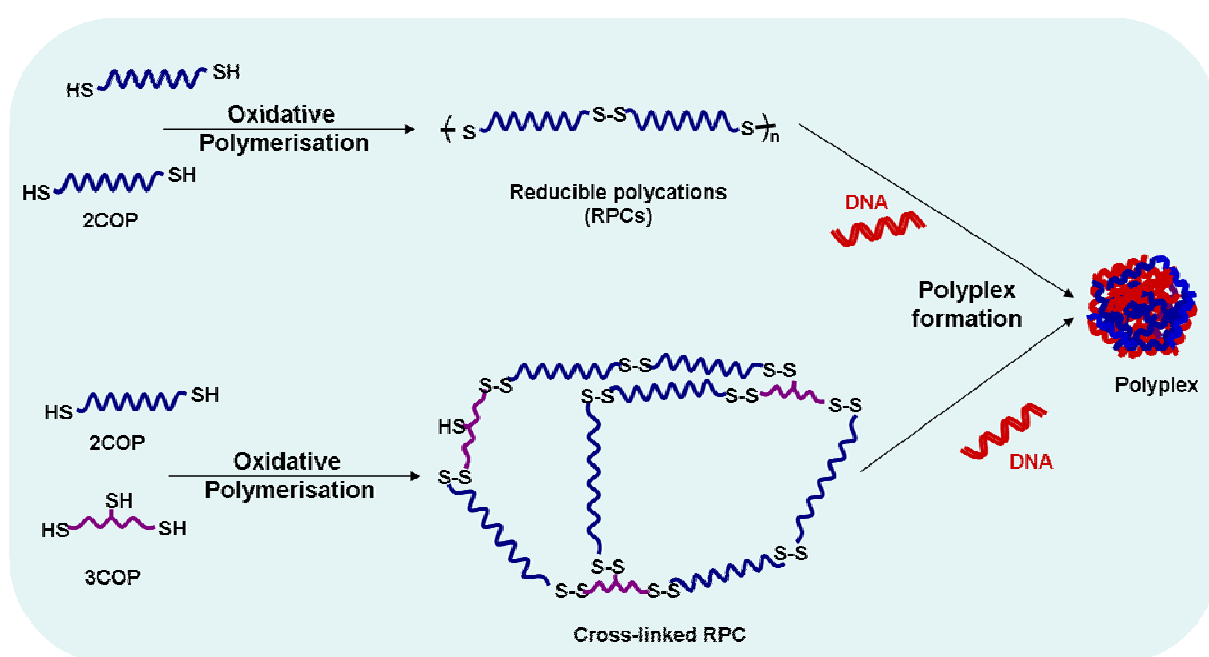


**Figure 1.25.** Polyplex formation from reducible polycations (RPCs) and *cross-linked* RPC

## 1.6.2 Known strategies

### 1.6.2.1 Electrostatic binding with DNA

The lysine residue has been widely used in peptide vectors because of the positive side chain that results upon protonation, that can bind electrostatically to the negative charged phosphate groups in DNA backbone.<sup>[89,124,127]</sup> Therefore, our designed vectors (cross-linked RPCs, RPCs, and RcPCs) which have lysine residues incorporated will bind strongly to the DNA resulting in extracellular stability of polyplexes (vector feature **I**). In addition, the cationic polyplexes will electrostatically bind to the negative groups of heparan sulfate proteoglycans on cell surface which facilitates cell uptake *via* endocytosis (vector feature **III**).

### 1.6.2.2 Disulfide bond backbone

In recent years, reducible polycations (RPCs) have been synthesized by oxidative polymerization of oligopeptides that have terminated cysteine residues.<sup>[85,89,133,152]</sup> These RPCs resulted in extracellular stability of polyplexes (vector feature **I**), as well as intracellular reduction of polyplexes leading to DNA release in the cytoplasm (vector feature **V**). Therefore, the RPCs and RcPCs are likely to provide extracellular stability and an intracellular disassembles mechanism to provide polyplexes with efficient transfection (**Figure 1.27d and e**). In contrast, PLL polyplex does not have disulfide linkage, thus, it is unable to be reduced in the cytoplasm resulting in poor transfection level (**Figure 1.27a**).

### 1.6.2.3 NLS incorporation

NLS has been widely used in non-viral vectors<sup>[115,118,144]</sup> as described previously in section 1.1.2.2b. The introduction of NLS into vectors could enhance the transfection level as the DNA is more likely to enter into nucleus in non-dividing cells (vector feature **VI**). Therefore, RcPC vectors (**Figure 1.26**) with TAT (NLS derived from HIV-1) should facilitate efficient transfection compared to other vectors that do not have TAT incorporation.

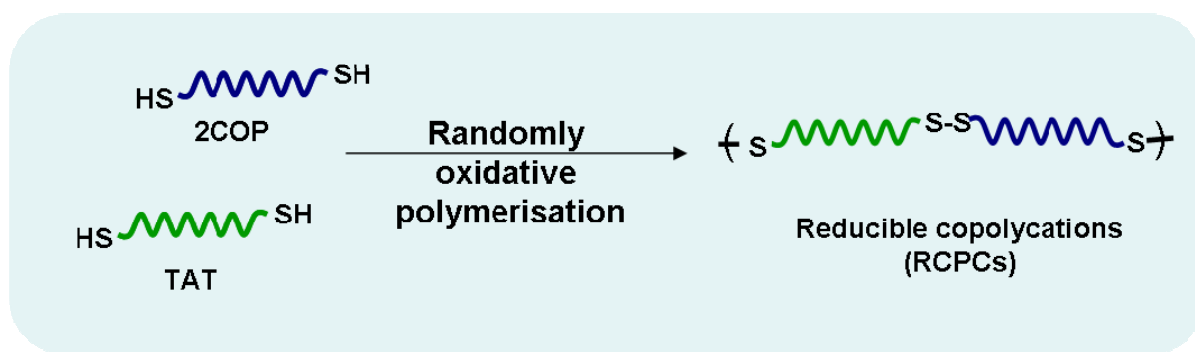


**Figure 1.26.** Reducible *copolymers* (RcPCs) synthesised by oxidative polymerisation between 2COPs and Bis-cysteine containing TAT oligopeptides

In addition, the RcPCs **2-5** contain 2COPs and TAT in order to combine the extracellular binding with DNA (**I**), cell uptake (**III**), endosomal escape (**IV**), intracellular degradability (**V**) and nuclear targeting (**VI**) could induce excellent transfection levels (**Figure 1.27e**).

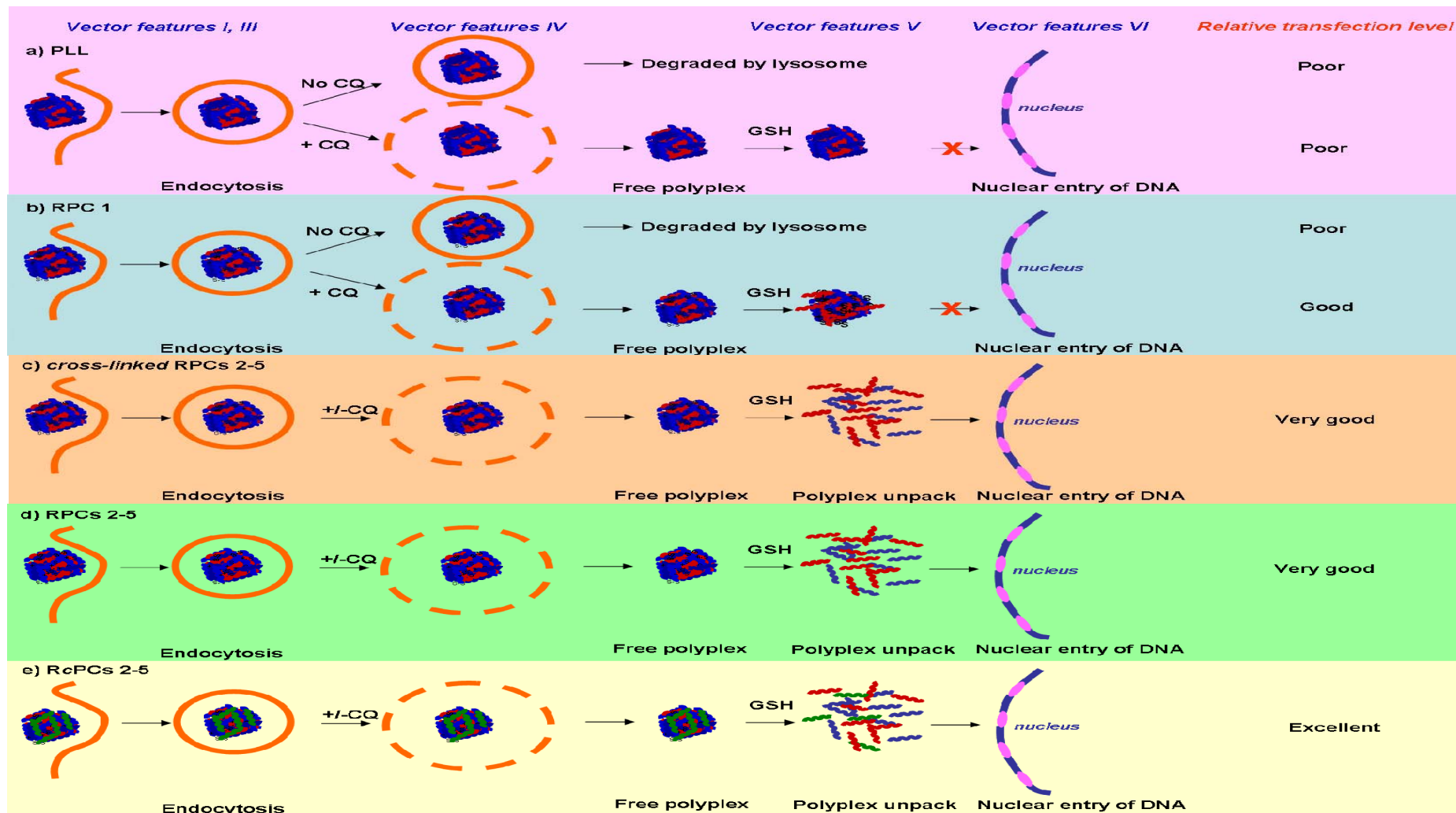


Figure 1.27. Schematic model of the transfection manner of RPCs and PLL polyplexes based on vector features I and III-VI: a) PLL, b) RPCs 1, c) cross-linked RPCs 2-5, d) RPCs 2-5 and e) RcPCs 2-5 polyplexes.

## 1.7 Overview of thesis

This PhD thesis will be divided into 4 chapters as described below:

- (i) In chapter 3, the oligopeptides (2COPs **1-6** and 3COP **7**) will be purified and characterised. The reducible polycations (RPCs **1-6**) will be synthesized from 2COPs **1-5** *via* disulfide bond formation by oxidative polymerisation. The DNA polyplexes from either RPCs or 2COPs will be produced and characterized in simulated *extra* – and *intracellularly* conditions based on vector features **I** and **III-V**. In addition, the oxidative polymerisation of the cross-linked RPCs between 2COPs and 3COP will also be studied.
  
- (ii) In chapter 4, the cell transfection of RPCs polyplexes based on vector feature **I** and **III-V** will be studied. The transfection of the RPCs polyplexes will be combined with the following compounds :
  - Chloroquine (CQ) will be added into cell lines as its ability to buffer endosome and to enhance the transfection efficiency.
  - Glutathione monoethyl ester (GSH-MEE), which is cell permeable and is converted to reduced glutathione intracellularly, will be added in order to boost intracellular GSH and enhance polypeptide vector cleavage of the disulfide bonds.
  - Buthionine sulfoximine (BSO), which is an inhibitor of intracellular GSH synthesis, will be used to deplete intracellular GSH, thus probing the reductive cleavage mechanism in the cells of the disulfide bonds.

- (iii) In chapter 5, the reducible *copoly*cations between 2COPs and TAT peptide (RcPCs) will be synthesized and characterized by randomly oxidative polymerisation in order to combine vector feature **I** and **III-V** of 2COPs and vector feature **VI** of TAT peptide.
  
- (iv) In Chapter 6, the cell transfection of RcPC polyplexes will be preformed in the same basis with Chapter 4 in order to compare with RPC polyplexes.

The transfections will be carried out in two representative cell lines, human lung carcinoma epithelial cell (A549) and mouse brain endothelial cell (bEND3). These cell lines were chosen because for therapeutic applications it is important to consider transduction of both epithelial and endothelial cells. The A549 cells are the representative of most types of common cancer, while the bEND3 cells serve as a model for the surfaces that are accessible following the bloodstream administration of the polyplexes.

PLL and PEI polyplexes at N:P 5 and 10, respectively were used as controls.

## 1.8 References

1. Watson, J.D., and Crick, F.H.C. (1953). Genetical implications of the structure of deoxyribonucleic acid. *Nature*, **171**, 964-967.
2. Slavotinek, A., and Biesecker, L.G. (2003). Genetic modifiers in human development and malformation syndromes, including chaperone proteins. *Human Molecular Genetics*, **12**, R45-50.
3. Rubanyi, G.M. (2001). The future of human gene therapy. *Molecular Aspects of Medicine*, **22**, 113-142.
4. Williams, D.A., and Orkin, S.H. (1986). Somatic gene therapy; current status and future prospects. *The Journal of Clinical Investigation*, **77**, 1053-1056.
5. Dorin, J. (1996). Somatic gene therapy. *British Medical Journal* **312**, 323-324.
6. Nielsen, T.O. (1997). Human germline gene therapy. *Mcgill Journal of Medicine*, **3**, 126-132.
7. Friedmann, T., and Roblin, R. (1972). Gene therapy for human genetic disease? *Science*, **175**, 949-955.
8. Rogers, S. (1959). Induction of arginase in rabbit epithelium by the Shope rabbit papilloma virus. *Nature*, **183**, 1815-1816.
9. Rogers, S., and Moore, M. (1963). Studies of mechanism of action of Shope rabbit papilloma virus. 1. Concerning nature of induction of arginase in infected cells. *Journal of Experimental Medicine*, **117**, 521-542.
10. Müller, H. (1987). Human gene therapy: possibilities and limitations. *Cellular and Molecular Life Sciences* **43**, 375-378.



11. Philipp, C.N., Sollinger, H.W., and Alam, T. (2003). Hepatic insulin gene therapy in insulin-dependent diabetes mellitus. *American Journal of Transplantation*, **3**, 1197-1203.
12. Lai, L.W., and Lien, Y.H.H. (1999). Homologous recombination based gene therapy. *Nephron Experimental Nephrology*, **7**, 11-14.
13. Wu, L.C., Sun, C.W., Ryan, T.M., Pawlik, K.M., Ren, J.X., and Townes, T.M. (2006). Correction of sickle cell disease by homologous recombination in embryonic stem cells. *Blood*, **108**, 1183-1188.
14. Flagler, K., Alexeev, V., Pierce, E.A., and Igoucheva, O. (2008). Site-specific gene modification by oligodeoxynucleotides in mouse bone marrow-derived mesenchymal stem cells. *Gene Therapy*, **15**, 1035-1048.
15. Bonaccorsi, L., Luciani, P., Nesi, G., Mannucci, E., Deledda, C., Dichiarà, F., Paglierani, M., Rosati, F., Masieri, L., Serni, S., Carini, M., Proietti-Pannunzi, L., Monti, S., Forti, G., Danza, G., Serio, M., and Peri, A. (2008). Androgen receptor regulation of the seladin-1/DHCR24 gene: altered expression in prostate cancer. *Laboratory Investigation*, **88**, 1049-1056.
16. Raty, J.K., Lesch, H.P., Wirth, T., and Ylä-Herttuala, S. (2008). Improving safety of gene therapy. *Current Drug Safety*, **3**, 46-53.
17. Boulaiz, H., Marchal, J.A., Prados, J., Melguizo, C., and Aranega, A. (2005). Non-viral and viral vectors for gene therapy. *Cellular and Molecular Biology*, **51**, 3-22.
18. Cohen, S.S. (1963). Biochemistry of viruses. *Annual Review of Biochemistry*, **32**, 83-&
19. El-Aneed, A. (2004). An overview of current delivery systems in cancer gene therapy. *Journal of Controlled Release*, **94**, 1-14.

20. Wei, C.M., Gibson, M., Spear, P.G., and Scolnick, E.M. (1981). Construction and isolation of a transmissible retrovirus containing the Src Gene of harvey murine sarcoma-virus and the thymidine kinase gene of herpes-simplex virus type-1. *Journal of Virology*, **39**, 935-944.
21. Coffin, J.M. (1979). Structure, replication, and recombination of retrovirus genomes - some unifying hypotheses. *Journal of General Virology*, **42**, 1-26.
22. Hermens, W.T.J.M.C., and Verhaagen, J. (1998). Viral vectors, tools for gene transfer in the nervous system. *Progress in Neurobiology*, **55**, 399-432.
23. Robbins, P.D., and Ghivizzani, S.C. (1998). Viral vectors for gene therapy. *Pharmacology and Therapeutics*, **80**, 35-47.
24. Wang, Y., and Yuan, F. (2006). Delivery of viral vectors to tumor cells: Extracellular transport, systemic distribution, and strategies for improvement. *Annals of Biomedical Engineering*, **34**, 114-127.
25. Schatzlein, A.G. (2003). Targeting of synthetic gene delivery systems. *Journal of Biomedicine and Biotechnology*, **2**, 149-158.
26. Chan, C.K., and Jans, D.A. (2002). Using nuclear targeting signals to enhance non-viral gene transfer. *Immunology and Cell Biology*, **80**, 119-130.
27. Klasse, P.J., Bron, R., and Marsh, M. (1998). Mechanisms of enveloped virus entry into animal cells. *Advanced Drug Delivery Reviews*, **34**, 65-91.
28. Lehn, P., Fabrega, S., Oudrhiri, N., and Navarro, J. (1998). Gene delivery systems: Bridging the gap between recombinant viruses and artificial vectors. *Advanced Drug Delivery Reviews*, **30**, 5-11.
29. Whittaker, G.R. (2003). Virus nuclear import. *Advanced Drug Delivery Reviews*, **55**, 733-747.

30. Pouton, C.W., and Seymour, L.W. (2001). Key issues in non-viral gene delivery. *Advanced Drug Delivery Reviews*, **46**, 187-203.
31. Khalil, I.A., Kogure, K., Akita, H., and Harashima, H. (2006). Uptake pathways and subsequent intracellular trafficking in nonviral gene delivery. *Pharmacological Reviews*, **58**, 32-45.
32. Merdan, T., Kopecek, J., and Kissel, T. (2002). Prospects for cationic polymers in gene and oligonucleotide therapy against cancer. *Advanced Drug Delivery Reviews*, **54**, 715-758.
33. Turk, M.J., Reddy, J.A., Chmielewski, J.A., and Low, P.S. (2002). Characterization of a novel pH-sensitive peptide that enhances drug release from folate-targeted liposomes at endosomal pHs. *Biochimica Et Biophysica Acta-Biomembranes*, **1559**, 56-68.
34. Tang, F.X., and Hughes, J.A. (1998). Introduction of a disulfide bond into a cationic lipid enhances transgene expression of plasmid DNA. *Biochemical and Biophysical Research Communications*, **242**, 141-145.
35. Gosselin, M.A., Guo, W.J., and Lee, R.J. (2001). Efficient gene transfer using reversibly cross-linked low molecular weight polyethylenimine. *Bioconjugate Chemistry*, **12**, 989-994.
36. Kichler, A., Leborgne, C., Coeytaux, E., and Danos, O. (2001). Polyethylenimine-mediated gene delivery: a mechanistic study. *Journal of Gene Medicine*, **3**, 135-144.
37. Kunath, K., von Harpe, A., Fischer, D., Peterson, H., Bickel, U., Voigt, K., and Kissel, T. (2003). Low-molecular-weight polyethylenimine as a non-viral vector for DNA delivery: comparison of physicochemical properties, transfection efficiency and in vivo distribution with high-molecular-weight polyethylenimine. *Journal of Controlled Release*, **89**, 113-125.

38. Boeckle, S., von Gersdorff, K., van der Piepen, S., Culmsee, C., Wagner, E., and Ogris, M. (2004). Purification of polyethylenimine polyplexes highlights the role of free polycations in gene transfer. *Journal of Gene Medicine*, **6**, 1102-1111.
39. Brus, C., Petersen, H., Aigner, A., Czubayko, F., and Kissel, T. (2004). Efficiency of polyethylenimines and polyethylenimine-graft-poly (ethylene glycol) block copolymers to protect oligonucleotides against enzymatic degradation. *European Journal of Pharmaceutics and Biopharmaceutics*, **57**, 427-430.
40. Boussif, O., Lezoualch, F., Zanta, M.A., Mergny, M.D., Scherman, D., Demeneix, B., and Behr, J.P. (1995). A versatile vector for gene and oligonucleotide transfer into cells in culture and *in vivo* - polyethylenimine. *Proceedings of the National Academy of Sciences of the United States of America*, **92**, 7297-7301.
41. Dufes, C., Uchegbu, I.F., and Schatzlein, A.G. (2005). Dendrimers in gene delivery. *Advanced Drug Delivery Reviews*, **57**, 2177-2202.
42. Stoddart, A. (2006). Gene delivery with dendrimers. *Molecular Biosystems*, **2**, B10-B10.
43. Chattoraj, D.K., Gosule, L.C., and Schellman, J.A. (1978). DNA condensation with polyamines. 2. Electron-microscopic studies. *Journal of Molecular Biology*, **121**, 327-337.
44. Gosule, L.C., and Schellman, J.A. (1976). Compact form of DNA induced by spermidine. *Nature*, **259**, 333-335.
45. Zhang, S.B., Xu, Y.M., Wang, B., Qiao, W.H., Liu, D.L., and Li, Z.S. (2004). Cationic compounds used in lipoplexes and polyplexes for gene delivery. *Journal of Controlled Release*, **100**, 165-180.
46. Felgner, P.L., Gadek, T.R., Holm, M., Roman, R., Chan, H.W., Wenz, M., Northrop, J.P., Ringold, G.M., and Danielsen, M. (1987). Lipofection - a highly efficient, lipid-

- mediated DNA-transfection procedure. *Proceedings of the National Academy of Sciences of the United States of America*, **84**, 7413-7417.
47. Simberg, D., Weisman, S., Talmon, Y., and Barenholz, Y. (2004). DOTAP (and other cationic lipids): Chemistry, biophysics, and transfection. *Critical Reviews in Therapeutic Drug Carrier Systems*, **21**, 257-317.
  48. Behr, J.P., Demeneix, B., Loeffler, J.P., and Mutul, J.P. (1989). Efficient gene-transfer into mammalian primary endocrine-cells with lipopolyamine-coated DNA. *Proceedings of the National Academy of Sciences of the United States of America*, **86**, 6982-6986.
  49. Gao, X., and Huang, L. (1991). A novel cationic liposome reagent for efficient transfection of mammalian-cells. *Biochemical and Biophysical Research Communications*, **179**, 280-285.
  50. Mahato, R.I. (2005). Water insoluble and soluble lipids for gene delivery. *Advanced Drug Delivery Reviews*, **57**, 699-712.
  51. Mahato, R.I., Rolland, A., and Tomlinson, E. (1997). Cationic lipid-based gene delivery systems: Pharmaceutical perspectives. *Pharmaceutical Research*, **14**, 853-859.
  52. Xu, Y.H., and Szoka, F.C. (1996). Mechanism of DNA release from cationic liposome/DNA complexes used in cell transfection. *Biochemistry*, **35**, 5616-5623.
  53. Wetzler, B., Byk, G., Frederic, M., Airiau, M., Blanche, F., Pitard, B., and Scherman, D. (2001). Reducible cationic lipids for gene transfer. *Biochemical Journal*, **356**, 747-756.
  54. Han, S.O., Mahato, R.I., and Kim, S.W. (2001). Water-soluble lipopolymer for gene delivery. *Bioconjugate Chemistry*, **12**, 337-345.

55. Lee, M., Rentz, J., Han, S.O., Bull, D.A., and Kim, S.W. Water-soluble lipopolymer as an efficient carrier for gene delivery to myocardium. *Gene Therapy*, **10**, 585-593.
56. Lungwitz, U., Breunig, M., Blunk, T., and Gopferich, A. (2005). Polyethylenimine-based non-viral gene delivery systems. *European Journal of Pharmaceutics and Biopharmaceutics*, **60**, 247-266.
57. Suh, J., Paik, H.J., and Hwang, B.K. (1994). Ionization of poly(ethylenimine) and poly(allylamine) at various pHs. *Bioorganic Chemistry*, **22**, 318-327.
58. Behr, J.P. (1997). The proton sponge: A trick to enter cells the viruses did not exploit. *Chimia*, **51**, 34-36.
59. Sonawane, N.D., Szoka, F.C., and Verkman, A.S. (2003). Chloride accumulation and swelling in endosomes enhances DNA transfer by polyamine-DNA polyplexes. *Journal of Biological Chemistry*, **278**, 44826-44831.
60. Min, S.H., Lee, D.C., Lim, M.J., Park, H.S., Kim, D.M., Cho, C.W., Yoon, D.Y., and Yeom, Y.I. (2006). A composite gene delivery system consisting of polyethylenimine and an amphipathic peptide KALA. *Journal of Gene Medicine*, **8**, 1425-1434.
61. Li, D., Tang, G.P., Li, J.Z., Kong, Y., Huang, H.L., Min, L.J., Zhou, J., Shen, F.P., Wang, Q.Q., and Yu, H. (2007). Dual-targeting non-viral vector based on polyethylenimine improves gene transfer efficiency. *Journal of Biomaterials Science-Polymer Edition*, **18**, 545-560.
62. Kircheis, R., Kichler, A., Wallner, G., Kurs, M., Ogris, M., Felzmann, T., Buchberger, M., and Wagner, E. (1997). Coupling of cell-binding ligands to polyethylenimine for targeted gene delivery. *Gene Therapy*, **4**, 409-418.
63. Baker, A., Saltik, M., Lehrmann, H., Killisch, I., Mautner, V., Lamm, G., Christofori, G., and Cotten, M. (1997). Polyethylenimine (PEI) is a simple, inexpensive and

- effective reagent for condensing and linking plasmid DNA to adenovirus for gene delivery. *Gene Therapy*, **4**, 773-782.
64. Wang, Y.X., Chen, P., and Shen, J.C. (2006). The development and characterization of a glutathione-sensitive cross-linked polyethylenimine gene vector. *Biomaterials*, **27**, 5292-5298.
65. Dufes, C., Uchegbu, I.F., and Schatzlein, A.G. (2005). Dendrimers in gene delivery. *Advanced Drug Delivery Reviews*, **57**, 2177-2202.
66. Lee, J.W., Kim, J.H., Kim, B.-K., Kim, J.H., Shin, W.S., and Jin, S.-H. (2006). Convergent synthesis of PAMAM dendrimers using click chemistry of azide-functionalized PAMAM dendrons. *Tetrahedron*, **62**, 9193-9200.
67. Martin, I.K., and Twyman, L.J. (2001). The synthesis of unsymmetrical PAMAM dendrimers using a divergent/divergent approach. *Tetrahedron Letters*, **42**, 1119-1121.
68. Loup, C., Zanta, M.A., Caminade, A.M., Majoral, J.P., and Meunier, B. (1999). Preparation of water-soluble cationic phosphorus-containing dendrimers as DNA transfecting agents. *Chemistry a European Journal*, **5**, 3644-3650.
69. Tomalia, D.A., Baker, H., Dewald, J., Hall, M., Kallos, G., Martin, S., Roeck, J., Ryder, J., and Smith, P. (1985). A new class of polymers - starburst-dendritic macromolecules. *Polymer Journal*, **17**, 117-132.
70. Svenson, S. (2009). Dendrimers as versatile platform in drug delivery applications. *European Journal of Pharmaceutics and Biopharmaceutics*, **71**, 445-462.
71. Haensler, J., and Szoka, F.C. (1993). Polyamidoamine cascade polymers mediate efficient transfection of cells in culture. *Bioconjugate Chemistry*, **4**, 372-379.
72. Maiti, P.K., Cagin, T., Lin, S.T., and Goddard, W.A. (2005). Effect of solvent and pH on the structure of PAMAM dendrimers. *Macromolecules*, **38**, 979-991.

73. Tomlinson, E., and Rolland, A.P. (1996). Controllable gene therapy - Pharmaceutics of non-viral gene delivery systems. *Journal of Controlled Release*, **39**, 357-372.
74. Ruponen, M., Honkakoski, P., Ronkko, S., Pelkonen, J., Tammi, M., and Urtti, A. (2003). Extracellular and intracellular barriers in non-viral gene delivery. *Journal of Controlled Release*, **93**, 213-217.
75. Davis, M.E. (2002). Non-viral gene delivery systems. *Current Opinion in Biotechnology*, **13**, 128-131.
76. Besterman, J.M., and Low, R.B. (1983). Endocytosis: a review of mechanisms and plasma membrane dynamics. *Biochemical Journal*, **210**, 1-13.
77. Owens Iii, D.E., and Peppas, N.A. (2006). Opsonization, biodistribution, and pharmacokinetics of polymeric nanoparticles. *International Journal of Pharmaceutics*, **307**, 93-102.
78. Norman, M.E., Williams, P., and Illum, L. (1992). Human serum albumin as a probe for surface conditioning (opsonization) of block copolymer-coated microspheres. *Biomaterials*, **13**, 841-849.
79. Patel, H.M. (1992). Serum opsonins and liposomes - their interaction and opsonophagocytosis. *Critical Reviews in Therapeutic Drug Carrier Systems*, **9**, 39-90.
80. Carlisle, R.C., Etrych, T., Briggs, S.S., Preece, J.A., Ulbrich, K., and Seymour, L.W. (2004). Polymer-coated polyethylenimine/DNA complexes designed for triggered activation by intracellular reduction. *Journal of Gene Medicine*, **6**, 337-344.
81. Dash, P.R., Read, M.L., Fisher, K.D., Howard, K.A., Wolfert, M., Oupicky, D., Subr, V., Strohalm, J., Ulbrich, K., and Seymour, L.W. (2000). Decreased binding to proteins and cells of polymeric gene delivery vectors surface modified with a multivalent hydrophilic polymer and retargeting through attachment of transferrin. *Journal of Biological Chemistry*, **275**, 3793-3802.



82. Fink, T.L., Klepcyk, P.J., Oette, S.M., Gedeon, C.R., Hyatt, S.L., Kowalczyk, T.H., Moen, R.C., and Cooper, M.J. (2006). Plasmid size up to 20 kbp does not limit effective *in vivo* lung gene transfer using compacted DNA nanoparticles. *Gene Therapy*, **13**, 1048-1051.
83. Lai, E., and van Zanten, J.H. (2001). Monitoring DNA/poly-L-lysine polyplex formation with time-resolved multiangle laser light scattering. *Biophysical Journal*, **80**, 864-873.
84. Petersson, K., Ilver, D., Johansson, C., and Krozer, A. (2006). Brownian motion of aggregating nanoparticles studied by photon correlation spectroscopy and measurements of dynamic magnetic properties. *Analytica Chimica Acta*, **573-574**, 138-146.
85. Read, M.L., Singh, S., Ahmed, Z., Stevenson, M., Briggs, S.S., Oupicky, D., Barrett, L.B., Spice, R., Kendall, M., Berry, M., Preece, J.A., Logan, A., and Seymour, L.W. (2005). A versatile reducible polycation-based system for efficient delivery of a broad range of nucleic acids. *Nucleic Acids Research*, **33**, e86.
86. Ogris, M., Brunner, S., Schuller, S., Kircheis, R., and Wagner, E. (1999). PEGylated DNA/transferrin-PEI complexes: reduced interaction with blood components, extended circulation in blood and potential for systemic gene delivery. *Gene Therapy*, **6**, 595-605.
87. Dash, P.R., Read, M.L., Barrett, L.B., Wolfert, M., and Seymour, L.W. (1999). Factors affecting blood clearance and *in vivo* distribution of polyelectrolyte complexes for gene delivery. *Gene Therapy*, **6**, 643-650.
88. McKenzie, D.L., Kwok, K.Y., and Rice, K.G. (2000). A potent new class of reductively activated peptide gene delivery agents. *Journal of Biological Chemistry*, **275**, 9970-9977.

89. Read, M.L., Bremner, K.H., Oupicky, D., Green, N.K., Searle, P.F., and Seymour, L.W. (2003). Vectors based on reducible polycations facilitate intracellular release of nucleic acids. *Journal of Gene Medicine*, **5**, 232-245.
90. Wang, S., and Low, P.S. (1998). Folate-mediated targeting of antineoplastic drugs, imaging agents, and nucleic acids to cancer cells. *Journal of Controlled Release*, **53**, 39-48.
91. Wagner, E., Curiel, D., and Cotten, M. (1994). Delivery of drugs, proteins and genes into cells using transferrin as a ligand for receptor-mediated endocytosis. *Advanced Drug Delivery Reviews*, **14**, 113-135.
92. Zenke, M., Steinlein, P., Wagner, E., Cotten, M., Beug, H., and Birnstiel, M.L. (1990). Receptor-mediated endocytosis of transferrin polycation conjugates - an efficient way to introduce DNA into hematopoietic cells. *Proceedings of the National Academy of Sciences of the United States of America*, **87**, 3655-3659.
93. Wagner, E., Zenke, M., Cotten, M., Beug, H., and Birnstiel, M.L. (1990). Transferrin-polycation conjugates as carriers for DNA uptake into cells. *Proceedings of the National Academy of Sciences of the United States of America*, **87**, 3410-3414.
94. Daniels, T.R., Delgado, T., Rodriguez, J.A., Helguera, G., and Penichet, M.L. (2006). The transferrin receptor part I: Biology and targeting with cytotoxic antibodies for the treatment of cancer. *Clinical Immunology*, **121**, 144-158.
95. von Gersdorff, K., Sanders, N.N., Vandenbroucke, R., De Smedt, S.C., Wagner, E., and Ogris, M. (2006). The internalization route resulting in successful gene expression depends on polyethylenimine both cell line and polyplex type. *Molecular Therapy*, **14**, 745-753.
96. Wu, G.Y., and Wu, C.H. (1988). Receptor-mediated gene delivery and expression *in vivo*. *Journal of Biological Chemistry*, **263**, 14621-14624.

97. Wattiaux, R., Laurent, N., Wattiaux-De Coninck, S., and Jadot, M. (2000). Endosomes, lysosomes: their implication in gene transfer. *Advanced Drug Delivery Reviews*, **41**, 201-208.
98. Mitra, B.N., Yasuda, T., Kobayashi, S., Saito-Nakano, Y., and Nozaki, T. (2005). Differences in morphology of phagosomes and kinetics of acidification and degradation in phagosomes between the pathogenic *Entamoeba histolytica* and the non-pathogenic *Entamoeba dispar*. *Cell Motility and the Cytoskeleton*, **62**, 84-99.
99. Bishop, N.E. (1997). An update on non-clathrin-coated endocytosis. *Reviews in Medical Virology*, **7**, 199-209.
100. Mousavi, S.A., Malerod, L., Berg, T., and Kjekken, R. (2004). Clathrin-dependent endocytosis. *Biochemical Journal*, **377**, 1-16.
101. Kim, C.W., Goldberger, O.A., Gallo, R.L., and Bernfield, M. (1994). Members of the syndecan family of heparan-sulfate proteoglycans are expressed in distinct cell-specific, tissue-specific, and development-specific patterns. *Molecular Biology of the Cell*, **5**, 797-805.
102. Bernfield, M., Gotte, M., Park, P.W., Reizes, O., Fitzgerald, M.L., Lincecum, J., and Zako, M. (1999). Functions of cell surface heparan sulfate proteoglycans. *Annual Review of Biochemistry*, **68**, 729-777.
103. Mislick, K.A., and Baldeschwieler, J.D. (1996). Evidence for the role of proteoglycans in cation-mediated gene transfer. *Proceedings of the National Academy of Sciences of the United States of America*, **93**, 12349-12354.
104. Kopatz, I., Remy, J.S., and Behr, J.P. (2004). A model for non-viral gene delivery: through syndecan adhesion molecules and powered by actin. *Journal of Gene Medicine*, **6**, 769-776.

105. Forrest, M.L., and Pack, D.W. (2002). On the kinetics of polyplex endocytic trafficking: Implications for gene delivery vector design. *Molecular Therapy*, **6**, 57-66.
106. Wiethoff, C.M., and Middaugh, C.R. (2003). Barriers to nonviral gene delivery. *Journal of Pharmaceutical Sciences*, **92**, 203-217.
107. Akinc, A., Thomas, M., Klibanov, A.M., and Langer, R. (2005). Exploring polyethylenimine-mediated DNA transfection and the proton sponge hypothesis. *Journal of Gene Medicine*, **7**, 657-663.
108. Foley, M., and Tilley, L. (1997). Quinoline antimalarials: Mechanisms of action and resistance. *International Journal for Parasitology*, **27**, 231-240.
109. Monsigny, M., Roche, A.C., Midoux, P., and Mayer, R. (1994). Glycoconjugates as carriers for specific delivery of therapeutic drugs and genes. *Advanced Drug Delivery Reviews*, **14**, 1-24.
110. Cheng, J.J., Zeidan, R., Mishra, S., Liu, A., Pun, S.H., Kulkarni, R.P., Jensen, G.S., Bellocq, N.C., and Davis, M.E. (2006). Structure-function correlation of chloroquine and analogues as transgene expression enhancers in nonviral gene delivery. *Journal of Medicinal Chemistry*, **49**, 6522-6531.
111. Tomlinson, R., Klee, M., Garrett, S., Heller, J., Duncan, R., and Brocchini, S. (2002). Pendant chain functionalized polyacetals that display pH-dependent degradation: A platform for the development of novel polymer therapeutics. *Macromolecules*, **35**, 473-480.
112. Tomlinson, R., Heller, J., Brocchini, S., and Duncan, R. (2003). Polyacetal-doxorubicin conjugates designed for pH-dependent degradation. *Bioconjugate Chemistry*, **14**, 1096-1106.
113. Pouton, C.W., Wagstaff, K.M., Roth, D.M., Moseley, G.W., and Jans, D.A. (2007). Targeted delivery to the nucleus. *Advanced Drug Delivery Reviews*, **59**, 698-717.

114. Stewart, M. (2007). Molecular mechanism of the nuclear protein import cycle. *Nature Reviews Molecular Cell Biology*, **8**, 195-208.
115. Zanta, M.A., Belguise-Valladier, P., and Behr, J.P. (1999). Gene delivery: A single nuclear localization signal peptide is sufficient to carry DNA to the cell nucleus. *Proceedings of the National Academy of Sciences of the United States of America*, **96**, 91-96.
116. Bremner, K.H., Seymour, L.W., Logan, A., and Read, M.L. (2004). Factors influencing the ability of nuclear localization sequence peptides to enhance nonviral gene delivery. *Bioconjugate Chemistry*, **15**, 152-161.
117. Pante, N., and Aebi, U. (1996). Toward the molecular dissection of protein import into nuclei. *Current Opinion in Cell Biology*, **8**, 397-406.
118. Collins, E., Birchall, J.C., Williams, J.L., and Gumbleton, M. (2007). Nuclear localisation and pDNA condensation in non-viral gene delivery. *Journal of Gene Medicine*, **9**, 265-274.
119. Plank, C., Oberhauser, B., Mechtler, K., Koch, C., and Wagner, E. (1994). The influence of endosome disruptive peptides on gene transfer using synthetic virus-like gene transfer Systems. *Journal of Biological Chemistry*, **269**, 12918-12924.
120. Chen, Q.R., Zhang, L., Stass, S.A., and Mixson, A.J. (2001). Branched co-polymers of histidine and lysine are efficient carriers of plasmids. *Nucleic Acids Research*, **29**, 1334-1340.
121. McKenzie, D.L., Smiley, E., Kwok, K.Y., and Rice, K.G. (2000). Low molecular weight disulfide cross-linking peptides as nonviral gene delivery carriers. *Bioconjugate Chemistry*, **11**, 901-909.
122. Cho, Y.W., Kim, J.D., and Park, K. (2003). Polycation gene delivery systems: escape from endosomes to cytosol. *Journal of Pharmacy and Pharmacology*, **55**, 721-734.

123. Leng, M., and Felsenfeld, G. (1966). The preferential interactions of polylysine and polyarginine with specific base sequences in DNA. *Proceedings of the National Academy of Sciences of the United States of America*, **56**, 1325-1332.
124. Zauner, W., Ogris, M., and Wagner, E. (1998). Polylysine-based transfection systems utilizing receptor-mediated delivery. *Advanced Drug Delivery Reviews*, **30**, 97-113.
125. Vermeersch, H., and Remon, J.P. (1994). Immunogenicity of poly-D-lysine, a potential polymeric drug carrier. *Journal of Controlled Release*, **32**, 225-229.
126. Ward, C.M., Read, M.L., and Seymour, L.W. (2001). Systemic circulation of poly(L-lysine)/DNA vectors is influenced by polycation molecular weight and type of DNA: differential circulation in mice and rats and the implications for human gene therapy. *Blood*, **97**, 2221-2229.
127. Wolfert, M.A., and Seymour, L.W. (1996). Atomic force microscopic analysis of the influence of the molecular weight of poly(L)lysine on the size of polyelectrolyte complexes formed with DNA. *Gene Therapy*, **3**, 269-273.
128. Wolfert, M.A., Dash, P.R., Nazarova, O., Oupicky, D., Seymour, L.W., Smart, S., Strohmalm, J., and Ulbrich, K. (1999). Polyelectrolyte vectors for gene delivery: Influence of cationic polymer on biophysical properties of complexes formed with DNA. *Bioconjugate Chemistry*, **10**, 993-1004.
129. Bettinger, T., Carlisle, R.C., Read, M.L., Ogris, M., and Seymour, L.W. (2001). Peptide-mediated RNA delivery: a novel approach for enhanced transfection of primary and post-mitotic cells. *Nucleic Acids Research*, **29**, 3882-3891.
130. Midoux, P., and Monsigny, M. (1999). Efficient gene transfer by histidylated polylysine pDNA complexes. *Bioconjugate Chemistry*, **10**, 406-411.

131. Zhang, X.H., Sawyer, G.J., Dong, X.B., Qiu, Y., Collins, L., and Fabre, J.W. (2003). The *in vivo* use of chloroquine to promote non-viral gene delivery to the liver *via* the portal vein and bile duct. *Journal of Gene Medicine*, **5**, 209-218.
132. Erbacher, P., Roche, A.C., Monsigny, M., and Midoux, P. (1996). Putative role of chloroquine in gene transfer into a human hepatoma cell line by DNA lactosylated polylysine complexes. *Experimental Cell Research*, **225**, 186-194.
133. Parker, A.L., Eckley, L., Singh, S., Preece, J.A., Collins, L., and Fabre, J.W. (2007). (LYS)(16)-based reducible polycations provide stable polyplexes with anionic fusogenic peptides and efficient gene delivery to post mitotic cells. *Biochimica Et Biophysica Acta-General Subjects*, **1770**, 1331-1337.
134. Gasparovic, C., Barba, I., Born, J., Barton, S., Arus, C., and Mann, P. (1998). A study of imidazole-based nuclear magnetic resonance probes of cellular pH. *Analytical Biochemistry*, **261**, 64-72.
135. Uster, P.S., and Deamer, D.W. (1985). pH-dependent fusion of liposomes using titratable polycations. *Biochemistry*, **24**, 1-8.
136. Wang, C.Y., and Huang, L. (1984). Polyhistidine mediates an acid-dependent fusion of negatively charged liposomes. *Biochemistry*, **23**, 4409-4416.
137. Cho, Y.W., Kim, J.D., and Park, K. (2003). Polycation gene delivery systems: escape from endosomes to cytosol. *Journal of Pharmacy and Pharmacology*, **55**, 721-734.
138. Pichon, C., Roufai, M.B., Monsigny, M., and Midoux, P. (2000). Histidylated oligolysines increase the transmembrane passage and the biological activity of antisense oligonucleotides. *Nucleic Acids Research*, **28**, 504-512.
139. Midoux, P., Kichler, A., Boutin, V., Maurizot, J.C., and Monsigny, M. (1998). Membrane permeabilization and efficient gene transfer by a peptide containing several histidines. *Bioconjugate Chemistry*, **9**, 260-267.

140. Daniel W. Pack, D.P.R.L. (2000). Design of imidazole-containing endosomolytic biopolymers for gene delivery. *Biotechnology and Bioengineering*, **67**, 217-223.
141. Bennis, J.M., Choi, J.S., Mahato, R.I., Park, J.S., and Kim, S.W. (2000). pH-Sensitive cationic polymer gene delivery vehicle: N-Ac-poly(L-histidine)-graft-poly(L-lysine) comb shaped polymer. *Bioconjugate Chemistry*, **11**, 637-645.
142. Asayama, S., Sekine, T., Hamaya, A., Kawakami, H., and Nagaoka, S. (2005). Poly(L-histidine) with several aminoethyl groups for a new pH-sensitive DNA carrier. *Polymers for Advanced Technologies*, **16**, 567-570.
143. Yu, W., Pirollo, K.F., Yu, B., Rait, A., Xiang, L.M., Huang, W.Q., Zhou, Q., Ertem, G., and Chang, E.H. (2004). Enhanced transfection efficiency of a systemically delivered tumor-targeting immunolipoplex by inclusion of a pH-sensitive histidylated oligolysine peptide. *Nucleic Acids Research*, **32**, e48.
144. Manickam, D.S., and Oupicky, D. (2006). Multiblock reducible copolypeptides containing histidine-rich and nuclear localization sequences for gene delivery. *Bioconjugate Chemistry*, **17**, 1395-1403.
145. Trubetskoy, V.S., Budker, V.G., Hanson, L.J., Slattum, P.M., Wolff, J.A., and Hagstrom, J.E. (1998). Self-assembly of DNA-polymer complexes using template polymerization. *Nucleic Acids Research*, **26**, 4178-4185.
146. Tung, C.H., and Weissleder, R. (2003). Arginine containing peptides as delivery vectors. *Advanced Drug Delivery Reviews*, **55**, 281-294.
147. Truant, R., and Cullen, B.R. (1999). The arginine-rich domains present in human immunodeficiency virus type 1 TAT and Rev function as direct importin beta-dependent nuclear localization signals. *Molecular and Cellular Biology*, **19**, 1210-1217.



148. Manickam, D.S., Bisht, H.S., Wan, L., Mao, G.Z., and Oupicky, D. (2005). Influence of TAT-peptide polymerization on properties and transfection activity of TAT/DNA polyplexes. *Journal of Controlled Release*, **102**, 293-306.
149. Rudolph, C., Plank, C., Lausier, J., Schillinger, U., Muller, R.H., and Rosenecker, J. (2003). Oligomers of the arginine-rich motif of the HIV-1 TAT protein are capable of transferring plasmid DNA into cells. *Journal of Biological Chemistry*, **278**, 11411-11418.
150. Meister, A. (1988). Glutathione metabolism and its selective modification. *The Journal of Biological Chemistry*, **263**, 17205-17208.
151. Nitin, N., LaConte, L., Rhee, W., and Bao, G. (2009). TATpeptide is capable of importing large nanoparticles across nuclear membrane in digitonin permeabilized cells. *Annals of Biomedical Engineering*, 1-10.
152. Stevenson, M., Ramos-Perez, V., Singh, S., Soliman, M., Preece, J.A., Briggs, S.S., Read, M.L., and Seymour, L.W. (2008). Delivery of siRNA mediated by histidine-containing reducible polycations. *Journal of Controlled Release*, **130**, 46-56.

# **CHAPTER 2**

## **Materials and Methods**

# CONTENTS

List of Figures

List of Tables

## 2 MATERIALS AND METHODS

<b>2.1 Suppliers of materials</b>	<b>79</b>
<b>2.2 Source of nucleic acids, oligopeptides and cell lines</b>	<b>79</b>
2.2.1 Source of nucleic acids	79
2.2.2 Source of oligopeptides	80
2.2.3 Source of cell lines	80
<b>2.3 Oligopeptide purification and characterization</b>	<b>81</b>
<b>2.4 p<i>K</i><sub>a</sub> determination of oligopeptides</b>	<b>86</b>
<b>2.5 Reducible polycations (RPCs) formation</b>	<b>87</b>
2.5.1 Oxidative polymerisation to form RPCs	87
2.5.2 Formation of <i>cross-linked</i> RPCs	88
2.5.3 Formation of reducible <i>copolypeptides</i> (RcPCs) and reducible polyTAT (RP-TAT)	89
2.5.4 Gel Permeation Chromatography (GPC)	90
2.5.5 Polymer purification	90
2.5.6 Polydispersity index (PDI) of polycations	91
<b>2.6 Amino acid analysis of RcPCs</b>	<b>92</b>
<b>2.7 Formation of polyplexes</b>	<b>93</b>
2.7.1 Calculation of charge ratio	93
2.7.2 Formation of polyplexes	94
<b>2.8 Physicochemical characterisation of polyplexes</b>	<b>94</b>
2.8.1 Analysis of polyplex diameter by photon correlation spectroscopy (PCS)	94
2.8.2 Analysis of polyplex surface charge by zeta potential	95
2.8.3 Atomic force microscopy	95
2.8.4 Agarose gel electrophoresis of DNA	96
2.8.5 Gel shift assay	96
2.8.5.1 Polyaspatic acid assay	96
2.8.5.2 Glutathione and NaCl assay	97
<b>2.9 Cell culture</b>	<b>97</b>

2.9.1	Maintainance of established cell lines	98
2.9.2	Determination of viable cell number	98
<b>2.10</b>	<b>Biological studies of polyplexes</b>	<b>99</b>
2.10.1	Cell transfection <i>in vitro</i>	99
2.10.2	Luciferase assay	100
2.10.3	Advanced protein assay	100
2.10.4	MTS cell proliferation assay	101
2.10.5	Intracellular glutathione analysis	102
<b>2.11</b>	<b>Expression of data</b>	<b>103</b>

## List of Figures

Figure 2.1.	Map of pCMV-Luc (5.9 kb)	80
Figure 2.2.	Structures of lysine and histidine	86
Figure 2.3.	$pK_a$ determination by plotting the change of chemical shift against the pH values	87
Figure 2.4.	PLL standard plotted between Log MW and GPC retention time	90
Figure 2.5.	Amino acid standard at $200 \text{ nmol ml}^{-1}$ (EZ:faast kits, phenomenex, UK) run with GC	92
Figure 2.6.	Amino acid standard plotted between the concentration of amino acid and the peak area obtained from GC	93
Figure 2.7.	BSA standard plotted between BSA concentration and absorbance	101

## List of Tables

Table 2.1.	Oligopeptides used in this work	81
Table 2.2.	Specific masses and volumes of peptides and reagents used in oxidative polymerization to synthesize RPCs	88
Table 2.3.	Specific masses and volumes of peptides and reagents used in oxidative polymerization to synthesize RP-TAT and RcPCs	89

## 2 MATERIALS AND METHODS

### *Abstract*

*In this chapter the experimental principles and procedures used during the course of this thesis are described. The techniques employed ranged from chemical characterization of synthesised peptides, formation of reducible polycations (RPCs) and reducible copolycations (RcPCs) and their DNA polyplexes through to determination of gene transfection studies of RPCs- and RcPCs-based vectors in endothelial (bEND3) and epithelial (A549) cell lines.*

### 2.1 Suppliers of materials

All materials were purchased from Sigma-Aldrich, Fisher Scientific or Applied Biosystems, in the UK unless otherwise stated. All solvents were laboratory reagent grade or anhydrous, with the exception for HPLC analysis, where HPLC grade solvents were used. All water was distilled, followed by purification to 18 M $\Omega$ .cm using an Elga water purifier.

### 2.2 Source of nucleic acids, oligopeptides and cell lines

#### 2.2.1 Source of nucleic acid

The expression vector used in all of the transfection studies was pCMV-Luc, a luciferase gene expression plasmid that contains CMV promoter and enhancer regions (**Figure 2.1**). Plasmid DNA was grown in *Escherichia coli*, and all nucleic acids were amplified by standard techniques followed by purification using preparation kits (Qiagen, Crawley, UK) or otherwise stated, and finally stored at -18°C in appropriate aliquot concentrations (1.2 mg/ml)

prior to use. The concentration and purity of DNA was checked on a spectrophotometer at  $A_{260}/A_{280}$  absorbance wavelengths.

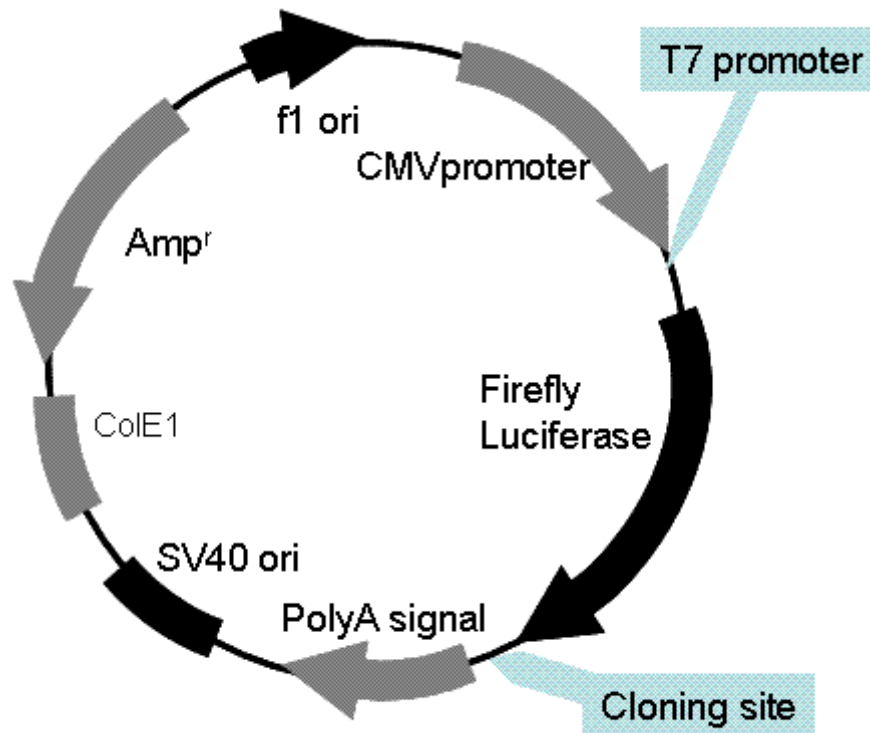


**Figure 2.1.** Map of pCMV-Luc (5.9 kb)

### 2.2.2 Source of oligopeptides

All of the oligopeptides were synthesized by Alta Biosciences (Birmingham, UK) and Peptide protein research Ltd (Wickham, UK) using standard Fmoc method. Oligopeptides used in the studies are shown in **Table 2.1**.

### 2.2.3 Source of cell lines

A549 (human lung carcinoma cells) and bEND3 (mouse brain carcinoma cells) were used in this study and were obtained from ATCC unless otherwise stated. Both cell lines were



maintained and grown in Dulbecco's modified Eagles media (DMEM, Gibco-BRL, Paisley, UK) supplemented with 2 mM L-glutamine and 10 % foetal calf serum (FCS). The media was supplemented with penicillin and streptomycin to prevent bacterial contamination of the cell lines

**Table 2.1 Oligopeptides used in this work**

Oligopeptide	Sequence <sup>a</sup>	Calculated
		Mass (g mol <sup>-1</sup> ) <sup>b</sup>
2COPs (bis-cysteine containing oligopeptides)		
<b>1</b>	CK <sub>8</sub> C	1249.70
<b>2</b>	CK <sub>4</sub> H <sub>4</sub> C	1285.56
<b>3</b>	CK <sub>2</sub> H <sub>2</sub> K <sub>2</sub> H <sub>2</sub> C	1285.56
<b>4</b>	CK <sub>2</sub> HKHKH <sub>2</sub> C	1285.56
<b>5</b>	CKHKHKHKHC	1285.56
<b>6</b>	CH <sub>8</sub> C	1321.43
<b>TAT</b>	CRKKRRQRRRC	1545.10
3COP (tris-cysteine containing oligopeptides)		
<b>7</b>	CK <sub>2</sub> CK <sub>2</sub> C	839.42

<sup>a</sup> C = Cysteine, K = Lysine, H = Histidine, R = Arginine, Q = Glutamine

<sup>b</sup> Molecular weight from the calculation

### 2.3 Oligopeptide purification and characterization

The crude oligopeptides **1-7** and TAT were purified by preparative RP-HPLC. Briefly, all crude peptides were analyzed by analytical RP-HPLC eluted with the gradient 0-100% of MeCN/water (60:40) plus 0.05% TFA for 60 minutes. The methods used in analytical RP-HPLC were then written separately for separating all peaks for each oligopeptide sample.

Analytical RP-HPLC runs were performed on a Luna (Phenomenex), C<sub>18</sub>, 250 mm × 4.6 mm ID, with 10 μm pore size column. The crude oligopeptides (~1mg) were dissolved in water (100 μl) and a 10 μl aliquot was injected at 1.0 ml/min flow rate and the UV absorbance at 210 nm was monitored. After finding the suitable method, all fractions were collected and their mass was determined by ElectroSpray Mass Spectrometry (TOF-ESI MS, Micromass, UK). Preparative RP-HPLC (Phenomenex), C<sub>18</sub> with 250 mm × 21.2 mm ID and 10 μm pore size, was utilized for oligopeptide purification. An aqueous solution of the crude oligopeptides (20 mg in 700 μl of water) were injected onto the column using of MeCN plus 0.05% TFA as an elution solvent at 10 ml/min flow (see below). The methods applied for purifying oligopeptides were those used in analytical HPLC. Fractions of the oligopeptides were collected, concentrated by rotary evaporation, lyophilized, purged with nitrogen or helium and stored dry at -20°C. The lyophilized samples were then analyzed by ESI-MS. The structures of the purified oligopeptides were determined using <sup>1</sup>H NMR 500 MHz (Bruker AC500) using deuterated solvents and the residual solvent as the lock. Purity of purified peptides was further analyzed by analytical RP-HPLC (preparative HPLC of crude peptides, analytical HPLC and <sup>1</sup>H NMR of purified peptides are shown in appendix).

Dr. Parvez Iqbal and Dr. Neil Spencer (School of Chemistry, University of Birmingham) characterized the 2COPs and TAT by <sup>1</sup>H NMR.

### **2COP 1 (CK<sub>8</sub>C)**

Preparative HPLC eluting time: ~24 minutes with MeCN (1%) plus TFA (0.05%) as an elution solvent at 10 ml/min flow rate for 60 minutes

Mass (g mol<sup>-1</sup>): 1249.9 [M]<sup>+</sup>, 625.4 [M+H]<sup>+2</sup>, 417.3 [M+H]<sup>+3</sup>

$^1\text{H}$  NMR  $\delta$  (ppm) ( $\text{D}_2\text{O}$ ): 4.61 (t,  $J = 5.23\text{Hz}$ , 1H,  $-\text{CO}-\underline{\text{CH}}-\text{N}-$ ), 4.36-4.24 (m, 9H,  $-\text{CO}-\underline{\text{CH}}-\text{N}-$ ), 2.98 (t,  $J = 6.99\text{ Hz}$ , 20H,  $\text{CH}-\text{C}_3\text{H}_6-\underline{\text{CH}}_2-\text{NH}_2$ ,  $-\underline{\text{CH}}_2-\text{SH}$ ), 1.79-1.66 (m, 32H,  $\text{CH}-\underline{\text{CH}}_2-\text{CH}_2-\text{CH}_2-\text{NH}_2$ ,  $\text{CH}-\text{CH}_2-\text{CH}_2-\underline{\text{CH}}_2-\text{CH}_2-\text{NH}_2$ ), 1.45-1.42 (m, 16H,  $\text{CH}-\text{CH}_2-\underline{\text{CH}}_2-\text{CH}_2-\text{CH}_2-\text{NH}_2$ )

### 2COP 2 ( $\text{CK}_4\text{H}_4\text{C}$ )

Preparative HPLC eluting time:  $\sim 35$  minutes with the gradient of MeCN (0-5%) plus TFA (0.05%) for the first 30 minutes, and with MeCN+TFA (5%) for further 10 minutes as an elution solvent at 10 ml/min flow rate

Mass ( $\text{g mol}^{-1}$ ): 1285.9  $[\text{M}]^+$ , 643.4  $[\text{M}+\text{H}]^{+2}$ , 429.3  $[\text{M}+\text{H}]^{+3}$

$^1\text{H}$  NMR  $\delta$  (ppm) ( $\text{D}_2\text{O}$ ): 8.63-8.61 (m, 4H, Im,  $-\text{N}=\underline{\text{CH}}-\text{NH}-$ ), 7.32-7.27 (m, 4H, Im,  $-\text{C}-\text{CH}-\text{N}-$ ), 4.69-4.63 (m, 4H,  $-\text{CO}-\underline{\text{CH}}-\text{N}-$ ), 4.54 (t, 1H,  $J = 5.73\text{ Hz}$ ,  $-\text{CO}-\underline{\text{CH}}-\text{N}-$ ), 4.35 (t,  $J = 5.73\text{ Hz}$ , 1H,  $-\text{CO}-\underline{\text{CH}}-\text{N}-$ ), 4.33-4.21 (m, 4H,  $-\text{CO}-\underline{\text{CH}}-\text{N}-$ ), 3.21-3.10 (m, 10H,  $-\text{NH}-\text{CH}-\underline{\text{CH}}_2-$ ,  $-\underline{\text{CH}}_2-\text{SH}$ ), 3.07-2.92 (m, 10H,  $\text{CH}-\text{C}_3\text{H}_6-\underline{\text{CH}}_2-\text{NH}_2$ ,  $-\underline{\text{CH}}_2-\text{SH}$ ), 1.74-1.66 (m, 16H,  $\text{CH}-\underline{\text{CH}}_2-\text{CH}_2-\text{CH}_2-\text{NH}_2$ ,  $\text{CH}-\text{CH}_2-\text{CH}_2-\underline{\text{CH}}_2-\text{CH}_2-\text{NH}_2$ ), 1.45-1.38 (m, 8H,  $\text{CH}-\text{CH}_2-\underline{\text{CH}}_2-\text{CH}_2-\text{CH}_2-\text{NH}_2$ )

### 2COP 3 ( $\text{CK}_2\text{H}_2\text{K}_2\text{H}_2\text{C}$ )

Preparative HPLC eluting time:  $\sim 32-34$  minutes with MeCN (3%) plus TFA (0.05%) as an elution solvent at 10 ml/min flow rate for 50 minutes

Mass ( $\text{g mol}^{-1}$ ): 1285.7  $[\text{M}]^+$ , 643.3  $[\text{M}+\text{H}]^{+2}$ , 429.2  $[\text{M}+\text{H}]^{+3}$

$^1\text{H}$  NMR  $\delta$  (ppm) ( $\text{D}_2\text{O}:\text{H}_2\text{O}=1:9$ ): 8.63-8.62 (m, 4H, Im,  $-\text{N}=\underline{\text{CH}}-\text{NH}-$ ), 7.31-7.26 (m, 4H, Im,  $-\text{C}-\text{CH}-\text{N}-$ ), 4.67-4.64 (m, 4H,  $-\text{CO}-\underline{\text{CH}}-\text{N}-$ ), 4.49 (t, 1H,  $J = 5.59\text{ Hz}$ ,  $-\text{CO}-\underline{\text{CH}}-\text{N}-$ ), 4.34-4.21 (m, 5H,  $-\text{CO}-\underline{\text{CH}}-\text{N}-$ ), 3.25-3.10 (m, 10H,  $-\text{NH}-\text{CH}-\underline{\text{CH}}_2-$ ,  $-\underline{\text{CH}}_2-\text{SH}$ ), 3.08-2.89 (m, 10H,

CH-C<sub>3</sub>H<sub>6</sub>-CH<sub>2</sub>-NH<sub>2</sub>, -CH<sub>2</sub>-SH), 1.77-1.65 (m, 16H, CH-CH<sub>2</sub>-CH<sub>2</sub>-CH<sub>2</sub>-CH<sub>2</sub>-NH<sub>2</sub>, CH-CH<sub>2</sub>-CH<sub>2</sub>-CH<sub>2</sub>-CH<sub>2</sub>-NH<sub>2</sub>), 1.45-1.35 (m, 8H, CH-CH<sub>2</sub>-CH<sub>2</sub>-CH<sub>2</sub>-CH<sub>2</sub>-NH<sub>2</sub>)

#### 2COP 4 (CK<sub>2</sub>HKHKH<sub>2</sub>C)

Preparative HPLC eluting time: ~32-34 minutes with MeCN (3%) plus TFA (0.05%) as an elution solvent at 10 ml/min flow rate for 50 minutes

Mass (g mol<sup>-1</sup>): 1285.7 [M]<sup>+</sup>, 643.3 [M+H]<sup>+2</sup>, 429.2 [M+H]<sup>+3</sup>

<sup>1</sup>H NMR δ (ppm) (D<sub>2</sub>O:H<sub>2</sub>O=1:9): 8.64-8.62 (m, 4H, im, -N=CH-NH-), 7.32-7.28 (m, 4H, im, -C-CH-N-), 4.69-4.63 (m, 4H, -CO-CH-N-), 4.53 (t, 1H, *J* = 5.66 Hz, -CO-CH-N-), 4.35 (m, 1H, -CO-CH-N-), 4.33-4.27 (m, 4H, -CO-CH-N-), 3.26-3.03 (m, 10H, -NH-CH-CH<sub>2</sub>-, -CH<sub>2</sub>-SH), 2.98-2.90 (m, 10 H, CH-C<sub>3</sub>H<sub>6</sub>-CH<sub>2</sub>-NH<sub>2</sub>, -CH<sub>2</sub>-SH), 1.76-1.65 (m, 32H, CH-CH<sub>2</sub>-CH<sub>2</sub>-CH<sub>2</sub>-CH<sub>2</sub>-NH<sub>2</sub>, CH-CH<sub>2</sub>-CH<sub>2</sub>-CH<sub>2</sub>-CH<sub>2</sub>-NH<sub>2</sub>), 1.43-1.35 (m, 8H, CH-CH<sub>2</sub>-CH<sub>2</sub>-CH<sub>2</sub>-CH<sub>2</sub>-NH<sub>2</sub>)

#### 2COP 5 (CKHKHKHKHC)

Preparative HPLC eluting time: ~35-37 minutes with MeCN (3%) plus TFA (0.05%) as an elution solvent at 10 ml/min flow rate for 50 minutes

Mass (g mol<sup>-1</sup>): 1285.8 [M]<sup>+</sup>, 643.3 [M+H]<sup>+2</sup>, 429.2 [M+H]<sup>+3</sup>

<sup>1</sup>H NMR δ (ppm) (D<sub>2</sub>O:H<sub>2</sub>O=1:9): 8.64-8.63 (m, 4H, Im, -N=CH-NH-), 7.34-7.30 (m, 4H, Im, -C-CH-N-), 4.69-4.63 (m, 4H, -CO-CH-N-), 4.55 (t, 1H, *J* = 5.62 Hz, -CO-CH-N-), 4.33-4.24 (m, 5H, -CO-CH-N-), 3.22-3.07 (m, 10H, -NH-CH-CH<sub>2</sub>-, -CH<sub>2</sub>-SH), 3.01-2.94 (m, 10 H, CH-C<sub>3</sub>H<sub>6</sub>-CH<sub>2</sub>-NH<sub>2</sub>, -CH<sub>2</sub>-SH), 1.74-1.64 (m, 16H, -CH-CH<sub>2</sub>-CH<sub>2</sub>-CH<sub>2</sub>-CH<sub>2</sub>-NH<sub>2</sub>, -CH-CH<sub>2</sub>-CH<sub>2</sub>-CH<sub>2</sub>-CH<sub>2</sub>-NH<sub>2</sub>), 1.45-1.38 (m, 8H, -CH-CH<sub>2</sub>-CH<sub>2</sub>-CH<sub>2</sub>-CH<sub>2</sub>-NH<sub>2</sub>)

#### 2COP 6 (CH<sub>8</sub>C)

Preparative HPLC eluting time: ~37 minutes with the gradient of MeCN (0-10%) plus TFA (0.05%) as an elution solvent at 10 ml/min flow rate for 40 min

Mass (g mol<sup>-1</sup>): 1321.9 [M]<sup>+</sup>, 661.4 [M+H]<sup>+2</sup>, 441.3 [M+H]<sup>+3</sup>

<sup>1</sup>H NMR δ (ppm) (D<sub>2</sub>O): 8.64-8.63 (m, 8H, Im, -N=CH-NH-), 7.28-7.26 (m, 8H, Im, -C-CH-N-), 4.73-4.63 (m, 8H, -CO-CH-N-), 4.45 (t, 1H, *J* = 5.38 Hz, -CO-CH-N-), 4.17 (t, *J* = 5.37 Hz, 1H, -CO-CH-N-), 3.00-2.84 (m, 20H, -NH-CH-CH<sub>2</sub>-, -CH<sub>2</sub>-SH)

### 3COP 7 (CK<sub>2</sub>CK<sub>2</sub>C)

Preparative HPLC eluting time: ~19 minutes with MeCN (3%) plus TFA (0.05%) as an elution solvent at 10 ml/min flow rate for 50 minutes

Mass (g mol<sup>-1</sup>): 840.5 [M]<sup>+</sup>, 420.7 [M+H]<sup>+2</sup>

<sup>1</sup>H NMR δ (ppm) (D<sub>2</sub>O:H<sub>2</sub>O=1:9): 4.54-4.49 (m, 2H, -CO-CH-N-), 4.36-4.31 (m, 4H, -CO-CH-N-), 3.13-2.90 (m, 14H, CH-C<sub>3</sub>H<sub>6</sub>-CH<sub>2</sub>-NH<sub>2</sub>, -CH<sub>2</sub>-SH), 1.81-1.66 (m, 16H, CH-CH<sub>2</sub>-CH<sub>2</sub>-CH<sub>2</sub>-CH<sub>2</sub>-NH<sub>2</sub>, CH-CH<sub>2</sub>-CH<sub>2</sub>-CH<sub>2</sub>-CH<sub>2</sub>-NH<sub>2</sub>), 1.45-1.42 (m, 8H, CH-CH<sub>2</sub>-CH<sub>2</sub>-CH<sub>2</sub>-NH)

### TAT (CRKKRRQRRRC)

Preparative HPLC eluting time: ~32 minutes with the gradient of MeCN (0-20%) plus TFA (0.05%) as an elution solvent at 10 ml/min flow rate for 60 min

Mass (g mol<sup>-1</sup>): 783.9 [M+H]<sup>+2</sup>, 515.6 [M+H]<sup>+3</sup>

<sup>1</sup>H NMR δ (ppm) (D<sub>2</sub>O:H<sub>2</sub>O=1:9): 8.78 (d, *J* = 6.41 Hz, 1H, -CH-CO-NH-), 8.48 (m, 9H, -CH-CO-NH-), 7.52 (m, 4H, -CH-CH<sub>2</sub>-CH<sub>2</sub>-CH<sub>2</sub>-NH<sub>2</sub>), 7.18-7.16 (m, 6H, -CH-CH<sub>2</sub>-CH<sub>2</sub>-CH<sub>2</sub>-NH-CNH-NH<sub>2</sub>, -N-CH-CH<sub>2</sub>-NH<sub>2</sub>), 4.34-4.24 (m, 4H, -CO-CH-N-), 3.20-3.16 (m, 12H, -CH-CH<sub>2</sub>-CH<sub>2</sub>-CH<sub>2</sub>-NH-CNH-NH<sub>2</sub>), 3.10 (dq, 2H, *J* = 17.42 Hz, 5.50 Hz, -N-CH-CH<sub>2</sub>-SH), 3.04-2.98 (m, 6H, -CH-CH<sub>2</sub>-CH<sub>2</sub>-CH<sub>2</sub>-CH<sub>2</sub>-NH<sub>2</sub>, -N-CH-CH<sub>2</sub>-SH), 2.34 (t, *J* = 8.14 Hz, 2H, -

CH-CH<sub>2</sub>-CH<sub>2</sub>-CO-NH<sub>2</sub>), 2.06-1.92 (m, 2H, -CH-CH<sub>2</sub>-CH<sub>2</sub>-CO-NH<sub>2</sub>), 1.82-1.61 (m, 32H, CH-CH<sub>2</sub>-CH<sub>2</sub>-CH<sub>2</sub>-CH<sub>2</sub>-NH<sub>2</sub>, -CH-CH<sub>2</sub>-CH<sub>2</sub>-CH<sub>2</sub>-NH-CN<sub>2</sub>-NH<sub>2</sub>), 1.44-1.36 (m, 4H, CH-CH<sub>2</sub>-CH<sub>2</sub>-CH<sub>2</sub>-NH<sub>2</sub>)

## 2.4 pK<sub>a</sub> determination of the olipeptides

NMR titration was used for the determination of the pK<sub>a</sub> values of the histidine moieties. 10 mg of each peptide was dissolved in deuterated water (D<sub>2</sub>O) (0.75 ml). An aliquot of NaOD solution (100 mM, 20 μl) was added to the peptide solution and then mixed by vortex for 2 minutes. The pH values were measured using a thin stem stainless pH reference probe (ISFET electrode). The NMR spectra were recorded using <sup>1</sup>H NMR (500 MHz). The NMR sample was left in the NMR instrument for 10 minutes at 27°C. The chemical shifts of H<sub>ε</sub> of lysine residues and H<sub>5</sub> and H<sub>6</sub> of the imidazole rings of histidine residues (**Figure 2.2**) were measured as a function of pH.

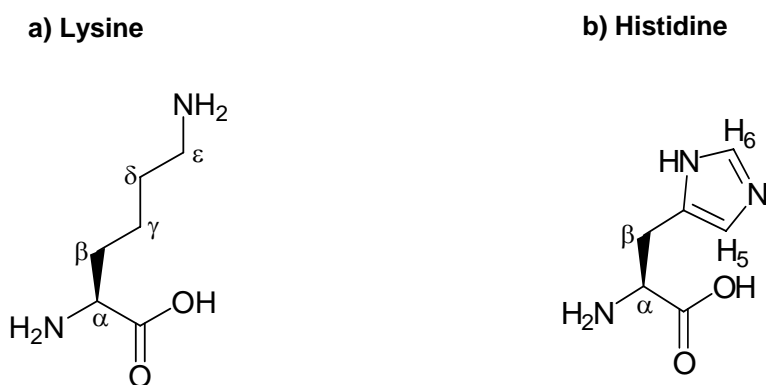


**Figure 2.2.** Structures of lysine (a) and histidine (b)

The pK<sub>a</sub> values were determined by plotting the change of chemical shift against the pH values (**Figure 2.3**)

Dr. Parvez Iqbal (School of Chemistry, University of Birmingham) performed the NMR experiments to calculate the  $pK_a$ . The NMR spectra examples from the NMR titration experiments are shown in appendix (section 8.3, **Figure 8.25-8.27**)

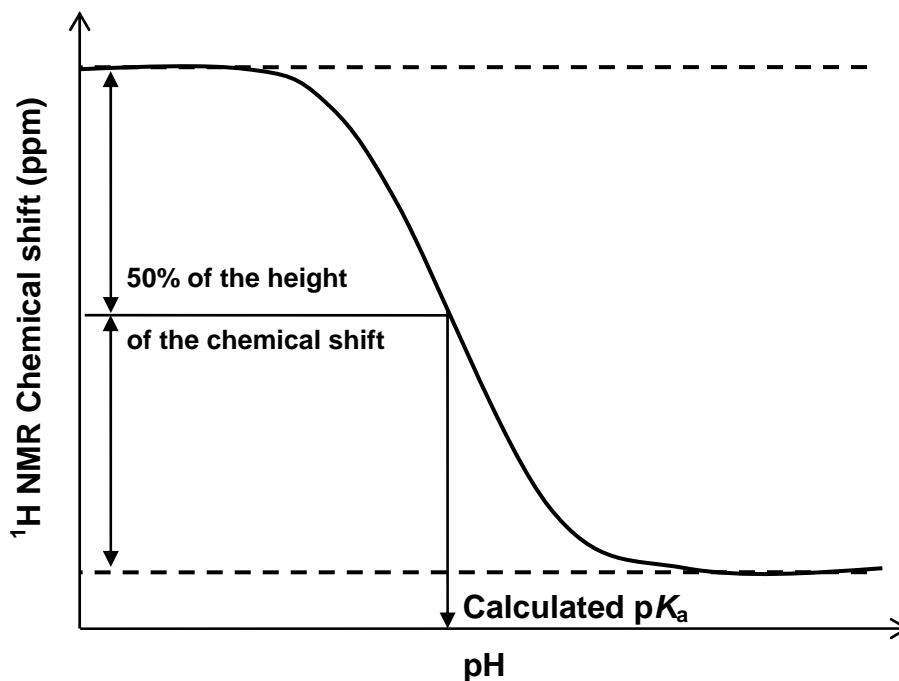


**Figure 2.3.**  $pK_a$  determinations by plotting the change of chemical shift against pH

## 2.5 Reducible polycations (RPCs) formation

### 2.5.1 Oxidative polymerisation to form RPCs

The purified oligopeptides were dissolved in PBS (0.5X PBS, pH 7.4, 70  $\mu$ l) and 30% DMSO (60  $\mu$ l) (~70 fold molar excess in respect to thiol groups) to form 200  $\mu$ l total volume mixtures at 18, 30 and 60 mM oligopeptide concentration (**Table 2.2**). The reactions were incubated at ambient or 40°C and the reaction progress was monitored by measuring the increase in molecular weight of the resulting polymers by gel permeation chromatography (section 2.5.4) as a function of time. Aliquots (5  $\mu$ l) of the reaction were removed and

terminated using fresh prepared aminoethanethiol (AET, 17  $\mu$ M, 40  $\mu$ l), unless otherwise stated, every 2 hours for the first 12 hours then 24, 30, 36 and 48 hours.

**Table 2.2. Specific masses and volumes of peptides and reagents used in oxidative polymerization to synthesize RPCs**

RPCs	2COPs used	Concentration of 2COPs (mM)	Mass of peptide used (mg)	Vol of PBS ( $\mu$ l)	Vol of DMSO ( $\mu$ l)
RPC 1	2COP 1	18	4.5	140	60
		30	7.5	140	60
		60	15.0	140	60
RPC 2	2COP 2	18	4.6	140	60
		30	7.7	140	60
		60	15.4	140	60
RPC 3	2COP 3	18	4.6	140	60
		30	7.7	140	60
		60	15.4	140	60
RPC 4	2COP 4	18	4.6	140	60
		30	7.7	140	60
		60	15.4	140	60
RPC 5	2COP 5	18	4.6	140	60
		30	7.7	140	60
		60	15.4	140	60
RPC 6	2COP 6	18	4.6	140	60
		30	7.9	140	60
		60	15.8	140	60



### 2.5.2 Formation of *cross-linked RPCs*

The reaction mixtures were performed at 30 mM concentration of 2COP **1-5** containing 3COP **7** at 4 and 32% mole fraction in PBS (0.5X PBS, 70  $\mu$ l) and 30% DMSO (30  $\mu$ l). The reactions were incubated at ambient and the reaction progress was monitored by measuring the increase in molecular weight of resulting polymer by gel permeation chromatography (section 2.5.4). Aliquots (5  $\mu$ l) of the reaction were removed and terminated using fresh prepared aminoethanethiol (AET, 17  $\mu$ M, 8 mol % excess, 40  $\mu$ l), unless otherwise stated, every 2 hours for the first 12 hours then 24, 30, 36 and 48 hours.

### 2.5.3 Formation of reducible *copolyations (RcPCs)* and reducible polyTAT (RP-TAT)

Reducible *copolyations* (RcPCs) were produced from 2COPs **1-5** and the TAT oligopeptide. 2COPs (30 mM) and TAT solution (30 mM) in 5x PBS and 30% DMSO at 2COPs:TAT molar ratios of 1:1 for RcPCs **1-5** and also 1:3 for RcPC **5** (**Table 2.3**) were incubated at ambient for 48 hours. In addition, the reducible polymer from TAT (RP-TAT) was synthesized from 60 mM TAT solution in 5x PBS and 30% DMSO, and was incubated at ambient form 48 hours. The progress of the polymerisation was measures by monitoring the increase in molecular weight of resulting polymer by gel permeation chromatography (section 2.5.4)

**Table 2.3. Specific masses and volumes of peptides and reagents used in oxidative polymerization to synthesize RP-TAT and RcPCs**

RP-TAT/RcPCs	2COP:TAT	Molar ratio	Mass of peptide used (mg)	Vol of PBS ( $\mu$ l)	Vol of DMSO ( $\mu$ l)
RP-TAT	TAT	-	18	140	60
RcPC 1	2COP 1:TAT	1:1	7.5:9.3	140	60
RcPC 2	2COP 2:TAT	1:1	7.7:9.3	140	60
RcPC 3	2COP 3:TAT	1:1	7.7:9.3	140	60
RcPC 4	2COP 4:TAT	1:1	7.7:9.3	140	60
RcPC 5	2COP 5:TAT	1:1	7.7:9.3	140	60
RcPC 5	2COP 5:TAT	1:3	3.9:14.0	140	60

#### 2.5.4 Gel permeation chromatography (GPC)

The molecular weight distributions of the quenched polymerization reactions (section 2.5.1 and 2.5.2) were analyzed by size exclusion chromatography (SEC). The SEC analysis was performed using HPLC with CATSEC-300 (250 mm x 4.5 mm ID) column (Hichrom, UK) eluted with 200 mM NaCl with 0.1% TFA. 10  $\mu$ l of the samples were injected with 0.5 ml/min flow rate (20  $\mu$ l injecting loop) using a UV detector system at 220 nm. Commercially available poly-L-lysine (PLL) (Sigma, UK) samples (5.6, 8.3, 21.3, 62.1 and 128.5 kDa) were used to estimate the molecular weight (**Figure 2.4**).

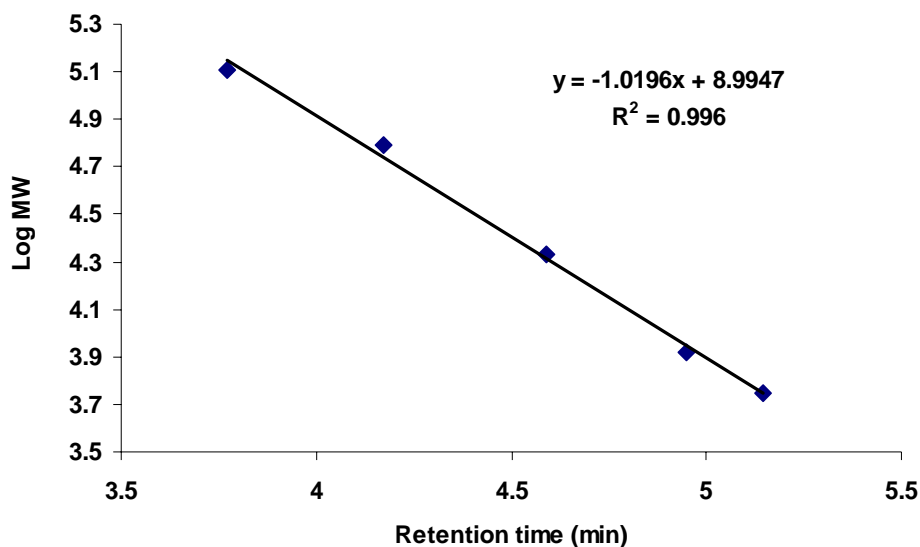


**Figure 2.4.** PLL standard plotted between Log MW and GPC retention time

### 2.5.5 Polymer purification

The reaction mixtures from section 2.5.1 and 2.5.2 were diluted in HEPES (15 ml, 15 mM, pH 7.4). The RPCs, R<sub>c</sub>PCs and RP-TAT were purified on centrifugal filter concentrators with molecular weight cut-off of 10,000 (Centricon Plus 2, Amicon Biosperation, Millipore, cellulose membrane, UK). The solution was spun down to 150 µl at 4000 rpm (repeated three times for this procedure). For the final time of the centrifugation, the sample was spun down until a final volume of 400-500 µl obtained. After purification of the polymers, the molecular weight of the polymers and the removal of DMSO and other impurities were verified by GPC (section 2.5.4).

### 2.5.6 Polydispersity index (PDI) of polycations

SEC-MALLS (size exclusion chromatography coupled to multi-angle laser light scattering) was used to detect absolute molecular weights and molecular weight distributions. The Wyatt Technology (Santa Barbara, USA) DAWN® HELEOS multi-angle laser light scattering photometer was coupled to TSK Gel G6000PW and G4000PW columns protected by a similarly packed guard column (Anachem Ltd., Luton, UK) and pre-equilibrated for at least 1 hour at 30°C before sample measurement. The eluent was aqueous acetic acid (0.5 M) and aqueous sodium nitrate (0.1 M) and the injection volume was 100 µl. A value for the refractive index change with concentration  $dn/dc$  of 0.155 was used. Polypeptide molar masses and polydispersities were analyzed using software Astra V 5.3.2.16. This measurement was carried out by Dr. Gordon Morris (National Centre for Macromolecular Hydrodynamics, Division of Food Sciences, School of Biosciences, University of Nottingham)

## 2.6 Amino acid analysis of RcPCs

Ratios of the 2COP and TAT sequences of RcPCs **1-5** were determined using amino acid analysis. RcPCs were hydrolysed by liquid phase hydrolysis by adding HCl (6N) with 4% of thioglycolic acid (100 µl) into polypeptide (500 µg). The reaction mixtures were placed in a heating block in a tightly capped vial at 110°C for 22 hr, to cleave the peptide bonds. The sample was then placed at -20°C for 24 h, unless stated otherwise. The samples were neutralised and analysed using EZ:faast kits (phenomenex, UK). An amino acid calibration standard (50, 100 and 200 nmol ml<sup>-1</sup>) (**Figure 2.5**) was run with gas chromatography (GC) to

allow quantification of the amount of unknown amino acids found in each sample, thereby enabling calculation of the % recovery of amino acids within the sample to be determined.

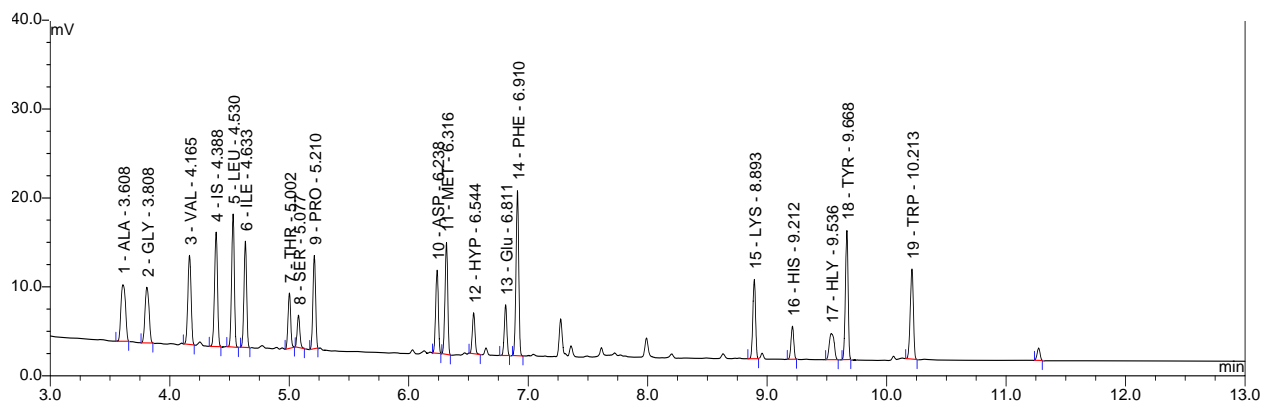


Figure 2.5. Amino acid standard at 200 nmol ml<sup>-1</sup> (EZ:faast kits, Phenomenex, UK) run with GC

The amino acid standards were plotted between the concentration of amino acid and the peak area obtained from GC (Figure 2.6).

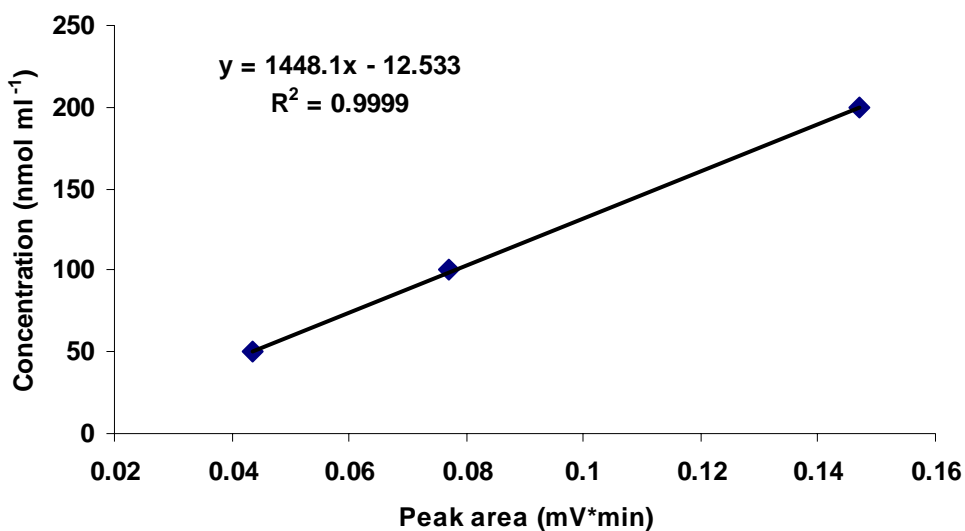


Figure 2.6. Amino acid standard plotted between the concentration of amino acid and the peak area obtained from GC

## **2.7 Formation of polyplexes**

### **2.7.1 Calculation of charge ratio**

An average mass of DNA per phosphate group is 325 Da and an average mass of PLL per amino group is 208. Hence, to obtain a theoretical charge ratio of PLL:DNA at 1:1, a weight/weight (w/w) ratio of 1:0.64 was required. For oligopeptides, PEI, RPCs and TAT-RPCs, the ratio of N:P was used rather than charge ratio, since the charge ratio is dependent on pH, and therefore, difficult to calculate accurately and only a proportion of the amino groups are fully ionised. The N:P ratio is defined as: N is the number of amino groups in the polycation, and P is the number phosphate groups in the DNA. The N:P ratio calculations have been used and will be discussed in detail in the appropriate chapters.

### **2.7.2 Formation of polyplexes**

The addition of the 2COPs, RPCs, R<sub>c</sub>PCs and RP-TAT as well as PLL and PEI, oligopeptides and RPCs to a solution of DNA results in an electrostatic interaction between the oppositely charged components resulting in partial charge neutralisation and hydrophobic collapse of the DNA into discrete nanomolecular sized polyplexes. Plasmid DNA was dissolved in 10 mM HEPES buffer, pH 7.4 (1 ml, 40 µg/ml DNA). Plasmid DNA solution (500 µl) was added into a polypropylene microcentrifuge tube. The amount of polycation to produce the polyplexes at the desired N:P ratios was dissolved in 10 mM HEPES buffer (1 ml) at pH 7.4 and then added (500 µl) into the plasmid DNA solution to give the final concentration at 20 µg/ml of plasmid DNA. The resulting suspension of polyplexes was mixed by inverting the tube 5 times. The

polyplexes were allowed to equilibrate overnight at ambient temperature, unless otherwise stated.

## **2.8 Physicochemical characterisation of polyplexes**

### **2.8.1 Analysis of polyplex diameter by photon correlation spectroscopy (PCS)**

The hydrodynamic diameters of the polyplexes were measured by dynamic light scattering (DLS) using a Zetasizer 3000 (Malvern Instruments, Worcestershire, UK), equipped with a 50 mW internal laser. Measurements were taken at 25°C at an angle of 90° to the incident light using disposable polymethacrylate cuvette. The machine was calibrated using latex spheres (204 nm diameter). Polyplexes for PCS measurements were prepared in 10mM HEPES buffer at pH 7.4 (1 ml)(section 2.7.2) in triplicate and analysed by monomodal analysis (where n = 3 (total of 30 sub-runs)).

### **2.8.2 Analysis of polyplex surface charge by zeta potential**

The polyplex solution was diluted with 10 mM HEPES buffer at pH 7.4 (3 ml) before injecting into the Zetamaster (Malvern Instruments, Worcestershire, UK) instrument. Measurements were taken at 25 °C and repeated 10 times. Before each measurement the flow cell was washed through with 18 ΩM.cm water (5 ml).

### **2.8.3 Atomic force microscopy**

An AFM liquid cell and oxidation-sharpened NP-S tips on a V-shaped, silicon nitride cantilever, with a spring constant of around 0.1 N/m (Nanoprobe, Veeco Instruments) and

resonant frequency between 9 and 10 kHz were used. All AFM imaging was carried out using a Tapping Mode on a Veeco Nanoscope (IIIa) MultiMode system (Veeco Instruments, Santa Barbara, CA). Topographical images were taken at 512X512 pixel resolution, plane-flattened, and analyzed by the computer program Nanoscope Software v 5.12.

The polyplexes were incubated at room temperature prior to immobilization onto freshly cleaved muscovite mica (Agar Scientific, Essex, UK) and being imaged directly in liquid.

For time-course experiments, the polyplexes (120  $\mu$ l, 97.8  $\mu$ g/ml) were deposited on freshly cleaved NiCl<sub>2</sub> modified mica and incubated for 10 minutes before being washed twice with deionized water (2 x 200  $\mu$ l). An aliquot of the fluid (100  $\mu$ l) in the cell was then exchanged with GSH (20mM, 100  $\mu$ l). The time for this exchange was defined as time zero and images were then captured according to stated times.

The AFM experiments were carried out by Mahmoud Soliman (School of Pharmacy, University of Nottingham, UK)

#### **2.8.4 Agarose gel electrophoresis of DNA**

All agarose gel electrophoresis used Horizon 11.14 horizontal gel tanks (Gibco BRL, Invitrogen Life Technologies, Paisley, UK). Low melting point agarose gel (Gibco, BRL) was prepared at 1 % in TBE buffer (50 mM Tris, 50 mM boric acid, 0.8 mM EDTA, 0.5X TBE). Ethidium bromide (5  $\mu$ l, 10 mg/ml) was added into melted gel (100 ml). The agarose gel was poured into the casting tray and allowed to set at room temperature before TBE (0.5X TBE) was added as running buffer. TBE buffer (0.5X) was used as the electrophoresis



running buffer. The samples were loaded into wells and the gel was run at 110 V (Biorad, UK) for 60 mins. The Typhoon gel scanner set at 533 nm/610 nm wavelengths and 550V was used to scan the gel and the quantity of DNA in particular bands analysed using ImageQuant™ software. Gels visualised on the transilluminator and the image captured using a Polaroid camera (Analysis software, FluorChem 8800, Alpha Innotech).

## **2.8.5 Gel shift assay**

### *2.8.5.1 Polyaspartic assay*

The simulated extracellular stability of the polyplexes was studied using polyaspartic acid (PAA). The polyplex solutions were prepared by mixing with PAA at 250 times of the plasmid DNA concentration. The gel was run (section 2.8.4) at 110 volt for 60 minutes in 0.5x TBE. The pCMV-Luc was loaded into gel in the equal amount with the plasmid DNA in the polyplex samples as control.

### *2.8.5.2 Glutathione and NaCl assay*

The intracellular stability of polyplexes was studied using glutathione (GSH) and NaCl for monitoring the reduction of the disulfide bonds. The polyplex solutions were prepared by mixing with 5mM. The mixtures were incubated at ambient for 1 hr before adding 0.15 M, 0.5 M or 1 M NaCl. The gel was run (section 2.8.4) at 110 volt for 60 minutes in 0.5x TBE. The pCMV-Luc was loaded onto the gel in the equal amount with the plasmid DNA in the polyplex samples as control.

## **2.9 Cell culture**

All cell cultures were performed using biological safety class II laminar flow cabinet (Class II Microbiological Safety Cabinet, Envair Ltd, UK), cleaned with 70 % ethanol before and after use. Cells were maintained in an incubator (MCO-17AIC, Sanyo, UK) at 37°C with a constant CO<sub>2</sub> level of 5 %. Cells were maintained and grown in Dulbecco's modified Eagles media (DMEM, Gibco-BRL, Paisley, UK) supplemented with L-glutamine (2mM) and 10 % foetal calf serum (FCS). The media was supplemented with penicillin and streptomycin to prevent the bacterial contamination to the cell lines. Phosphate buffered saline (1x PBS, Gibco-BRL, Paisley, UK) was used for washing cells. All media and PBS buffer were stored at 4°C.

### **2.9.1 Maintenance of established cell lines**

Cells were grown as a monolayer in 75 cm<sup>3</sup> flasks containing of DMEM with 10% FCS (10 ml) at 37°C, 5% CO<sub>2</sub>. The culture medium was replaced every 3-4 days to avoid depletion of essential nutrients and build up of toxic metabolites. Cells were routinely passaged at 80 % confluence at a ratio of 1:10 to prevent overgrowth and loss of surface contact. To the sub-culture, the medium was removed and the cells were washed briefly with 1x PBS buffer (10 ml). The cells were suspended by trypsinising by adding trypsin/EDTA (5 ml; 0.05/0.02 %, respectively) and incubated at 37°C, 5% CO<sub>2</sub> for 5 mins. Cells were resuspended in fresh media and aliquoted (10 ml) into fresh flasks, unless otherwise stated.

## 2.9.2 Determination of viable cell number

An aliquot of the cell suspension (20  $\mu$ l) was added to aqueous trypan blue solution (20  $\mu$ l). Only viable cells take up the trypan blue dye, thereby allowing the number of viable cell numbers to be determined microscopically by discounting blue cells using a haemocytometer of fixed volume. The cell concentration was calculated as the equation below.

$$\left( \frac{\text{number of cell counted}}{\text{proportion of chamber counted} \times \text{volume of chamber}} \right) \times \left( \frac{\text{volume of sample dilution}}{\text{volume of original mixture in sample}} \right)$$

## 2.10 Biological studies of polyplexes

### 2.10.1 Cell transfection *in vitro*

Cells were prepared in 96 well plates ( $10^4$  cells per well) in DMEM (100  $\mu$ l) containing 10% FCS and 1% penstrep. The cells were allowed to adhere for 18 hours at 37°, 5% CO<sub>2</sub>. The media was removed from the wells and the cells were washed with PBS (100  $\mu$ l) and replaced with the serum free DMEM (50  $\mu$ l). The polyplex solutions (25  $\mu$ l) were mixed with serum free DMEM (25  $\mu$ l) then added 50  $\mu$ l of the mixture to each well of the cells (3 replicates were performed for each polyplex). The polyplexes were incubated at 37°C with 5% CO<sub>2</sub> for 4 hours then removed from the wells. The cells were washed with PBS (100  $\mu$ l) and replaced with DMEM (100  $\mu$ l) containing 10% FCS and 1% penstrep. The plates were incubated at 37°C with 5% CO<sub>2</sub> for a further 44 hours. The media was removed from the wells and the cells were washed with PBS (100  $\mu$ l) and replaced with 1x cell lysis buffer (50  $\mu$ l). The plates were kept at -80°C for at least 30 minutes and then thawed at room temperature. The cell

lysate were further analyzed by luciferase assay (section 2.10.2) to obtain the relative light units (RLU), and the amount of protein produced by the advanced protein assay (section 2.10.3). Thus, the gene expression will be shown in relative light units per milli gram of protein (RLU/mg protein).

In some experiments, cells were incubated in the DMEM (100  $\mu$ l) containing chloroquine (100  $\mu$ M), glutathione monoethyl ester (5 mM) or buthionine sulfoximin (100  $\mu$ M) at 37°C with 5% CO<sub>2</sub> for 1, 3 and 24 hours, respectively. The cells were washed with PBS before transfecting with the polyplexes.

### **2.10.2 Luciferase assay**

The luciferase assay is used to determine the luminescence produced by luciferase enzyme in the cell lysate (section 2.10.1).

The cell lysate (25  $\mu$ l) was added into the appropriate Rohren tube. The luminescence of the samples was analysed automatically by the luminormeter (EG and G Berthold, Bundoora, Australia) using the luciferase assay reagent (25  $\mu$ l) (Promega, Madison, WI, USA). Luminescence was integrated over 10 sec and normalised to total cell protein, obtained using the advanced protein assay (section 2.10.3).

### **2.10.3 Advanced protein assay**

The advanced protein assay is a colorimetric method for determining the protein concentration of cell lysate. It was performed in a 96 well plate.

The cell lysate (5  $\mu\text{l}$ ) was added into each well (triplicate per sample) and the advanced protein assay reagent (250  $\mu\text{l}$ , 1x APAR) (Totam Biologicals, Northampton, UK) was added into sample. The absorbance was measured at 590 nm using the Victor plate reader (Wallec, Perkin Elmer Life Sciences, UK). Blank was also performed by adding 1x lysis buffer (5  $\mu\text{l}$ ) instead of protein sample. The absorbance of each measurement was deducted from the blank. Bovine serum albumin (BSA) at different concentrations (7.8, 15.6, 31.2, 62.5, 125, 250 and 500  $\mu\text{g ml}^{-1}$ ) was used to produce a standard curve (**Figure 2.7**).

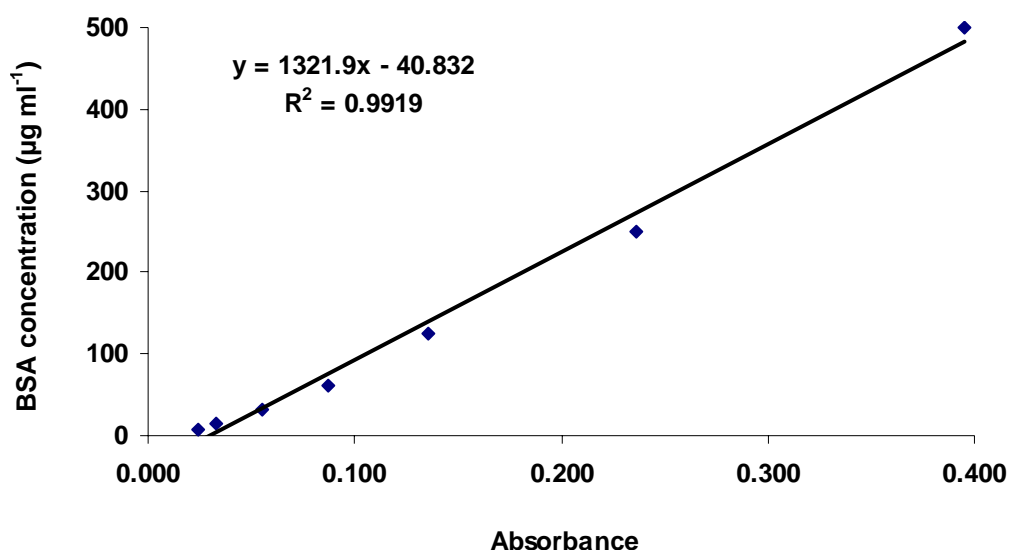


**Figure 2.7.** BSA standard plotted between BSA concentration and absorbance

#### 2.10.4 MTS cell proliferation assay

MTS cell proliferation assay is a colourimetric method to identify the cytotoxic potential of a test agent. The active agent of this assay is [3-(4,5-dimethylthiazol-2-yl)-5-(3-carboxymethoxyphenyl)-2-(4-sulphophenyl)-2H-tetrazolium, inner salt] (Owen's reagent or

MTS). The MTS agent is bio-reduced by NADPH and NADH produced by dehydrogenase enzymes in metabolically active cells, producing a yellow/orange formazan product. The amount of formazan product is directly proportional to the number of living cells. Thus, the cell proliferation or death can be quantified by reading the plate at 490 nm.

After cell transfection for 96 hrs, cells were washed with PBS (200  $\mu$ l) and reaction media (120  $\mu$ l), containing DMEM (100  $\mu$ l) with 10% FCS and MTS reagent (20  $\mu$ l) (Promega, Madison, WI, USA) was added to the cells. Cells were incubated at 37°C with 5% CO<sub>2</sub> for 45 minutes. The quantity of formazan product was measured by the amount of absorbance at 490 nm. A blank was also performed by adding the reaction media into empty wells. The absorbance was read using the Victor plate reader (Wallace, Perkin Elmer Life Sciences, UK). Each measurement was deducted from the blank before calculating the percentage cell viability.

### **2.10.5 Intracellular glutathione analysis**

Monochlorobimane (mBCl) fluorometric method was used to measure the intracellular GSH in this thesis. Adding the membrane-permeant mBCl into culture medium leads the intracellular GSH to form GSH-mBCl adduct which can be measured fluorometrically.

A stock solution of mBCl (8mM) was prepared in DMSO and stored at -80°C. The working solution of mBCl was prepared immediately before using by adding PBS to give the 800  $\mu$ M final concentration.

Following the cell incubation with chemical agents such as GSH-MEE, BSO or CQ at appropriate time (section 2.10.1), the cells were washed with PBS (100  $\mu$ l) and the mBCl (5  $\mu$ l, 800  $\mu$ M) was added into DMEM (95  $\mu$ l), then added into cells to give final concentration at 40  $\mu$ M. The cells were incubated at 37°C with 5% CO<sub>2</sub> for 60 min. The fluorescence of the cells was measured at  $\lambda_{\text{ex}}$  355 nm and  $\lambda_{\text{em}}$  460 using the Victor plate reader (Wallace, Perkin Elmer Life Sciences, UK). A blank was also performed by measuring the cell fluorescence before adding fluorescent probe mBCl. Each measurement was deducted from the blank before calculating the relative fluorescence.

## **2.11 Expression of data**

All error bars shown represent the mean and standard deviation of the data from three independent experiments.

## **CHAPTER 3**

# **Synthesis and characterization of oligopeptides, reducible polycations (RPCs) and polyplexes**



# CONTENTS

List of Figures

List of Tables

## 3 SYNTHESIS AND CHARACTERIZATION OF OLIGOPEPTIDES, REDUCIBLE POLYCATIONS (RPCs) AND POLYPLEXES

<b>3.1</b>	<b>Introduction</b>	<b>109</b>
<b>3.2</b>	<b>Objectives</b>	<b>111</b>
<b>3.3</b>	<b>Methodology</b>	<b>112</b>
<b>3.4</b>	<b>Results and discussion</b>	<b>116</b>
3.4.1	Oligopeptide purification and characterization	116
3.4.2	Determination of the $pK_a$ of the oligopeptides	117
3.4.3	Formation and characterization of reducible polycations (RPCs)	121
3.4.3.1	Polymerization as a function of oligopeptide concentration	122
3.4.3.2	Polymerization as a function of temperature for 2COP 1	125
3.4.3.3	Polymer stability in HEPES buffer	126
3.4.4	Formation and characterization of polyplexes	126
3.4.4.1	Weight per charge and N:P ratio calculation	126
3.4.4.2	RPCs polyplexes formation and characterization	129
3.4.4.2a	Diameter and zeta potential of polyplexes	129
3.4.4.2b	Shape of polyplexes	131
3.4.4.2c	Extracellular stability studies of polyplexes	133
3.4.4.2d	Intracellular reduction studies of polyplexes	134
3.4.4.3	Formation of polyplexes with low molecular weight RPCs	144
3.4.4.3a	Diameter and zeta potential of polyplexes	144
3.4.4.3b	Extracellular stability studies of polyplexes	145
3.4.4.3c	Intracellular reduction studies of polyplexes	146
3.4.4.4	Oligopeptide polyplexes formation and characterization	149
3.4.5	Formation and characterization of <i>cross-linked</i> RPCs	151
<b>3.5</b>	<b>Conclusions</b>	<b>155</b>
<b>3.6</b>	<b>References</b>	<b>160</b>

## List of Figures

Figure 3.1.	Schematic overview of characterisation and analysis of oligopeptides and polyplexes in this chapter	114
Figure 3.2.	Schematic overview of experimental processes of a) 2COPs and polyplexes and b) 3COPs and <i>cross-linked RPC</i>	115
Figure 3.3.	$pK_a$ calculation by $^1\text{H}$ NMR titration plotting the change in chemical shift of reporter proton resonances against pH	117
Figure 3.4.	$pK_a$ determination of oligopeptides by plotting the change in chemical shift from $\text{H}_5$ , $\text{H}_6$ or $\text{H}_\epsilon$ against pH	118
Figure 3.5.	Average $pK_a$ of histidine-containing oligopeptides	120
Figure 3.6.	The oxidative polymerization procedure of 2COP <b>2</b> ( $\text{CK}_4\text{H}_4\text{C}$ )	121
Figure 3.7.	Oxidative polymerization of 2COPs (bis-cysteine containing peptides) at various peptide concentrations incubated at ambient	123
Figure 3.8.	Oxidative polymerization compared between all 2COPs at different peptide concentration incubated at ambient	124
Figure 3.9.	Oxidative polycondensation of 2COP <b>1</b> ( $\text{CK}_8\text{C}$ ) at 18 mM concentration reacted at ambient and $40^\circ\text{C}$	125
Figure 3.10.	The chemical shift changing between pH 2-10	128
Figure 3.11.	Length persistency of the lysine and histidine based sequences	131
Figure 3.12.	Aqueous phase atomic force microscopy of RPCs polyplexes at N:P 5	132
Figure 3.13.	Gel shift assay with and without polyaspartic acid (PAA) of polyplexes formed from RPCs <b>1-5</b> at N:P 5 and PEI polyplex at N:P 10	134
Figure 3.14.	DNA binding and release demonstrated by agarose gel electrophoresis (gel shift assays)	135
Figure 3.15.	Percentage of DNA release from RPCs <b>1-5</b> after incubating with GSH (5mM) in combination with NaCl (0, 0.15, 0.5 and 1 M)	136
Figure 3.16.	Aqueous phase atomic force microscopy of RPC <b>1</b> polyplexes at N:P 5 showing effect of reduction by GSH (20 mM)	138
Figure 3.17.	Aqueous phase atomic force microscopy of RPC <b>2, 3</b> polyplexes at N:P 5 showing effect of reduction by GSH (20 mM)	139
Figure 3.18.	Aqueous phase atomic force microscopy of PLL/DNA polyplexes at N:P 5 showing effect of reduction by GSH (20 mM) at the different times	140

Figure 3.19.	Diameters of RPC polyplexes <b>1-5</b> following incubation with 20 mM glutathion	141
Figure 3.20.	Model of polyplex reduction by GSH	141
Figure 3.21.	The models of PLL and RPC polyplexes after treating with PAA or GSH+NaCl	143
Figure 3.22.	Gel shift assay with and without polyaspartic acid (PAA) of polyplexes formed from low molecular weight RPCs <b>1-5</b> (N:P 5), PEI (N:P 10) and PLL (N:P 5)	146
Figure 3.23.	DNA binding and release demonstrated by gel shift assays of low molecular weight RPC polyplexes	148
Figure 3.24.	The model of cross-linking polymerization to form <i>cross-linked RPC</i> via disulfide bond formation	151
Figure 3.25.	Oxidative polymerization of 2COPs <b>1-5</b> at 30mM concentration with and without 4% and 30% mole fraction of 3COP <b>7</b> (CK <sub>2</sub> CK <sub>2</sub> C) incubated at ambient	152
Figure 3.26.	Oxidative polymerization compared between 2COPs <b>1-5</b> at 30mM concentration with and without 4% (a) and 30% (b) mole fraction of 3COP <b>7</b> (CK <sub>2</sub> CK <sub>2</sub> C) incubated at ambient	154

## List of Tables

Table 3.1.	The synthetic oligopeptides studied in this chapter	112
Table 3.2.	The purity and mass of purified oligopeptides	116
Table 3.3.	p <i>K</i> <sub>a</sub> value of oligopeptides determined by <sup>1</sup> H NMR titration (500 MHz)	119
Table 3.4.	Weight per charge (wpc) of 2COPs	128
Table 3.5.	Properties of RPCs and their polyplexes	130
Table 3.6.	Properties of RPCs at different molecular weight and their polyplexes formed at N:P 5	144
Table 3.7.	Diameter of polyplexes from 2COPs <b>1-5</b> at N:P 5 and PEI at N:P 10 after 6, 24 and 48 hr of the formation	150

# 3 SYNTHESIS AND CHARACTERIZATION OF OLIGOPEPTIDES, REDUCIBLE POLYCATIONS (RPCs) AND POLYPLEXES

## *Abstract*

*As described previously there are several barriers to be overcome to deliver a gene in vitro and in vivo, which provided the key features to achieve the efficient gene delivery including. In this chapter, the synthetic oligopeptides were designed by combining with lysine, histidine and cysteine residues which will bind DNA extracellularly, internalise via endocytosis, provide a tunable endosomal release mechanism and provide a degradable backbone in order that the DNA can be released once in the cytoplasm. The design, synthesis, characterize molecular and biologically of  $pK_a$  modulatable oligopeptides and reducible polycations (RPCs) will be described. The sizes, surface charges and the stability of RPC polyplexes under the simulated physiological conditions extra- and intracellularly suggested that these RPCs are the promising vectors for gene delivery, especially the low molecular weight RPCs.*

## 3.1 Introduction

For efficient gene delivery, DNA or RNA must be taken across a number of formidable biological barriers. In the case of DNA, delivery is to the cell nuclei, while for RNA only cytoplasmic delivery is required. For both nucleic acids, a challenging step is to cross the cell membrane and gain entry into cellular cytoplasm which can be achieved *via* endocytosis.<sup>[1,2]</sup> Cationic polymers can be used as non-viral gene carriers by condensing nucleic acids with polycations to form polyelectrolyte complexes, known as ‘polyplexes’.<sup>[3]</sup> When internalized into the cytoplasm, *via* endocytosis, the polyplexes must be able to escape from endosomal compartments: and a means to do this is *via* a buffering capacity as the pH in the maturing endosome drops – this is known as the proton sponge hypothesis.<sup>[4]</sup> This hypothesis specifically describes the buffering action of polyethylenimine (PEI)/DNA polyplexes in the endosome during acidification and subsequent lysis of the endosome, due to an influx of

water due to the change in osmolarity. This hypothesis can be extended to describe the activity of polyplexes which contain other basic groups which are capable of buffering the endosome.<sup>[5]</sup>

In recent years, lysine (K) and histidine (H) have been incorporated into vectors on account of their varying abilities to deliver genes *in vitro* and *in vivo*,<sup>[6-13]</sup> which in turn may stem from their varying basicities. The degree of success of these vectors may be related to the ability of the polycation to buffer acidification in the endosome sufficiently. For example, polyplexes formed from poly(L)lysine (PLL) are not very efficient for gene delivery when used alone because the primary amine on the side chain of lysine has a  $pK_a$  of  $\sim 10.5$ , and thus, is highly protonated at physiological pH ( $\sim 7.4$ ),<sup>[14]</sup> and is therefore unable to buffer the pH effectively. Therefore, an endosomolytic agent, chloroquine, is used to increase the transfection efficiency of PLL.<sup>[7]</sup> The rationale for the addition of the chloroquine is that it is a weaker base with  $pK_a$  of 8.1 and 10.2 and is able to diffuse into low-pH compartments, whereupon it is protonated and buffers acidic vesicles, which aids the lysis of the endosome.<sup>[15]</sup> Thus, the lack of buffering capacity of the protonated amine groups in PLL results in low transfection activity of the polyplexes, without chloroquine. Therefore, histidine residues have been incorporated into synthetic peptides in order to enhance endosomal release, since the  $pK_a$  of an imidazole group in the histidine side chain is approximately 6.0.<sup>[16]</sup> It was found that poly(L)histidines were able to promote buffering in endosomal compartments allowing the polyplexes to escape from the endosome *via* the proton sponge hypothesis.<sup>[17-21]</sup>

The use of cysteines in bioconjugates is a well-known strategy for linking molecular fragments together *via* a covalent disulfide bond, and is an appealing option in gene delivery chemistries owing to the ready reversibility of the disulfide bonds by the reducing agent

intracellular glutathione (GSH).<sup>[9,22]</sup> Polyplexes have been formed with disulfide bonds in the polymer backbone which are stabilized in the extracellular matrix,<sup>[23,24]</sup> but are cleaved efficiently by high concentration of intracellular glutathione, leading to the vector falling apart and efficient release of the DNA. These polyplexes are also reasonable gene delivery agents.

## 3.2 Objectives

In this chapter, we focus on producing a vector from synthetic oligopeptides, that incorporate 3 amino acids – lysine, histidine and cysteine – in order to combine the vector features as described previously in Chapter 1 (**Table 1.5**). Thus, the vectors should address several of the key features highlighted on page 40.

- bind DNA extracellularly (**I**),
- cell uptake *via* endocytosis (**III**),
- provide a tunable endosomal release mechanism (**IV**),
- and provide a degradable backbone in order that the DNA can be released once in the cytoplasm (**V**).

The design of the oligopeptides (**Table 3.1**) used in this study was described in section 1.5.

**Table 3.1. The synthetic oligopeptides used in this study**

Oligopeptide	Sequence <sup>a</sup>
<b>Bis-(cysteine containing oligopeptides) (2COPs)</b>	
1	CK <sub>8</sub> C
2	CK <sub>4</sub> H <sub>4</sub> C
3	CK <sub>2</sub> H <sub>2</sub> K <sub>2</sub> H <sub>2</sub> C
4	CK <sub>2</sub> HKHKH <sub>2</sub> C
5	CKHKHKHKHKHC
6	CH <sub>8</sub> C
<b>Tris-(cysteine containing oligopeptides) (3COP)</b>	
7	CK <sub>2</sub> CK <sub>2</sub> C

<sup>a</sup> C = Cysteine, K = Lysine, H = Histidine

### 3.3 Methodology

The experimental processes in this chapter will be divided into 5 sections as described below and show in diagrammatically in **Figure 3.1** and **3.2**.

(i) *The purification and characterisation of the oligopeptides:* The crude oligopeptides 2COPs and 3COPs were purified and characterized (**Figure 3.1** and **3.2a-b, step 1**) using high performance liquid chromatography (HPLC), electrospray mass spectrometry (ESI-MS) and nuclear magnetic resonance (NMR). The pK<sub>a</sub> values of the oligopeptides were then determined using <sup>1</sup>H NMR titration.

(ii) *The formation and characterization of RPCs:* The reducible polycations (RPCs) were synthesized via oxidative polymerisation from 2COPs (**Figure 3.1, step 2**).



The characterisation of RPCs was carried out using gel permeation chromatography (GPC) and multi-angle laser light scattering (MALLS).

(iii) *The formation and characterization of RPCs polyplexes*: The formation of RPCs polyplex with the DNA was performed in a condensation reaction (**Figure 3.1, step 4**), and the stability of the polyplexes under extra- and intracellularly simulated conditions was carried out (**Figure 3.1, step 5-7**).

(iv) *The formation and characterisation of oligopeptide polyplexes*: 2COPs **1-5** were used to form the polyplexes with the DNA (**Figure 3.2a, step 2**) in order to compare their characteristic with RPCs polyplexes. The characterization of 2COPs polyplexes was carried out using dynamic light scattering (DLS) (**Figure 3.2a, step 3**).

(v) *The synthesis of cross-linked RPCs*: The *cross-linked RPCs* were synthesized *via* oxidative polymerisation between 2COPs and 3COPs (**Figure 3.2b, step 2**) in order to compare with the synthesis of the *linear RPCs*. The characterization of the *cross-linked RPCs* was performed using GPC (**Figure 3.2b, step 3**).

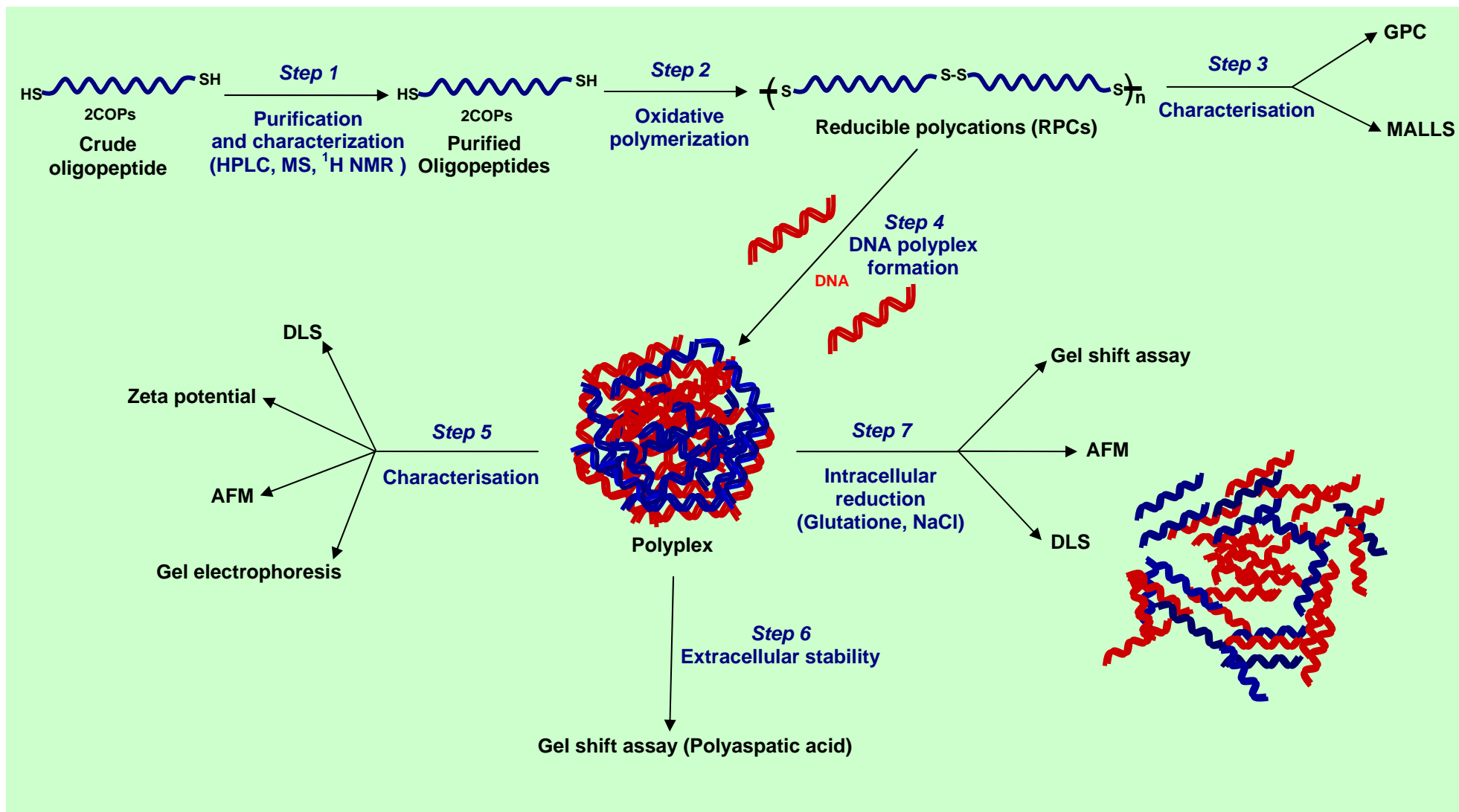


Figure 3.1. Schematic overview of characterisation and analysis of oligopeptides and polyplexes in this chapter  
References for Chapter 3 are on page 160-163.

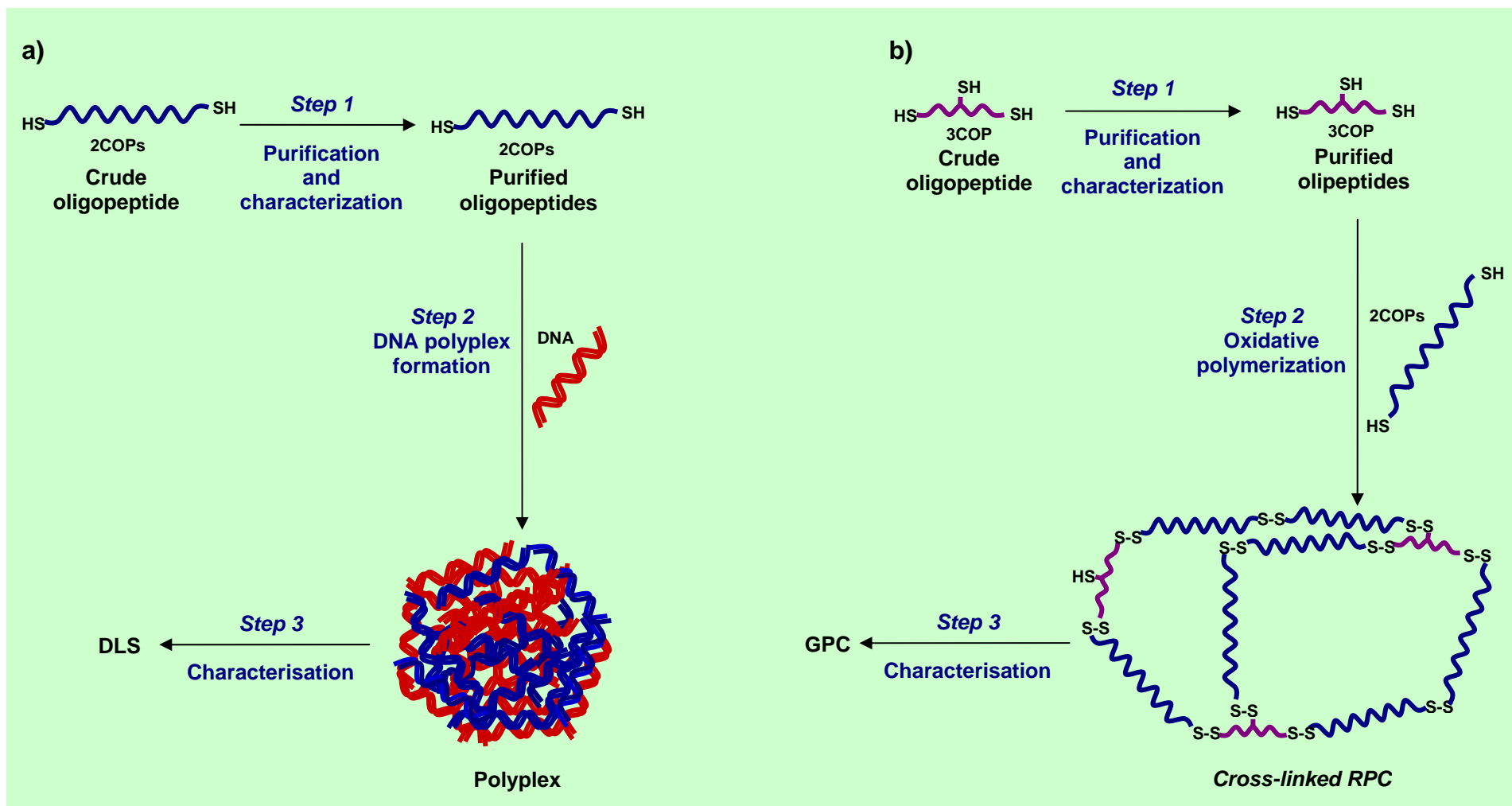


Figure 3.2. Schematic overview of experimental processes of a) 2COPs and polyplexes and b) 3COPs and *cross-linked RPC*

## 3.4 Results and discussion

### 3.4.1 Oligopeptide purification and characterization (Figure 3.1 and Figure 3.2a-b, Step 1)

Crude samples of oligopeptides **1-7** synthesized by Alta Bioscience (Birmingham, UK) using Fmoc procedure were purified by preparative reverse phase HPLC as described in section 2.3. The final purity of each oligopeptide was determined by analytical reverse phase HPLC, the experimental and calculated mass was determined by electrospray-MS and is shown in **Table 3.2**. The purity of all oligopeptides was between 97.35-99.64 % by analytical RP-HPLC. The purified oligopeptides were then characterized by <sup>1</sup>H NMR (500 MHz) and ESI-MS to confirm their structures (section 2.3).

**Table 3.2. The purity and mass of purified oligopeptides**

Oligopeptide	Sequence <sup>a</sup>	Purity (%) <sup>b</sup>	Experimental Mass	Calculated
			[M] <sup>+</sup> (g mol <sup>-1</sup> ) <sup>c</sup>	Mass (g mol <sup>-1</sup> ) <sup>d</sup>
2COPs				
<b>1</b>	CK <sub>8</sub> C	99.59	1249.90	1249.70
<b>2</b>	CK <sub>4</sub> H <sub>4</sub> C	97.42	1285.90	1285.56
<b>3</b>	CK <sub>2</sub> H <sub>2</sub> K <sub>2</sub> H <sub>2</sub> C	98.45	1285.70	1285.56
<b>4</b>	CK <sub>2</sub> HKHKH <sub>2</sub> C	97.35	1285.70	1285.56
<b>5</b>	CKHKHKHKHKHC	97.41	1285.80	1285.56
<b>6</b>	CH <sub>8</sub> C	97.56	1321.90	1321.43
3COP				
<b>7</b>	CK <sub>2</sub> CK <sub>2</sub> C	99.64	840.50	839.42

<sup>a</sup> C = Cysteine, K = Lysine, H = Histidine

<sup>b</sup> Purity determined by analytical RP-HPLC (see appendix)

<sup>c</sup> Mass analyzed by ESI-MS

<sup>d</sup> Mass from the calculation

### 3.4.2 Determination of the $pK_a$ of the oligopeptides (Figure 3.1 and Figure 3.2a-b, Step 1)

The  $pK_a$  values of the purified oligopeptides was determined using  $^1\text{H}$  NMR titration (section 2.4). The  $pK_a$  values were calculated by plotting the change in chemical shift of reporter proton resonances against pH (Figure 3.3). At 50% of the height of the change in chemical shift the equilibrium position of protonated and unprotonated amino groups is 1:1. Thus, the pH at this point is referred as the  $pK_a$ .

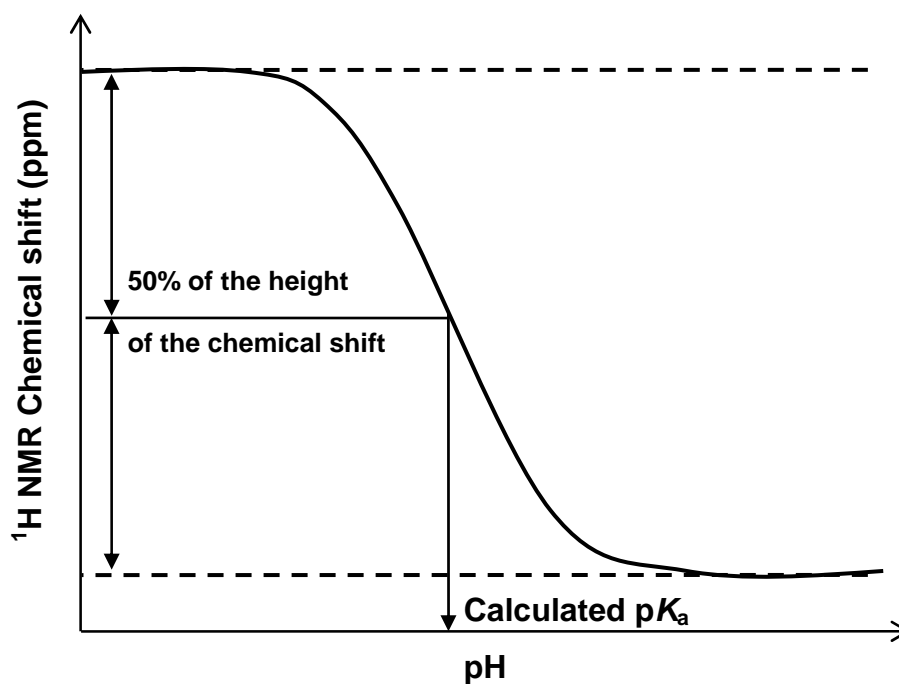


Figure 3.3.  $pK_a$  calculation by  $^1\text{H}$  NMR titration plotting the change in chemical shift of reporter proton resonances against pH

For 2COP 1 and 3COP 7 the lysine moieties  $pK_a$  were measured by observing the  $H_\epsilon$  proton of the side chain (Table 3.3). Whilst, 2COPs 2-6, the  $H_5$  and  $H_6$  proton on the imidazole ring were monitored as shown in Figure 3.4 and Table 3.3. The NMR spectra examples from the NMR titration experiments are shown in the appendix (section 8.3, Figure 8.25-8.27).

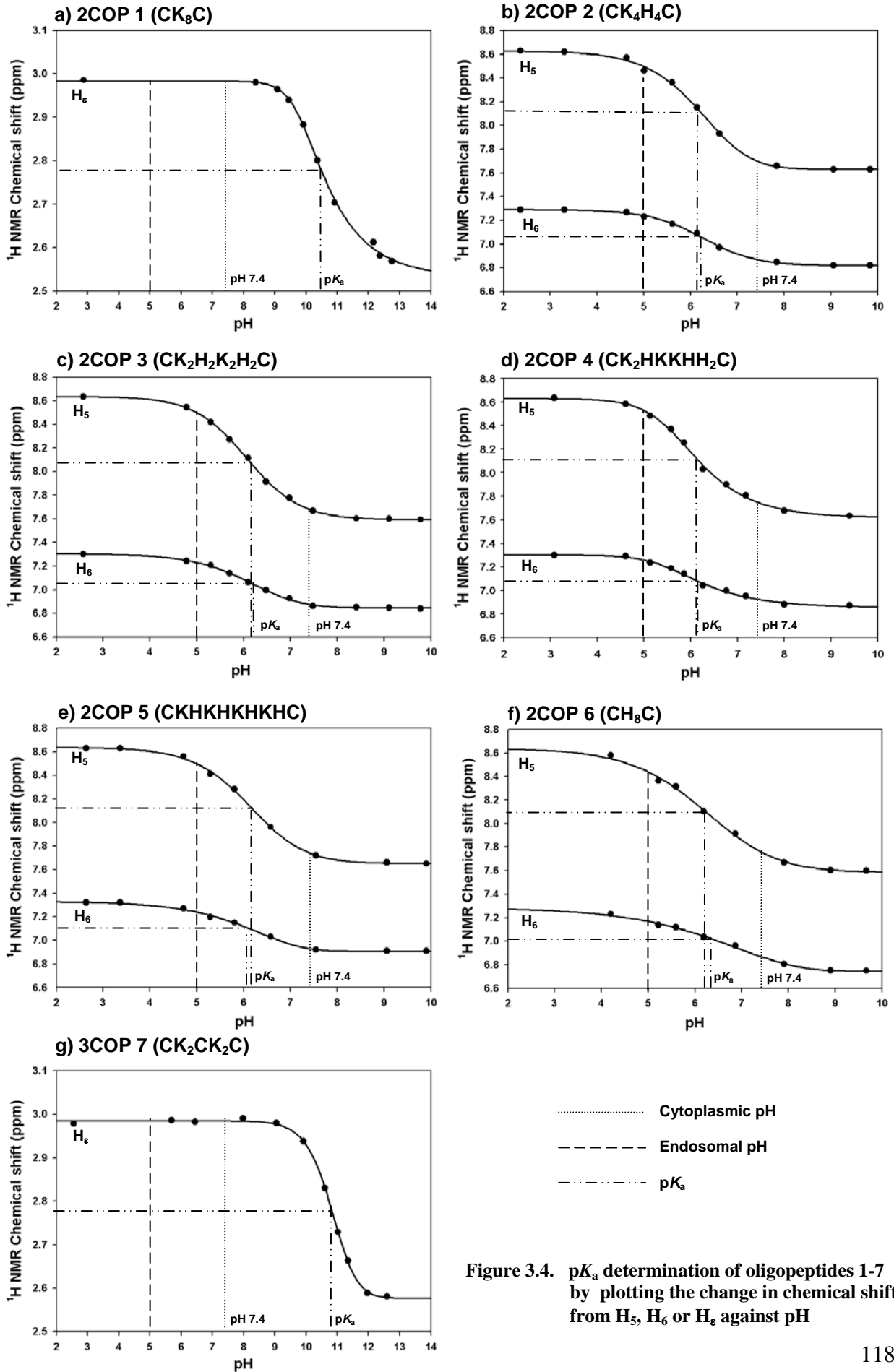
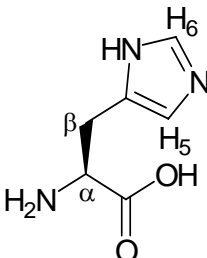
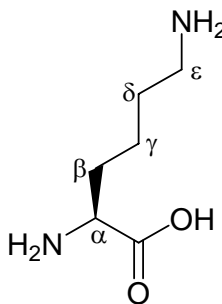


Figure 3.4. pK<sub>a</sub> determination of oligopeptides 1-7 by plotting the change in chemical shift from H<sub>5</sub>, H<sub>6</sub> or H<sub>ε</sub> against pH

The determination of the  $pK_a$  of the lysine residues in 2COPs **2-5** is not possible because of overlapping proton resonance with the  $\beta$ -methylene group of the histidine. However, the  $pK_a$  of the lysine is so much greater ( $\sim 10.5$ ) than the physiological pH ( $\sim 7.4$ ), leading to it being highly protonated at pH 7.4. Hence small pH shifts will not affect the DNA binding significantly.

**Table 3.3.**  $pK_a$  value of oligopeptides determined by  $^1\text{H}$  NMR titration (500 MHz)

Oligopeptide	Histidine		Lysine	
				
	$pK_a$			
	$H_5$	$H_6$	$H_\epsilon$	Average
<b>2COPs</b>				
CK <sub>8</sub> C ( <b>1</b> )	-	-	10.51	10.51
CH <sub>4</sub> K <sub>4</sub> C ( <b>2</b> )	6.18	6.22	-	6.20
CH <sub>2</sub> K <sub>2</sub> H <sub>2</sub> K <sub>2</sub> C ( <b>3</b> )	6.15	6.17	-	6.16
CH <sub>2</sub> KHKHK <sub>2</sub> C ( <b>4</b> )	6.10	6.12	-	6.11
CHKHKHKHKC ( <b>5</b> )	6.14	6.04	-	6.09
CH <sub>8</sub> C ( <b>6</b> )	6.2	6.3	-	6.25
<b>3COP</b>				
CK <sub>2</sub> CK <sub>2</sub> C ( <b>7</b> )	-	-	10.81	10.81

For 2COP 1 and 3COP 7 the  $pK_a$  of the lysine residue were 10.51 and 10.81, respectively. For 2COPs 2-6 the  $pK_a$  of the histidine residues were 6.20, 6.16, 6.11, 6.09 and 6.25, respectively. As expected the  $pK_a$  of the imidazole residues in the histidine decreases from 2COPs 2-5 (Figure 3.5), due to charge repulsion of the subphase protons by the protonated lysine residues as described in section 1.6.1.1 and Figure 1.24.

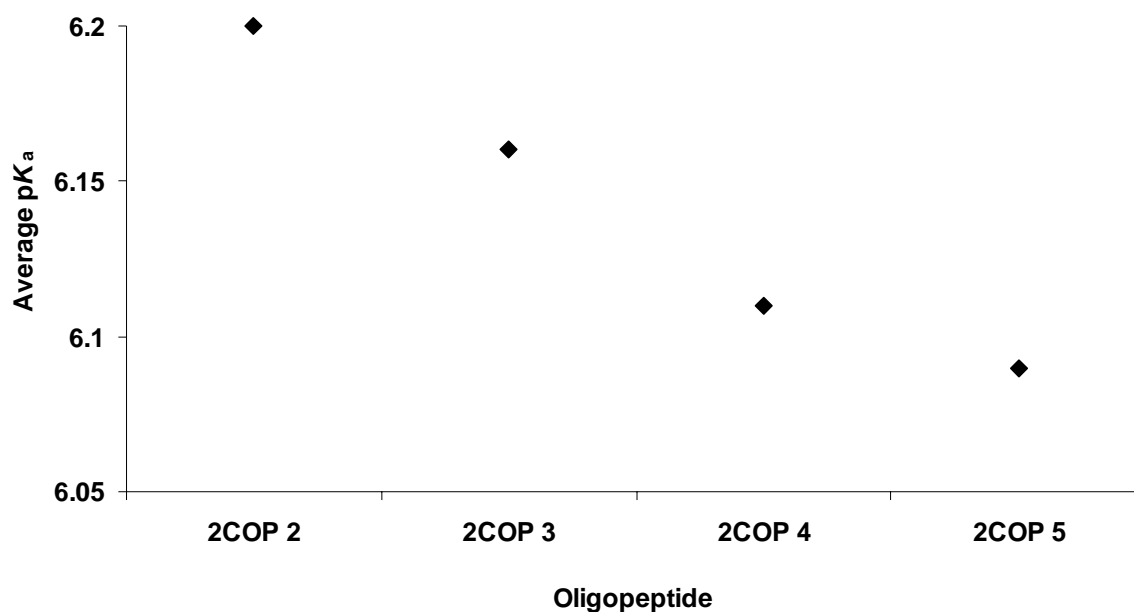


Figure 3.5. Average  $pK_a$  of histidine-containing oligopeptides

In addition, as can be seen in Figure 3.4, at physiological pH (pH 7.4) 2COP 1 is fully protonated as there is no chemical shift of  $H_\epsilon$  at pH less than 8, whereas there is only partial protonation in 2COPs 2-6. Furthermore, the 2COPs 2-6 are still not fully protonated at endosomal pH (pH ~5), suggesting that 2COPs 2-6 will have a buffering capacity in the endosome leading to endosomal disruption *via* the proton sponge mechanism.<sup>[4]</sup>



### 3.4.3 Formation and characterization of reducible polycations (RPCs) (Figure 3.1, Step 2, 3)

2COPs **1-6** were oxidative polymerized to form linear polymers *via* disulfide bond formation (referred to reducible polycations, RPCs) (section 2.5.1). The polymerization is shown for 2COP **2** in **Figure 3.6**.

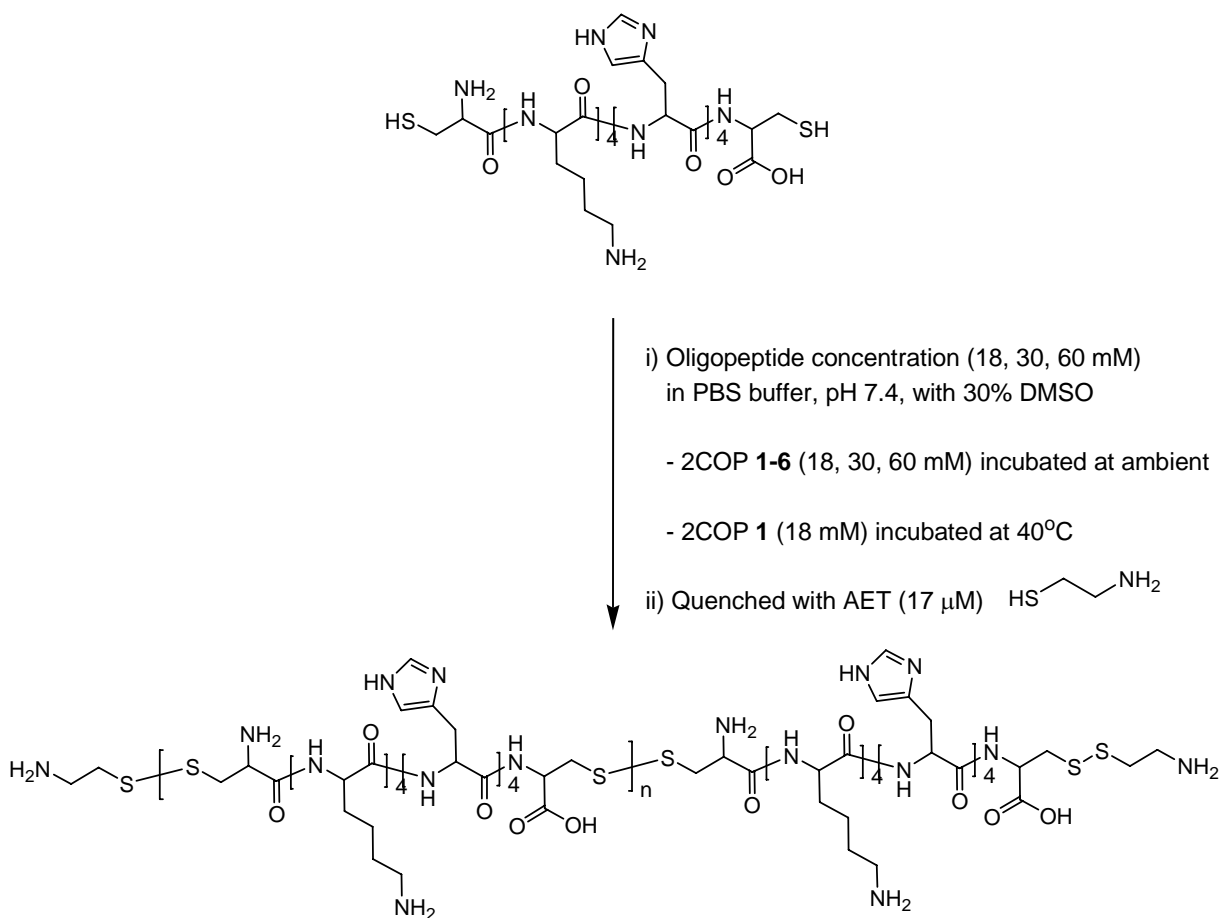


**Figure 3.6.** The oxidative polymerization procedure of 2COP **2** ( $\text{CK}_4\text{H}_4\text{C}$ )

We investigated for 2COPs **1-6** the effect of concentration of the oligopeptides on the degree of polymerization, and for 2COP **1**, we investigated the effect of temperature (ambient and 40°C)

The growth of the RPCs molecular weights was monitored by gel permeation chromatography (GPC) (section 2.5.4). At various time intervals 5  $\mu$ l aliquots were removed and quenched with aminoethanethiol (AET, 17  $\mu$ M, 40  $\mu$ l). This aliquot was analysed by GPC eluting with 200 mM NaCl with 0.1% TFA, in order to get the molecular weight against PLL standards (5.6, 8.3, 21.3, 62.1 and 128.5 kDa). The GPC chromatogram examples of some polymerization reactions are shown in the appendix (**Figure 8.28-8.30**).

#### *3.4.3.1 Polymerization as a function of oligopeptide concentration*

The polymerizations were performed at three 2COP concentrations (18, 30 and 60 mM (ambient temperature)) and the molecular weights were determined as a function of time. This data is shown in **Figure 3.7**. Due to the nature of the step growth polymerization mechanism,<sup>[25]</sup> in which monomers react to form dimers, then trimers, oligomers and finally long chain polymers, unsurprisingly, to produce the higher the molecular weight of the RPCs the higher concentration of 2COPs is needed in order to increase the chance of interacting to the adjacent monomers. At 2COP concentrations of 18, 30 and 60 mM, the relative conversions are 40, 60 and 80 %, respectively (data not shown). We propose at the lower 2COP concentration there may be a competing oxidation forming R-SO-O<sup>-</sup>,<sup>[26,27]</sup> resulting in the lower polymerization yields, for example, at lower peptide concentration reaction there is more chance of thiol groups to be oxidized to R-SO-O<sup>-</sup> which resulted in less conversion of monomers. All 2COPs showed the same general pattern of the RPC growth. During the first 12 hr the RPC molecular weight grew slowly and increased rapidly after 12 hr. The maximum molecular weight of the RPCs generally reduced after 36 hrs.

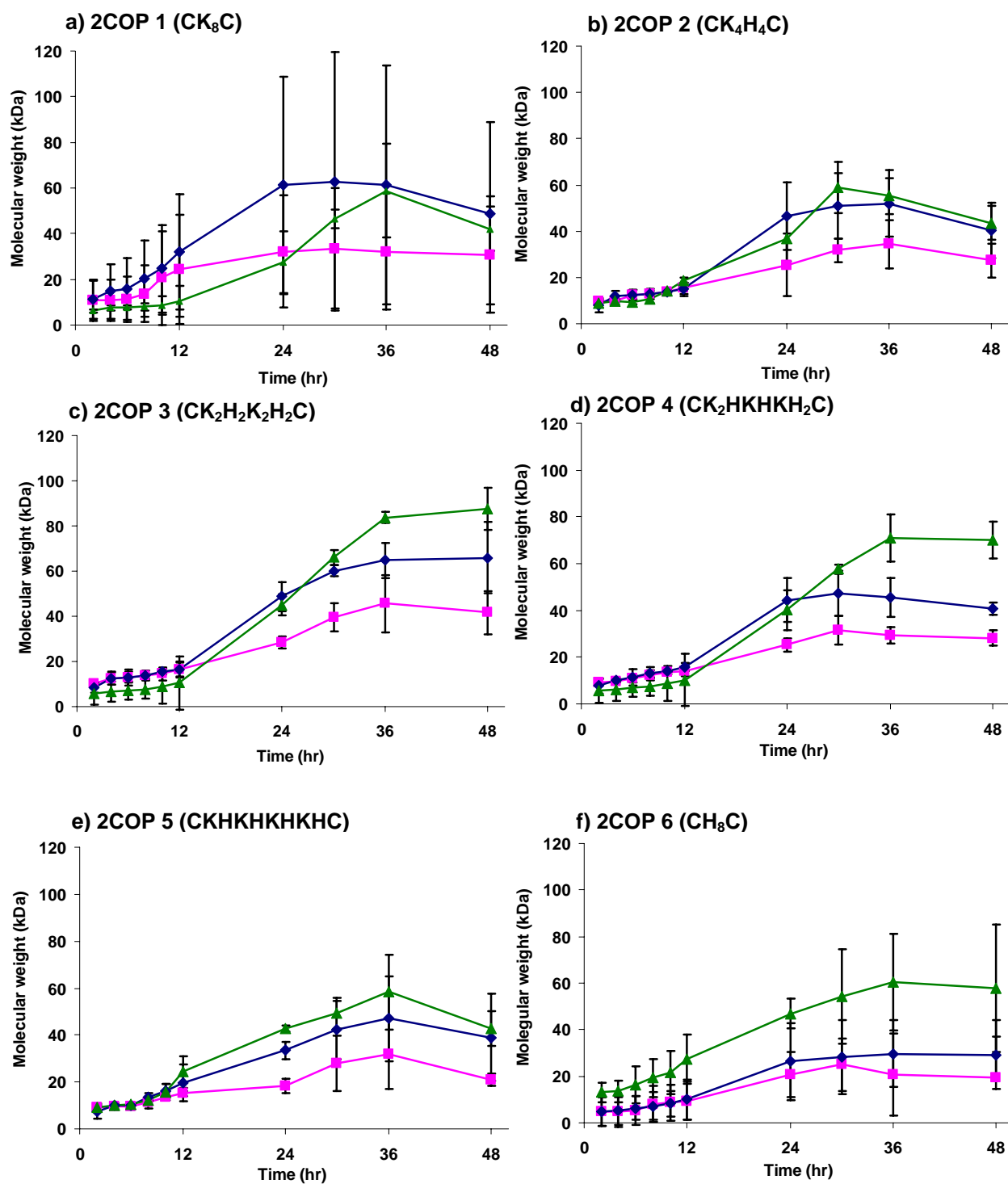


**Figure 3.7. Oxidative polymerization of 2COPs (bis-cysteine containing peptides) at various peptide concentrations incubated at ambient. [18mM —■—, 30mM —◆— and 60mM —▲—]**

The molecular weight was analyzed by GPC using PLL at 5.6, 8.3, 21.3, 62.1 and 128.5 kDa as standard curve (all data are an average of the triplicate experiments).

The maximum RPC molecular weight for all 2COPs at 18 mM, 30mM and 60mM are approximately 25-45, 30-65, and 50-90 kDa, respectively, as can be seen in **Figure 3.8**.

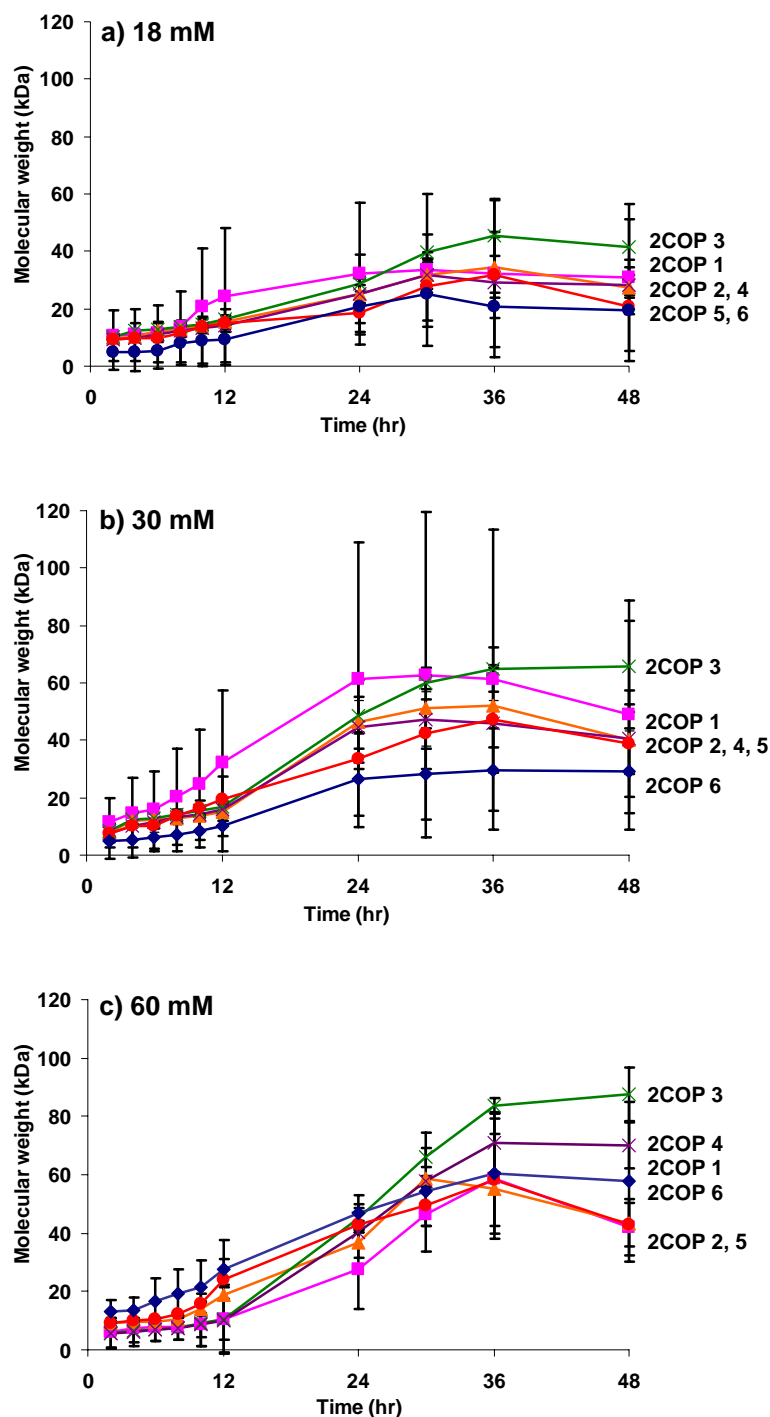


**Figure 3.8.** Oxidative polymerization compared between all 2COPs at different concentrations incubated at ambient. All data are an average of triplicate experiments.

[peptide 1 —■—, 2 —▲—, 3 —×—, 4 —×—, 5 —●—, and 6 —◆—]

### 3.4.3.2 Polymerization as a function of temperature for 2COP 1 (ambient and 40 °C)

The reaction mixtures were incubated at ambient and 40°C. Unsurprisingly the polymerization at 40°C proceeds more rapidly than that at ambient, reaching a molecular weight of approximately 45 kDa after 4 hr, followed by a decrease in molecular weight (~25% over 70 hrs) (**Figure 3.9a**). The ambient polymerization reaches approximately the same maximum molecular weight, but after ~24 hr, at which point there is 3% decrease of the RPC molecular weight. Both temperatures proceed only to ~37% (40°C) and 41% (ambient) yield (**Figure 3.9b**). The remaining ~60% of material that is eluted has a retention time of 2COP 1. The GPC chromatograms are shown in the appendix (**Figure 8.30**).

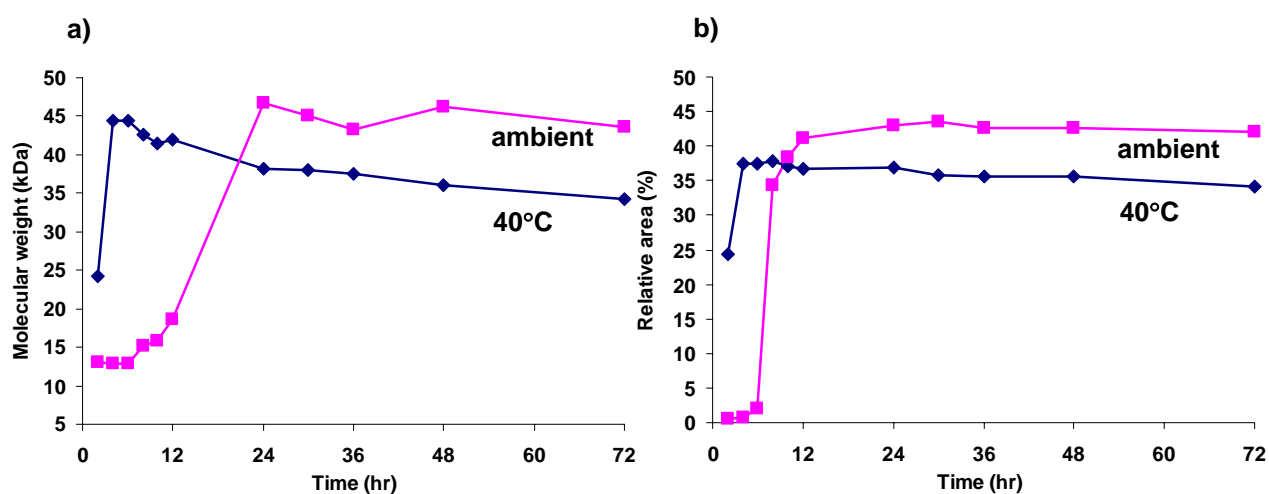


Figure 3.9. Oxidative polymerization of 2COP 1 (CK<sub>8</sub>C) at 18 mM concentration reacted at ambient —■— and 40°C —◆— ; a) molecular weight growth, and b) relative area of polymer yield

#### 3.4.3.3 *RPCs stability in HEPES buffer*

The purified RPCs were stored in the HEPES buffer at -20°C for a period of 2-3 days and then reanalyzed by GPC. All the RPCs were stable, except for the RPC formed from 2COP 6, which degraded to form a material of molecular weight less than 10 kDa (data not shown).

#### 3.4.4 **Formation and characterization of polyplexes**

The polyplexes were prepared by mixing the plasmid DNA (pCMV-Luc or pEGFP-C1) in HEPES buffer with the vectors (RPCs or oligopeptides) in HEPES buffer. The ratio of protonated basic groups (lysine and imidazole) of the vectors to the negative phosphate group on the DNA backbone is defined as the N:P ratio. Previously, RPCs (RPC(59) (CH<sub>3</sub>K<sub>3</sub>H<sub>3</sub>C, 59 kDa) and RPC (113) (CH<sub>6</sub>K<sub>3</sub>H<sub>6</sub>C, 113 kDa)<sup>[8]</sup> revealed an N:P ratio of 5:1 gave polyplexes of ~100 nm diameter, which were non toxic to cells (95% cell viability). Therefore, the experiments here were carried out at N:P ratio of 5:1, with controls PLL and PEI at N:P ratios of 5:1 and 10:1, respectively, as these represented the most effective system in the literature.<sup>[28,29]</sup> High N:P ratios were not tested for toxicity and transfection because N:P ratios greater than 10:1 lead to high level of cell death and result in decrease in transfection,<sup>[30]</sup> because of a high free concentration of the polycations.

##### 3.4.4.1 *Weight per charge and N:P ratio calculation*

The weight per charges (wpc) were calculated on the actual mass of the oligopeptides (2COPs), taking into consideration the counterion associated with the protonation of the

amino groups on the lysine and histidine residues at physiological pH. During the synthesis, the 10 mer peptides were deprotected in an acidic cocktail containing trifluoroacetic acid (TFA), which acts as the counterion forming a TFA salt. Therefore, the number of TFA counterions of 2COP **1-5** is 9, due to the TFA counterion forming a salt molecule with the 4 ammonium ions and 4 imidazolium ions of the 2COP backbone and the protonated N-terminus of the oligopeptide. The following calculation was used to determine the wpc of all oligopeptides in this study.

$$wpc = \frac{(MW \text{ of peptide}) + (\text{number of TFA counterions} \times MW \text{ of TFA})}{\text{number of protonated basic (lysine/histidine) groups at physiological pH}}$$

$$\text{MW of TFA} = 114 \text{ g/mol}$$

$$\text{TFA counterion} = \text{CF}_3\text{COO}^-$$

For example, in the case of 2COP **1** (CK<sub>8</sub>C), as can be seen in **Figure 3.4a**, there is no change in chemical shift of H<sub>ε</sub> at pH 7.4 which mean the amino groups on the side chain of lysine residues are fully protonated at physiological pH. Therefore, the number of positive amino groups of this 2COP **1** is 9.

In the cases of 2COPs **2-5**, the basic nitrogen atom on the imidazole rings of histidine residues are not fully protonated. However, there is a change in the chemical shift of H<sub>5</sub> and H<sub>6</sub> at pH 7.4, as can be seen in **Figure 3.4b-e**, which means there is a degree of protonation of the histidine side chain. Therefore, the number of protonated amino groups of the histidine based sequences was calculated from the average percentage of the chemical shift changing at pH 7.4 of H<sub>5</sub> (b) and H<sub>6</sub> (b') (**Figure 3.10**).

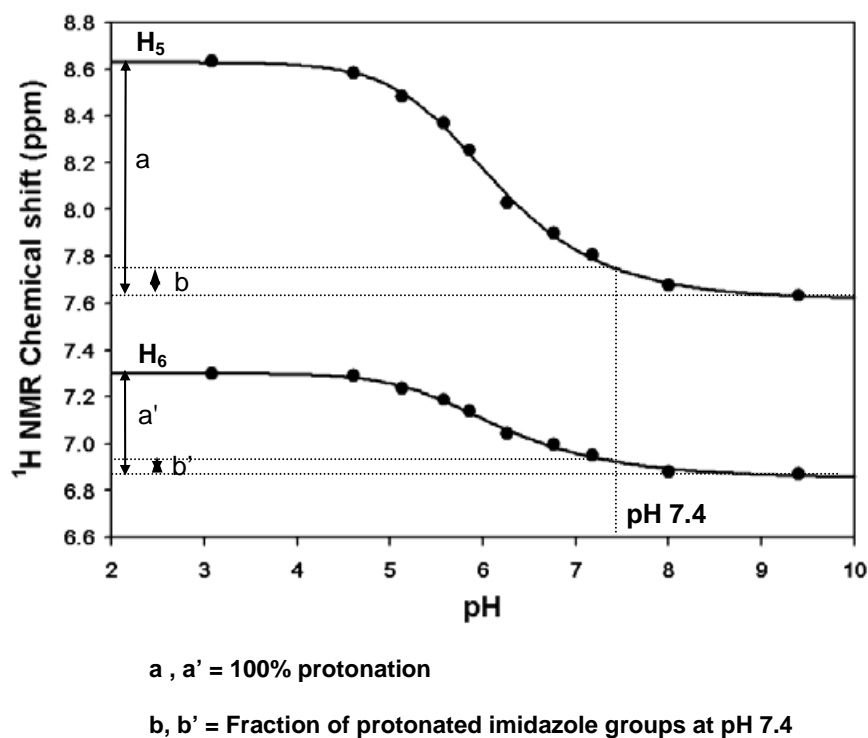


Figure 3.10. The chemical shift change between pH 2-10

Weight per charge (wpc) of 2COPs 1-5 is shown in Table 3.4.

Table 3.4. Weight per charge (wpc) of 2COPs

2COPs	Number of TFA counterions	Number of positive charges at pH 7.4	Peptide Mw (g mol <sup>-1</sup> )	wpc (g mol <sup>-1</sup> )
CK <sub>8</sub> C (1)	9	9	1249.90	252.8
CK <sub>4</sub> H <sub>4</sub> C (2)	9	5.7	1285.90	405.6
CK <sub>2</sub> H <sub>2</sub> K <sub>2</sub> H <sub>2</sub> C (3)	9	5.2	1285.70	444.6
CK <sub>2</sub> HKHKH <sub>2</sub> C (4)	9	5.4	1285.70	428.1
CKHKHKHKHKHC (5)	9	5.3	1285.80	436.2



The wpc value is used to calculate the N:P ratio, which is the number of possible protonatable basic groups with respect to the negative phosphate groups on the backbone of the nucleic acid. The concentration of 2COPs or RPCs calculated to form the polyplexes at final concentration of plasmid DNA at 20 µg/ml and at the N:P ratios used in this study is shown by the following equation.

$$\text{Peptides conc. } (\mu\text{g ml}^{-1}) = \frac{\text{Final concentration of plasmid DNA}}{\text{average mass of DNA per phosphate group}} \times N : P \times \text{wpc}$$

Final concentration of plasmid DNA = 20 µg ml<sup>-1</sup>

Average mass of DNA per phosphate group = 325 g mol<sup>-1</sup>

wpc = weight per charge

#### 3.4.4.2 RPC polyplex formation and characterization (**Figure 3.1, step 4-7**)

##### 3.4.4.2a Diameter and zeta potential of polyplexes (**Figure 3.1, Step 4-5**)

Polyplexes were formed from RPCs **1-5** as described in section 2.7.1 and 2.7.2 at N:P 5. PEI (25 kDa) and PLL (70 kDa) were used as controls to form the polyplexes at N:P 10 and 5 by leaving the condensation mixtures overnight at ambient temperature. The resultant polyplex dispersion was analyzed by zeta potential and dynamic light scattering (**Table 3.5**).

Zeta potentials were positive in all cases, which will allow the polyplexes to promote the internalization *via* syndecan-mediated endocytosis<sup>[31]</sup> (**Figure 1.22**) by electrostatic interaction between the positively charged polyplexes and the negatively charged cell membrane.

**Table 3.5. Properties of RPCs and their polyplexes**

RPCs/ polymer	Average $pK_a$	MW (kDa) <sup>a</sup>	Polydispersity index <sup>b</sup>	N:P ratio	Zetapotential (mV) <sup>c</sup>	Polyplex size (nm) <sup>d</sup>
RPC 1 (CK <sub>8</sub> C)	10.51	111.4	1.119	5	10.0 ± 10.9	132.1 ± 4.5
RPC 2 (CK <sub>4</sub> H <sub>4</sub> C)	6.20	118.0	1.142	5	14.3 ± 9.7	98.3 ± 0.6
RPC 3 (CK <sub>2</sub> H <sub>2</sub> K <sub>2</sub> H <sub>2</sub> C)	6.16	115.1	1.167	5	13.5 ± 7.2	99.8 ± 0.9
RPC 4 (CK <sub>2</sub> HKHKH <sub>2</sub> C)	6.11	102.9	1.063	5	5.8 ± 3.6	101.1 ± 2.8
RPC 5 (CKHKHKHKHC)	6.09	94.8	1.125	5	17.4 ± 11.3	95.5 ± 1.1
PEI	-	25	-	10	3.4 ± 0.2	108.7 ± 8.6
PLL	-	70	-	5	11.3 ± 9.0	81.0 ± 0.9

<sup>a</sup> Molecular weight of RPCs was analyzed by GPC using CATSEC300 column compared to PLL standard.

<sup>b</sup> Polydispersity index (PDI) of RPCs was measured by size exclusion chromatography (Anachem Ltd., Luton, UK) coupled with multi-angle laser light scattering photometer (Wyatt Technology (Santa Barbara, USA).

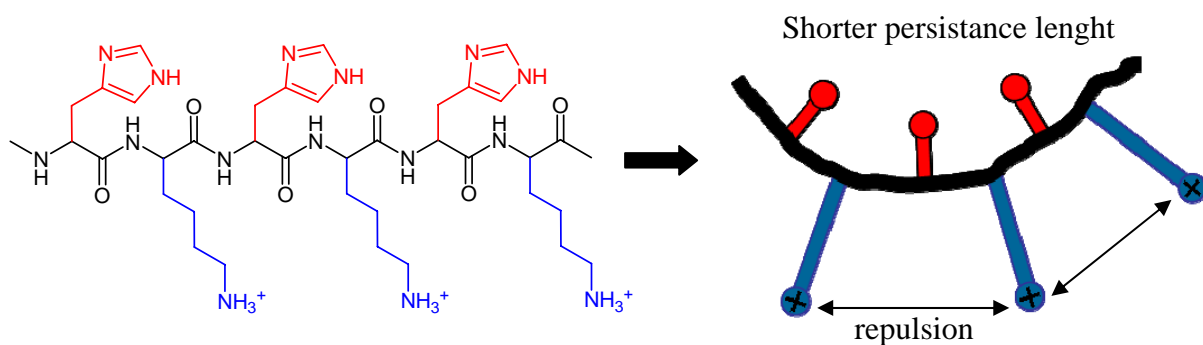
<sup>c</sup> Zetapotential was measured by using Zetamaster (Malvern Instruments, Worcestershire, UK).

<sup>d</sup> Hydrodynamic diameters of the polyplexes were measured by dynamic light scattering using a Zetasizer 3000 (Malvern Instruments, Worcestershire, UK).

The diameters by DLS for each RPC/DNA polyplex were in the range between 95.5-132.1 nm (**Table 3.5**). However, the polyplexes of RPCs 2-5 were all smaller than for RPC 1, suggesting better compaction through the introduction of histidine residues. On first inspection this result is counter-intuitive as RPC 1 is more highly charged and one might expect tight compaction, as a result of the greater electrostatic interaction. However, the incorporation of histidine residues, which are only slightly protonated at physiological pH (pH 7.4)(**Figure 3.4**) results in the polymer chains maybe having a shorter persistence length

(**Figure 3.11a**) that may result in better compaction of the histidine containing polyplexes over **RPC 1** with its more potentially rigid structure (**Figure 3.11b**).

**a) -Lys-His-Lys-His-**



**b) -Lys-Lys-Lys-Lys-**

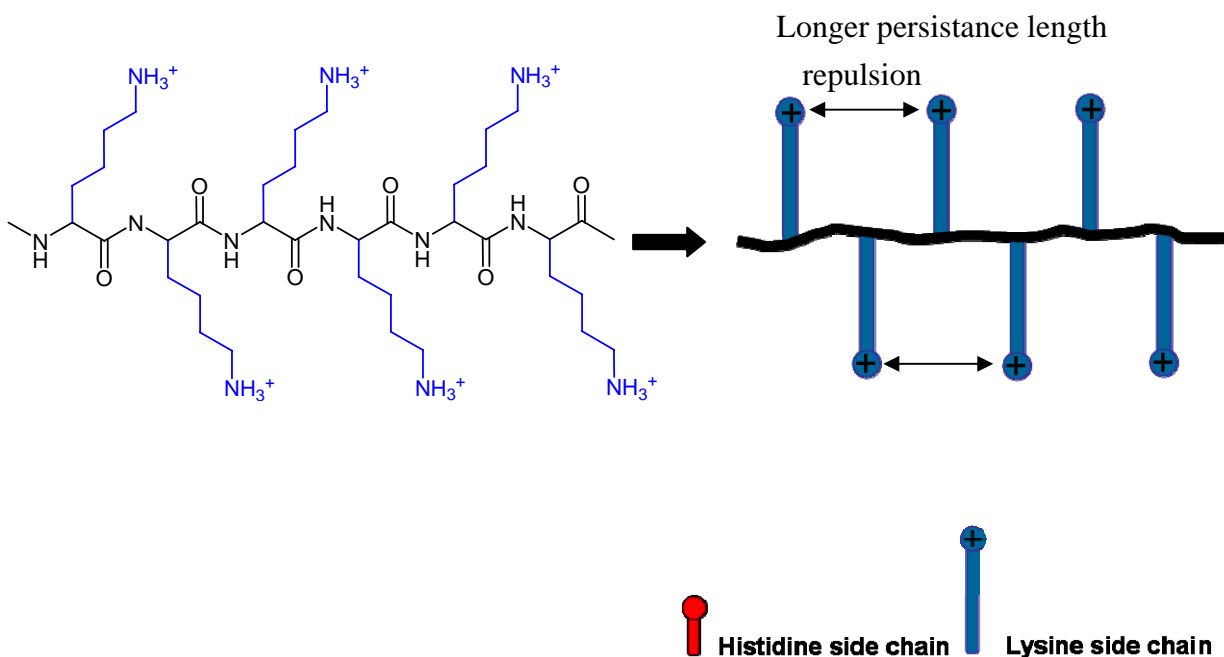


**Figure 3.11.** Length persistency of the lysine and histidine based sequences; a) -Lys-His-Lys-His and b) -Lys-Lys-Lys-Lys

3.4.4.2b Shape of polyplexes (**Figure 3.1, Step 5**)

Polyplexes imaged in a solution AFM cell on mica all revealed nanoparticulate matter with diameters as indicated by DLS. Comparing the AFM images for **RPC 1** (**Figure 3.12a** and **b**) against **RPC 2-5** (**Figure 3.12c-f**), it can be seen that **RPC 1** architectures are less symmetric

and appear to have a ‘halo’ around the bright core. These images would suggest and support the lower degree of compact for RPC 1, as its ‘halo’ is likely to be non-condensed DNA (see **Figure 3.16** and associated text).

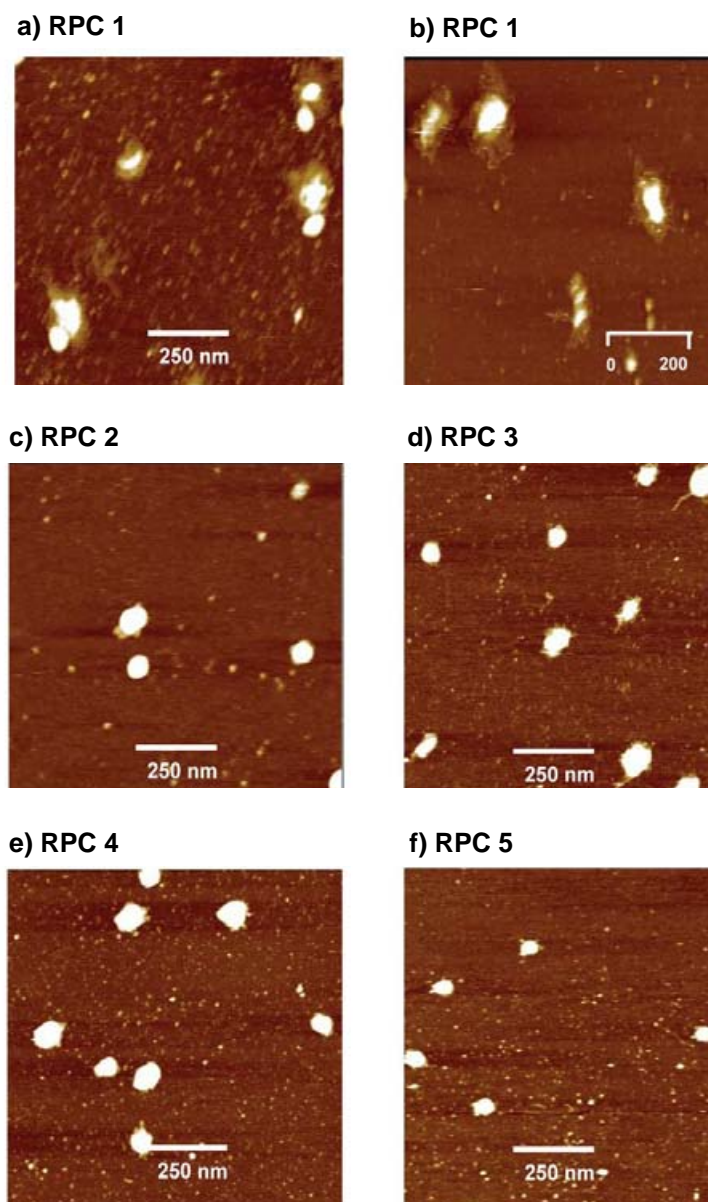


**Figure 3.12.** Aqueous phase atomic force microscopy of RPCs polyplexes at N:P 5. Images show polyplexes of pEGFP-C1 with (a,b) RPC 1; (c) RPC 2 ; (d) RPC 3 ; (e) RPC 4 ; and (f) RPC 5. Note that RPC 1 polyplex (CK<sub>8</sub>C) displays several morphologies consistent with the more rigid structure of the fully protonated polylysine backbone at pH 7.4, as seen clearly in plate b) at higher magnification. (Studied by Mahmoud Soliman at School of Pharmacy, University of Nottingham, UK)

#### 3.4.4.2c Extracellular stability studies of polyplexes (**Figure 3.1, Step 6**)

The stability of polyplexes can be investigated by studying the polyelectrolyte exchange reaction. The simple method to determine the stabilisation of polyplexes is to evaluate the susceptibility to disruption by polyanions. Therefore, polyaspartic acid (PAA) was used as a model polyanions to investigate the stability of polyplexes against polyelectrolyte exchange reaction. <sup>[32,33]</sup> The results (**Figure 3.13**) without PAA all RPCs, PEI and PLL were able to form stable polyplexes as shown by no loss of DNA in the gel electrophoresis assay (**lane a1-g1**). Furthermore, the polyplexes formed with RPCs **2-5** were found to be stable even after incubating with PAA (**lane b2-e2**), and were more stable than the polyplex formed with RPC **1** (**lane a2**), PEI (**lane f2**) and PLL (**lane g2**). The rationale of lower stability of RPC **1** (slightly released DNA with PAA, **lane a2**) fits with the hypothesis of the higher length persistency of the polymer chain resulting in less compaction with DNA (as described in **section 3.4.4.2a** and **Figure 3.11**) leading to PAA competitively replacing the DNA with greater than RPC **2-5**. Thus, RPC/DNA binding is not entirely due to electrostatic interaction, but also due to some steric contribution, such as molecular entanglement.

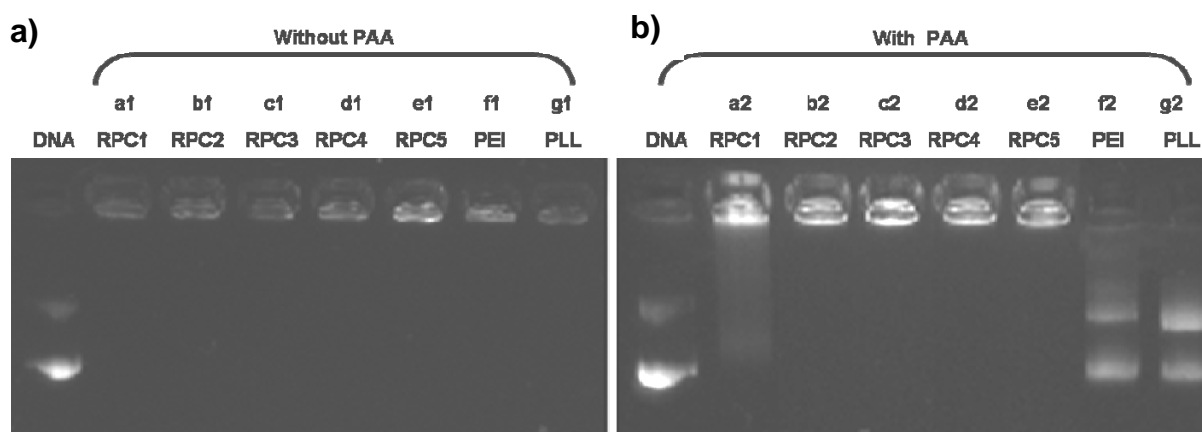


**Figure 3.13.** Gel shift assay with (a) and without (b) polyaspartic acid (PAA) of polyplexes formed from RPCs 1-5 (N:P 5), PEI (N:P 10) and PLL (N:P 5). Polyaspartic acid at 250 times of DNA concentration was mixed into the polyplex solution. Lanes a1-g1 on the left panel are for polyplexes without incubating with PAA. Lanes a2-g2 on the right panel are for polyplexes incubated with PAA. pCMV-Luc was used to run as standard DNA. Agarose gel electrophoresis was run using 1% agarose gel with EtBr (0.5  $\mu$ g.ml) at 110 V for 60 mins in 0.5x TBE buffer.

#### 3.4.4.2d Intracellular reduction studies of polyplexes (Figure 3.1, Step 7)

##### (i) Gel shift assay with salt and GSH

Another key aspect of the vector design criteria was the inbuilt release mechanism aimed at destabilising vector-DNA association through the cleavage of the disulfide bonds forming the polypeptide. Thus, the stability against physiological concentrations of salt and a biological reducing agent, glutathione, was assessed. GSH is thought to be present in the cytoplasm at concentrations varying between 5-20 mM dependent on the cell cycle, thus 5 mM GSH was used in these studies.<sup>[34]</sup> Gel electrophoresis assays were carried out on polyplexes with NaCl (0.15, 0.5 and 1 M) to evaluate primary binding stability in the presence of electrolytes, with GSH and GSH with NaCl to assess polyplex destabilisation (Figure 3.14).

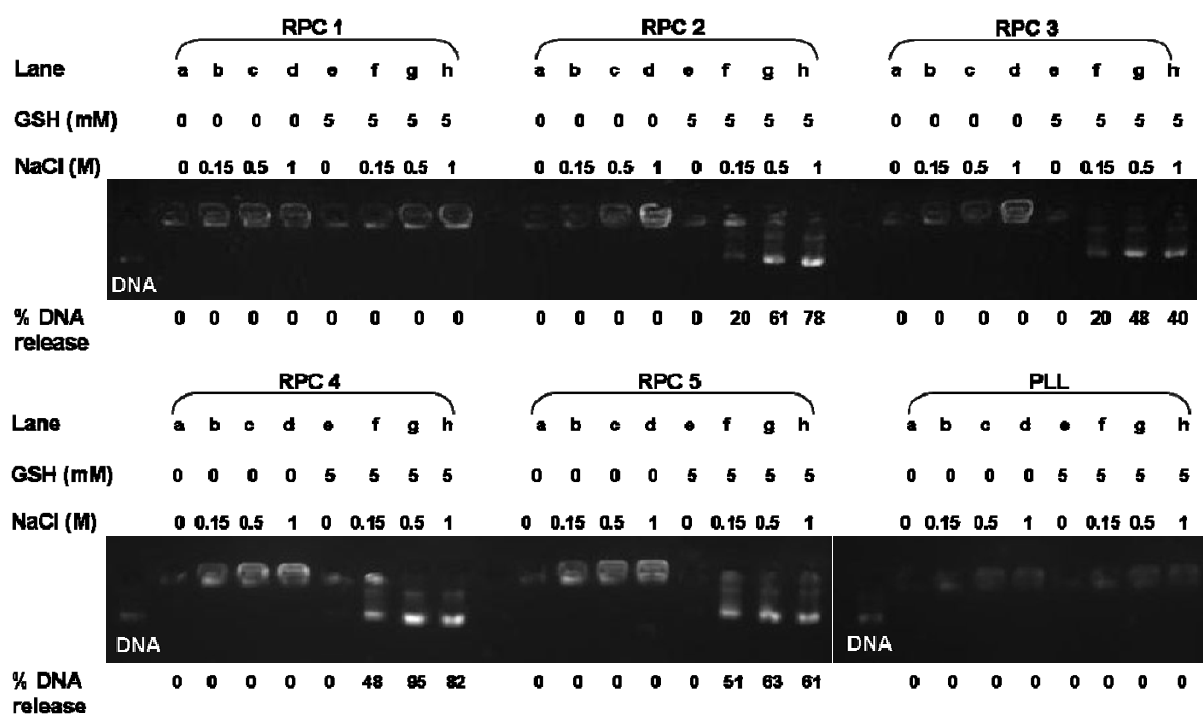


**Figure 3.14.** DNA binding and release demonstrated by agarose gel electrophoresis (gel shift assays). All polyplexes formed at N:P 5. Top panel: polyplexes of RPCs 1-3 with pDNA; bottom panel shows RPCs 4, 5 compared against non-cleavable polypeptide poly(lysine). Gel shift assays demonstrate tight binding of DNA and stability to dissociation by NaCl solutions (lanes a-d for all RPCs) but release of DNA following addition of GSH (lanes f-h) for RPCs 1-5. Agarose gel electrophoresis was run using 1% agarose gel with EtBr (0.5 µg.ml) at 110 V for 60 mins in 0.5x TBE buffer

The percentage of DNA release against salt concentration in the presence of GSH (5 mM) in plotted in **Figure 3.15**.

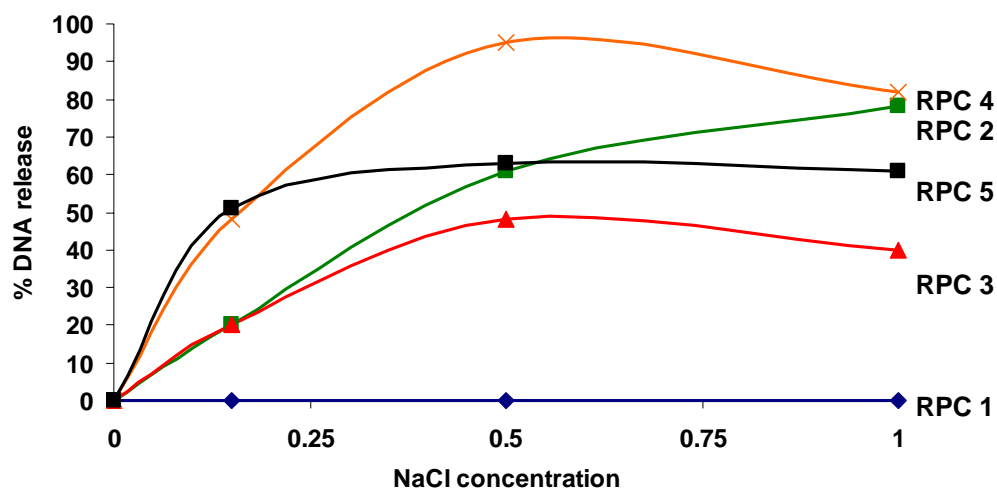


**Figure 3.15.** Percentage of DNA release from RPCs 1-5 after incubating with GSH (5mM) in combination with NaCl (0, 0.15, 0.5 and 1 M)

[RPC 1 —◆— , RPC 2 —■— , RPC 3 —▲— , RPC 4 —×— , RPC 5 —■— ]

These gel shift assays reveals

(a) RPC 1 produced polyplexes that were both stable in salt alone and GSH alone. Data presented later (**Figure 3.16**) suggested that the GSH does indeed cleave the RPC 1. Thus we concluded the short oligopeptide 2COP 1 that probably results, after GSH treatment, binds strongly to DNA, and therefore does not release it in the gel. Indeed even salt and GSH in combination does not release the DNA from RPC 1/2COP 1 (**Figure 3.15**). This result is in contrast to RPCs 2-5 (described below) presumably due to the higher charge of 2COP 1, that results in much stronger electrostatic binding to the DNA.

(b) RPCs 2-5 produced the polyplexes that were stable in salt (0.15-1 M) as can be seen from **lanes b-d** of RPCs 2-5. Furthermore, these RPCs polyplexes were also stable in GSH alone (5mM) (**lane e** of RPCs 2-5). Importantly, however, addition of GSH (5mM) in the presence of salt destabilised the polyplexes, leading to



release of the DNA in all cases (**lane f-h** of RPCs **2-5** and **Figure 3.15**). Thus, the combination of GSH under physiological salt concentrations was able to both cleave the polydisulfide bonds in the polyplexes leading to lower a molecular weight peptides that had a lower affinity for the DNA in the salt solution, leading to disassociate of the polyplexes.

(c) poly L-lysine (PLL), the non-cleavable RPC **1** analogue, used as a control, was found not to release DNA in salt alone, GSH alone and in combination as can be seen in **lanes b-d, e** and **f-h of PLL**, respectively, as would be expected.

*(ii) AFM analysis of degradation by GSH*

Disassembly of the polyplexes under reducing conditions was apparent in aqueous phase AFM imaging in the presence of GSH. Polyplexes formed from RPC **1** with pEGFP-C1 were imaged sequentially following the addition of the reducing agent and marked changes were observed in the structures of the individual polyplexes over a period of 220 minutes (**Figure 3.16 a-d**). Initially the polyplexes appeared a compact spherical structure (**Figure 3.16a**). However, after 25 minutes expose to GSH (20mM), the polyplexes became less dense, and DNA strands were observed to protrude from the core (**Figure 3.16**). After prolonged times (**Figure 3.16c-d**), a DNA ‘halo’ is visible and the core area is diminished, although complete DNA release is not observed for RPC **1**. This ‘halo’ suggested that interactions of the cationic components with DNA were diminishing with time, and that condensation of the DNA by the vector components was less effective, in line with the earlier gel shift results, which suggest disulfide bond cleavage.

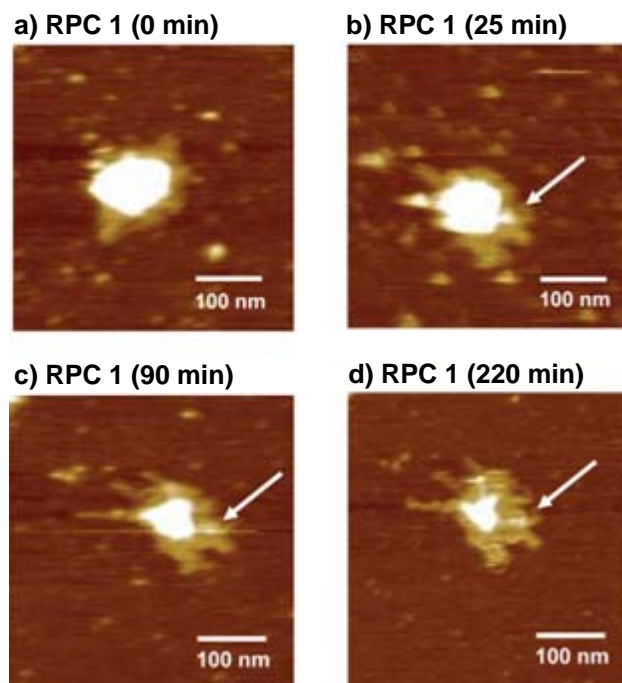


**Figure 3.16.** Aqueous phase atomic force microscopy of RPC 1 polyplexes at N:P 5 showing effect of reduction by GSH (20 mM). Images (a-d) show individual RPC 1-pEGFP-C1 polyplexes immediately after addition of glutathione and after 25, 90 and 220 minutes, respectively. (Studied by Mahmoud Soliman at School of Pharmacy, University of Nottingham, UK)

Polyplexes formed from RPC 2 and 3 with pEGFP-C1 were also imaged before (**Figure 3.17a** and **c**) and 4 hrs after addition of GSH (20 mM) (**Figure 3.17b** and **d**). Polyplexes are fewer in number after incubating with GSH for both RPCs, and strands of free DNA are visible for both RPCs after incubating with GSH (images **b,d** arrows).

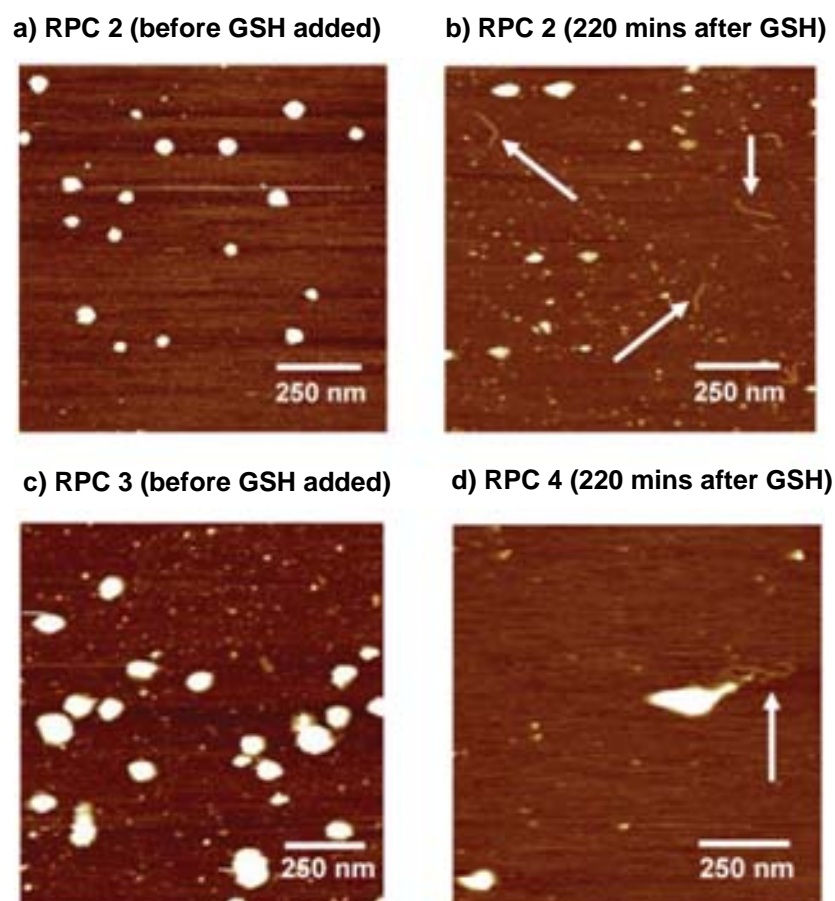


**Figure 3.17.** Aqueous phase atomic force microscopy of RPC 2, 3 polyplexes at N:P 5 showing effect of reduction by GSH (20 mM). Image (a,b) and (g,h) depicts RPC 2 and RPC 3 polyplexes with pEGFP-C1, respectively, before GSH added and after 220 minutes of incubating with GSH. (Studied by Mahmoud Soliman at School of Pharmacy, University of Nottingham, UK)

The control experiments with non-cleavable PLL vectors did not show polyplex breakdown under the same conditions (NaCl, GSH) over a time period of 223 minutes (**Figure 3.18**). Compared to RPC 1 in **Figure 3.16**, the core area of PLL polyplex did not diminish with time, as would be expected there are no disulfide bonds that the GSH might cleave.

Thus, the gel shift assay (**Figure 3.14**) and AFM data have established RPCs 2-5 vectors release the DNA under physiological reducing conditions, whereas RPC 1 and PLL do not.

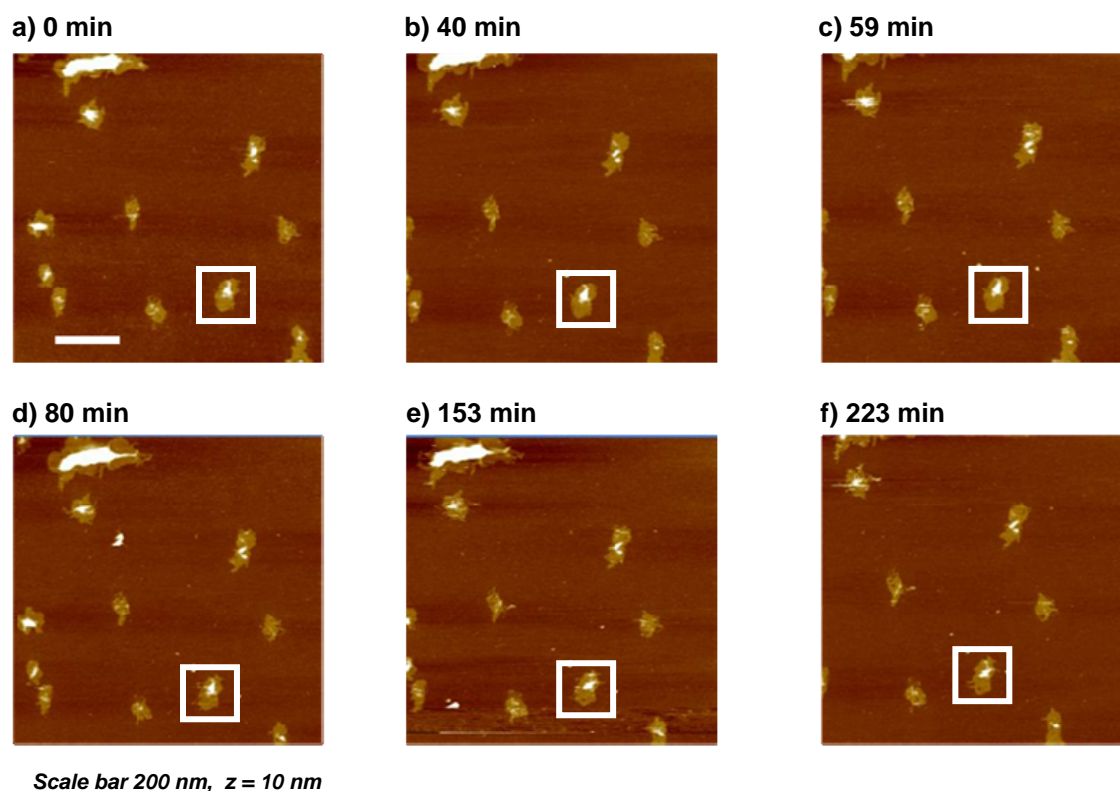


**Figure 3.18.** Aqueous phase atomic force microscopy of PLL/DNA polyplexes at N:P 5 showing effect of reduction by GSH (20 mM) at the different times. (Studied by Mahmoud Soliman at School of Pharmacy, University of Nottingham, UK)

*(iii) Dynamic light scattering analysis of degradable by GSH*

Further confirmation of RPCs polyplex breakdown under reducing conditions was obtained by dynamic light scattering after incubating RPCs polyplexes with GSH (20mM) over a time period of 210 minutes (**Figure 3.19**).

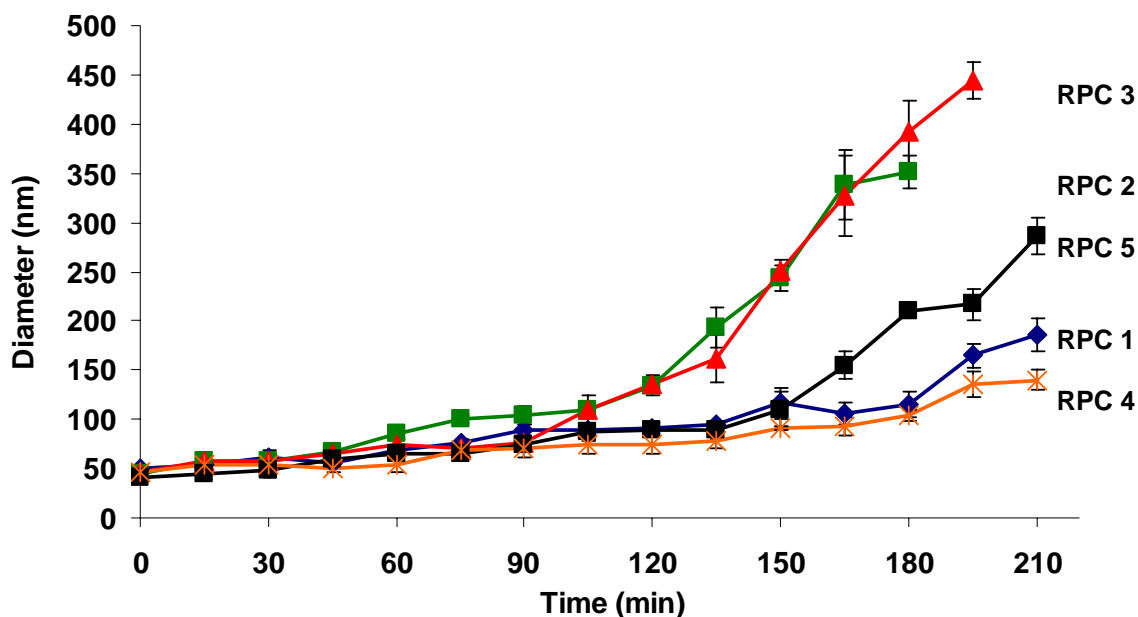


Figure 3.19. Diameters of RPC polyplexes 1-5 following incubation with 20 mM glutathione

[RPC 1—◆ , RPC 2—■ , RPC 3—▲ , RPC 4—× , RPC 5—■ ]

The model in **Figure 3.20** explains why this should occur. The GSH cleaves the disulfide bonds and leads to unpacking of the polyplexes and thus expansion. This model is corroborated with the DLS experiments (**Figure 3.19**).

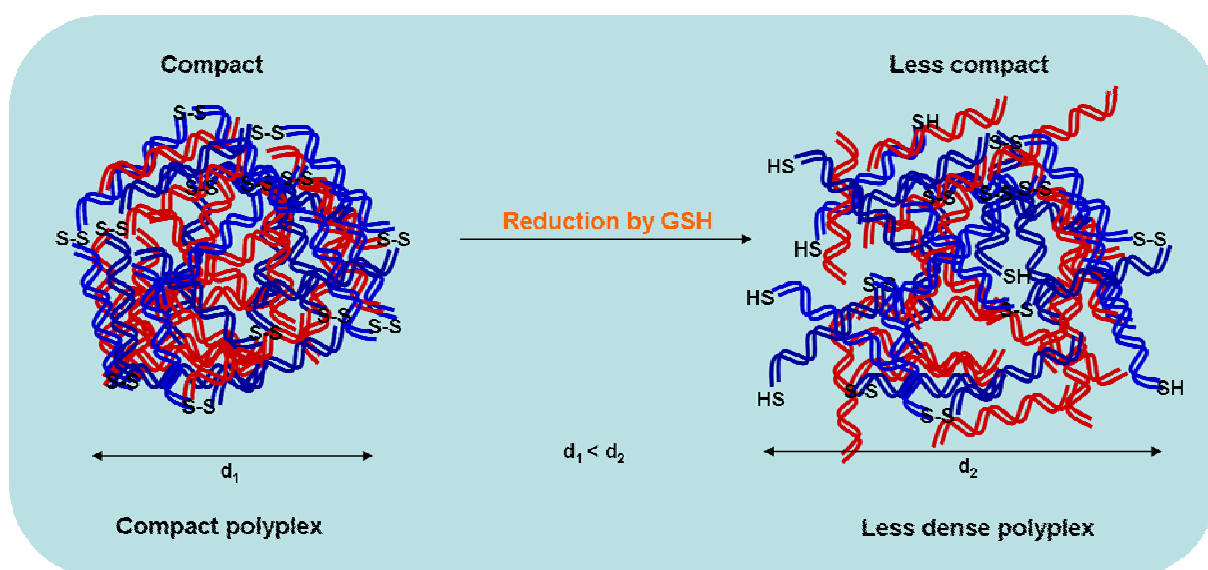


Figure 3.20. Model of polyplex reduction by GSH

In summary, the PLL polyplex is disassembled by PAA (**Figure 3.21a**) to a greater extent than **RPC 1** (**Figure 3.21b**). Presumably, this is because PLL has a higher persistence length than **RPC 1**. This reduction in persistence length of **RPC 1** is a result of the reduction in charge repulsion of the protonated lysine groups either side of the reducible disulfide bond from the cysteines, allow the s-s bond to act as a molecular hinge. Whereas, **RPCs 2-5** are stable to PAA (**Figure 3.21c**) because of the greater compaction of the polyplexes, which we hypothesized, is a result of the lower persistence length of **RPCs 2-5** over **RPC 1** and PLL.

PLL polyplex is unable to be disassembled by GSH and NaCl due to the lack of the disulfide bonds (**Figure 3.21a**). **RPC 1** polyplex is cleaved by GSH (**Figure 3.21b**). However, the short **2COP 1** that results still binds strongly to the DNA resulting in it being unable to release the DNA. **RPC 2-5** polyplexes are cleavable by GSH and NaCl and the resulting **2COPs** are less strongly bound to the DNA, than **2COP 1**, and hence the DNA is released (**Figure 3.21c**).

Therefore, with these stability models, **RPCs 2-5** could be promising vectors for non-viral gene delivery system.

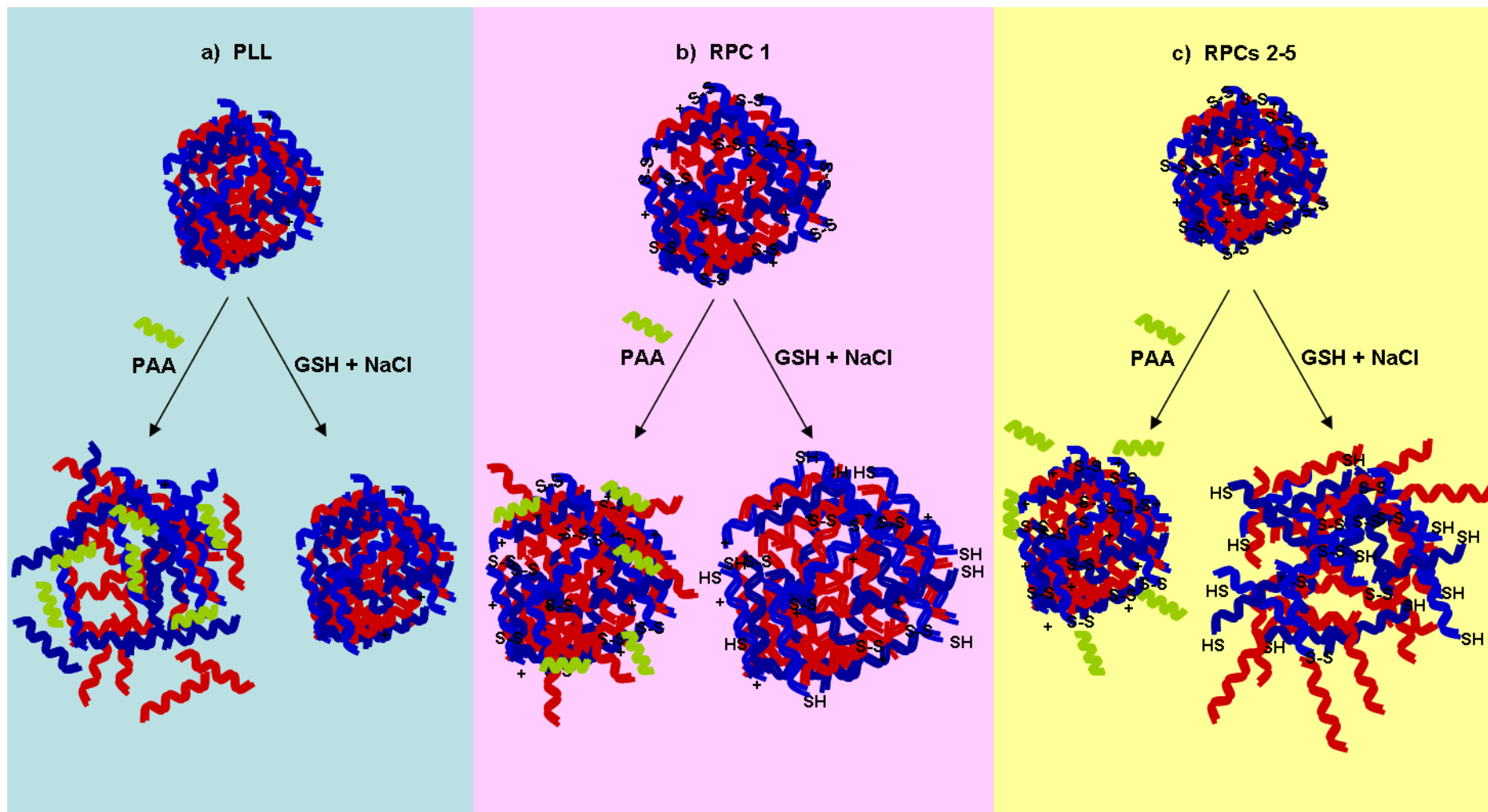


Figure 3.21. The models of PLL and RPC polyplexes after treating with PAA or GSH+NaCl: a) PLL, b) RPC 1 and c) RPCs 2-5

3.4.4.3 Formation of polyplexes with lower molecular weight RPCs (**Figure 3.1, step 4-7**)

3.4.4.3a Diameter and zeta potential of polyplexes (**Figure 3.1, Step 3-4**)

DNA polyplexes were prepared from the lower molecular weight (~50 kDa) RPCs at N:P ratio 5 in order to compare their properties with the high molecular weight (~100 kDa) RPCs (**Table 3.6**).

**Table 3.6. Properties of RPCs at different molecular weight and their polyplexes formed at N:P 5**

RPCs	MW (kDa) <sup>a</sup>	Polydispersity index <sup>b</sup>	Diameter (nm) <sup>c</sup>	Zeta potential (mV) <sup>d</sup>
RPC 1	53.9	1.563	99.9 ± 8.3	16.8 ± 11.0
(CK <sub>8</sub> C)	111.4	1.119	132.1 ± 4.5	10.0 ± 10.9
RPC 2	60.8	1.339	98.4 ± 0.7	10.1 ± 14.0
(CK <sub>4</sub> H <sub>4</sub> C)	118.0	1.142	98.3 ± 0.6	14.3 ± 9.7
RPC 3	40.4	1.318	94.7 ± 1.5	15.5 ± 15.5
(CK <sub>2</sub> H <sub>2</sub> K <sub>2</sub> H <sub>2</sub> C)	115.1	1.167	99.8 ± 0.9	13.5 ± 7.2
RPC 4	48.5	1.279	101.1 ± 2.2	5.3 ± 5.7
(CK <sub>2</sub> HKHKH <sub>2</sub> C)	102.9	1.063	101.1 ± 2.8	5.8 ± 3.6
RPC 5	42.3	1.292	90.7 ± 3.4	12.6 ± 12.3
(CKHKHKHKHC)	94.8	1.125	95.5 ± 1.1	17.4 ± 11.3

<sup>a</sup> Molecular weight of RPCs was analyzed by GPC using CATSEC300 column compared to PLL standard.

<sup>b</sup> Polydispersity index (PDI) of RPCs was measured by size exclusion chromatography (Anachem Ltd., Luton, UK) coupled with multi-angle laser light scattering photometer (Wyatt Technology (Santa Barbara, USA).

<sup>c</sup> Hydrodynamic diameters of the polyplexes were measured by dynamic light scattering using a Zetasizer 3000 (Malvern Instruments, Worcestershire, UK).

<sup>d</sup> Zetapotential was measured by using Zetamaster (Malvern Instruments, Worcestershire, UK).



As can be seen in **Table 3.6**, the diameters for all N:P ratios for each RPC/DNA polyplex at lower molecular weight were in the range between 90.7-101.1 nm, compared to the polyplexes produced from higher molecular weight RPCs were in the range between 95.5-132.1 nm. The polyplex diameters and zeta potential values of RPC polyplexes which formed from the RPCs at the different molecular weight were similar in all cases. Thus, revealing reduction in molecular weight of the RPCs greater than 50% do not affect the diameter and surface charge of the polyplexes.

#### 3.4.4.3b Extracellular stability studies of polyplexes (**Figure 3.1, Step 5**)

The extracellular stability of the polyplexes of lower molecular weight RPCs was also studied using the gel shift assay by incubating the polyplexes with polyaspartic acid (PAA) as shown in **Figure 3.22**. PEI polyplexes at N:P 10 and PLL polyplexes at N:P 5 were used as a control.

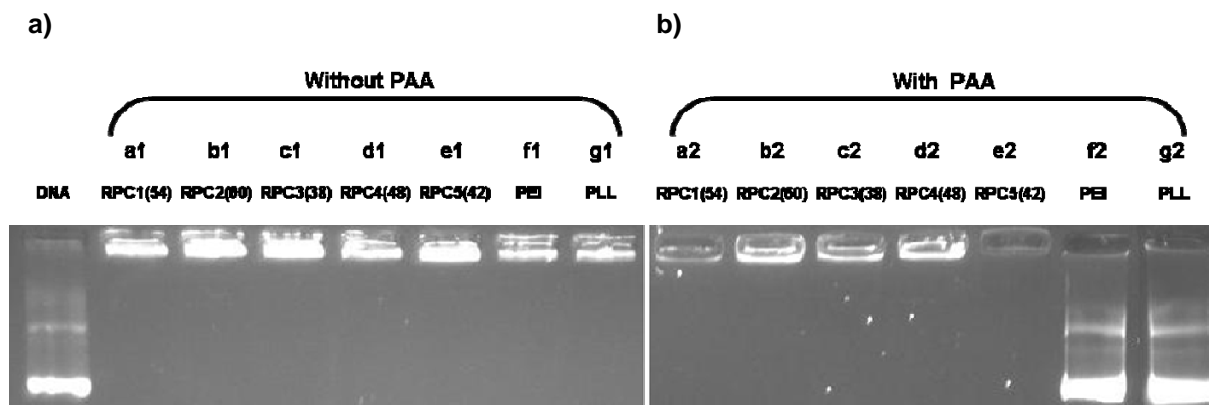


**Figure 3.22.** Gel shift assay with (a) and without (b) polyaspartic acid (PAA) of polyplexes formed from low molecular weight RPCs 1-5 (N:P 5), PEI (N:P 10) and PLL (N:P 5). Polyaspartic acid at 250 times of DNA concentration was mixed into the polyplex solution. Lanes a1-g1 on the left panel are for polyplexes without incubating with PAA. Lanes a2-g2 on the right panel are for polyplexes incubated with PAA. pCMV-Luc was used to run as standard DNA. Agarose gel electrophoresis was run using 1% agarose gel with EtBr (0.5  $\mu\text{g}.\text{ml}$ ) at 110 V for 60 mins in 0.5xTBE buffer.

The results revealed that all RPCs at low molecular weight were able to form stable polyplexes with DNA as no DNA was released (**lane a1-e1**). Furthermore, after incubating with PAA (**lane a2-e2**) they did not release DNA, and were more stable than the polyplex formed with PEI and PLL (**lane f2 and g2, respectively**).

#### 3.4.4.3c Intracellular reduction studies of polyplexes (**Figure 3.1, Step 7**)

Stability of the lower molecular weight RPCs polyplexes against physiological concentrations of salt and GSH, was assessed by gel electrophoresis by treatment with GSH alone (5 mM), salt alone (NaCl 0.15 and 0.5 M), and combination of salt (NaCl 0.15 and 0.5 M and GSH (5 mM) to assess polyplex destabilisation (**Figure 3.23**). PLL polyplexes at N:P 5 were used as controls. These gel shift assays demonstrate that:

(a) Polyplexes produced from lower molecular weight RPCs **2-5** slightly released the DNA when in the presence of GSH (5mM) without NaCl (**Figure 3.23, lane b**), suggesting that they are more easily reducible than polyplexes with higher molecular weight RPCs (**Figure 3.14, lane e**). However, these lower molecular weight RPCs polyplexes were stable in salt alone (0.15-0.5M) as can be seen in **Figure 3.23, lane c,d** which is similar to the high molecular weight RPC polyplexes (**Figure 3.14, lane b,c**). Importantly, however, addition of GSH (5mM) in the presence of salt destabilised the polyplexes, leading to a greater release of the DNA in all cases (**Figure 3.23, lane e-f**), relative to the higher molecular weight RPC polyplexes (**Figure 3.14, lane f,g**).

(b) RPC **1(54)** produced polyplexes that were stable in GSH alone, salt alone and a combination of both as can be seen in **lane b, c-d** and **e-f (Figure 3.23)**, respectively, and are similar to RPC **1(111)** (**Figure 3.14, lane a-h**). These results reveal that the molecular weight of RPCs in both cases does not affect the stability of polyplexes: Electrostatic interaction dominate the stability it would seem.

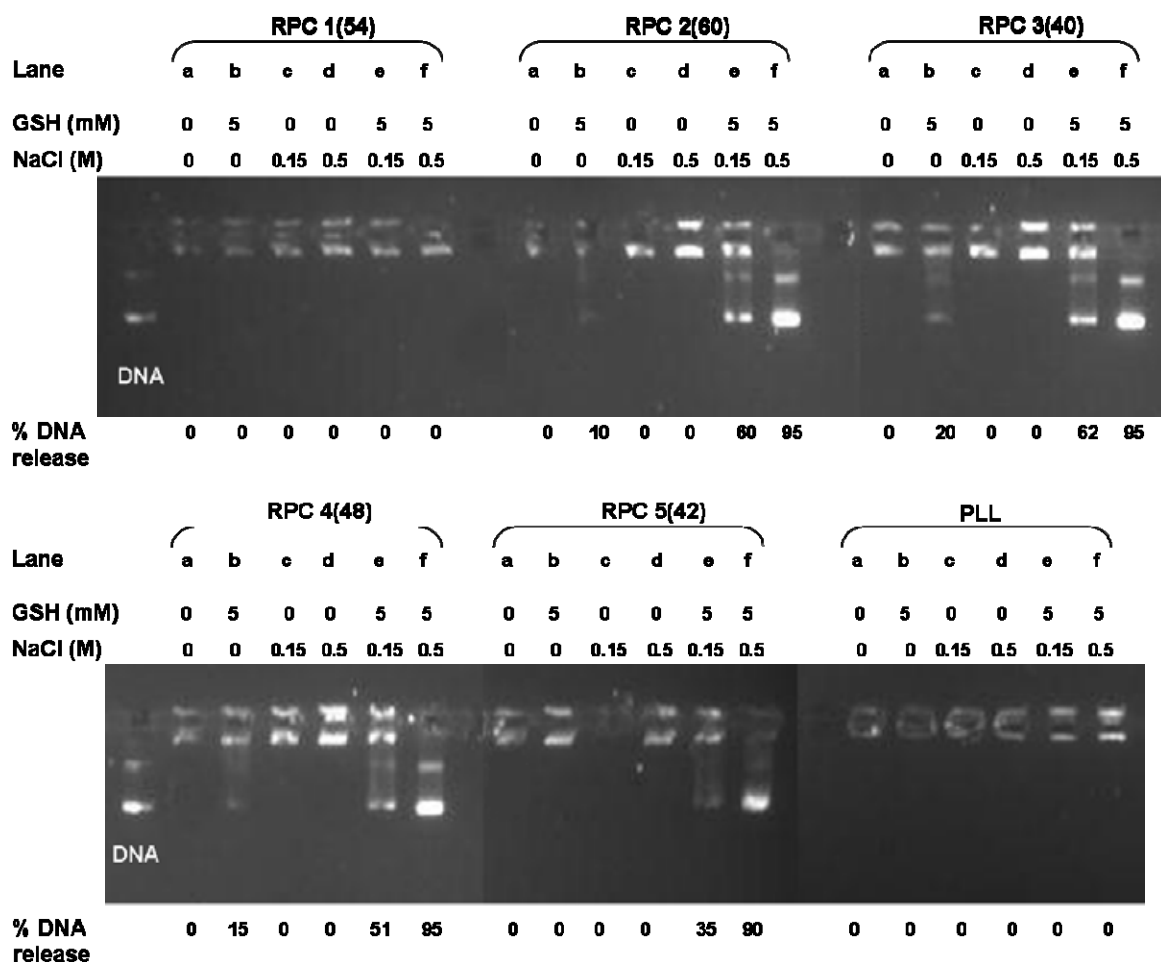


**Figure 3.23. DNA binding and release demonstrated by gel shift assays of low molecular weight RPC polyplexes.** All polyplexes formed at N:P 5. Top panel: polyplexes of RPC 1(54), RPC 2(60) and RPC 3(40) with pDNA; bottom panel shows RPCs 4(48), RPC 5(42) compared against non-cleavable polypeptide poly(lysine). Agarose gel electrophoresis was run using 1% agarose gel with EtBr (0.5  $\mu\text{g}/\text{ml}$ ) at 110 V for 60 mins in 0.5x TBE buffer

In combination, the diameters, surface charges and gel shift assays of polyplexes from low molecular weight RPCs 2-5 compared to high molecular weight RPCs 2-5 suggest that the low molecular weight RPCs could be promising vectors for gene therapy. However, the cell transfections of these polyplexes have to be further investigated to confirm (Chapter 4).

#### 3.4.4.4 *Oligopeptide polyplex formation and characterization (Figure 3.2a, Step 2-3)*

As shown in the previous section, the DNA polyplexes were synthesized from RPCs with molecular weight of approximately 100 kDa. In this section, the DNA polyplexes were formed from the oligopeptides (2COPs 1-5) in order to compare their properties with the associated RPCs polyplexes.

DNA polyplexes were formed from 2COP 1-5 at N:P ratio 5 as described in section 2.7.1 and 2.7.2. PEI (25 kDa) was also used to form polyplexes at N:P 10 as control. Briefly, the polyplexes were formed by mixing the oligopeptides in HEPES buffer and the DNA in HEPES buffer in the appropriate molar ratios. Diameter of the polyplexes were analyzed by dynamic light scattering (section 2.8.1) after approximately 6, 24 and 48 hr of the polyplex formation. The diameters of the polyplexes over the course of 48 hr are shown in **Table 3.7**.

**Table 3.7. Diameter of polyplexes from 2COPs 1-5 at N:P 5 and PEI at N:P 10 after 6, 24 and 48 hr of the formation.**

Polyplexes	N:P ratio	Diameter (nm) <sup>a</sup>		
		6 hr	24 hr	48 hr
2COP 1 (CK <sub>8</sub> C)	5	2848.0 ± 1500.0	1080.8 ± 135.2	741.6 ± 12.4
2COP 2 (CK <sub>4</sub> H <sub>4</sub> C)	5	5217.9 ± 1091.5	1563.7 ± 1103.6	7017.2 ± 10211.4
2COP 3 (CK <sub>2</sub> H <sub>2</sub> K <sub>2</sub> H <sub>2</sub> C)	5	8643.8 ± 3779.3	4438.7 ± 4186.8	2248.6 ± 2669.6
2COP 4 (CK <sub>2</sub> HKHKH <sub>2</sub> C)	5	4830.5 ± 640.7	2415.0 ± 990.6	2320.8 ± 1430.1
2COP 5 (CKHKHKHKHC)	5	7116.9 ± 2546.1	11399.1 ± 10939.3	2150.4 ± 2400.5
PEI	10	98.0 ± 3.8	126.1 ± 4.6	87.7 ± 1.2

<sup>a</sup> The hydrodynamic diameters of the polyplexes were measured by dynamic light scattering using a Zetasizer 3000 (Malvern Instruments, Worcestershire, UK).

As can be seen in **Table 3.7** the diameters of polyplexes reduced over the time course of 48 hrs. 2COP 1 formed the smallest polyplexes (~741 nm) compared to 2COPs 2-5 (greater than 1 µm diameter in most cases). The polyplexes formed from 2COP 1 are smaller than those from 2COPs 2-5 as a result of higher charged on 2COP 1. Compared to RPC polyplexes diameter (~100 nm), the 2COPs polyplexes are much larger suggesting that the 2COPs polyplexes are not suitable for use as vectors for gene delivery, because polyplexes that are larger than 1 µm more readily interact with blood components or fixed macrophages resulting in the clearance from the blood stream before reaching the cells.<sup>[35]</sup>

### 3.4.5 Formation and characterization of *cross-linked RPCs* (Figure 3.2b, step 2-3)

In this section, *cross-linked RPCs* were synthesized and characterized in order to compare their properties with the *linear RPCs*.

Bis-cysteine containing oligopeptides (2COPs **1-5**) were oxidative polymerized with tris-cysteine containing oligopeptide (3COP **7**) to form *cross-linked RPCs* via disulfide bond formation (section 2.5.2). The scheme of the cross-linking polymerization is shown in **Figure 3.24**.

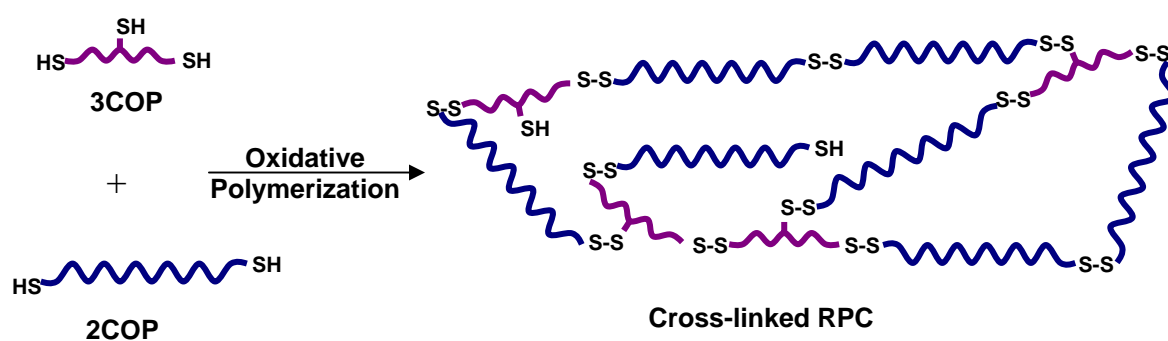


**Figure 3.24.** The model of cross-linking polymerization to form *cross-linked RPC* via disulfide bond formation

The reactions were performed at ambient temperature with 30mM concentration of 2COPs **1-5** containing 3COP **7** at 4% and 32 % mole fractions. The growth of the *cross-linked RPC* molecular weights was monitored by gel permeation chromatography (GPC) (section 2.5.4). At various time intervals 5  $\mu$ l aliquot were removed from the polymerization vessel and AET was added to terminate the polymerization. This aliquot was injected onto the GPC eluting with 200 mM NaCl with 0.1% TFA. The eluting time was used to determine the molecular

weight against calibration data from PLL standards 5.6, 8.3, 21.3, 62.1, and 128.5 kDa. This data is plotted in **Figure 3.25**.

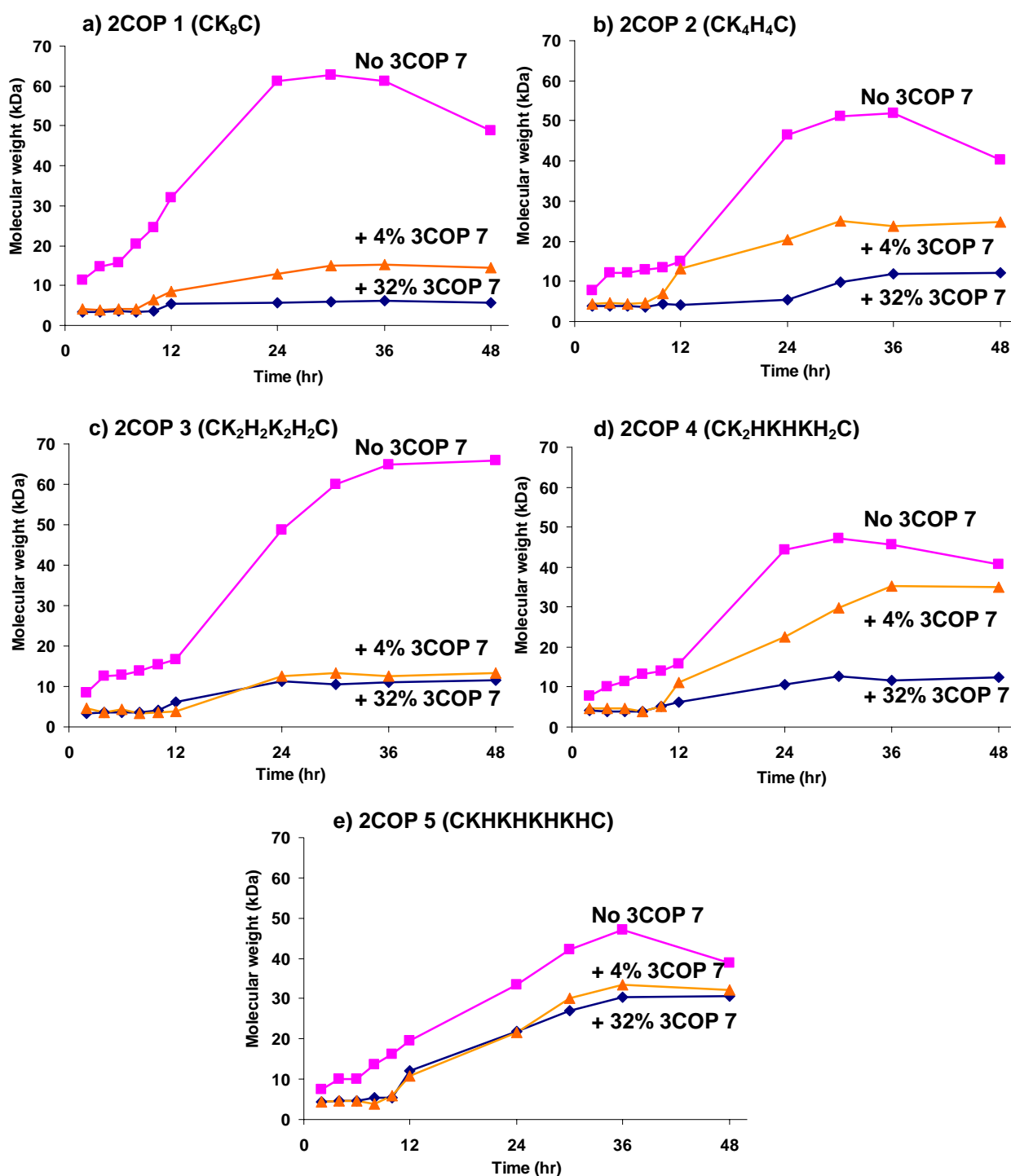


**Figure 3.25.** Oxidative polymerization of 2COPs 1-5 at 30mM concentration with and without 4% and 30% mole fraction of 3COP 7 (CK<sub>2</sub>CK<sub>2</sub>C) incubated at ambient. The molecular weight was analyzed by GPC using PLL as standard curve.

[no 3COP 7 —■—, + 4% 3COP 7 —▲— and + 32% 3COP 7 —◆—]



The polymerization mixtures of each 2COP without 3COP **7** gave higher molecular weight RPCs over an extended time compared to those with 4% and 32% mole fractions of 3COP **7**. During the first 12 hr the RPCs from 2COP itself grew slowly and increased rapidly after 12 hr of incubation. The maximum molecular weights of the RPCs (2COP alone) were observed between 30 to 36 hr. After 36 hr the molecular weight of the polymers generally reduced. However, when 3COP **7** at 4% and 32% mole fractions were present this reduced the growth of polymers. For all oligopeptide reactions, the growth of *cross-linked RPCs* at 32% mole fraction of 3COP **7** was lower than those at 4% mole fraction. Therefore, using higher mole fraction of 3COP **7** resulted in lower molecular weight of polymers over 4% and 32% 3COP.

The maximum molecular weight of *cross-linked RPCs* synthesized from all oligopeptides varied from approximately 10-35 kDa when carried out with 3COP **7** at 4% mole fraction. Synthesis at 32% mole fraction of 3COP **7** in the mixture produced the highest polymer molecular weight with 2COP **5** (~30 kDa). The molecular weight of the *cross-linked RPCs* produced from other 2COPs at 32% mole fraction of 3COP **7** are only in the range of approximately 5-10 kDa as can be seen in **Figure 3.26**.

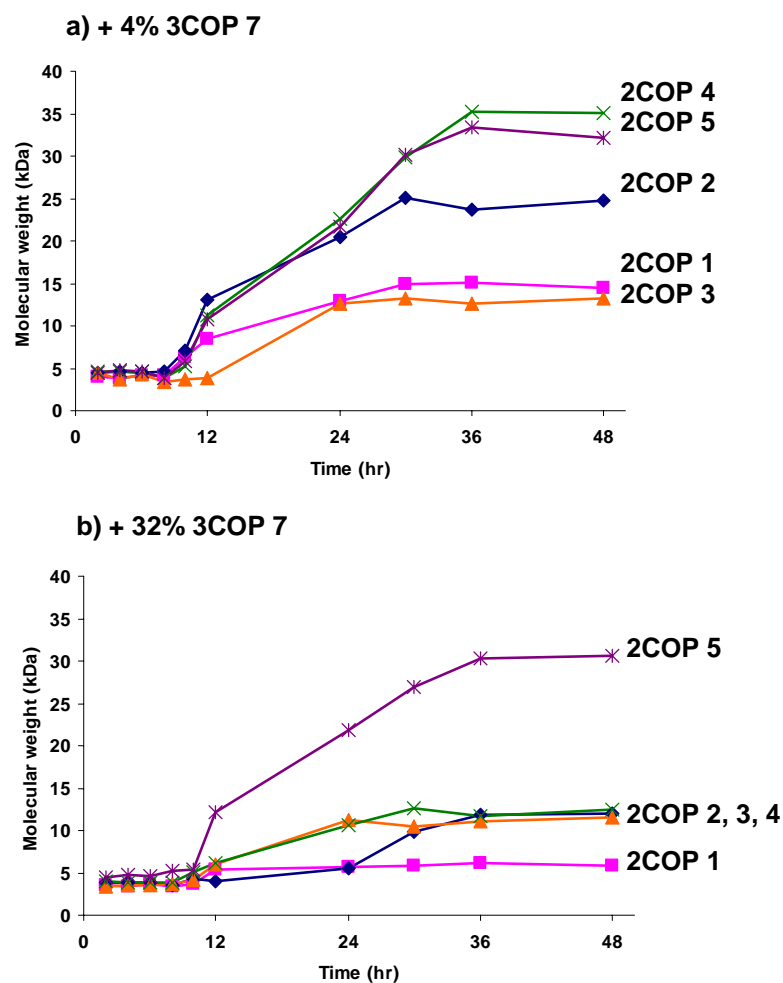


**Figure 3.26.** Oxidative polymerization compared between 2COPs 1-5 at 30mM concentration with and without 4% (a) and 30% (b) mole fraction of 3COP 7 (CK<sub>2</sub>CK<sub>2</sub>C) incubated at ambient. (all data are an average of the triplicate experiments).

[2COP 1 —■—, 2 —◆—, 3 —▲—, 4 —×— and 5 —\*— ]

Due to the inability of the cross-linking polymerization to produce high molecular weight polymers, these *cross-linked RPCs* were not considered further as vectors.

## 3.5 Conclusions

### 3.5.1 RPC conclusion

The work presented in this chapter has shown the design of synthetic vectors by combining lysine, histidine and cysteine residues to provide the key features to hopefully achieve efficient gene delivery. These vectors are designed to bind DNA extracellularly (**I**), achieve cell uptake *via* endocytosis (**III**), provide a tunable endosomal release mechanism (**IV**) and provide a degradable backbone in order that the DNA can be released once in the cytoplasm (**V**).

Crude samples of bis-cysteine containing oligopeptides (2COPs **1-6**) and tris-cysteine containing oligopeptide (3COP **7**) (CK<sub>8</sub>C (**1**), CK<sub>4</sub>H<sub>4</sub>C (**2**), CK<sub>2</sub>H<sub>2</sub>K<sub>2</sub>H<sub>2</sub>C (**3**), CK<sub>2</sub>HKHKH<sub>2</sub>C (**4**), CKHKHKHKHC (**5**), CH<sub>8</sub>C (**6**) and CK<sub>2</sub>CK<sub>2</sub>C (**7**)) synthesized by Alta Bioscience (Birmingham, UK) were purified by the preparative reverse phase HPLC. All purified oligopeptides were analyzed by analytical RP-HPLC, ESI-MS and <sup>1</sup>H NMR to obtain the purity and to characterize the oligopeptides. The purity of all oligopeptides is shown to be between 97.35-99.64 %.

The pK<sub>a</sub> values of the oligopeptides **1-7** were determined *via* <sup>1</sup>H NMR titration method. For 2COP **1** and 3COP **7**, the pK<sub>a</sub> of the lysine residue were 10.51 and 10.81, respectively. For 2COP **6** (CH<sub>8</sub>C) and RPCs **2-5** the pK<sub>a</sub> of the histidine residues were 6.25, 6.20, 6.16, 6.11 and 6.09, respectively. The increase in the mixing of the constitution of the histidine residues in the lysine residues results in the reduction of the pK<sub>a</sub> for 2COPs **2-5** because of the charge repulsion of subphase protons by its proximity to the protonated lysine residues.

2COPs **1-6** were oxidative polymerized to form linear reducible polycations (RPCs) *via* disulfide bond formation. The polymerization as a function of oligopeptide concentration produced higher molecular weight RPCs at high oligopeptides concentration. The maximum RPCs molecular weight obtained for all the oligopeptides at 18 mM, 30mM and 60mM are approximately 25-45, 30-65, and 50 -90 kDa, respectively. The maximum molecular weights of the RPCs were observed between 30 to 36 hr. After 36 hr the molecular weight of the RPCs generally reduced. The RPCs produced from 2COP **3** did not show this decrease in molecular weight after 36 hr and produced the longest RPCs at all oligopeptide concentrations. All RPCs were stable to the degradation in the HEPES buffer at -20°C over a period of 2-3 days, with the exception of the RPC formed from 2COP **6** (CH<sub>8</sub>C) which degraded. Therefore, the 2COP **6** was not used for further studies.

The polymerization as a function of temperature revealed that the growth of the RPCs at 40°C was more rapid than that at ambient. However, approximately the same maximum molecular weight was observed (~45 kDa). The polymerisation proceed only to ~37% (40°C) and 41% (ambient), the remaining ~60% of material that was eluted has a retention time of 2COP **1**.

DNA polyplexes were then formed from RPCs **1-5** (~100 kDa) at N:P ratios 5 and their diameters and surface charges were measured. The polyplexes produced from RPCs-DNA condensation showed their diameters were at ~100 nm. However, the RPCs **2-5** introduced better compaction of the DNA than RPC **1**. We hypothesize RPCs **2-5** are more flexible than RPC **1**, as a result of the incorporation of histidine residues in the lysine based peptides giving them a shorter persistence length.

The surface charges were positive for all polyplexes, enabling them to electrostatically interact with the negatively charged cell membrane and promote the internalization into cell *via* syndecan-mediated endocytosis.<sup>[31]</sup> These primary characteristics of RPC polyplexes suggested that they are suitable for further cell transfection.

Simulated extracellular stability of these polyplexes was examined. PAA (found in blood serum) was used as a competitively polyanionic agent to destabilize the polyplexes. The polyplexes from RPCs **2-5** were stable in this simulated extracellular condition. However, the RPC **1** polyplex was slightly unstable in PAA assay. The PEI polyplex was completely disrupted under these conditions.

In addition, to the simulated extracellular destabilized conditions, GSH was used as a biological intracellular reducing agent, since GSH is present in the cytoplasm (the stability under physiological salt concentrations was studied). The polyplexes from RPCs **2-5** were stable in salt solution alone in the range 0.15 – 1 M. However, after adding GSH (5 mM), all polyplexes released DNA. However, the polyplex from RPC **1** did not release DNA. These results suggested that RPCs **2-5** are able to facilitate intracellular reduction resulting in DNA releasing for further gene expression mechanisms. Whereas, RPC **1** although probably does undergo the disulfide bonds reduction the high net charge on the 2COP **1** that results is still bound the DNA more strongly than 2COPs **2-5**.

*In conclusion, the sizes, surface charges, stability of these polyplexes under simulated physiological conditions combined with their sensitivity to levels of GSH which are likely to be encountered inside cells (as evidenced by combined gel shift, AFM and DLS) indicated that these systems might be effective transfection reagents in vitro.*

### 3.5.2 RPC molecular weight conclusion

DNA polyplexes were then formed from low molecular weight RPCs **1-5** (38-60 kDa) at N:P 5 in order to compare their characteristic as a function of RPC molecular weight. The polyplexes produced from low molecular weight RPCs were similar to those from high molecular weight RPCs (~100 kDa). The surface charges were similar to polyplexes from high molecular weight RPCs. These primary characteristics suggested the lower molecular weight RPC polyplexes may also be suitable vectors.

Extracellular stability of these polyplexes were further examined by the PAA assay, and revealed that the polyplexes from low molecular weight RPCs **1-5** were stable in this simulated extracellular condition.

The intracellular stability of these lower molecular weight RPC polyplexes against physiological salt concentrations (0.15-0.5 M) and GSH (5 mM) was studied. The polyplexes from RPCs **2-5** were stable in salt solution alone. However, these RPCs polyplexes are less stable to GSH compared to the polyplexes from high molecular weight RPCs. Therefore, unsurprisingly, when combined salt and GSH in the RPCs polyplex solutions, they released more DNA, which might promote enhanced gene delivery over the higher molecular weight RPC polyplexes.

*In conclusion, the diameters, surface charges and gel shift assays of polyplexes from low molecular weight RPCs **2-5** were similar to high molecular weight RPCs **2-5**, but had enhanced release of DNA when treated with GSH suggesting that the low molecular weight RPCs could also be promising vectors for gene therapy.*

### 3.5.3 Oligopeptide polyplexes conclusion

DNA polyplexes were then formed from 2COPs **1-5** at N:P 5 and their diameters were measured. All polyplexes from 2COPs **1-5** formed large particles which were greater than 1  $\mu\text{m}$  diameter over time course of 48 hr. In general, the particle diameter less than 1  $\mu\text{m}$  circulate longer in the bloodstream than the larger particles if there are no interactions with blood components or fixed macrophages.<sup>[35]</sup> Therefore these polyplexes suggest that they are not suitable for further cell transfection.

### 3.5.4 Cross-linked RPCs conclusion

The oxidative polymerization to form *cross-linked RPCs* was also studied by mixing between 2COP **1-5** and 3COP **7** at 4% and 32% mole fraction of 3COP **7**. The results showed termination in the growth of *cross-linked RPCs* producing low molecular weight in all cases. The higher the mole fraction of 3COP used, the lower the polymer molecular weight produced. We believe the 3COP leads to the termination of the *cross-linked RPCs* during the reaction. The maximum molecular weight of cross-linked RPCs for all 2COPs varied from approximately 10-35 kDa with 3COP at 4% mole fraction, whereas reacting with 32% mole fraction of 3COP the maximum molecular weight was only 5-10 kDa. With such low molecular weights of these polymers, they not considered further study as gene delivery carriers.

### 3.6 References

1. Wattiaux, R., Laurent, N., Wattiaux-De Coninck, S., and Jadot, M. (2000). Endosomes, lysosomes: their implication in gene transfer. *Advanced Drug Delivery Reviews*, **41**, 201-208.
2. Besterman, J.M., and Low, R.B. (1983). Endocytosis: a review of mechanisms and plasma membrane dynamics. *Biochemical Journal*, **210**, 1-13.
3. Davis, M.E. (2002). Non-viral gene delivery systems. *Current Opinion in Biotechnology*, **13**, 128-131.
4. Behr, J.P. (1997). The proton sponge: A trick to enter cells the viruses did not exploit. *Chimia*, **51**, 34-36.
5. Moore, N.M., Sheppard, C.L., Barbour, T.R., and Sakiyama-Elbert, S.E. (2008). The effect of endosomal escape peptides on in vitro gene delivery of polyethylene glycol-based vehicles. *Journal of Gene Medicine*, **10**, 1134-1149.
6. Chen, Q.R., Zhang, L., Stass, S.A., and Mixson, A.J. (2001). Branched co-polymers of histidine and lysine are efficient carriers of plasmids. *Nucleic Acids Research*, **29**, 1334-1340.
7. Read, M.L., Bremner, K.H., Oupicky, D., Green, N.K., Searle, P.F., and Seymour, L.W. (2003). Vectors based on reducible polycations facilitate intracellular release of nucleic acids. *Journal of Gene Medicine*, **5**, 232-245.
8. Read, M.L., Singh, S., Ahmed, Z., Stevenson, M., Briggs, S.S., Oupicky, D., Barrett, L.B., Spice, R., Kendall, M., Berry, M., Preece, J.A., Logan, A., and Seymour, L.W. (2005). A versatile reducible polycation-based system for efficient delivery of a broad range of nucleic acids. *Nucleic Acids Research*, **33**, e86.



9. McKenzie, D.L., Kwok, K.Y., and Rice, K.G. (2000). A potent new class of reductively activated peptide gene delivery agents. *Journal of Biological Chemistry*, **275**, 9970-9977.
10. Bennis, J.M., Choi, J.S., Mahato, R.I., Park, J.S., and Kim, S.W. (2000). pH-Sensitive cationic polymer gene delivery vehicle: N-Ac-poly(L-histidine)-graft-poly(L-lysine) comb shaped polymer. *Bioconjugate Chemistry*, **11**, 637-645.
11. Pichon, C., Goncalves, C., and Midoux, P. (2001). Histidine-rich peptides and polymers for nucleic acids delivery. *Advanced Drug Delivery Reviews*, **53**, 75-94.
12. Goncalves, C., Pichon, C., Guerin, B., and Midoux, P. (2002). Intracellular processing and stability of DNA complexed with histidylated polylysine conjugates. *Journal of Gene Medicine*, **4**, 271-281.
13. Leng, Q.X., and Mixson, A.J. (2005). Modified branched peptides with a histidine-rich tail enhance in vitro gene transfection. *Nucleic Acids Research*, **33**, e40.
14. Leng, M., and Felsenfe, G. (1966). Preferential interactions of polylysine and polyarginine with specific base sequences in DNA. *Proceedings of the National Academy of Sciences of the United States of America*, **56**, 1325-1332.
15. Foley, M., and Tilley, L. (1997). Quinoline antimalarials: Mechanisms of action and resistance. *International Journal for Parasitology*, **27**, 231-240.
16. Gasparovic, C., Barba, I., Born, J., Barton, S., Arus, C., and Mann, P. (1998). A study of imidazole-based nuclear magnetic resonance probes of cellular pH. *Analytical Biochemistry*, **261**, 64-72.
17. Cho, Y.W., Kim, J.D., and Park, K. (2003). Polycation gene delivery systems: escape from endosomes to cytosol. *Journal of Pharmacy and Pharmacology*, **55**, 721-734.

18. Pichon, C., Roufai, M.B., Monsigny, M., and Midoux, P. (2000). Histidylated oligolysines increase the transmembrane passage and the biological activity of antisense oligonucleotides. *Nucleic Acids Research*, **28**, 504-512.
19. Daniel W. Pack, D.P.R.L. (2000). Design of imidazole-containing endosomolytic biopolymers for gene delivery. *Biotechnology and Bioengineering*, **67**, 217-223.
20. Midoux, P., and Monsigny, M. (1999). Efficient gene transfer by histidylated polylysine pDNA complexes. *Bioconjugate Chemistry*, **10**, 406-411.
21. Manickam, D.S., and Oupicky, D. (2006). Multiblock reducible copolypeptides containing histidine-rich and nuclear localization sequences for gene delivery. *Bioconjugate Chemistry*, **17**, 1395-1403.
22. Saito, G., Swanson, J.A., and Lee, K.D. (2003). Drug delivery strategy utilizing conjugation via reversible disulfide linkages: role and site of cellular reducing activities. *Advanced Drug Delivery Reviews*, **55**, 199-215.
23. McKenzie, D.L., Smiley, E., Kwok, K.Y., and Rice, K.G. (2000). Low molecular weight disulfide cross-linking peptides as nonviral gene delivery carriers. *Bioconjugate Chemistry*, **11**, 901-909.
24. Oupicky, D., Konak, C., Ulbrich, K., Wolfert, M.A., and Seymour, L.W. (2000). DNA delivery systems based on complexes of DNA with synthetic polycations and their copolymers. *Journal of Controlled Release*, **65**, 149-171.
25. Reimschuessel, H.K. (1975). General aspects in polymer synthesis. *Environmental Health Perspectives*, **11**, 9-20.
26. Turell, L., Carballal, S., Botti, H., Radi, R., and Alvarez, B. (2009). Oxidation of the albumin thiol to sulfenic acid and its implications in the intravascular compartment. *Brazilian Journal of Medical and Biological Research*, **42**, 305-311.

27. Quijano, C., Alvarez, B., Gatti, R.M., Augusto, O., and Radi, R. (1997). Pathways of peroxynitrite oxidation of thiol groups. *Biochemical Journal*, **322**, 167-173.
28. Akinc, A., Thomas, M., Klivanov, A.M., and Langer, R. (2005). Exploring polyethylenimine-mediated DNA transfection and the proton sponge hypothesis. *Journal of Gene Medicine*, **7**, 657-663.
29. Sirirat Choosakoonkriang, Brian A. Lobo, Gary S. Koe, Janet G. Koe, and Middaugh, C.R. (2003). Biophysical characterization of PEI/DNA complexes. *Journal of Pharmaceutical Sciences*, **92**, 1710-1722.
30. Fischer, D., Bieber, T., Li, Y., Elsässer, H.-P., and Kissel, T. (1999). A novel non-viral vector for DNA delivery based on low molecular weight, branched polyethylenimine: effect of molecularweight on transfection efficiency and cytotoxicity. *Pharmaceutical Research*, **16**, 1273-1279.
31. Mislick, K.A., and Baldeschwieler, J.D. (1996). Evidence for the role of proteoglycans in cation-mediated gene transfer. *Proceedings of the National Academy of Sciences of the United States of America*, **93**, 12349-12354.
32. Carlisle, R.C., Etrych, T., Briggs, S.S., Preece, J.A., Ulbrich, K., and Seymour, L.W. (2004). Polymer-coated polyethylenimine/DNA complexes designed for triggered activation by intracellular reduction. *Journal of Gene Medicine*, **6**, 337-344.
33. Oupicky, D., Carlisle, R.C., and Seymour, L.W. (2001). Triggered intracellular activation of disulfide crosslinked polyelectrolyte gene delivery complexes with extended systemic circulation in vivo. *Gene Therapy*, **8**, 713-724
34. Meister, A. (1988). Glutathione metabolism and its selective modification. *The Journal of Biological Chemistry*, **263**, 17205-17208.
35. Patel, H.M. (1992). Serum opsonins and liposomes - their interaction and opsonophagocytosis. *Critical Reviews in Therapeutic Drug Carrier Systems*, **9**, 39-90.

## **CHAPTER 4**

### **Delivery of nucleic acid using lysine, histidine and cysteine based oligopeptides and reducible polycations (RPCs)**

# CONTENTS

List of Figures

List of Tables

## 4 DELIVERY OF NUCLEIC ACID USING LYSINE, HISTIDINE AND CYSTEINE BASED OLIGOPEPTIDES AND REDUCIBLE POLYCATIONS (RPCs)

<b>4.1 Introduction</b>	<b>168</b>
<b>4.2 Objectives</b>	<b>170</b>
<b>4.3 Methodology</b>	<b>171</b>
<b>4.4 Results and discussion</b>	<b>175</b>
4.4.1 Cytotoxicity of RPC polyplexes	176
4.4.2 Cell transfection of RPCs polyplexes	181
4.4.2.1 Cell transfection of RPCs polyplexes based on endosomolytic buffering: effect of CQ	182
4.4.2.2 Cell transfection of RPCs polyplexes based on intracellularly reducible property: effect of GSH-MEE/BSO	187
4.4.2.2a Artificially increase the intracellular GSH level: effect of GSH-MEE	188
4.4.2.2b Artificially depleting the intracellular GSH level: effect of BSO	191
4.4.2.2c Assessing intracellular GSH level in A549 and bEND3 cells treated with GSH-MEE and BSO	192
4.4.2.3 Cell transfection of RPCs polyplexes based on the combination of endosomolytic and intracellularly reducible properties	195
4.4.2.4 Cell transfection of RPCs polyplexes as a function of RPCs molecular weight	198
4.4.3 Cell transfection of oligopeptide polyplexes	197
<b>4.5 Conclusions</b>	<b>199</b>
<b>4.6 References</b>	<b>211</b>

## List of Figures

Figure 4.1.	Physiology of artery, endothelium and capillaries	172
Figure 4.2.	Schematic overview of cell transfection in this chapter	173
Figure 4.3.	Schematic processes of cytotoxicity and cell transfection studies of polyplexes with CQ, GSH-MEE or BSO	176
Figure 4.4.	Schematic diagram showing cellular metabolism resulting in the conversion of MST agent to formazan in MTS assay	177
Figure 4.5.	Cell viability following exposure to RPCs (~50 and ~100 kDa) polyplexes <b>1-5</b> at N:P 5, PLL polyplex at N:P 5, PEI polyplex at N:P 10 and cell controls	179
Figure 4.6.	Transfection based on CQ with RPC polyplexes <b>1-5</b> at N:P 5, PLL polyplex at N:P 5, PEI polyplex at N:P 10 and cell control	184
Figure 4.7.	Structures of glutathione monoethyl ester (GSH-MEE) and buthionine sulfoximine (BSO)	188
Figure 4.8.	Transfection based on GSH-MEE and BSO with RPC polyplexes <b>1-5</b> at N:P 5, PLL polyplex at N:P 5, PEI polyplex at N:P 10 and cell control	190
Figure 4.9.	Inhibition of glutathione synthesis by buthionine sulfoximine (BSO) in $\gamma$ -glutamly cycle	191
Figure 4.10.	The schematic process of intracellular GSH determination	193
Figure 4.11.	Relative fluorescence of intracellular GSH based on the addition of GSH-MEE and BSO in bEND3 and A549 cells	194
Figure 4.12.	Transfection based on CQ and GSH-MEE with RPC polyplexes <b>1-5</b> at N:P 5, PLL polyplex at N:P 5, PEI polyplex at N:P 10 and cell control	196
Figure 4.13.	Transfection based on CQ and GSH-MEE with RPC polyplexes 1-5 (~50 kDa) at N:P 5, PLL polyplex at N:P 5, PEI polyplex at N:P 10 and cell control	200
Figure 4.14.	The transfection efficiency in bEND3 and A549 of RPCs polyplexes at different molecular weight (~50 and ~100 kDa), PEI and PLL polyplexes	202

Figure 4.15.	Transfection in bEND3 and A549 based on CQ and GSH-MEE of polyplexes from the RPCs <b>1-5</b> at the different molecular weight, PEI and PLL	204
Figure 4.16.	Relative transfection efficiency of 2COPs, RPCs at N:P 5 and PEI at N:P 10 in A549 cells	206
Figure 4.17.	The transfection efficiency in bEND3 and A549 of RPCs polyplexes based on the $pK_a$ values	208

### List of Tables

Table 4.1.	RPCs, polymers and their polyplexes used in cell transfection studies	183
Table 4.2.	The characteristic of RPCs and their polyplexes	199

## 4 DELIVERY OF NUCLEIC ACID USING LYSINE, HISTIDINE AND CYSTEINE BASED OLIGOPEPTIDES AND REDUCIBLE POLYCATIONS (RPCs)

### *Abstract*

*In this chapter the cell transfections based on endosomolytic and intracellularly reducible characteristics of the  $pK_a$  modulated-reducible polycations (RPCs) were carried out. These RPCs are not only more active at transfection than current systems such as PEI and PLL, but importantly are also much better tolerated by two different cell types, bEND3 and A549. Furthermore, they can facilitate endosomal buffering and intracellular reduction. The highest transfection efficiencies in both cell types were with RPC 2. In addition, using low molecular weight RPCs (~50 kDa) as a vector induces higher transfection levels than the high molecular weight RPCs (~100 kDa). The oligopeptides were shown to be unsuitable to be vectors.*

### 4.1 Introduction

Nature employs a number of highly evolved strategies to package and process nucleic acids. Proteins such as histones condense DNA within a cell *via* the spatially-controlled display of protonatable peptide side-chains.<sup>[1]</sup> Viruses have developed polymeric structures that compact nucleic acids for transfer across cellular barriers, then release the ‘foreign’ genetic material *via* specific biological triggers.<sup>[2]</sup> For the delivery of nucleic acids for therapy, synthetic carrier molecules that combine advantageous features of DNA condensing agents, but without the infection and immune response problems of viruses are needed.<sup>[3-8]</sup> The most efficient synthetic gene delivery agents for many applications are partially protonated branched poly(ethyleneimine)s (PEI), a polycation that can transfect cells *in vitro* and *in vivo*.<sup>[9-13]</sup> Unfortunately, PEI exhibits unacceptable toxicity,<sup>[14]</sup> which arises in part from the combination of a non-degradable polymer backbone and a residual high polycation content.



As described in Chapter 1, chloroquine has the ability to buffer the endosomal pH, resulting in endosomal membrane disruption.<sup>[15]</sup> Therefore, polyplexes that have no buffering capacity such as those contain PLL need chloroquine to promote the endosomal escape.<sup>[16, 17]</sup> However, the use of chloroquine results in cell toxicity.<sup>[17]</sup>

Therefore in our group's previous work,<sup>[18]</sup> The RPC(59) (CH<sub>3</sub>K<sub>3</sub>H<sub>3</sub>C, 59 kDa) and RPC(113) (CH<sub>6</sub>K<sub>3</sub>H<sub>6</sub>C, 113 kDa) were developed by incorporating histidine residues which help promote the endosomal buffering. These RPCs were synthesized by oxidative polymerization, and they have an average pK<sub>a</sub> of ~5-6. These RPCs formed stable polyplexes with plasmid DNA at N:P ratio of 5 with the polyplex sizes ~100 nm in diameter. Addition of chloroquine increased the transfection of RPC(59) ~3.2-12.7 fold. However, there was no enhancement in RPC(113). These previous results indicated that incorporating histidine improves the transfection ability. In addition, RPCs containing disulfide linkages have previously been shown to be stable in the extracellular matrix,<sup>[18-20]</sup> but cleaved efficiently by intracellular glutathione, leading to disassemble of the vector to oligomers, which also reduces the toxicity, and efficient release of the nucleic acid payload.

However, the coupling of reducible vector backbones with modulated pK<sub>a</sub> DNA-binding side-chains has not hitherto been investigated. Therefore, we planned to exploit proximities of protonatable groups on a peptide side chain in order to control the pK<sub>a</sub> range (shown in Chapter 3, page 119 and discussed in term of the hypothesis in Chapter 1, page 48). Therefore, the pK<sub>a</sub> of vectors that promotes the endosomal escape in cell transfection will be optimized.

## 4.2 Objectives

Therefore, the six  $pK_a$ -moduatable decameric peptides containing lysine and/or histidine and terminated with cysteine residues (CK<sub>8</sub>C (1), CK<sub>4</sub>H<sub>4</sub>C (2), CK<sub>2</sub>H<sub>2</sub>K<sub>2</sub>H<sub>2</sub>C (3), CK<sub>2</sub>HKHKH<sub>2</sub>C (4), CKHKHKHKHC (5) and CH<sub>8</sub>C (6)), prepared in Chapter 3, have 4 key criteria to enhance gene delivery. These are:

- i) Peptide-side-chain functionality provide electrostatic interaction with the DNA *via* the incorporation of lysine residues, which will be fully protonated at physiological pH, leading to strong extracellular binding to DNA,
- ii) Modulatable endosome release *via* buffering by the mixing of lysine and histidine residues to modulate the  $pK_a$  of vectors,
- iii) Biodegradation to promote the release of the DNA, by introducing the disulfide backbone, which will be reduced by intracellular GSH, and
- iv) Biodegradation to reduce the toxicity, as the polyplexes can be reduced by intracellular GSH, resulting in small fragments of oligopeptides which will be cleared more readily than high molecular weight polymers.

Therefore, in this chapter, the cell transfection of these vectors will be studied *via* experiments that manipulate the endosomolysis (addition of CQ) and the intracellular reduction (addition of BSO (GSH depleter) and GSH-MEE (GSH raiser)).

### 4.3 Methodology

The transfections were carried out in two representative cell lines, mouse brain endothelial cells (bEND3) and human lung carcinoma epithelial cells (A549). These cell lines were chosen because for therapeutic applications it is important to consider transduction of both endothelial (bEND3) and epithelial cells (A549). The bEND3 cells serve as a model for the surfaces that are accessible following bloodstream administration of the polyplexes, while A549 cells are representative of most types of common cancer cells. Therefore, for efficient *in vivo* transfection polyplexes should not attach and/or transfect endothelial cells if they are injected into bloodstream, otherwise they are unable to reach the target tissue that needs to be treated (**Figure 4.1**).

The controls, PLL and PEI polyplexes, were used, and the background of cell transfection was performed by cell lines with no transfection agent (the polyplexes).

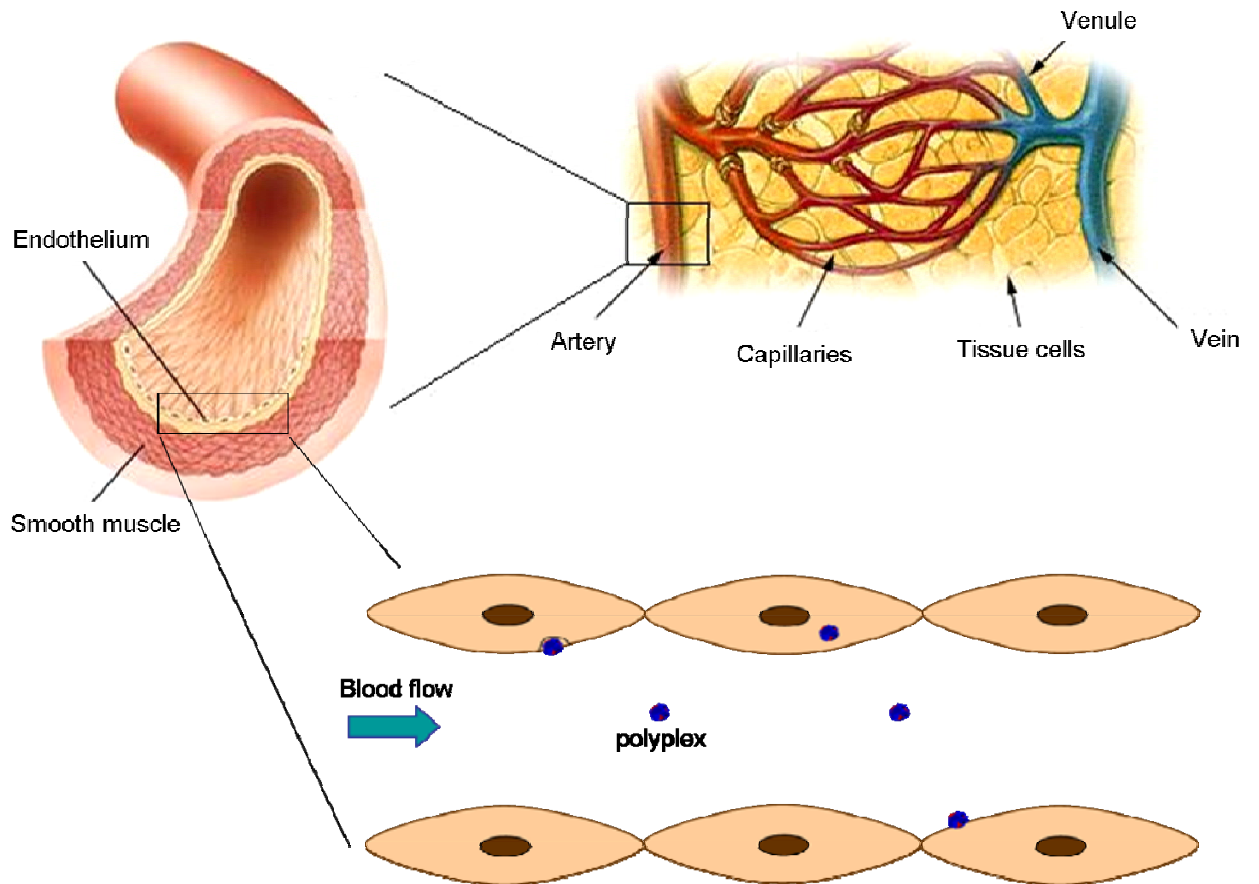


**Figure 4.1. Physiology of artery, endothelium and capillaries;** Image modified from:

<http://www.webbooks.com/eLibrary/Medicine/Physiology/Cardiovascular/capillary.jpg> , and

<http://cache-media.britannica.com/eb-media/83/98483-004-FD45DAA5.jpg>

The experimental processes in this chapter will be divided into 2 sections as described below and shown in **Figure 4.2**.

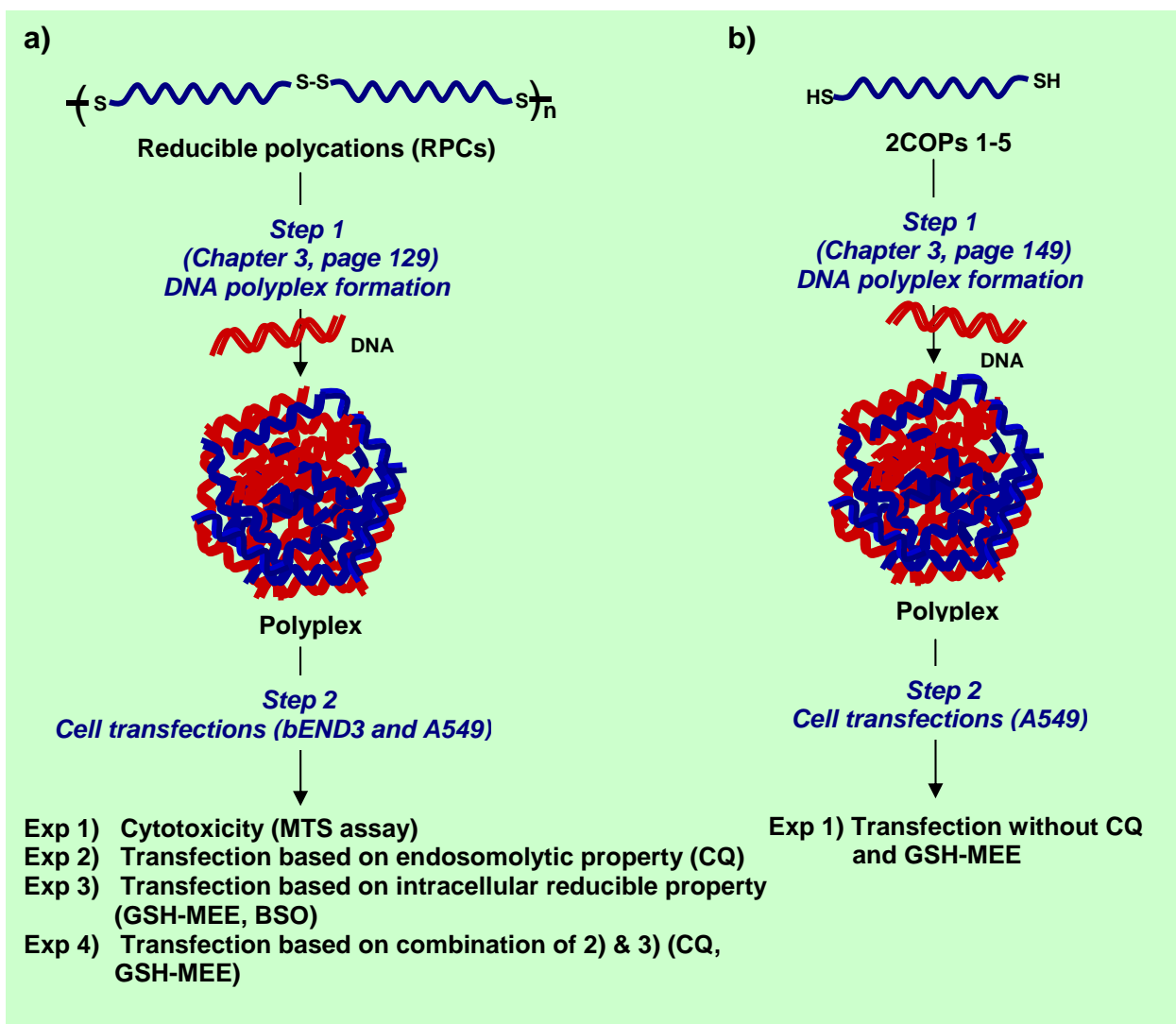


**Figure 4.2.** Schematic overview of cell transfection in this chapter; a) transfection with RPCs polyplexes and b) transfection with 2COPs polyplexes

#### 4.3.1 Cell transfections of RPCs polyplexes

The cell transfections of RPC polyplexes were carried out based on four experiments (**Figure 4.2a, step 2**).

*Exp 1. Investigate the cytotoxicity of RPCs polyplexes:* The cytotoxicity of RPCs polyplexes was investigated using the MTS assay.

*Exp 2. Investigate the endosomolytic buffering:* The transfection of the  $pK_a$  modulated RPCs based on the endosomal buffering and endosomal escape was investigated. Chloroquine (CQ) was added to the cell lines for its ability to buffer the endosome. The transfection efficiencies of polyplexes with and without CQ were investigated, in order to assess the ability of the histidine moieties to buffer the endosome.

*Exp 3. Investigate the intracellular reducible property:* The intracellular cleavage of the disulfide bonds in the RPCs polyplexes by GSH was studied as a function of transfection. Intracellular GSH levels were boosted by adding glutathione monoethyl ester (GSH-MEE), which is cell permeable and is hydrolysed to GSH intracellularly.<sup>[21]</sup> In addition, an experiment using buthionine sulfoximine (BSO) which inhibits the synthesis of the intracellular GSH was studied as a function of transfection. Thus, an assessment of the nature of the disulfide bonds can be made on transfection efficiency.

*Exp 4. Investigate the endosomolytic buffering and intracellular reducible properties:* The combination of CQ and GSH-MEE was also carried out in the cell transfection studies. The transfections of polyplexes with CQ, GSH-MEE, CQ+GSH-MEE and only polyplexes were investigated, to make a combined assessment of both the nature of the histidine moieties and the disulfide bonds on the transfection efficiency.

In addition, the characterization of lower molecular weight RPCs (~40-60 kDa) and their polyplexes at N:P 5 studied in Chapter 3 (section 3.3.4.3) also suggested that they were suitable for cell transfection. Therefore, the transfection efficiency of RPCs as a function of molecular weight will be investigated in this chapter as well.

### 4.3.2 Cell transfections of oligopeptides polyplexes

Although, the polyplexes produced from 2COPs (see section 3.4.4.4) revealed that they were not suitable for using as vectors as the polyplex diameters were large, the transfection of these polyplexes was also investigated (**Figure 4.2b**) to compare with RPCs.

## 4.4 Results and discussion

The overview of cytotoxicity and transfection experiments are shown in **Figure 4.3** and described in detail in section 2.10.1. Briefly, cell lines ( $10^4$  cells/well) were grown in 96 well plates for 18 hr. The cells were washed (**step 1**) and serum free DMEM medium and CQ (100  $\mu$ M), GSH-MEE (5 mM) or BSO (100  $\mu$ M) (**step 2**) was added. Cells were incubated for 1, 3 or 24 hrs with CQ, GSH-MEE or BSO, respectively, before washing and transfecting cells with the polyplexes (**step 3**). Further serum containing DMEM medium was added to the washed cells, and the cells were further incubated for 96 or 44 hrs for cytotoxicity determination (**step 5-6**) or transfection level determination (**step 7-9**), respectively.

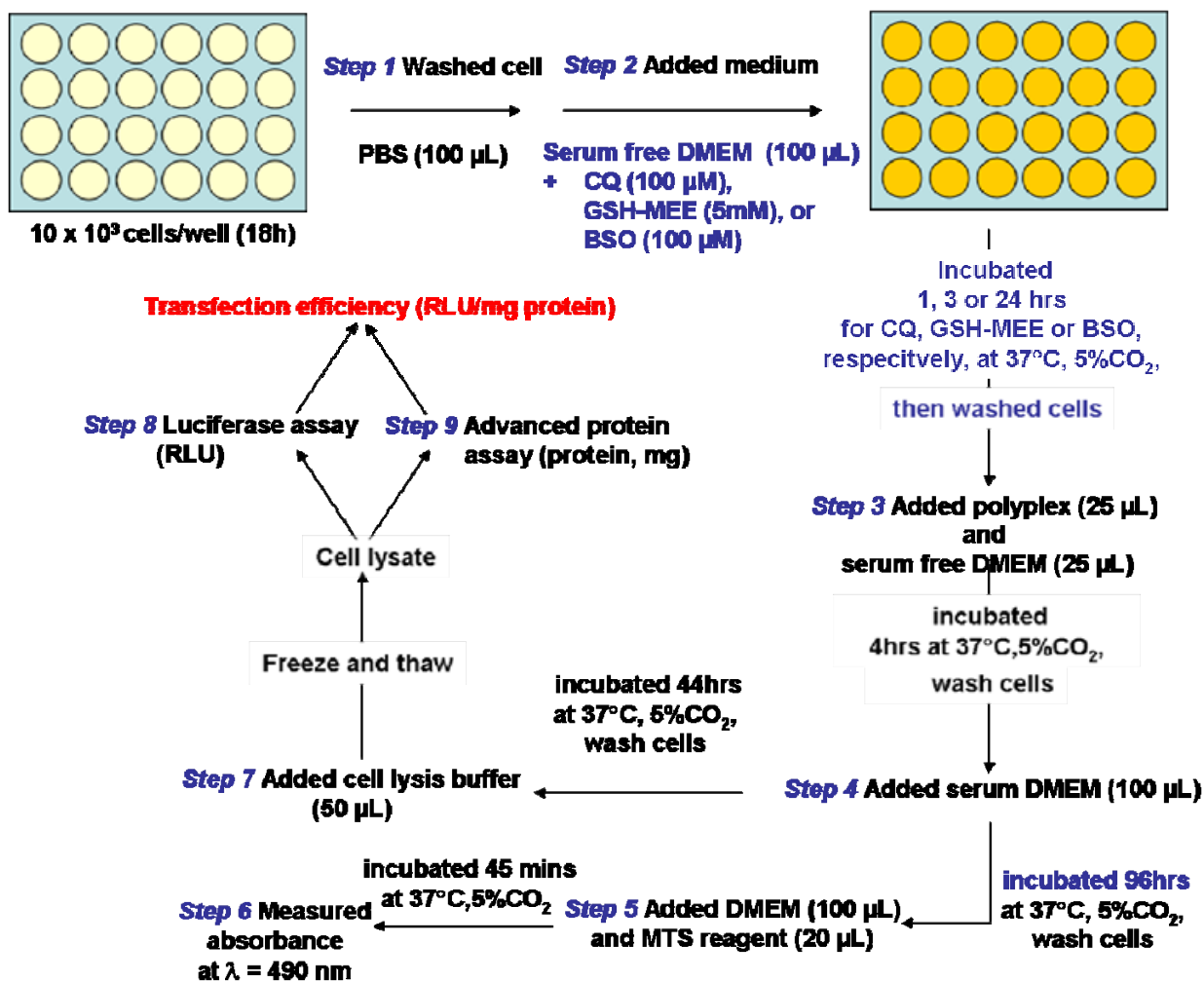


Figure 4.3. Schematic processes of cytotoxicity and cell transfection studies of polyplexes with CQ, GSH-MEE or BSO

#### 4.4.1 Cytotoxicity of RPC polyplexes (Figure 4.2a, step 2, Exp 1)

The MTS cell proliferation assay was utilized to determine the cytotoxicity of all polyplexes at both high and low molecular weight as described in section 2.10.4. The MTS reagent is bio-reduced by NAD<sup>+</sup> and NADH produced by dehydrogenase enzymes in metabolically active cells, producing a yellow/orange formazan product (Figure 4.4). The amount of



formazan product is directly proportional to the number of living cells. Thus, the cell proliferation or death can be quantified by reading the absorbance of the plate at 490 nm.

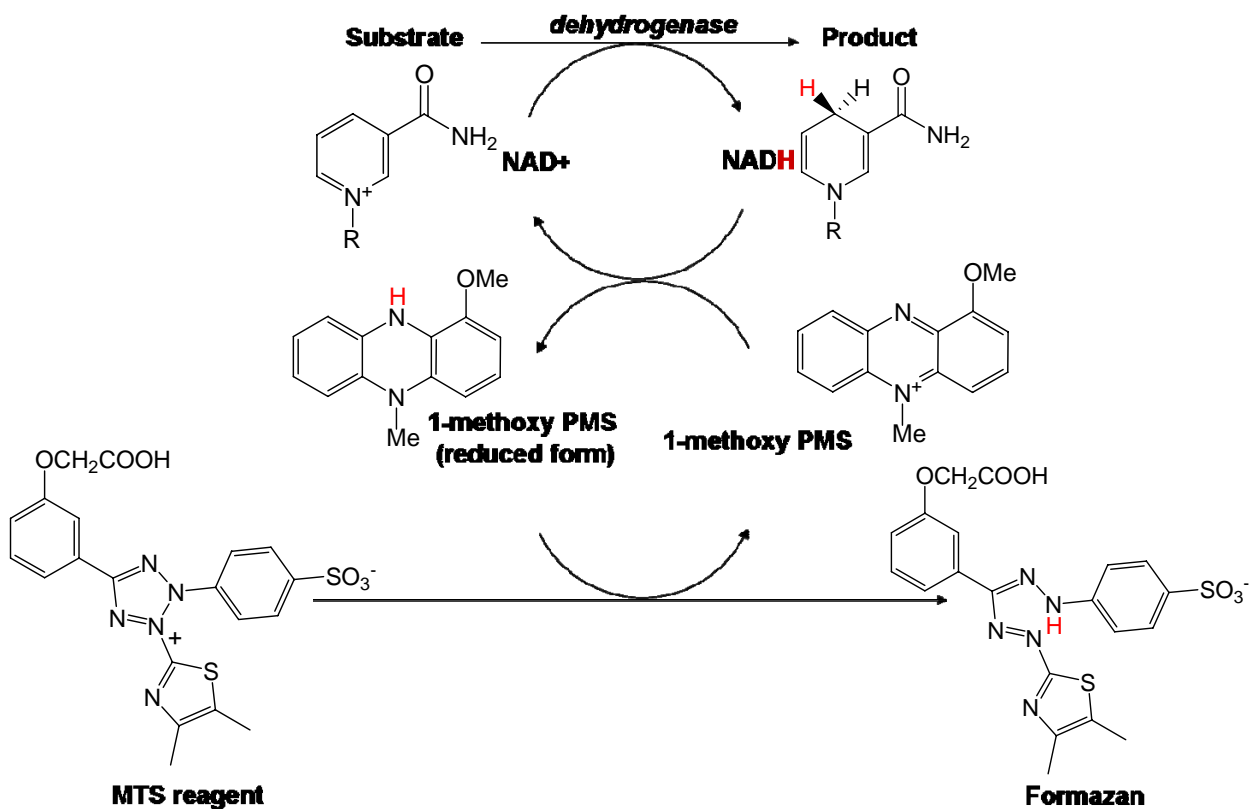


**Figure 4.4.** Schematic diagram showing cellular metabolism resulting in the conversion of MST agent to formazan in MTS assay

The process of cytotoxicity determination of the transfected cells is shown in **Figure 4.3**. Briefly, after transfecting cells with polyplexes (**step 1-4**) with or without the combination with the additive compounds (CQ or GSH-MEE), the cells were further incubated for 96 hrs. The incubated cells were washed and subjected to the MTS assay by adding the MTS reagent (**step 5**) and further incubated for 45 minutes. The absorbance was then measured at  $\lambda = 490$  nm. A blank was also performed by adding the reaction media into empty wells. The blank

was deducted before calculating the percentage of cell viability relative to non-transfected cells.

In addition, in order to compare with our group's previously developed RPCs (CH<sub>6</sub>K<sub>3</sub>H<sub>6</sub>C, RPC(113) and CH<sub>3</sub>K<sub>3</sub>H<sub>3</sub>, RPC(59))<sup>[18]</sup> which shown that they are less toxic to cell (~95% cell viability) the same amount of DNA polyplexes (with 0.5 µg DNA per well) was used in this thesis.

The cell viability after 96 hours of the transfection is illustrated in **Figure 4.5**.

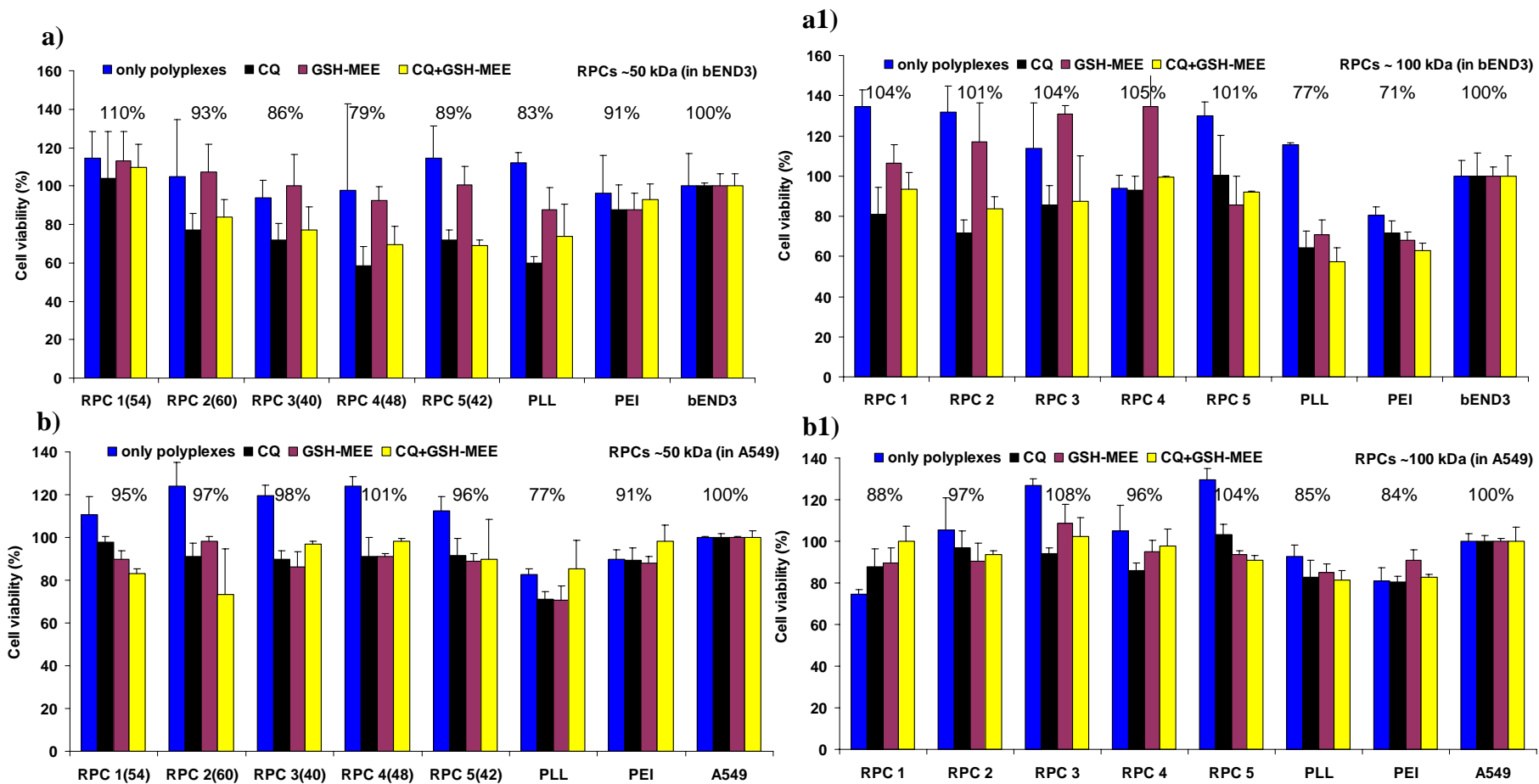


**Figure 4.5.** Cell viability following exposure to RPCs (~50 and ~100 kDa) polyplexes 1-5 at N:P 5, PLL polyplex at N:P 5, PEI polyplex at N:P 10 and cell controls; (a, b) : cell viability of transfected cells with RPCs at lower molecular weight (~50 kDa) in bEND3 and A549, respectively. and (a1,b1) : cell viability of transfected cells with RPCs at high molecular weight (~100 kDa) into bEND3 and A549, respectively. Note: The percentage of cell viability shown in this diagram derived from the average cell viability (%) of cells treated with polyplex alone and in the combination of polyplexes and CQ, GSH-MEE and CQ+GSH-MEE in each cases

As can be seen in **Figure 4.5** the data demonstrated that using RPCs alone at both molecular weights as vectors were tolerated well by both cell lines (blue bars), apart from RPC 1 (~100 kDa) which is slightly toxic to A549 (~75% viability after 96 hours post transfection). In addition, GSH-MEE does not decrease the cell viability. However, both CQ (black bars) and CQ+GSH-MEE (yellow bars) treated cells are less viable. This data indicates that CQ caused toxicity to cells. In addition, there was previous study that also indicated cells may be exposed to relative low concentration of chloroquine (100  $\mu$ M) during the transfection, but the concentration within cells is found to be much higher resulting in cell toxicity and substantial loss of cell viability.<sup>[17]</sup>

Furthermore, the average cell viability in the transfections with PLL and PEI polyplexes when in combination with CQ, GSH-MEE and GSH-MEE+CQ in both cells showed that they are slightly toxic to both cells (~80-87% cell viability).

*In summary, the overall cytotoxicity data indicated that RPCs 1-5 at low and high molecular weight are less toxic to both cell lines (~84-108% cell viability) and similar to ( $CH_6K_3H_6C$ -RPC<sub>113</sub> and  $CH_3K_3H_3$ -RPC<sub>59</sub>)<sup>[18]</sup> (~95% cell viability) relative to PLL (77-85% cell viability) and PEI (71-91% cell viability) polyplexes.*

#### 4.4.2 Cell transfection of RPCs polyplexes (Figure 4.2a, step 2)

The process of transfection experiments is shown in **Figure 4.3**. Briefly, after transfecting cells with polyplexes (**step 1-4**) with or without the combination with the additive compounds (CQ or GSH-MEE), the cells were further incubated for 44 hrs. The cells were washed and the cell lysis buffer was added to the cells (**step 7**). The cell lysate (from freezing and thawing the cells were analysed by luciferase assay to obtain the relative light units (RLU) (**step 8**) (section 2.10.2) and the amount of protein produced by the advanced protein assay (**step 9**) (section 2.10.3). Thus, the gene expression will be shown in relative light units per milli gram of protein (RLU/mg protein). NB. The luciferase assay is a chemiluminescence assay that is directly proportional to the amount of protein that is produced upon transfection.

PLL and PEI polyplexes at N:P 5 and 10, respectively were used as controls.

A background experiment was carried out with cell lines in which the process outlined in **Figure 4.3** was repeated, but whereby the polyplex was not added in **step 3**.

*4.4.2.1 Cell transfection of RPCs polyplexes based on the endosomolytic buffering: effect of CQ (Figure 4.2a, step 2, Exp 2)*

The mixing of the position of the constitution of the histidine and lysine in 2COPs **2-5** provided a subtle way of modulating the  $pK_a$  of the imidazole residues. The average  $pK_a$  of 2COPs **2-5** were 6.2-6.09 (section 3.4.2, page 117), thus at physiological pH ( $\sim 7.4$ ) they will not be fully protonated and will have different buffering capacities when in the early endosome, whose pH is  $\sim 6$ . Therefore, using the reducible polycations (RPCs) of these 2COPs, their buffering will promote modulatable endosomolysis as described earlier (page 27) under the proton sponge hypothesis.<sup>[22]</sup>

In this experiment, we investigated the cell transfection with RPCs/pCMV-luc polyplexes. The RPCs used as vectors are shown in **Table 4.1**.

**Table 4.1. RPCs, polymers and their polyplexes used in cell transfection studies**

RPCs/polymers	$pK_a^a$	MW of RPCs (kDa) <sup>b</sup>	N:P of polyplexes	Diameter of polyplexes (nm) <sup>c</sup>	Zeta potential of polyplexes (mV) <sup>d</sup>
RPC 1 (CK <sub>8</sub> C)	10.51	111.4	5	132.1 ± 4.5	10.0 ± 10.9
RPC 2 (CK <sub>4</sub> H <sub>4</sub> C)	6.20	118.0	5	98.3 ± 0.6	14.3 ± 9.7
RPC 3 (CK <sub>2</sub> H <sub>2</sub> K <sub>2</sub> H <sub>2</sub> C)	6.16	115.1	5	99.8 ± 0.9	13.5 ± 7.2
RPC 4 (CK <sub>2</sub> HKHKH <sub>2</sub> C)	6.11	102.9	5	101.1 ± 2.8	5.8 ± 3.6
RPC 5 (CKHKHKHKHC)	6.09	94.8	5	95.5 ± 1.1	17.4 ± 11.3
PLL	-	70	5	81.0 ± 0.9	11.3 ± 9.0
PEI	-	25	10	108.7 ± 8.6	3.4 ± 0.2

<sup>a</sup> average  $pK_a$  values analysed by <sup>1</sup>H NMR titration

<sup>b</sup> Molecular weight of RPCs was analyzed by GPC using CATSEC300 column compared to PLL standard.

<sup>c</sup> Hydrodynamic diameters of the polyplexes measured by dynamic light scattering using a Zetasizer 3000 (Malvern Instruments, Worcestershire, UK).

<sup>d</sup> Zetapotential measured by using Zetamaster (Malvern Instruments, Worcestershire, UK).

Chloroquine (CQ) (section 1.1.2.2a), a quinoline base with a protonatable diamine containing side-chain, was used for its ability to buffer endosomes.<sup>[23]</sup> The ability of these polyplexes to act as proton sponges for endosome escape could be inferred from the studies with added chloroquine: for example if the polyplexes had good buffering capacity, then the addition of CQ would have a reduced impact on the transfection than if the polyplexes had poor buffering capacity.

Cell lines were incubated with or without CQ (100 μM) for 1 hr (**Figure 4.3, step 2**) before washing and transfecting cells with polyplexes. The transfections of polyplexes with or without CQ were compared and shown in **Figure 4.6**.

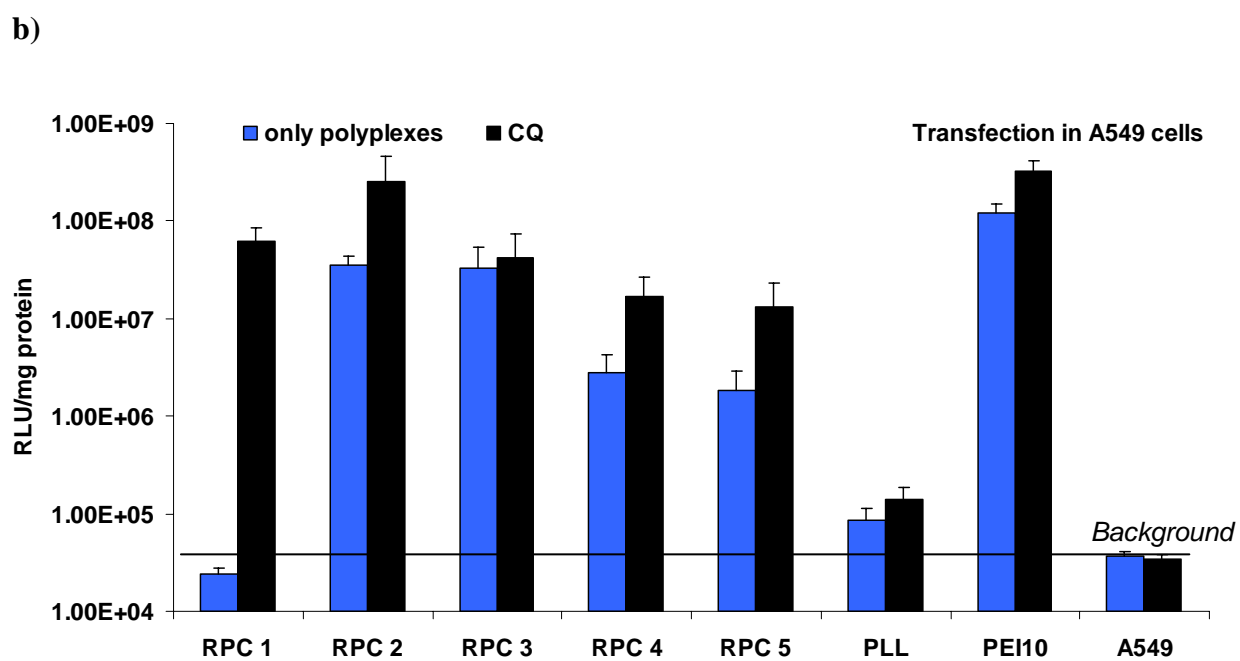
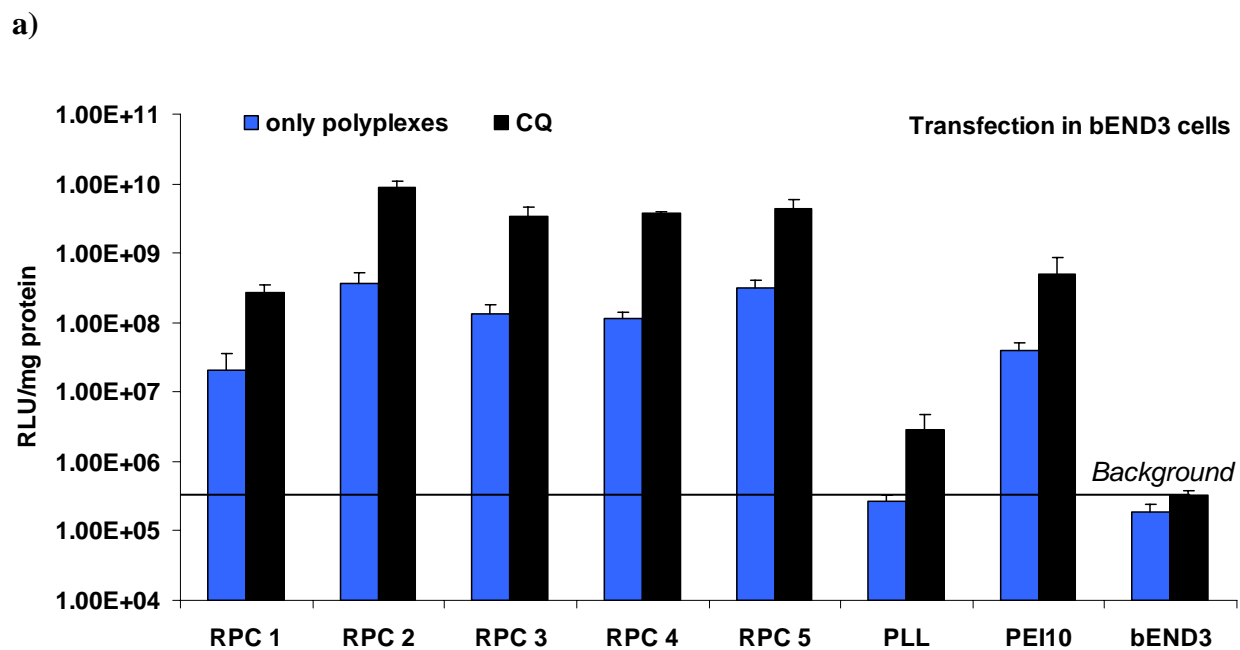


Figure 4.6. Transfection based on CQ with RPC polyplexes 1-5 at N:P 5, PLL polyplex at N:P 5, PEI polyplex at N:P 10 and cell control; a) transfection in bEND3 and b) transfection in A549



bEND3 cells (**Figure 4.5a**):

Without CQ

As can be seen in **Figure 4.6a** RPCs **1-5** polyplexes alone all transfect with significant levels above the background. RPC **1** polyplex gives the lowest level of transfection of the RPCs **1-5**, indicating the histidine moieties are playing a significant part in the transfection ability, i.e. increasing the endosomal release. Furthermore, RPC **1** polyplex has ~2 order of magnitude increase transfection over the non-reducible PLL polyplex, i.e. the reducible disulfide bond is playing a significant part in the transfection efficiencies.

RPCs **2-5** polyplexes have ~1 to ~4 orders of magnitude greater transfection ability than PEI10 and PLL, respectively.

With CQ

The addition of CQ increases the transfection ability by ~1 order of magnitude for all the polyplexes studied, indicating that these polyplexes need CQ to promote endosomal buffering.

A549 cells (**Figure 4.6b**):

#### Without CQ

The first point to note is that RPC **1** alone does not transfect the cells (RLU is below background), whereas, RPCs **2-5** all transfect the cells. Thus, indicating that RPC **1** does not have an efficient mechanism for escaping the endosome.

#### With CQ

As expected, there is ~3 orders of magnitude increase in transfection with cells incubated with CQ and RPC **1** polyplex relative to the polyplex alone. This enhancement is because the RPC **1** has no histidine residues which promote the buffering capacity in the endosomes, therefore it has no efficient mechanism to escape from the endosome by itself for gene expression.

In contrast, there is a modest increase (less than one order of magnitude) in transfection with cells (A549) incubated with CQ and polyplexes of RPCs **2-5** (black bars) than the cells incubated with the polyplexes alone (blue bars). This result suggests that RPCs **2-5** are buffering the endosome, indicating the importance of the intermediate  $pK_a$  of these RPCs.

There is only a slight increase in the transfection of cells incubated with CQ and PLL and the transfection level is near to the background. This result indicates both the lack of a buffering mechanism in the endosome and the lack of DNA release once subsequently in the cytoplasm.

*In summary, from the results of this transfection study based on the endosomolytic buffering capacity of the RPCs 1-5 it can be inferred that histidine moiety is important for gene transfection.*

*4.4.2.2 Cell transfection of RPCs polyplexes based on intracellularly reducible property: effect of GSH-MEE/ BSO (Figure 4.2a, step 2, Exp 3)*

It was established that the RPCs 1-5 polyplexes are stable in the extracellular matrix (section 3.4.4.2c), and they are cleavable in GSH and salt solution (section 3.4.4.2d). In this study we investigated the intracellular reduction of these polyplexes as a function of transfection. Glutathione monoethyl ester (GSH-MEE) (**Figure 4.7a**) was incubated with the cell lines in order to increase the intracellular concentration of GSH. The GSH-MEE is transported into cells effectively by incubation, and is converted into GSH intracellularly.<sup>[21]</sup> Thus, transfection efficiency of RPCs 1-5 should be boosted. Conversely, another set of cells was incubated with buthionine sulfoximine (BSO) (**Figure 4.7b**) which inhibits GSH production, and hence should knock down the transfection efficiency.

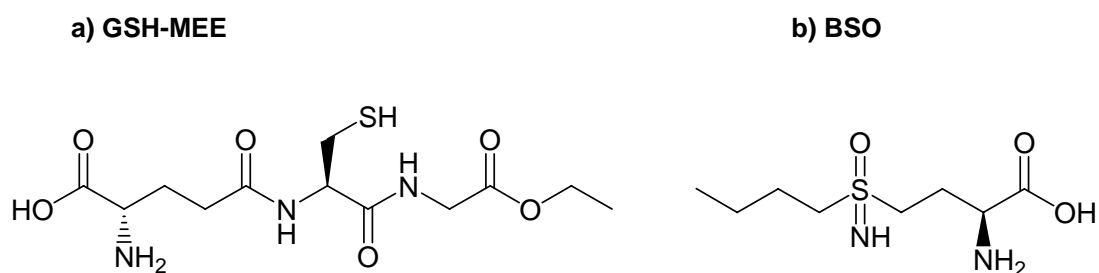


**Figure 4.7. Structures of Glutathion monoethyl ester (GSH-MEE) (a), and buthionine sulfoximine (BSO) (b)**

#### 4.4.2.2a Artificially increase the intracellular GSH level: effect of GSH-MEE (5mM)

The GSH-MEE was used to boost the intracellular GSH in order to probe the reductive cleavage mechanism in the cells. Briefly (**Figure 4.3**), cell lines were incubated with GSH-MEE (5mM) (**step 2**) containing medium for 3 hrs before washing and transfecting the cells with the polyplexes (section 2.10.1). The transfection cells (bEND3 and A549) with polyplexes without (blue bars) and with incubation with GSH-MEE (pink bars) are shown in **Figure 4.8**.

bEND3 cells (**Figure 4.8a**):

Transfection of cells incubated with GSH-MEE (pink bars) has in all cases increased the transfection ability over no incubation with GSH-MEE (blue bars). This result is as expected as we have raised the intracellular GSH levels and hence the DNA should be released more efficiently once in the cytoplasm, *via* more rapid cleavage of the disulfide bonds in the RPCs.

A549 cells (**Figure 4.8b**):

The case with A549 cells is not so clear cut as for bEND3 cells. Here polyplexes from RPCs **1, 2, 4** and PLL observed the expected results of an increase in transfection, whereas RPC **3** saw a reduction in the transfection and RPC **5** has no change in transfection. However, taken as a series we conclude the transfection efficiencies have increased as one might expect.

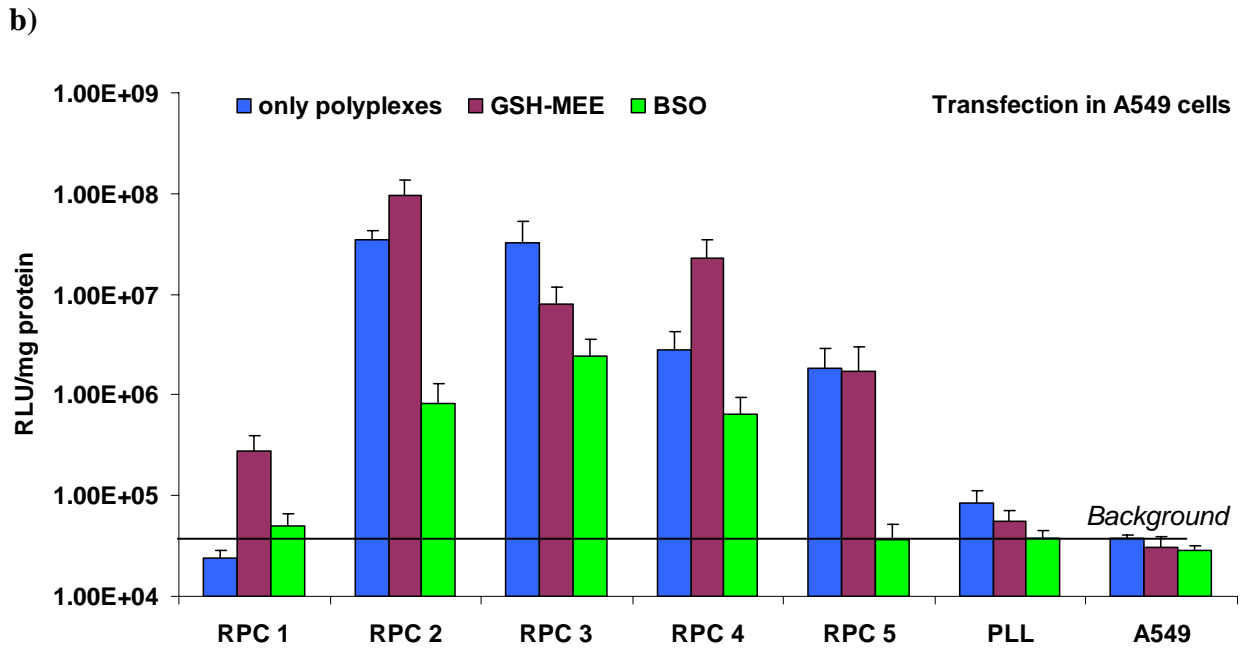
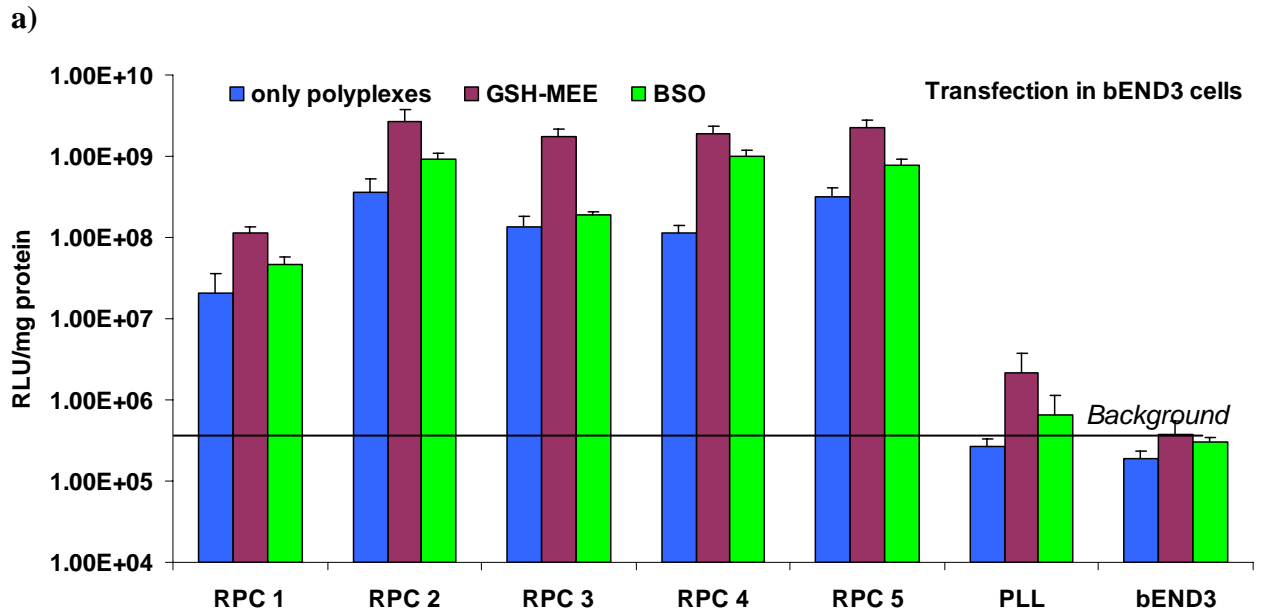


Figure 4.8. Transfection based on GSH-MEE and BSO with RPC polyplexes 1-5 at N:P 5, PLL polyplex at N:P 5, PEI polyplex at N:P 10 and cell control; a) transfection in bEND3 and b) transfection in A549

4.4.2.2b Artificially depleting the intracellular GSH level: effect of BSO

BSO is a GSH biosynthesis inhibitor by inhibiting the  $\gamma$ -glutamylcysteine synthetase in the glutamyl cycle for glutathione synthesis (**Figure 4.9**).<sup>[24]</sup> Therefore, BSO was used to deplete intracellular GSH.<sup>[25]</sup> Briefly (**Figure 4.3**), cell lines were incubated with BSO (100  $\mu$ M) (**step 2**) containing medium for 24 before washing and transfecting the cells with the polyplexes (section 2.10.1).

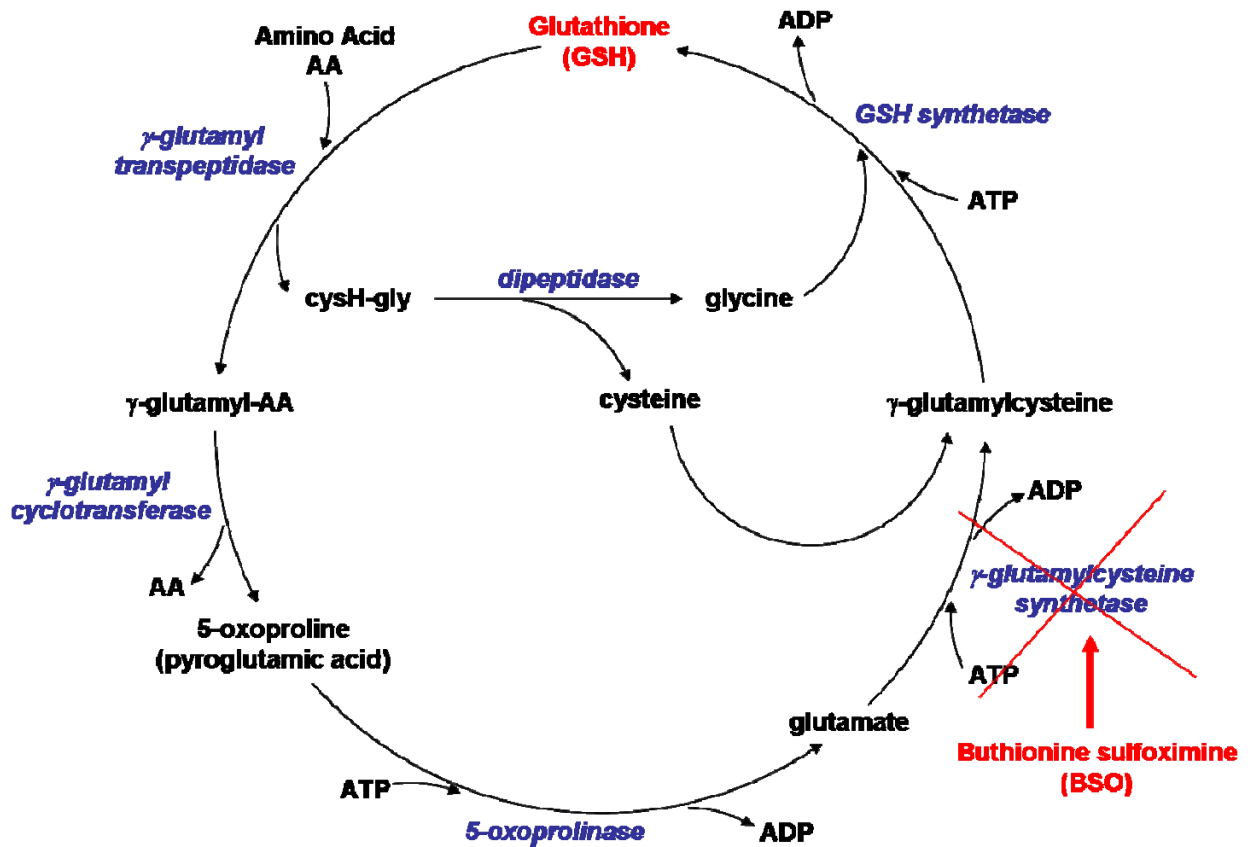


Figure 4.9. Inhibition of glutathione synthesis by buthionine sulfoximine (BSO) in  $\gamma$ -glutamyl cycle

The transfection cells (bEND3 and A549) with polyplexes without (blue bars) and with BSO (green bars) are shown in **Figure 4.8**.

bEND3 cells (**Figure 4.8a**):

The transfection ability of cells incubated with BSO (green bars) and treated with the polyplexes increased. Clearly, this result is contrary to what was expected as the BSO should deplete the amount of intracellular GSH, resulting in poorer release of DNA from the polyplex in the cytoplasm and hence reduced transfection.

A549 cells (**Figure 4.8b**):

In contrast, the A549 cells behaved as expected and all the transfections were knocked down by BSO treatment.

#### 4.4.2.2c Assessing intracellular GSH levels in A549 and bEND3 cells treated with GSH-MEE and BSO

As noted earlier (section 4.4.2.2b) the bEND3 cells treated with BSO had increased levels of transfection over the cells not treated with BSO. This result appears anomalous, as the BSO should knock down intracellular GSH levels and hence the polyplexes should not be degraded less efficiently in the cytoplasm. Therefore, we examined the glutathione content of both cell lines with and without treatment with GSH-MEE and BSO. Monochlorobimane (mBCI) was utilized to probe the intracellular GSH (section 2.10.5) (**Figure 4.10**). Briefly, after incubating cells with GSH-MEE or BSO at appropriate times (**step 1, 2**), the background fluorescence was measured ( $\lambda_{\text{ex}}$  at 355 nm and  $\lambda_{\text{em}}$  at 460 nm) (**step 3**). The monochlorobimane (mBCI) was added into cells (**step 4**) and further incubated for 60 minutes before measuring the



fluorescence again (**step 5**). The relative fluorescence was calculated after subtracting the background.

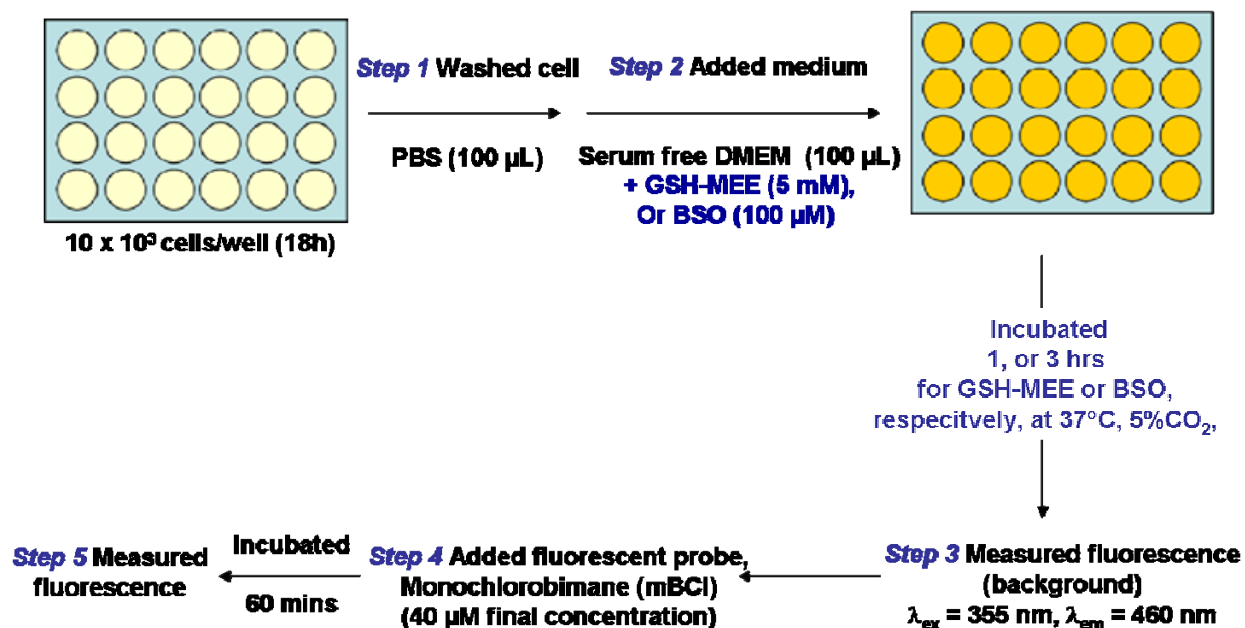
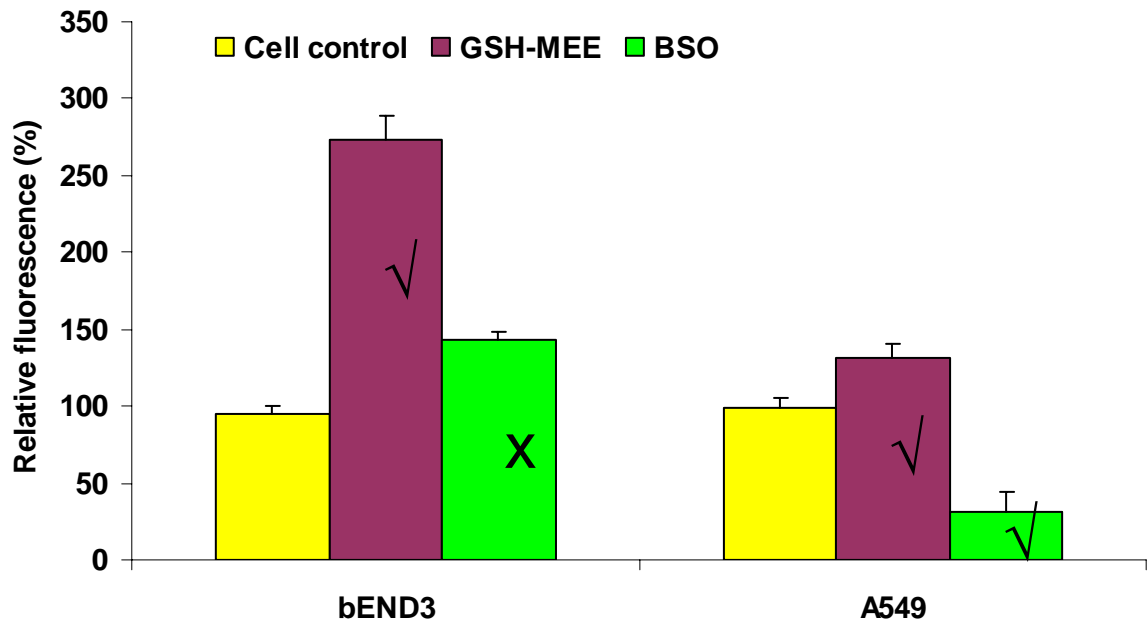


Figure 4.10. The schematic processes of intracellular GSH determination

The intracellular GSH levels of cell lines incubated with GSH-MEE or BSO are shown in

**Figure 4.11.**



**Figure 4.11.** Relative fluorescence of intracellular GSH based on the addition of GSH-MEE and BSO in bEND3 and A549 cells

There is boosting in intracellular GSH level in both cell lines incubated with GSH-MEE (bEND3 and A549, pink bars) relative to the cell control (bEND3 and A549, yellow bars). However the effect is more enhanced in bEND3 as the relative fluorescence increases ~ 175% compared to ~ 40% in A549.

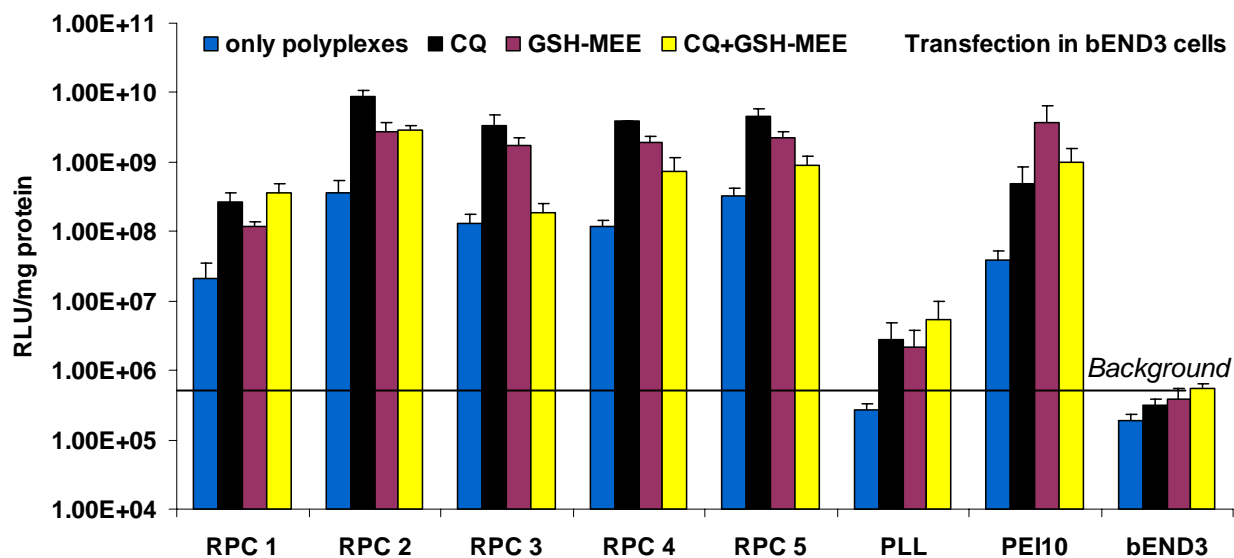
However, There is no reduction of the intracellular GSH in bEND3 cells incubated with BSO (bEND3, green bar) relative to the cell control (bEND3, yellow bar), indeed, there is ~50% increase. In contrast, the intracellular GSH in A549 cells incubated with BSO (A549, green bar) decreases relative to the cell control (A549, yellow bar) by 75%.

We do not understand why the intracellular GSH levels rise when the bEND3 cells are treated with BSO. However, now known this the data present in **Figure 4.8a** (green bars) is not anomalous.

*4.4.2.3 Cell transfection of RPCs polyplexes based on the combination of endosomolytic and intracellularly reducible properties (Figure 4.2a, step 2, Exp 4)*

The transfection of RPCs polyplexes based on endosomolytic and intracellularly reducible properties were also investigated. The transfections were carried out by adding CQ alone, GSH-MEE alone and the combination of CQ and GSH-MEE into cell lines, as well as incubation with the polyplexes alone (section 2.10.1). The transfection processes are shown in **Figure 4.3**. The transfection levels by the polyplexes with CQ alone, GSH-MEE alone, or CQ+GSH-MEE and the polyplexes alone are shown in **Figure 4.12**.

a)



b)

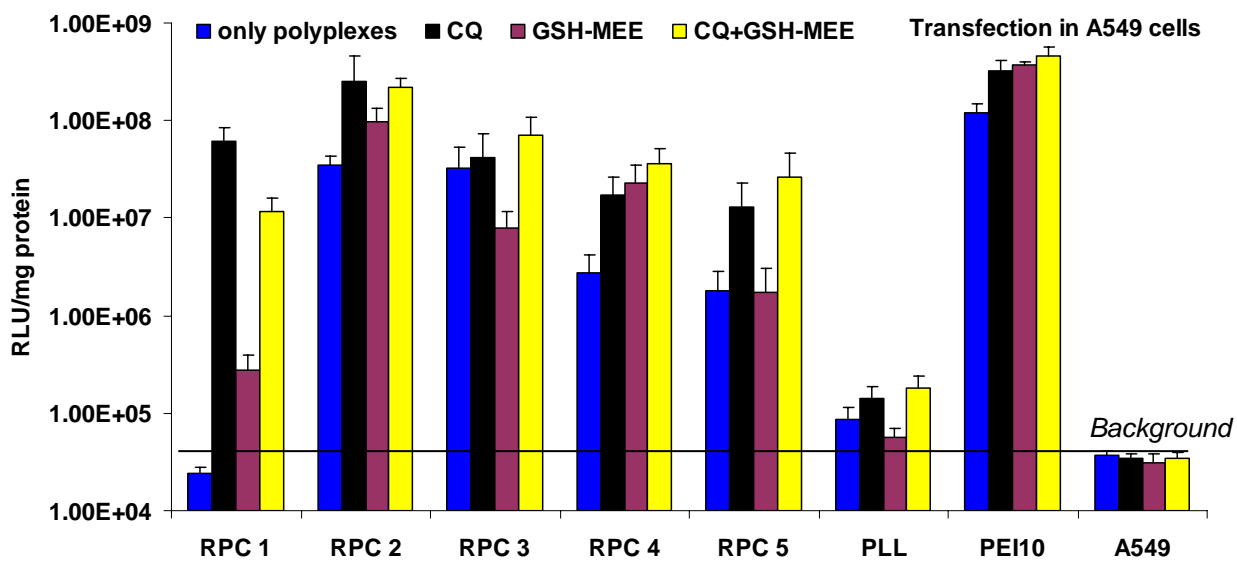


Figure 4.12. Transfection based on CQ and GSH-MEE with RPC polyplexes 1-5 at N:P 5, PLL polyplex at N:P 5, PEI polyplex at N:P 10 and cell control; a) transfection in bEND3 and b) transfection in A549

bEND3 cells (**Figure 4.12a**):

In all cases addition of CQ alone (black bars) and GSH-MEE alone (pink bars) increases the transfection ability of the polyplexes. However, the combination of CQ and GSH-MEE does not give a cumulative effect on the transfection ability (yellow bars).

A549 cells (**Figure 4.12b**):

As with bEND3 cells there is no cumulative effect of adding CQ and GSH-MEE in combination. As can be seen in **Figure 4.12b** for RPCs **2-5**, there is no significant change in transfection efficiencies of RPCs **2** and **4** in A549 incubated with the combination of CQ and GSH-MEE relative to CQ alone and GSH-MEE alone. In addition, for RPCs **2** and RPC **3** there is a modest increase (less than one order of magnitude) in the transfection ability in cells incubated with the combination of CQ and GSH-MEE (yellow bars) relative to the cells incubated with the polyplexes alone (blue bars). This result may suggest that RPCs **2** and **3** do not require the addition of CQ and extra GSH in the transfection. However, the combination of CQ and GSH-MEE appeared to improve the transfection efficiencies of RPCs **4** and **5** (~one order of magnitude relative to the polyplexes alone).

#### 4.4.2.4 *Cell transfection of RPCs polyplexes as a function of RPCs molecular weight (Figure 4.2a, step 2)*

In the previous chapter the set of RPCs based on the oligopeptides were prepared with molecular weights of ~50 kDa and ~100 kDa. Characterizations of these polyplexes showed that RPCs of lower molecular weight bound DNA as well as the higher molecular weight RPCs, but released DNA more efficiently upon treatment with GSH and NaCl, as shown by gel shift assay experiments (Chapter 3, **Figure 3.14** and **3.22**). Therefore, it is expected that these lower molecular weight RPCs might induce higher transfection efficiency than the high molecular weight RPCs as the DNA is released more efficiently from the polyplexes. The properties of these RPCs and their polyplexes are shown in **Table 4.2**.

**Table 4.2. The characteristic of RPCs and their polyplexes**

RPCs/ polymer	MW of RPCs (kDa) <sup>a</sup>	Diameter of polyplexes (nm) <sup>b</sup>	Zeta potential of polyplexes (mV) <sup>c</sup>	DNA released (%) <sup>d</sup> from polyplexes by GSH (5mM)+NaCl (0.5 mM)
RPC 1	53.9	99.9 ± 8.3	16.8 ± 11.0	0
(CK <sub>8</sub> C)	111.4	132.1 ± 4.5	10.0 ± 10.9	0
RPC 2	60.8	98.4 ± 0.7	10.1 ± 14.0	95
(CK <sub>4</sub> H <sub>4</sub> C)	118.0	98.3 ± 0.6	14.3 ± 9.7	61
RPC 3	40.4	94.7 ± 1.5	15.5 ± 15.5	95
(CK <sub>2</sub> H <sub>2</sub> K <sub>2</sub> H <sub>2</sub> C)	115.1	99.8 ± 0.9	13.5 ± 7.2	48
RPC 4	48.5	101.1 ± 2.2	5.3 ± 5.7	95
(CK <sub>2</sub> HKHKH <sub>2</sub> C)	102.9	101.1 ± 2.8	5.8 ± 3.6	95
RPC 5	42.3	90.7 ± 3.4	12.6 ± 12.3	90
(CKHKHKHKHC)	94.8	95.5 ± 1.1	17.4 ± 11.3	63

<sup>a</sup> Molecular weight of RPCs was analyzed by GPC using CATSEC300 column compared to PLL standard.

<sup>b</sup> Hydrodynamic diameters of the polyplexes were measured by dynamic light scattering using a Zetasizer 3000 (Malvern Instruments, Worcestershire, UK).

<sup>c</sup> Zetapotential was measured by using Zetamaster (Malvern Instruments, Worcestershire, UK).

<sup>d</sup> DNA released (%) was determined by gel electrophoresis.

The transfection levels of lower molecular weight RPCs based on CQ, GSH-MEE, and the combination of CQ and GSH-MEE in both cell lines are shown in **Figure 4.13**.

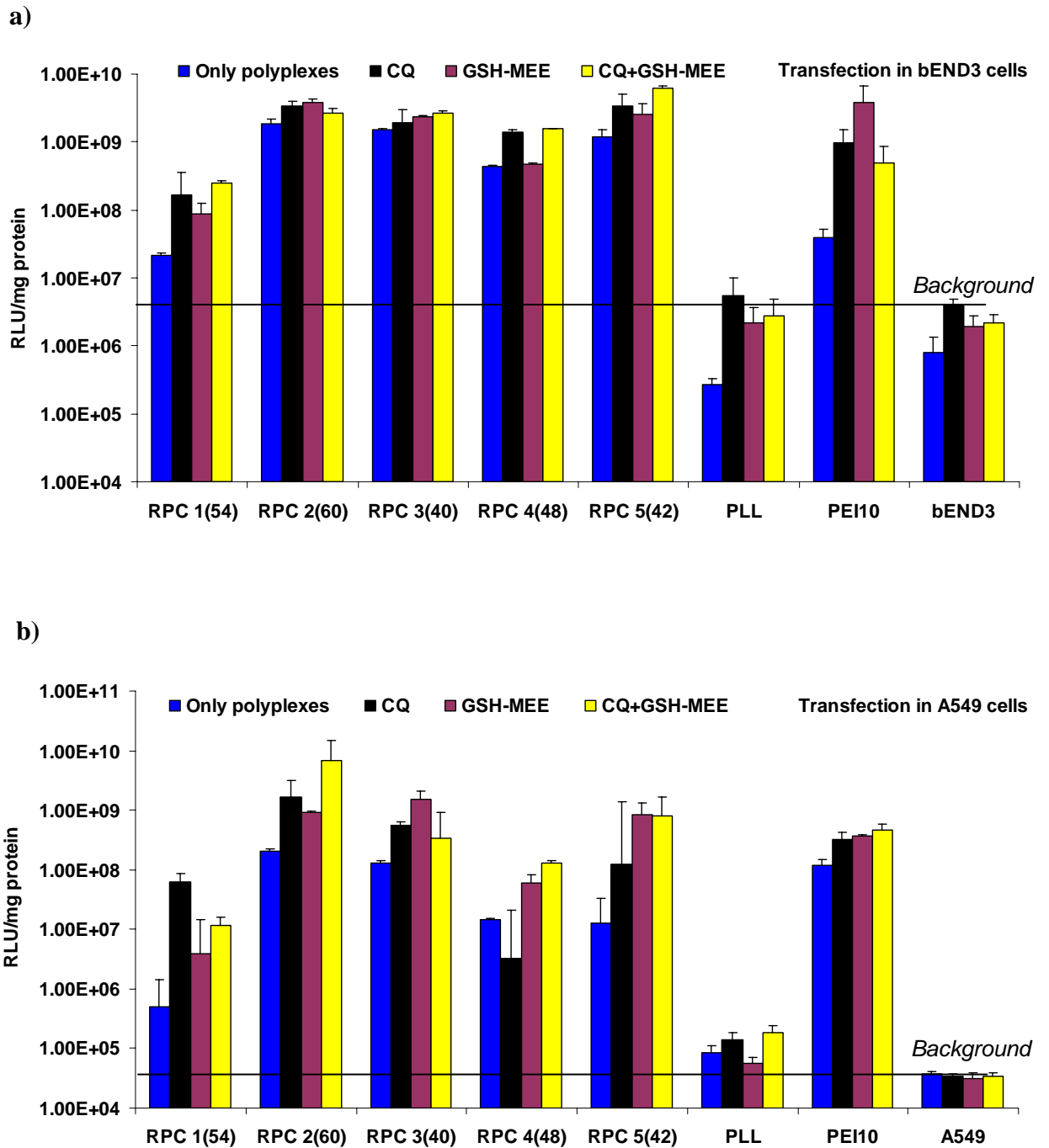


**Figure 4.13.** Transfection based on CQ and GSH-MEE with RPC polyplexes 1-5 (~50 kDa) at N:P 5, PLL polyplex at N:P 5, PEI polyplex at N:P 10 and cell control; a) transfection into bEND3 and b) transfection into A549



As can be seen in **Figure 4.13** there is similar trend of the transfection efficiencies of lower molecular weight RPCs compared to high molecular weight RPCs (**Figure 4.12**). Thus, similarity suggests that transfection mechanism is similar for both low and high molecular weights (~50 kDa and ~100 kDa).

A plot of transfection levels versus polyplex types is shown in **Figure 4.14** for both sets of molecular weight. These graphs clearly show that the lower molecular weight RPCs show greater transfection levels for both cell types. In addition, all profiles are similar with a maximum transfection levels at a  $pK_a$  between 6.20-6.16.

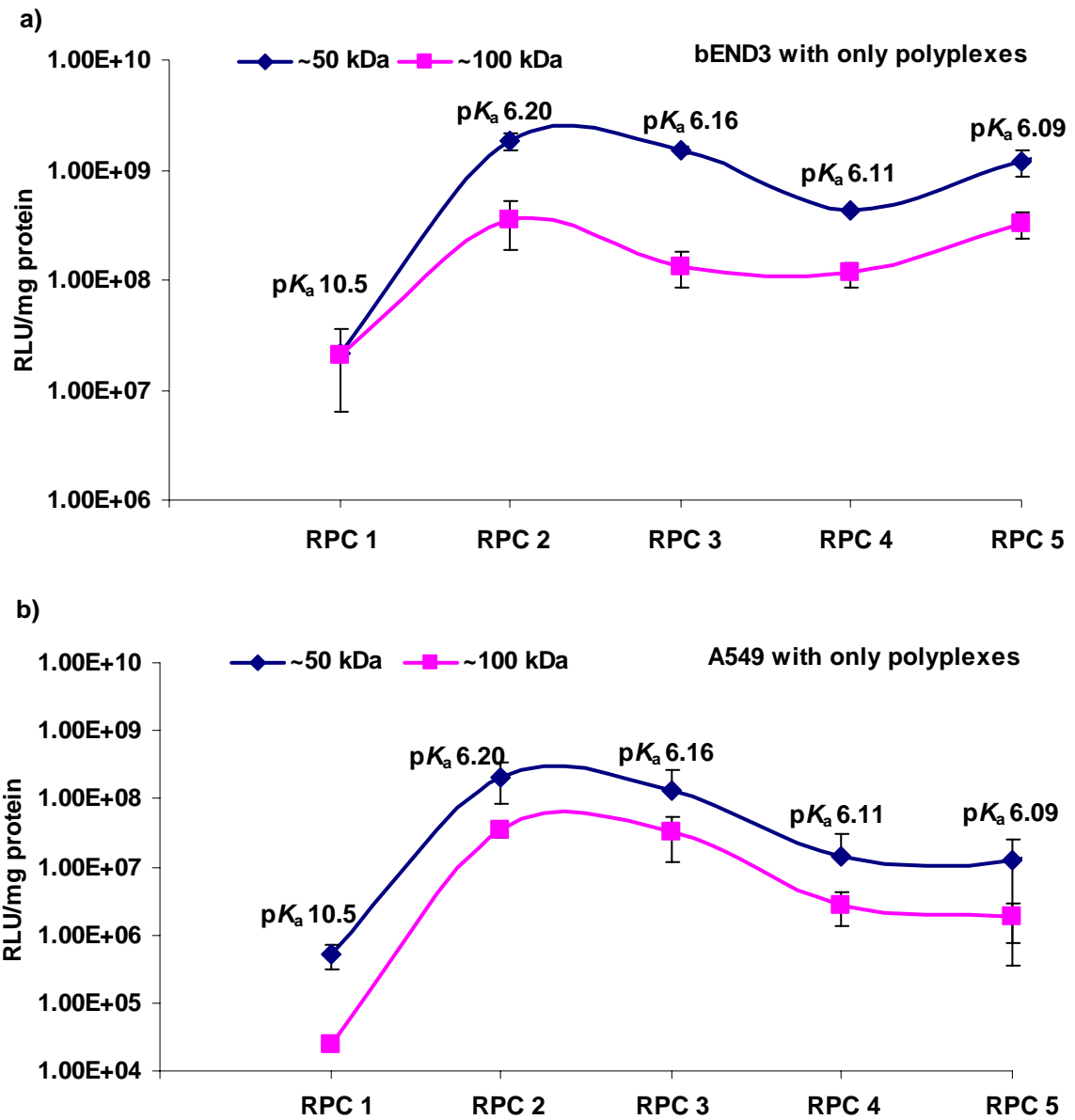


**Figure 4.14.** The transfection efficiency in bEND3 and A549 of RPCs polyplexes at different molecular weight (~50 and ~100 kDa), PEI and PLL polyplexes; a) Transfection in bEND3 and b) Transfection in A549

The transfection efficiency of the pair of polyplexes from RPCs at different molecular weights were carried out based on the endosomolytic (added CQ) and intracellular reducible (added GSH-MEE) properties in both A549 and bEND3 cell lines in a similar fashion to the higher molecular weight RPC polyplexes (**Figure 4.14a and b**). The comparisons of the various transfection levels of RPCs at low and high molecular weight are shown in **Figure 4.15**.

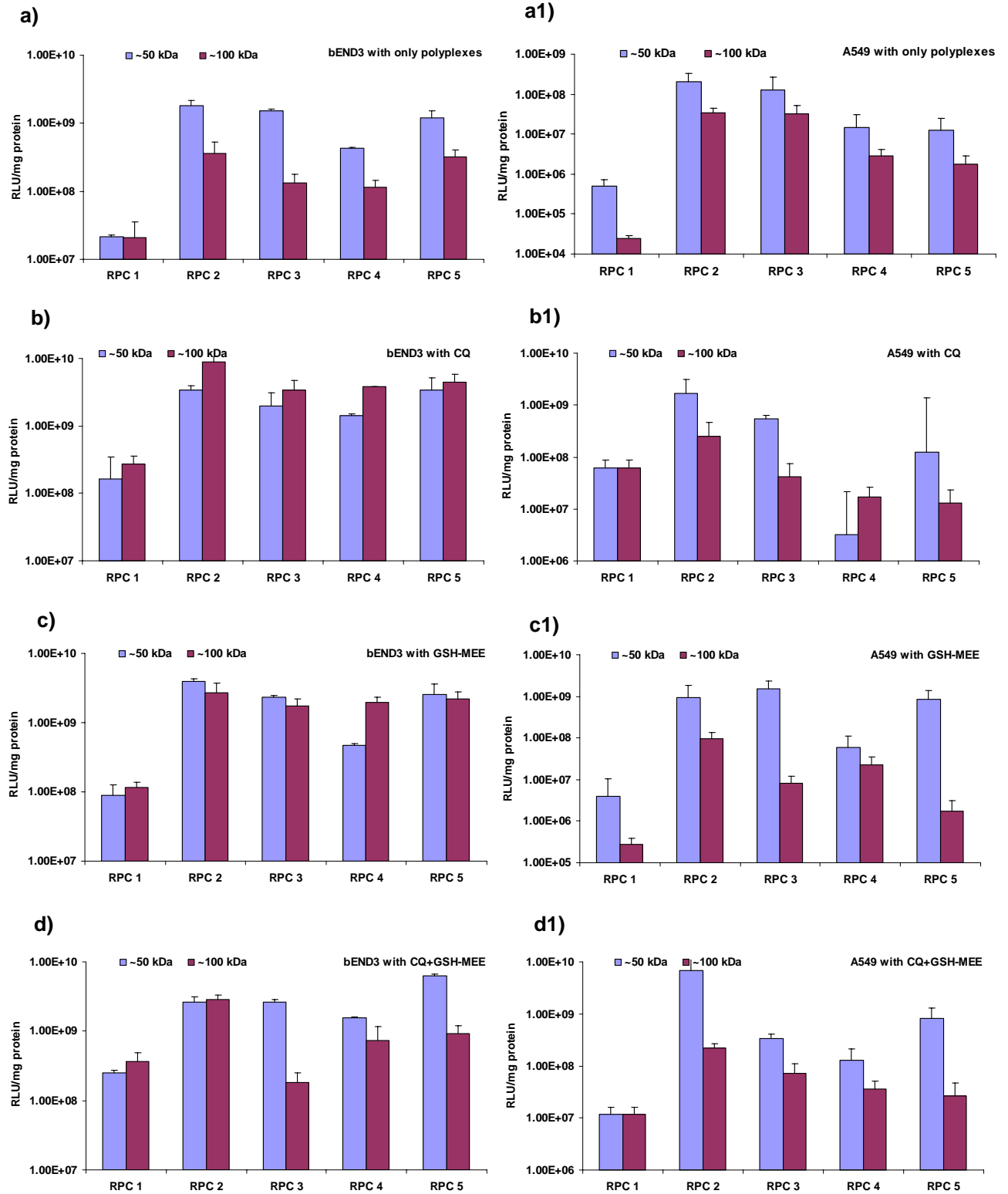


**Figure 4.15.** Transfection in bEND3 and A549 based on CQ and GSH-MEE of polyplexes from the RPCs 1-5 at the different molecular weight; (a)-(d): transfections in bEND3, (a1)-(d1): transfections in A549

As can be seen in **Figure 4.15** the transfection results showed the similar trend by using different molecular weight RPCs as vectors in most cases of both cell lines.

bEND3 cells (**Figure 4.15a-d**):

As can be seen the treatment of the cells with both CQ (**Figure 4.15b**), GSH-MEE (**Figure 4.15c**) and in combination (**Figure 4.15d**) reduces the differential between the transfection levels and molecular weight considerably when compared to no such treatment (**Figure 4.15a**).

A549 cells (**Figure 4.15a1-d1**):

In contrast, A549 cells maintain a differential in transfection cells as a function of molecular weight when treated with CQ (**Figure 4.15b1**), GSH-MEE (**Figure 4.15c1**) and in combination (**Figure 4.15c1**) when compared to no such treatment (**Figure 4.15a1**)

*In summary, lower molecular weight RPC polyplexes (~50kDa) give higher transfection levels than high molecular weight RPC polyplexes (~100 kDa).*

#### **4.4.3 Cell transfection of oligopeptide polyplexes**

Oligopeptide (2COPs **1-5**) polyplexes were prepared at N:P 5 (See section 3.6.2), and were found that their sizes were greater than 1  $\mu\text{m}$  over the time course of 48 hrs (**Table 3.7** and **Figure 3.23**). However, the transfection efficiency of these polyplexes was still determined, although it was expected that this would be poor *in vivo*, because the large polyplexes would interact with blood components or macrophages, resulting in the clearance from the blood

stream before reaching the cells.<sup>[26]</sup> In addition, we might expect poor transfection *in vitro* because of polyplex uptake by endocytosis is poor for polyplexes larger than 200 nm.<sup>[27]</sup>

The PEI polyplexes formed at N:P 10 were utilized as positive control. The human lung carcinoma cells, A549, were used in the *in vitro* transfection (section 2.10.1). The cell transfections with these polyplexes were carried out in the same manner as with RPCs polyplexes as shown in **Figure 4.3**. However, the experiments with GSH and CQ were not performed. Therefore, after 18 hrs of growing cells, the polyplexes were added directly to the washed cells (**Figure 4.3, step 3**). The relative transfection efficiencies are shown in **Figure 4.16**.

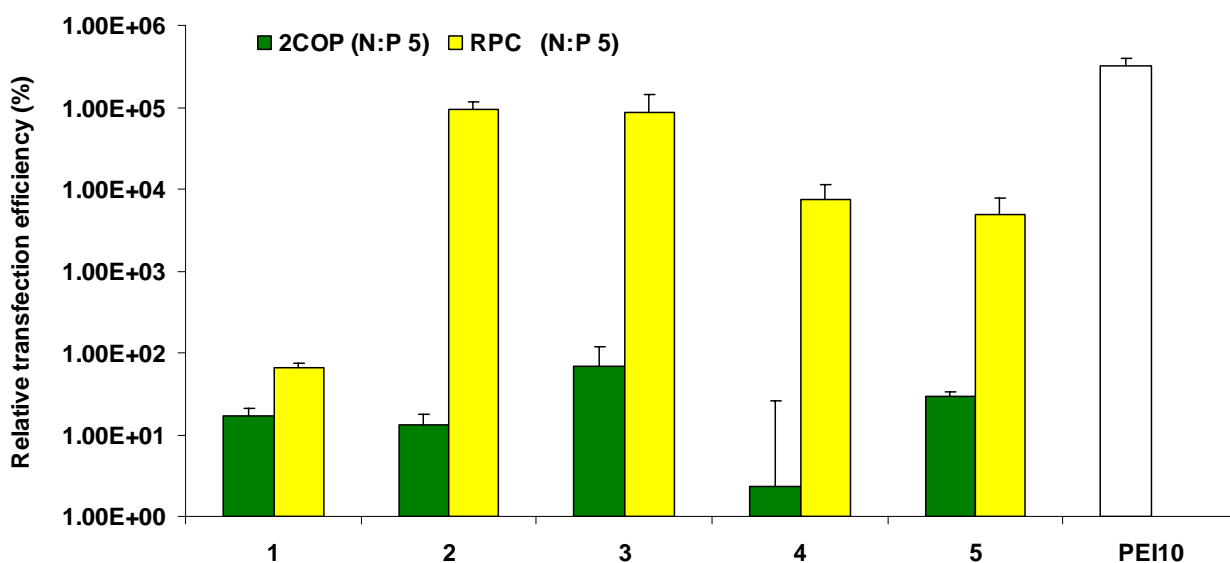


**Figure 4.16.** Relative transfection efficiency of 2COPs, RPCs at N:P 5 and PEI at N:P 10 in A549 cells

As predicted the oligopeptides 2COPs were poorly transfecting the cells relative to the RPCs that they formed (**Figure 4.16**). This result is presumably due to the series of the polyplexes formed from the 2COPs.

## 4.5 Conclusions

The work presented in this chapter involved evaluating the cytotoxicity and transfection of RPCs **1-5** (~50 kDa and ~100 kDa) in order to investigate the endosomolytic and intracellularly reducible properties and the affect of different molecular weight RPCs on transfection efficiency. The transfection efficiency of 2COPs **1-5** was also investigated in comparison with RPCs.

### 4.5.1 Cytotoxicity of RPCs polyplexes

Transfections in combination with CQ causes toxicity to cells. However, the overall cytotoxicity data indicated that RPCs **1-5** at lower and high molecular weight are less toxic to both cell lines relative to PLL and PEI polyplexes as its ability to unpackage in the cytoplasm suggested a reduced cytotoxicity compared to PEI and PLL, as it would be expected to degrade to readily cleared fragments (2COPs).

### 4.5.2 Cell transfection of RPC polyplexes

Our overall data of both cells indicates that RPCs **2-5** (with 40% histidine content) – which are less aided by CQ relative RPC **1** – is behaving in a similar way to PEI, in term of the proton sponge mechanism, escaping to the cytoplasm without developing into the lysosome<sup>[28]</sup> and does not require addition of the endosome buffering agent CQ to achieve high transfection efficiencies, whereas PLL and RPC **1** polyplexes do. These findings are in agreement with the study by Read and colleagues<sup>[29]</sup> which revealed that RPCs (45, 187 kDa)

oxidatively polymerized from CK<sub>10</sub>C required combining with CQ or DOTAP for efficient transfection because CK<sub>10</sub>C-RPC itself lacked endosomal buffering capacity. In addition, by incorporation of histidine moieties in our group's previous work<sup>[18]</sup> also indicated that histidine-containing RPCs (RPC(59) (CH<sub>3</sub>K<sub>3</sub>H<sub>3</sub>C, 59 kDa) and RPC (113) (CH<sub>6</sub>K<sub>3</sub>H<sub>6</sub>C, 113 kDa) promote the endosomal escape mechanism. However, using the new strategy to modulate the p*K*<sub>a</sub> of RPCs in this study revealed that the range of p*K*<sub>a</sub> of RPCs **2-5** (6.09-6.20) indeed buffer in a similar way to PEI. In addition, the highest transfection efficiencies in both cell types were with RPC **2**, the 'poly(diblock)' [CK<sub>4</sub>H<sub>4</sub>C]<sub>n</sub> polymer, which was 4 orders of magnitude better than PEI and 100-fold better than PLL in bEND 3 cells. In addition, comparing the p*K*<sub>a</sub> of RPCs **2-5** (p*K*<sub>a</sub> 6.20-6.09) suggested that the optimum p*K*<sub>a</sub> that induced the highest transfection efficiency in both cells is at p*K*<sub>a</sub> 6.20 (RPC **2**) (**Figure 4.17**).

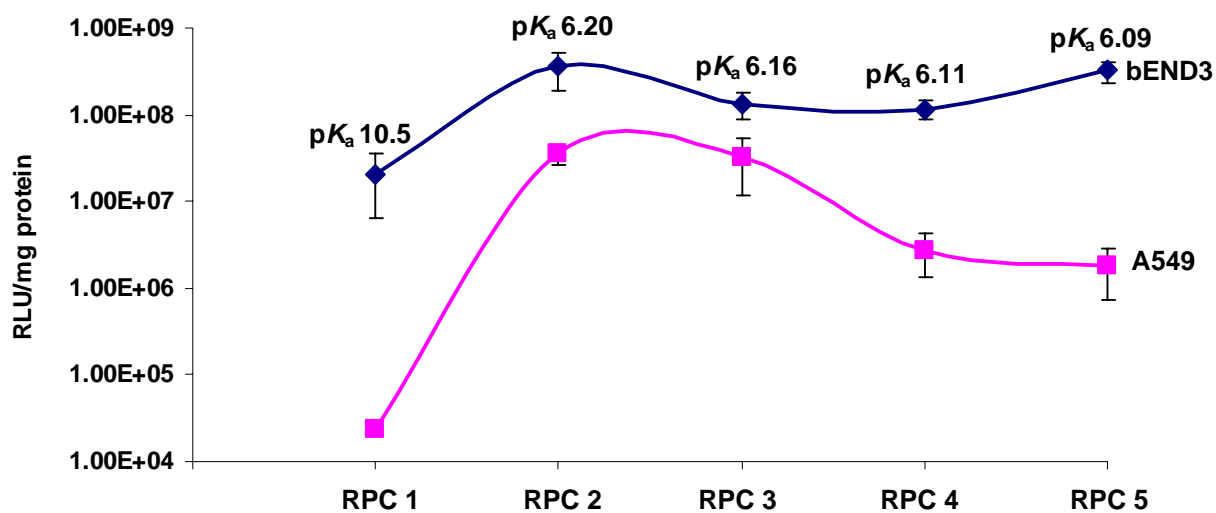


**Figure 4.17.** The transfection efficiency in bEND3 and A549 of RPCs polyplexes based on the p*K*<sub>a</sub> values

[ Transfection in bEND3—◆— and transfection in A549 —■— ]



From the results of the artificial depletion and increase of the intracellular GSH level studies, it could be shown that these RPCs are reduced by intracellular GSH (vector feature V).

The difference observed between transfection efficiencies in bEND3 and A549 cell lines was most likely due to the different rate of cell growth *in vitro*. Change in growth rates would have affected the level of intracellular glutathione and the protein expression. Concomitant degradation of the nuclear membrane would, therefore, have led to the release of high level of glutathione into cytoplasm.

#### **4.5.3. Cell transfection of RPCs polyplexes as a function of RPCs molecular weight**

The trend of transfection efficiency of lower molecular weight RPCs and high molecular weight RPCs were similar in both cells: The lower molecular weight RPCs induced higher transfection efficiency.

#### **4.5.4 Cell transfection of oligopeptides polyplexes**

As predicted the oligopeptides 2COPs were poor transfection agents relative to the RPCs as they formed large polyplexes which are not efficiently internalized into the cells *via* endocytosis effectively.<sup>[26]</sup> Manpreet and colleagues<sup>[30]</sup> also revealed that condensing DNA with low molecular weight peptides (DiCWK<sub>3</sub>, AlkCWK<sub>8</sub> and K<sub>19</sub>) failed to produce significant gene transfection which was put down to their large particle diameters (724, 2412 and 3102 nm, respectively).

*In summary, incorporation of lysine, histidine, and cysteine residues in RPCs provide promising vectors that bind DNA extracellularly and protect against nucleases and protein-mediated disassembly (vector feature **I**), cell uptake via syndecan mediated endocytosis (vector feature **III**), provide a tunable endosomal release mechanism (vector feature **IV**), and release DNA into the cytoplasm via glutathione reduction mechanisms (vector feature **V**) leading to further gene expression. In addition, these RPCs are non-toxic to cells.*

*However, using endothelium (bEND3) and epithelium cell lines (A549) in the in vitro transfection could suggest these polyplexes may not be suitable to inject into blood vessels as they could internalize into endothelium cells that line the interior surface of the blood vessels before they get to epithelium cells, which are the tissues to be treated. However, injecting the polyplexes to the specific tissue could be the alternative way to overcome this hurdle.*

## **4.6 References**

1. Lipps, H.J., Jenke, A.C.W., Nehlsen, K., Scinteie, M.F., Stehle, I.M., and Bode, J. (2003). Chromosome-based vectors for gene therapy. *Gene*, **304**, 23-33.
2. Koonin, E., Senkevich, T., and Dolja, V. (2006). The ancient virus world and evolution of cells. *Biology Direct*, **1**, 1:29.
3. Torchilin, V.P. (2006). Recent approaches to intracellular delivery of drugs and DNA and organelle targeting. *Annual Review of Biomedical Engineering*, **8**, 343-375.
4. Dobson, J. (2006). Gene therapy progress and prospects: Magnetic nanoparticle-based gene delivery. *Gene Therapy*, **13**, 283-287.

5. Mastrobattista, E., van der Aa, M., Hennink, W.E., and Crommelin, D.J.A. (2006). Artificial viruses: A nanotechnological approach to gene delivery. *Nature Reviews Drug Discovery*, **5**, 115-121.
6. Nishiyama, N., and Kataoka, K. (2006). Current state, achievements, and future prospects of polymeric micelles as nanocarriers for drug and gene delivery. *Pharmacology and Therapeutics*, **112**, 630-648.
7. Rawat, M., Singh, D., Saraf, S., and Saraf, S. (2006). Nanocarriers: Promising vehicle for bioactive drugs. *Biological and Pharmaceutical Bulletin*, **29**, 1790-1798.
8. Wagner, E. (2007). Programmed drug delivery: Nanosystems for tumor targeting. *Expert Opinion on Biological Therapy*, **7**, 587-593.
9. Kim, Y.H., Park, J.H., Lee, M., Kim, Y.H., Park, T.G., and Kim, S.W. (2005). Polyethylenimine with acid-labile linkages as a biodegradable gene carrier. *Journal of Controlled Release*, **103**, 209-219.
10. Varga, C.M., Tedford, N.C., Thomas, M., Klibanov, A.M., Griffith, L.G., and Lauffenburger, D.A. (2005). Quantitative comparison of polyethylenimine formulations and adenoviral vectors in terms of intracellular gene delivery processes. *Gene Therapy*, **12**, 1023-1032.
11. Merdan, T., Kunath, K., Petersen, H., Bakowsky, U., Voigt, K.H., Kopecek, J., and Kissel, T. (2005). PEGylation of poly(ethylene imine) affects stability of complexes with plasmid DNA under in vivo conditions in a dose-dependent manner after intravenous injection into mice. *Bioconjugate Chemistry*, **16**, 785-792.
12. Brownlie, A., Uchegbu, I.F., and Schatzlein, A.G. (2004). PEI-based vesicle-polymer hybrid gene delivery system with improved biocompatibility. *International Journal of Pharmaceutics*, **274**, 41-52.

13. Erbacher, P., Bettinger, T., Brion, E., Coll, J.L., Plank, C., Behr, J.P., and Remy, J.S. (2004). Genuine DNA/polyethylenimine (PEI) complexes improve transfection properties and cell survival. *Journal of Drug Targeting*, **12**, 223-236.
14. Moghimi, S.M., Symonds, P., Murray, J.C., Hunter, A.C., Debska, G., and Szewczyk, A. (2005). A two-stage poly(ethylenimine)-mediated cytotoxicity: Implications for gene transfer/therapy. *Molecular Therapy*, **11**, 990-995.
15. Foley, M., and Tilley, L. (1997). Quinoline antimalarials: Mechanisms of action and resistance. *International Journal for Parasitology*, **27**, 231-240.
16. Zauner, W., Ogris, M., and Wagner, E. (1998). Polylysine-based transfection systems utilizing receptor-mediated delivery. *Advanced Drug Delivery Reviews*, **30**, 97-113.
17. Monsigny, M., Roche, A.C., Midoux, P., and Mayer, R. (1994). Glycoconjugates as carriers for specific delivery of therapeutic drugs and genes. *Advanced Drug Delivery Reviews*, **14**, 1-24.
18. Read, M.L., Singh, S., Ahmed, Z., Stevenson, M., Briggs, S.S., Oupicky, D., Barrett, L.B., Spice, R., Kendall, M., Berry, M., Preece, J.A., Logan, A., and Seymour, L.W. (2005). A versatile reducible polycation-based system for efficient delivery of a broad range of nucleic acids. *Nucleic Acids Research*, **33**, e86.
19. Hong, R., Han, G., Fernandez, J.M., Kim, B.J., Forbes, N.S., and Rotello, V.M. (2006). Glutathione-mediated delivery and release using monolayer protected nanoparticle carriers. *Journal of the American Chemical Society*, **128**, 1078-1079.
20. Carlisle, R.C., Etrych, T., Briggs, S.S., Preece, J.A., Ulbrich, K., and Seymour, L.W. (2004). Polymer-coated polyethylenimine/DNA complexes designed for triggered activation by intracellular reduction. *Journal of Gene Medicine*, **6**, 337-344.

21. Anderson, M.E., Powrie, F., Puri, R.N., and Meister, A. (1985). Glutathione monoethyl ester-preparation, uptake by tissues, and conversion to glutathione. *Archives of Biochemistry and Biophysics*, **239**, 538-548.
22. Behr, J.P. (1997). The proton sponge: A trick to enter cells the viruses did not exploit. *Chimia*, **51**, 34-36.
23. Cheng, J.J., Zeidan, R., Mishra, S., Liu, A., Pun, S.H., Kulkarni, R.P., Jensen, G.S., Bellocq, N.C., and Davis, M.E. (2006). Structure-function correlation of chloroquine and analogues as transgene expression enhancers in nonviral gene delivery. *Journal of Medicinal Chemistry*, **49**, 6522-6531.
24. Ristoff, E., and Larsson, A. (2007). Inborn errors in the metabolism of glutathione. *Orphanet Journal of Rare Diseases*, **2**.
25. Reliene, R., and Schiestl, R.H. (2006). Glutathione depletion by buthionine sulfoximine induces DNA deletions in mice. *Carcinogenesis*, **27**, 240-244.
26. Patel, H.M. (1992). Serum opsonins and liposomes - their interaction and opsonophagocytosis. *Critical Reviews in Therapeutic Drug Carrier Systems*, **9**, 39-90.
27. Bishop, N.E. (1997). An update on non-clathrin-coated endocytosis. *Reviews in Medical Virology*, **7**, 199-209.
28. Akinc, A., Thomas, M., Klibanov, A.M., and Langer, R. (2005). Exploring polyethylenimine-mediated DNA transfection and the proton sponge hypothesis. *Journal of Gene Medicine*, **7**, 657-663.
29. Read, M.L., Bremner, K.H., Oupicky, D., Green, N.K., Searle, P.F., and Seymour, L.W. (2003). Vectors based on reducible polycations facilitate intracellular release of nucleic acids. *Journal of Gene Medicine*, **5**, 232-245.

30. Wadhwa, M.S., Collard, W.T., Adami, R.C., McKenzie, D.L., and Rice, K.G. (1997). Peptide-mediated gene delivery: Influence of peptide structure on gene expression. *Bioconjugate Chemistry*, **8**, 81-88.

## **CHAPTER 5**

### **Synthesis and characterization of reducible *copoly*cations (RcPCs) containing lysine, histidine and cysteine based sequences and TAT peptide**

# CONTENTS

List of Figures

List of Tables

## 5 SYNTHESIS AND CHARACTERIZATION OF REDUCIBLE *COPOLYCATIONS* (RcPCs) CONTAINING LYSINE, HISTIDINE AND CYSTEINE BASED SEQUENCES AND TAT PEPTIDE

<b>5.1 Introduction</b>	<b>219</b>
<b>5.2 Objectives</b>	<b>221</b>
<b>5.3 Methodology</b>	<b>222</b>
<b>5.4 Results and discussion</b>	<b>225</b>
5.4.1 TAT oligopeptide purification and characterization	225
5.4.2 Formation and characterization of reducible <i>copolycations</i> (RcPCs)	226
5.4.3 2COP and TAT sequence ratio analysis	228
5.4.4 Formation and characterization of TAT and RcPC polyplexes	231
5.4.4.1 Weight per charge and N:P ratio calculation	231
5.4.4.2 TAT and RcPCs polyplex formation and characterization	234
5.4.4.2a Diameter and zeta potential of polyplexes	234
5.4.4.2b Extracellular stability studies of polyplexes	236
5.4.4.2c Intracellular reduction studies of polyplexes	238
<b>5.5 Conclusions</b>	<b>241</b>
<b>5.6 References</b>	<b>244</b>



## List of Figures

Figure 5.1.	The amino acid sequence of human immunodeficiency virus 1 (HIV-1) TAT protein	222
Figure 5.2.	Schematic overview of characterisation and analysis of oligopeptides and polyplexes in this chapter	224
Figure 5.3.	Schematic model of reducible <i>c</i> opolycations (RcPCs) synthesis <i>via</i> random oxidative polymerization	226
Figure 5.4.	Oxidative polymerization compared between RcPCs <b>1-5</b> prepared from 2COPs ( <b>1-5</b> ):TAT at 1:1 and RcPC 5 (1:3) incubated at ambient	228
Figure 5.5.	Amino acid standard at 200 nmol ml <sup>-1</sup> run with GC	229
Figure 5.6.	Gel shift assay with (a) and without (b) polyaspartic acid (PAA) of polyplexes formed from RP-TAT (N:P 5), RcPCs 1-5 (N:P 5), PEI (N:P 10) and PLL (N:P 5)	237
Figure 5.7.	DNA binding and release demonstrated by gel shift assays of RP-TAT and RcPC polyplexes	240

## List of Tables

Table 5.1.	The purity and mass of purified oligopeptides	225
Table 5.2.	RP-TAT and RcPCs produced from TAT and 2COPs <b>1-5</b>	227
Table 5.3.	2COP and TAT sequence ratios of RcPCs 1-5 analysed by amino acid analysis	230
Table 5.4.	Weight per charge (wpc) of 2COPs, RP-TAT and RcPCs used in this chapter	233
Table 5.5.	Properties of RPCs, RP-TAT and RcPCs their polyplexes formed at N:P 5	235

# 5 SYNTHESIS AND CHARACTERIZATION OF REDUCIBLE COPOLYCATIONS (RcPCs) CONTAINING LYSINE, HISTIDINE AND CYSTEINE BASED SEQUENCES AND TAT PEPTIDE

## *Abstract*

*As shown previously in Chapters 3 and 4 the reducible polycations (RPCs) are promising vectors for gene delivery in non-viral system. However, these vectors have no nuclear targeting signal. Therefore, in this chapter we design to incorporate the nuclear targeting signal (TAT) in the vectors in order to potentially improve the transfection ability. The RP-TAT was synthesized via oxidative polymerisation of TAT oligopeptide (CRKKRRQRRRC). The RcPCs 1-5 (~50 kDa) were synthesized via random oxidative polymerisation of 2COPs 1-5 and TAT oligopeptide at molar ratio 1:1. The RcPC 5 was also synthesized at 1:3 molar ratio of 2COP 5:TAT. The DNA polyplexes of RP-TAT and RcPCs 1-5 were formed at N:P 5 and characterized. The RP-TAT and RcPCs polyplexes are approximately 100 nm in diameter, and are all positively charged. Gel shift assay revealed that the RP-TAT and RcPCs polyplexes are unpacked by interacting with PAA (extracellularly simulated condition) and GSH+NaCl (intracellularly simulated condition). These results suggested that the RcPCs have less potential than RPCs to be used as vectors as they are less stable to PAA than the RPCs, and hence may be degraded in the blood before they are internalized into the cells.*

## 5.1 Introduction

As described in Chapter 1 (page 22), there are several cellular barriers that need to be overcome in order for a gene to be delivered to the nucleus.<sup>[1]</sup> In Chapters 3 and 4, we have shown that the RPCs incorporating lysine, histidine and cysteine residues are promising vectors for non-viral gene delivery. In particular, these polyplexes were stable in an extracellular environment. The positively charged polyplexes could internalize into cells *via* syndecan-mediated endocytosis,<sup>[2,3]</sup> whilst the histidine residues help to buffer the endosomes,

resulting in endosomal disruption and release of the polyplexes into the cytoplasm.<sup>[4]</sup> Disulfide bonds in the backbone of the polycations provide the reducible property of the polyplexes (cleavage by intracellular GSH) leading to release of the nucleic acid for further enhancements in the gene expression mechanism.<sup>[5,6]</sup>

However, there is another key challenge to improve these cationic vectors, which is the nuclear import property.<sup>[7,8]</sup> The DNA must be internalized into the nucleus in order to either replace the non-functional gene or transcribe to mRNA for furthering translation to the therapeutic protein.<sup>[9]</sup> The nuclear membrane is a barrier for most macromolecules that are greater than 45 kDa, unless they are able to interact with the nuclear pore active transport system<sup>[10]</sup> as described in Chapter 1 (section 1.1.2.2b). The nuclear localization signals (NLS) are peptide sequences that are recognized by this nuclear transport system. Therefore, to improve the non-viral RPCs **1-5** vectors designed in Chapters 3 and 4, the conjugation of an NLS with 2COPs **1-5** to afford reducible copolycations (RcPCs **1-5**) has been considered in the research described in Chapters 5 and 6.

The most common NLS peptide that has been used in non-viral vectors derives from the simian virus 40 large tumor antigen (PKKKRKV)<sup>[7,11,12]</sup> that mediates binding of cargo protein to the importin- $\alpha$ , which in turn binds to importin- $\beta$ . The heterotrimer then binds to cytoplasmic filaments of NPCs and translocates through the nucleus pore complex (see section 1.1.2.2b).

The basic region (<sup>49</sup>RKKRRQRRR<sup>57</sup>) of the TAT protein from human immunodeficiency virus 1 (HIV-1) has widely been known as a cell penetrating peptide (CPP)<sup>[13-17]</sup>. However, TAT has also been investigated as a novel class of NLSs.<sup>[18,19]</sup> The mechanism for its nuclear

active transport is different from SV40 NLS. Instead of targeting to importin- $\alpha$ , TAT binds to importin- $\beta$  directly.<sup>[19]</sup> In addition, recently, it has been found that TAT could trigger the nuclear import faster than SV40 NLS and is capable of importing nanoparticles (5-90 nm).<sup>[20]</sup>

There was a study by Manickam and colleagues<sup>[21]</sup> in which reducible copolypeptides containing histidine-rich peptides (CKHHHKHHHKC) and nuclear localization signal peptides (CGAGPKKKRKVC) from SV40, which combined the endosomal buffering capacity and nuclear localization capability features. The transfection efficiency of the reducible copolypeptides increased when the content of histidine increased. However, it was still unclear as to the effect of the NLS sequence in the transfection. Therefore, in our study the TAT peptide was used as nuclear importing factor instead of NLS from SV40, and by combining with  $pK_a$  modulation we investigate the effect of the NLS.

## 5.2 Objectives

In Chapter 4 we have shown that the reducible polycations (RPCs) produced from 2COPs **2-5** were promising vectors for non-viral delivery system. The incorporation of a nuclear localisation signal could improve the transfection efficiency of these polycations even further. Therefore, in this Chapter, the basic region of **TAT**-peptide 49-57 sequence (RKKRRQRRR) (**Figure 5.1**) that functions as a nuclear targeting signal was used, and terminally modified with cysteine moieties (CRKKRRQRRRC) in order that it could be copolymerized with 2COPs **1-5** to form a series of reducible *copolycations* (RcPCs).

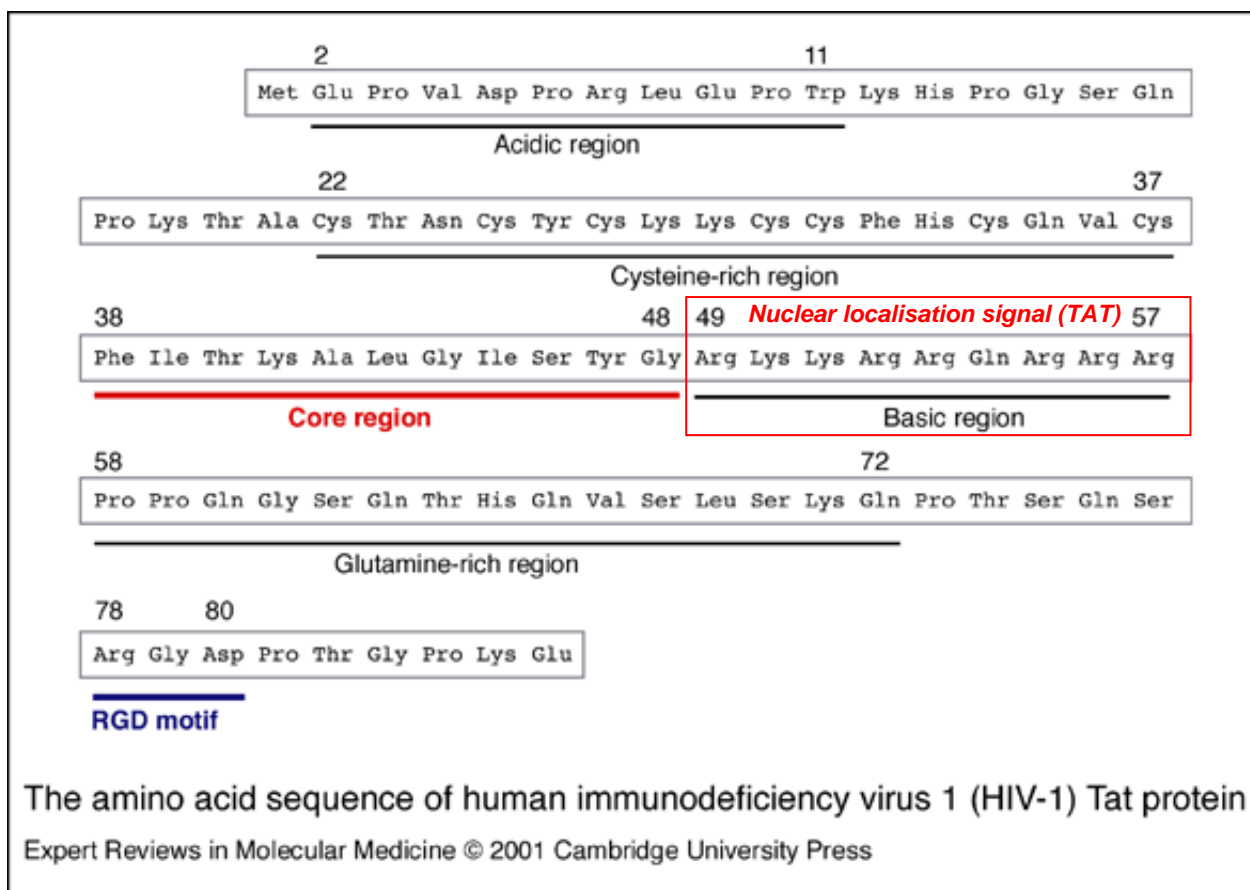


Figure 5.1. The amino acid sequence of human immunodeficiency virus 1 (HIV-1) TAT protein

### 5.3 Methodology

In this chapter we show the synthesis and characterization of the RcPCs and the physiochemical properties of the polyplexes. In order to achieve these objectives the following overview of the experimental process was devised as shown in **Figure 5.2**.

(i) *The purification and characterisation of TAT oligopeptide:* The crude TAT oligopeptide (CRKKRRQRRRC) was purified and characterized (**Figure 5.2 step 1**) using high performance liquid chromatography (HPLC), electrospray mass spectrometry (ESI-MS) and nuclear magnetic resonance ( $^1\text{H}$  NMR)

(ii) *The formation and characterization of TAT polycation and RcPCs:* The TAT reducible polycation (RP-TAT) was synthesized from TAT oligopeptide (CRKKRRQRRRC) *via* oxidative polymerisation (**Figure 5.2, step 2**). In addition, the reducible copolycations (RcPCs) were synthesized *via* random oxidative polymerization between TAT and 2COPs 1-5 (**Figure 5.2, step 2**). The characterisation of the RP-TAT and RcPCs was carried out using gel permeation chromatography (GPC), multi-angle laser light scattering (MALLS) and amino acid analysis.

(iii) *The formation and characterization of RcPC and RP-TAT polyplexes:* The formation of RcPC and RP-TAT polyplexes with the DNA (pCMV-Luc) was performed in a condensation reaction (**Figure 5.2, step 4**), and the stability of the polyplexes under extra- and intracellularly simulated conditions was carried out (**Figure 5.2, step 5-7**).

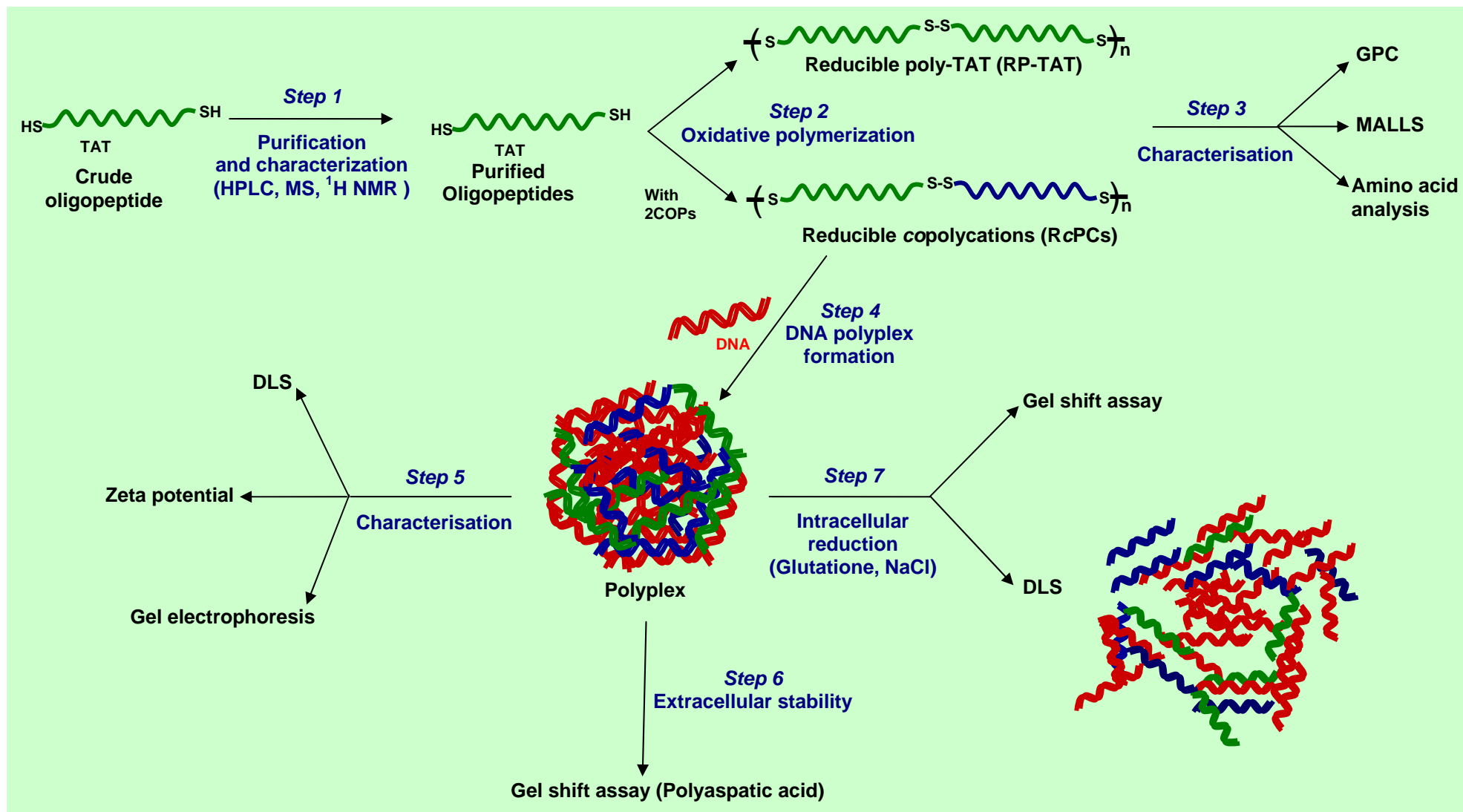


Figure 5.2. Schematic overview of characterisation and analysis of oligopeptides and polyplexes in this chapter  
References for Chapter 5 are on page 244-246.



## 5.4 Results and discussion

### 5.4.1 TAT oligopeptide purification and characterization (Figure 5.2, Step 1)

Crude samples of TAT oligopeptide synthesized by Alta Bioscience (Birmingham, UK) using Fmoc procedure were purified by preparative reverse phase HPLC as described in section 2.3. The final purity of TAT was determined by analytical reverse phase HPLC, the experimental and calculated mass was determined by electrospray-MS (**Table 5.1**). The purity of all oligopeptides was between 97.35-99.59 % by analytical RP-HPLC (see appendix). The purified oligopeptides were additionally characterized by <sup>1</sup>H NMR (500 MHz) (see appendix) and ESI-MS to confirm their structures (section 2.3). Selected data of the purified TAT and the oligopeptides from Chapter 3 used in this chapter are shown in **Table 5.1**.

**Table 5.1.** The purity and mass of purified oligopeptides

Oligopeptide	Sequence <sup>a</sup>	Purity (%) <sup>b</sup>	Experimental Mass	Calculated
			[M] <sup>+</sup> (g mol <sup>-1</sup> ) <sup>c</sup>	Mass (g mol <sup>-1</sup> ) <sup>d</sup>
TAT	CRKKRRQRRRC	98.73	1545.40	1545.10
<i>2COPs</i>				
1	CK <sub>8</sub> C	99.59	1249.90	1249.70
2	CK <sub>4</sub> H <sub>4</sub> C	97.42	1285.90	1285.56
3	CK <sub>2</sub> H <sub>2</sub> K <sub>2</sub> H <sub>2</sub> C	98.45	1285.70	1285.56
4	CK <sub>2</sub> HKHKH <sub>2</sub> C	97.35	1285.70	1285.56
5	CKHKHKHKHKHC	97.41	1285.80	1285.56

<sup>a</sup> C = Cysteine, K = Lysine, H = Histidine, R = Arginine, Q = Glutamine

<sup>b</sup> Purity determined by analytical RP-HPLC (see appendix)

<sup>c</sup> Mass analyzed by ESI-MS

<sup>d</sup> Mass from the calculation

#### 5.4.2 Formation and characterization of reducible copolycations (RcPCs) (Figure 5.1, Step 2, 3)

Reducible *copolycations* (RcPCs) were produced from 2COPs **1-5** and the TAT oligopeptide (section 2.5.3). Briefly, 2COPs (30 mM) and TAT solution (30 mM) in 5x PBS and 30% DMSO at 2COPs:TAT molar ratios of 1:1 for RcPCs **1-5** and also 1:3 for RcPC **5** were incubated at room temperature for 48 hrs. In addition, the RP-TAT was synthesized from 60 mM TAT solution in 5x PBS and 30% DMSO, and was incubated at room temperature for 48 hrs (Figure 5.3).

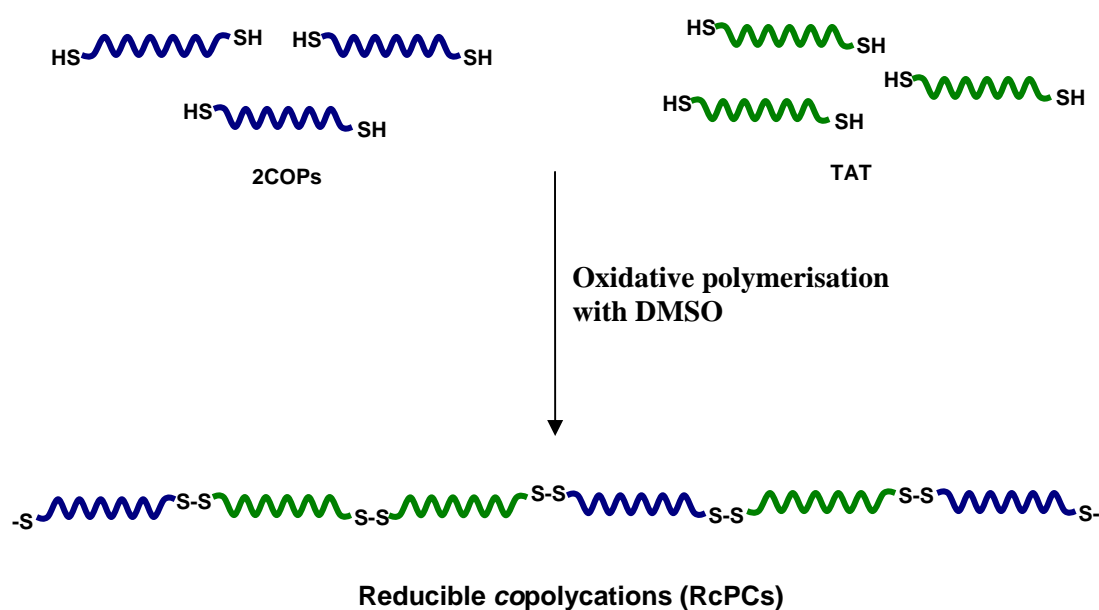


Figure 5.3. Schematic model of reducible *copolycations* (RcPCs) synthesis *via* random oxidative polymerization

The growth of the RcPCs and RP-TAT molecular weights was monitored by gel permeation chromatography (GPC) (Table 5.2 and Figure 5.4) (section 2.5.4). At various time intervals over 48 hrs, 5  $\mu$ l aliquots were removed and quenched with aminoethanethiol (AET). This

aliquot was analysed by GPC eluting with 200 mM NaCl with 0.1% TFA, in order to obtain the molecular weight against PLL standards (5.6, 8.3, 21.3, 62.1 and 128.5 kDa). The sequence ratio of 2COP and TAT in RcPCs was analysed and calculated using amino acid analysis (EZ:faast kits, phenomenex, UK) (section 2.6).

**Table 5.2. RP-TAT and RcPCs produced from TAT and 2COPs 1-5**

Entry	RP-TAT/ RcPCs	2COPs and TAT		2COP :		MW (kDa) <sup>a</sup>	PDI <sup>b</sup>
		in reaction mixtures		TAT	Incubation		
		2COPs	TAT	molar ratio	time (hr)		
i	RP-TAT (40)	-	CRKKRRQRRRC	-	48	39.7	1.260
ii	RcPC 1 (37)	2COP 1 (CK <sub>8</sub> C)	CRKKRRQRRRC	1:1	48	36.8	1.275
iii	RcPC 2 (52)	2COP 2 CK <sub>4</sub> H <sub>4</sub> C	CRKKRRQRRRC	1:1	48	51.6	1.265
iv	RcPC 3 (45)	2COP 3 CK <sub>2</sub> H <sub>2</sub> K <sub>2</sub> H <sub>2</sub> C	CRKKRRQRRRC	1:1	48	44.7	1.169
v	RcPC 4 (39)	2COP 4 CK <sub>2</sub> HKHKH <sub>2</sub> C	CRKKRRQRRRC	1:1	48	38.5	1.222
vi	RcPC 5 (45)	2COP 5 CKHKHKHKHC	CRKKRRQRRRC	1:1	48	45.1	1.211
vii	RcPC 5 (22)	2COP 5 CKHKHKHKHC	CRKKRRQRRRC	1:1	24	22.3	1.168
vii	RcPC 5 (23)	2COP 5 CKHKHKHKHC	CRKKRRQRRRC	1:3	24	23.3	1.213

<sup>a</sup> Molecular weight of RP-TAT and RcPCs was analyzed by GPC using CATSEC300 column compared to PLL standards.

<sup>b</sup> Polydispersity index (PDI) of TAT and RcPCs was measured by size exclusion chromatography (Anachem Ltd., Luton, UK) coupled with multi-angle laser light scattering photometer (Wyatt Technology (Santa Barbara, USA)).

From **Table 5.2** and **Figure 5.4** the molecular weight of RP-TAT and R<sub>c</sub>PCs **1-5** (1:1) were ~40~50 kDa when synthesized over 48 hrs. In addition, R<sub>c</sub>PC **5** (1:1) when synthesized over 24 hrs has molecular weight of ~22 kDa which is similar to R<sub>c</sub>PC **5** (1:3) synthesized over 24 hrs.

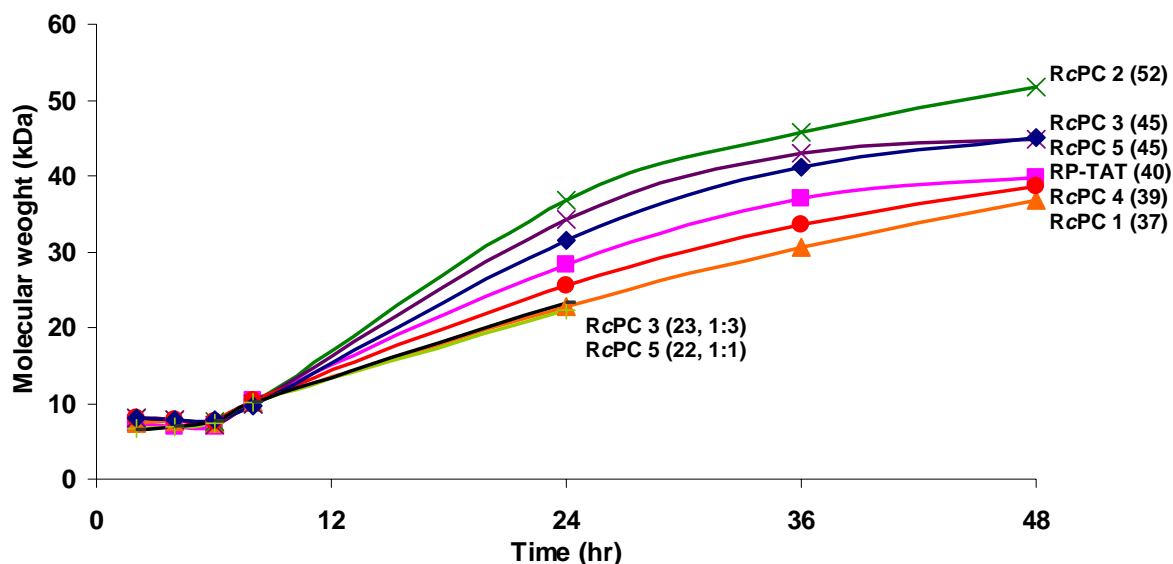


**Figure 5.4.** Oxidative polymerization compared between R<sub>c</sub>PCs **1-5** prepared from 2COPs (**1-5**) : TAT at **1:1** and R<sub>c</sub>PC **5** (**1:3**) incubated at ambient

[RP-TAT —■— , R<sub>c</sub>PCs **1** —▲— , **2** —×— , **3** —•— , **4** —●— , **5** —◆— , R<sub>c</sub>PC **5** (**22**) —+— and R<sub>c</sub>PC **5** (**23**) —— ]

### 5.4.3 2COPs and TAT sequence ratio analysis

The ratios of 2COP and TAT content of the R<sub>c</sub>PCs **1-5** were determined using amino acid analysis (section 2.6). Briefly, R<sub>c</sub>PCs (500 μg) were hydrolysed by liquid phase hydrolysis with 6N HCl with 4% of thioglycolic acid. The reaction mixtures were placed in a heating block in a tightly capped vial at 110°C for 22 hr, to break peptide bonds. The sample was then placed at -20°C for 24 h, unless stated otherwise. The samples were neutralised and analysed using EZ:faast kits (phenomenex, UK). An amino acid calibration standard at 50, 100 and 200

nmol ml<sup>-1</sup> (**Figure 5.5**) was run by gas chromatography (GC) to allow quantification of the amount of unknown amino acids found in each sample, thereby enabling calculation of the quantity of amino acids within the sample to be determined.

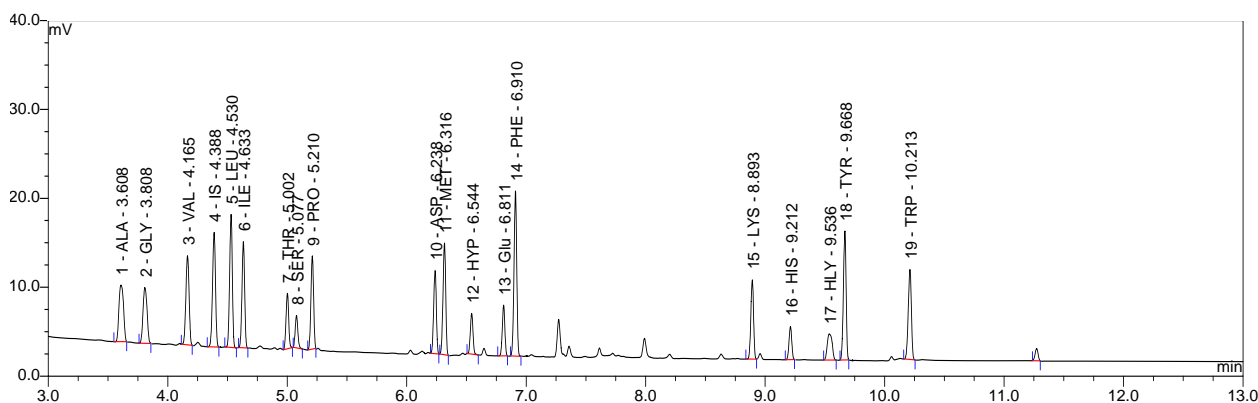


**Figure 5.5.** Amino acid standard at 200 nmol ml<sup>-1</sup> (EZ:faast kits, phenomenex, UK) run with GC.

To determine the ratios of 2COPs and TAT in RcPCs, the quantities of lysine (Lys), histidine (His) and glutamic acid (Glu) (glutamine (Gln, Q) is converted to glutamic acid (Glu, E) during acid hydrolysis) were considered. Therefore, in case of RcPC 1 (2COP 1 + TAT), the ratio of Lys:Glu was determined. In cases of RcPC 2-5 (2COP 2-5 + TAT), the ratios of Lys:Glu, Lys:His and His:Glu were determined (**Table 5.3**). 2COP 2 and TAT were also analyzed as controls.

As can be seen in **Table 5.3** the ratios of 2COP and TAT were derived from the calculation of the number of lysine, histidine and glutamic acid residues obtained from amino acid analysis. Using TAT oligopeptide (CRKKRRQRRRC, 2 Lys and 1 Gln) as a control should have produced the number of Lys per Glu at 2. Thus, the experimental result from TAT is unreliable (the number of Lys per Glu is 4.8). However, using 2COP 2 (CK<sub>4</sub>H<sub>4</sub>C, 4 Lys and 4 His) as a control produced the experimental result (the number of Lys per His is 1.0) as expected. Therefore, we presume that the calculation of amino acid ratio between Lys and His

is reliable. The glutamic acid analysis is not accurate and may result from the nonquantitative conversion of glutamine to glutamic acid. Therefore, in this study we only relied on the calculation between Lys and His. Therefore, as can be seen in **Table 5.3**, based on the number of Lys per His from feed ratio, the calculated numbers of Lys per His from RcPC **2-5** (~50 kDa) and RcPC **5** (22) indicated that they have 2COP:TAT ratio content 1:1, and RcPC **5** (23) has 2COP:TAT ratio content 1:3. We could not indicate the 2COP:TAT ratio content for RcPC **1** as the calculated number of Lys per Glu is unreliable. However, we presumed that it is 1:1.

**Table 5.3. 2COP and TAT sequence ratios of RcPCs 1-5 analyzed by amino acid analysis**

TAT/ 2COP/RcPC	Feed ratio of 2COP:TAT	Calculated number of Lys per Glu or His based on feed ratio		Calculated number of Lys per Glu/His from experimental data		2COP:TAT ratio content <sup>b</sup>
		Number of	Number of	Number of	Number of	
		Lys per Glu	Lys per His	Lys per Glu <sup>a</sup>	Lys per His	
TAT	0:1	2	-	4.8 ± 1.6	-	-
2COP <b>2</b>	1:0	-	1	-	1.0 ± 0.1	-
RcPC <b>1</b> (37)	1:1	6	1.5	17.2 ± 10.6	-	1:1 <sup>c</sup>
RcPC <b>2</b> (52)	1:1	6	1.5	12.3 ± 0.1	1.3 ± 0.1	1:1
RcPC <b>3</b> (45)	1:1	6	1.5	10.1 ± 0.3	1.3 ± 0.1	1:1
RcPC <b>4</b> (39)	1:1	6	1.5	11.8 ± 1.2	1.3 ± 0.1	1:1
RcPC <b>5</b> (45)	1:1	6	1.5	14.9 ± 2.1	1.3 ± 0.6	1:1
RcPC <b>5</b> (22)	1:1	6	1.5	11.0 ± 0.2	1.4 ± 0.1	1:1
RcPC <b>5</b> (23)	1:3	3.33	2.5	5.3 ± 0.1	2.4 ± 0.2	1:3

<sup>a</sup> The number of Lys per Glu from the experiments are unreliable as they are much higher than the expecting number base on feed ratio

<sup>b</sup> 2COP:TAT ratio content of RcPCs indicated from the calculated number of Lys per His

<sup>c</sup> The 2COP:TAT ratio content of RcPC **1** is unable to indicate as the experimental number of Lys per Glu is unreliable, however, we presumed that it is 1:1.

#### 5.4.4 Formation and characterization of TAT and RcPC polyplexes

The polyplexes were prepared by mixing the plasmid DNA (pCMV-Luc) in HEPES buffer, pH 7.4, with the vectors RPCs **1-5** (~50kDa), TAT (40) or RcPC s **1-5** in HEPES buffer (pH 7.4). The ratio of basic groups (lysine (K), imidazole (H) and arginine (R)) of the vectors to the negative phosphate group on the DNA backbone (N:P ratio) was calculated.

##### *5.4.4.1 Weight per charge and N:P ratio calculation*

The calculation of weight per charges (wpc) of 2COPs for polyplexes formation at appropriate N:P ratio was described previously in Chapter 3 (section 3.4.4.1). However, there is a difference in the weight per charge calculation of the RcPCs because there is a mixture of 2COP and TAT sequences. Therefore, to calculate the wpc of RcPC s the ratio of 2COP and TAT sequence was considered. The calculation of wpc was calculated on the actual mass of the 2COP and TAT, taking into consideration the counterion associated with the protonation of the amino groups on the lysine, histidine and arginine residues at physiological pH. In addition, during the synthesis, the 2COPs and TAT were deprotected in an acidic cocktail containing trifluoroacetic acid (TFA), which acts as the counterion forming a TFA salt. Therefore, the number of TFA counterions of 2COP **1-5** is 9, due to the TFA counterion forming a salt with the 4 ammonium ions of lysine residues and 4 imidazolium ions of histidine residues of the 2COP backbone and the protonated N-terminus of the oligopeptide. Moreover, the number of TFA counterions of TAT is 9, due to the TFA counterion forming a salt with the 9 ammonium ions of the lysine and arginine residues of the TAT backbone and the protonated N-terminus of the oligopeptide. Therefore, the number of TFA counterions of this polycation is 18. The following calculation was used to determine the wpc of all oligopeptides in this study.

$$wpc = \frac{(MW \text{ of peptide}) + (\text{number of TFA counterions} \times MW \text{ of TFA})}{\text{number of protonated basic (lysine/histidine/arginine) groups at physiological pH}}$$

MW of TFA = 114 g/mol

TFA counterion =  $\text{CF}_3\text{COO}^-$

For example, in the case of RcPC **1** (2COP **1** (CK<sub>8</sub>C):TAT (CRKKRRQRRRC) = 1:1), the p*K*<sub>a</sub> of lysine (K) and arginine (R) side chain are approximately 10.5 and 12.5, respectively. Therefore, the side chains of the lysine (p*K*<sub>a</sub> ~10.5) and arginine (p*K*<sub>a</sub> ~12.5) residues are fully protonated at physiological pH (pH 7.4). Thus, the number of positive amino groups of this RcPC **1** is 18.

In the cases of RcPC s **2-5** (2COP **2-5**:TAT = 1:1), the basic nitrogen atom on the imidazole rings of histidine residues are not fully protonated as shown in the p*K*<sub>a</sub> determination in Chapter 3 (**Figure 3.4**). Therefore, the number of protonated amino groups of the histidine based sequences was calculated from the average percentage of the chemical shift changing at pH 7.4 described in Chapter 3 (**Figure 3.10**). Weight per charge (wpc) of 2COPs **1-5** (Chapter 3, section 3.3.4.1), TAT and RcPC **1-5** at 2COPs and TAT for ratios are 1:1 and 1:3 are shown in **Table 5.4**.



**Table 5.4. Weight per charge (wpc) of 2COPs, RP-TAT and RcPCs used in this chapter**

2COPs	2COP:TAT ratio	Number of TFA counterions	Number of	Peptide MW (g mol <sup>-1</sup> )	wpc (g mol <sup>-1</sup> )
			positive charges at pH 7.4		
2COP 1	-	9	9	1249.9	252.8
2COP 2	-	9	5.7	1285.9	405.6
2COP 3	-	9	5.2	1285.7	444.6
2COP 4	-	9	5.4	1285.7	428.1
2COP 5	-	9	5.3	1285.8	436.2
RP-TAT	-	9	9	1545.4	285.7
RcPC 1(2COP 1+TAT)	1:1	18	18	2793.3	269.2
RcPC 2 (2COP 2+TAT)	1:1	18	14.7	2829.3	332.1
RcPC 3(2COP 3+TAT)	1:1	18	14.2	2829.1	343.7
RcPC 4 (2COP 4+TAT)	1:1	18	14.4	2829.1	339.0
RcPC 5 (2COP 5+TAT)	1:1	18	14.3	2829.2	341.3
RcPC 5 (2COP 5+TAT)	1:3	36	32.3	5916.0	310.2

The wpc value is used to calculate the N:P ratio, which is the number of possible protonatable basic groups with respect to the negative phosphate groups on the backbone of the nucleic acid. The concentration of RPCs, RP-TAT or RcPCs calculated to form the polyplexes at final concentration of plasmid DNA at 20 µg/ml and at the N:P ratios used in this study is shown by the following equation.

$$\text{Peptides conc. } (\mu\text{g ml}^{-1}) = \frac{\text{Final concentration of plasmid DNA}}{\text{average mass of DNA per phosphate group}} \times N : P \times \text{wpc}$$

Final concentration of plasmid DNA = 20  $\mu\text{g ml}^{-1}$

Average mass of DNA per phosphate group = 325  $\text{g mol}^{-1}$

wpc = weight per charge

#### 5.4.4.2 TAT and RcPCs polyplex formation and characterization (**Figure 5.2, step 4-7**)

##### 5.4.4.2a Diameter and zeta potential of polyplexes (**Figure 5.2, Step 4-5**)

Polyplexes from RP-TAT, RPCs **1-5** and RcPCs **1-5** were formed with plasmid DNA (pCMV-Luc) as described in section 2.7.1 and 2.7.2 at N:P 5. The polyplexes were analysed by dynamic light scattering (section 2.8.1) and zeta potentiometry (section 2.8.2) (**Table 5.5**).

As can be seen in **Table 5.5**, the diameter of the RP-TAT polyplex was 95.2 nm. The polyplex diameters from RcPCs **1-5** (~40-50 kDa), 2COP:TAT at 1:1 ratio, were in the range between 98.1-111.4 nm. Comparison of the diameter of RPCs **1-5** polyplexes and RcPC **1-5** polyplexes reveals only marginal differences of at most ~10%, from the corresponding RPCs. Zeta potentials were positive in all cases and were similar for RPCs and RcPCs (**Table 5.5**), which will allow the polyplexes to promote the internalization *via* syndecan-mediated endocytosis<sup>[2]</sup> (**Figure 1.22**) by electrostatic interaction between the positively charged polyplexes and the negatively charged cell membrane.

**Table 5.5. Properties of RP-TAT, RPCs, RcPCs and their polyplexes formed at N:P 5**

RP-TAT/ RPCs/ RcPCs	2COP : TAT ratio	Polymer		Polyplexes	
		MW (kDa) <sup>a</sup>	Polydispersity index <sup>b</sup>	Diameter (nm) <sup>c</sup>	Zeta potential (mV) <sup>d</sup>
RP-TAT (40)	-	39.7	1.260	95.2 ± 0.3	14.4 ± 9.3
RPC 1 (54)	-	53.9	1.563	99.9 ± 8.3	16.8 ± 11.0
RcPC 1 (37)	1:1	36.8	1.275	104.1 ± 1.4	13.5 ± 10.0
RPC 2 (60)	-	60.8	1.339	98.4 ± 0.7	10.1 ± 14.0
RcPC 2 (52)	1:1	51.6	1.265	111.4 ± 2.6	8.8 ± 8.0
RPC 3 (40)	-	40.4	1.318	94.7 ± 1.5	15.5 ± 15.5
RcPC 3 (45)	1:1	44.7	1.169	105.7 ± 3.7	17.8 ± 12.8
RPC 4 (48)	-	48.5	1.279	101.1 ± 2.2	5.3 ± 5.7
RcPC 4 (39)	1:1	38.5	1.222	98.1 ± 3.7	10.3 ± 9.1
RPC 5 (42)	-	42.3	1.292	90.7 ± 3.4	12.6 ± 12.3
RcPC 5 (45)	1:1	45.1	1.211	108.1 ± 1.6	11.6 ± 14.3
RcPC 5 (22)	1:1	22.3	1.168	98.4 ± 0.9	12.6 ± 8.4
RcPC 5 (23)	1:3	23.	1.213	110.3 ± 1.1	12.9 ± 12.0

<sup>a</sup> Molecular weight of RP-TAT, RPCs and RcPCs were analyzed by GPC using CATSEC300 column compared to PLL standard.

<sup>b</sup> Polydispersity index (PDI) of RPCs was measured by size exclusion chromatography (Anachem Ltd., Luton, UK) coupled with multi-angle laser light scattering photometer (Wyatt Technology (Santa Barbara, USA).

<sup>c</sup> Hydrodynamic diameters of the polyplexes were measured by dynamic light scattering with a Zetasizer 3000 (Malvern Instruments, Worcestershire, UK).

<sup>d</sup> Zetapotential was measured by with a Zetamaster (Malvern Instruments, Worcestershire, UK).

#### 5.4.4.2b Extracellular stability studies of polyplexes (**Figure 5.2, Step 6**)

The extracellular stability of the RP-TAT and RcPCs polyplexes was studied using the gel shift assay by incubating the polyplexes with polyaspartic acid (PAA) (**Figure 5.6**). PEI polyplexes at N:P 10 and PLL polyplexes at N:P 5 were used as a control. The results without PAA revealed that RP-TAT and all RcPCs were able to form stable polyplexes as shown by no loss of DNA in the gel electrophoresis assay (**lanes a1-h1**).

However, the polyplexes formed with RP-TAT and all RcPCs were found to be unstable after incubating with PAA (**lanes a2-h2**) which is similar to PEI (**lane i2**) and PLL (**lane j2**), indicating that RP-TAT and RcPCs polyplexes are less stable than RPCs (Chapter 3, **Figure 3.22**). Thus, to use RcPCs vectors may not be suitable *in vivo* as they may unpack and release the DNA by blood components before reaching the target cells.

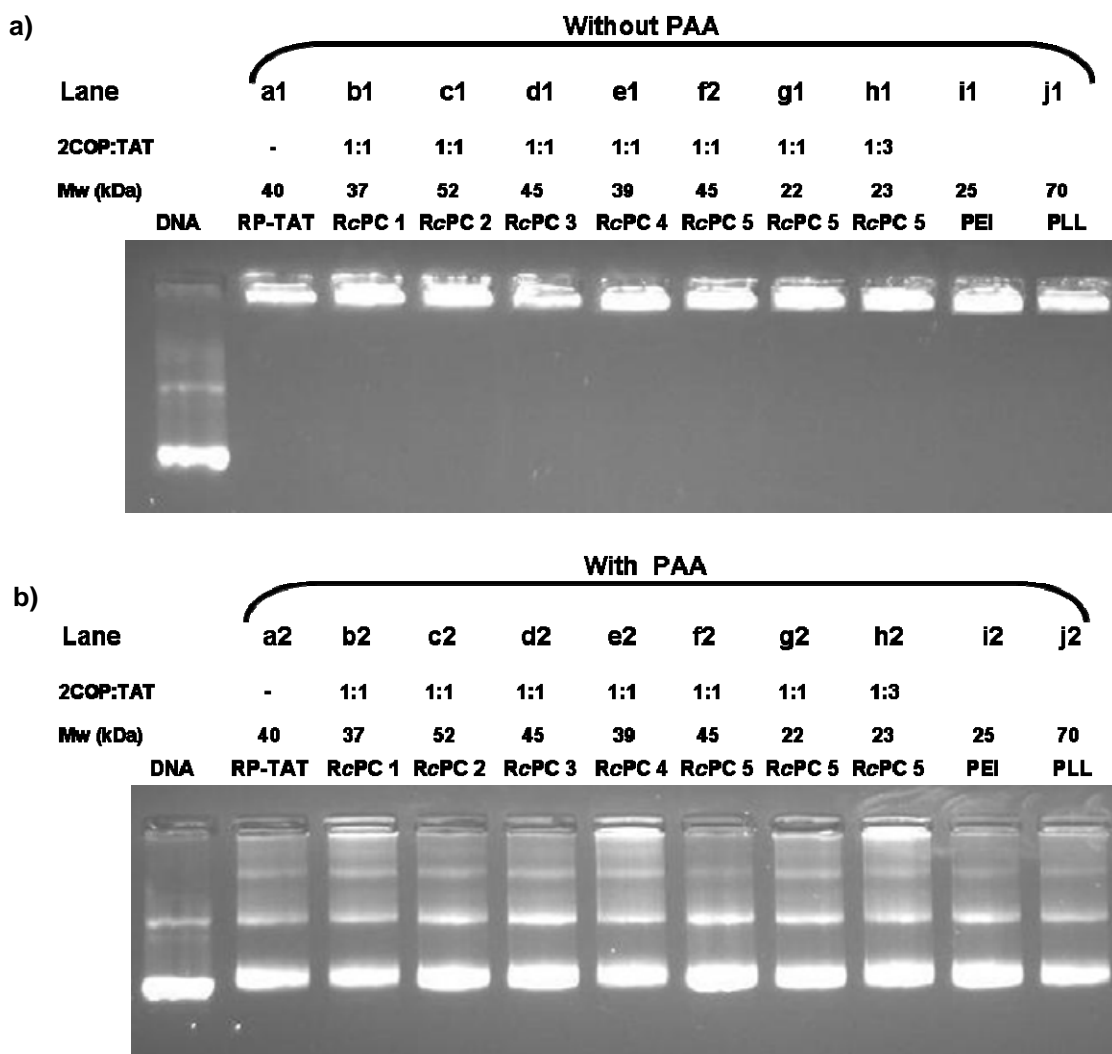


**Figure 5.6.** Gel shift assay with (a) and without (b) polyaspartic acid (PAA) of polyplexes formed from RP-TAT (N:P 5), RcPCs 1-5 (N:P 5), PEI (N:P 10) and PLL (N:P 5). Polyaspartic acid at 250 times of DNA concentration was mixed into the polyplex solution. Lanes a1-j1 on the top panel (a) are for polyplexes without incubating with PAA. Lanes a2-j2 on the bottom panel (b) are for polyplexes incubated with PAA. Agarose gel electrophoresis was run using 1% agarose gel with EtBr (0.5  $\mu\text{g}.\text{ml}$ ) at 110 V for 60 mins in 0.5x TBE buffer

#### 5.4.4.2c Intracellular reduction studies of polyplexes (**Figure 5.2,**

##### **Step 7)**

Stability of the RP-TAT and RcPCs polyplexes against physiological concentrations of salt and GSH, was assessed by gel electrophoresis *via* treatment with (i) GSH alone (5 mM), (ii) salt alone (NaCl 0.15 and 0.5 M), and (iii) combination of NaCl (0.5 and 0.5 M) and GSH (5 mM) to assess polyplexes destabilisation (**Figure 5.7**). PLL polyplexes at N:P 5 were used as controls. These gel shift assays demonstrate that:

(a) RP-TAT produced polyplexes that were stable in GSH alone, salt alone as can be seen from **lanes b-d** of RP-TAT. Importantly, however, addition of GSH (5mM) in the presence of salt destabilised the polyplexes, leading to release of the DNA (**lanes e-f** of RP-TAT). Thus, the combination of GSH under physiological salt concentrations was able to both cleave the polydisulfide bonds in the polyplexes leading to lower a molecular weight peptides that had a lower affinity for the DNA in the salt solution, leading to disassociation of the polyplexes.

(b) RcPC **1** produced polyplexes that were both stable in GSH alone, salt alone and in the combination of GSH and salt (**lanes b-f** of RcPC **1**). These results are probably due to the short oligopeptide 2COP **1** that probably results, after GSH treatment, binding strongly to DNA, and therefore does not release the DNA into the gel. This result is in contrast to RcPCs **2-5** (described below) presumably due to the lower charge on 2COP **2-5**, that results in weaker electrostatic binding to the DNA, and hence it release.

(c) RcPCs **2-5** produced polyplexes that were stable in GSH alone (5mM) as can be seen from **lanes b** of RcPCs **2-5**. Furthermore, these RcPC polyplexes

were also stable in salt (0.15-0.5 M) (**lanes c, d** of RcPCs **2-5**). Importantly, however, addition of GSH (5mM) in the presence of salt destabilised the polyplexes, leading to release of the DNA in all cases (**lanes e, f** of RcPCs **2-5**). Therefore, these results probably indicate that the combination of GSH under physiological salt concentrations was able to both cleave the disulfide bonds in the polyplexes leading to lower a molecular weight peptides that had a lower affinity for the DNA in the salt solution, leading to disassociation of the polyplexes.

(d) The lower molecular weight RcPC **5** (22) polyplex was stable in GSH alone and salt alone as can be seen in **Figure 5.7**. (**lanes b-d** of RcPC **5** (22)) which is similar to the high molecular weight RcPC **5** (45) polyplex (**Figure 5.7, lane b-d** of RcPC **5** (45)). However, the polyplex produced from the lower molecular weight RcPC **5** (22) released more DNA than the polyplex with higher molecular weight (RcPC **5** (45)) when treated with GSH and NaCl in combination (**lanes e, f** of RcPC **5**(45) and RcPC **5**(22)). This suggests that the kinetics of release is more rapid, as would be expected, due to small fragments of the polycations dissociate more rapidly from the DNA.

(e) Polyplexes produced from RcPC **5** at different 2COP:TAT ratios (RcPC **5** (22, 1:1) and RcPC **5** (23, 1:3) indicated that there is no ratio effect of 2COP to TAT, as they are stable in GSH alone (**lane b**), salt alone (**lanes c, d**), and released the similar amount of DNA in the combination with GSH and salt (**lanes e, f**).

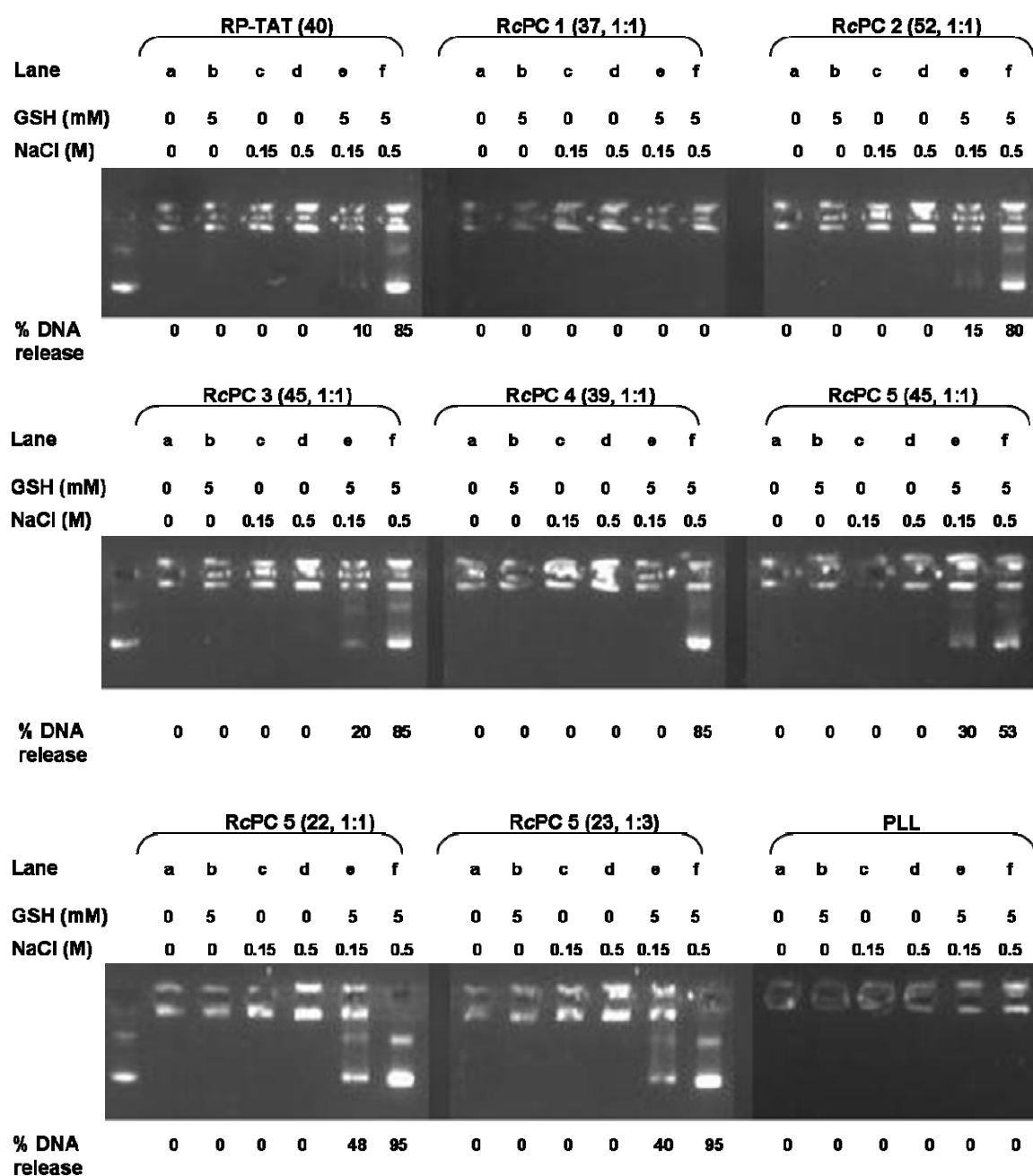


**Figure 5.7.** DNA binding and release demonstrated by gel shift assays of RP-TAT and RcPC polyplexes. All polyplexes formed at N:P 5. Top panel: polyplexes of RP-TAT (40), RcPC 1 (37) and RcPC 2 (52, 1:1) with pDNA; middle panel shows RcPC 3 (45, 1:1), RcPC 4 (39, 1:1) and RcPC 5 (45, 1:1); bottom panel shows RcPC 5(22, 1:1), RcPC 5(23, 1:3) compared against non-cleavable polypeptide poly(lysine). Agarose gel electrophoresis was run using 1% agarose gel with EtBr (0.5  $\mu\text{g}.\text{ml}$ ) at 110 V for 60 mins in 0.5x TBE buffer



## 5.5 Conclusions

The work in Chapters 3 and 4 has shown that the reducible polycations (RPCs) are promising vectors for non-viral gene delivery. However, these vectors have no nuclear targeting signal. Therefore, the work in this chapter has highlighted a vector design that combines 5 vector features together (**Table 1.4**, page 38): the extracellular binding with DNA (**I**), cell uptake *via* endocytosis (**III**), endosomal escape (**IV**), intracellular degradability (**V**), and *nuclear targeting* (**VI**).

### 5.5.1 TAT oligopeptide purification and characterization

TAT oligopeptide (CRKKRRQRRRC) synthesized by Alta Bioscience (Birmingham, UK) was purified by the preparative reverse phase HPLC. All purified oligopeptides were analyzed by analytical RP-HPLC, ESI-MS and <sup>1</sup>H NMR to obtain the purity and to characterize the oligopeptides. The purity of TAT oligopeptide is 98.73%.

### 5.5.2 Formation and characterization of RP-TAT and RcPC

2COPs **1-5** and TAT oligopeptide at 2COP:TAT molar ratio 1:1 were randomly oxidative polymerized to form reducible *copolycations* (RcPCs) *via* disulfide bond formation. The RcPC **1-5** molecular weights obtained are approximately 37-52 kDa with a 2COP:TAT ratio is 1:1. RP-TAT was synthesized, and the molecular weight is approximately 40 kDa. RcPC **5** with 2COP:TAT is 1:1 at molecular weight approximately 22 kDa, and the RcPC **5** with 2COP:TAT is 1:3 at molecular weight approximately 23 kDa were also synthesized in order to investigate the vectors as a function of RcPC molecular weight and 2COP:TAT ratio.

### 5.5.3 Formation and characterization of RP-TAT and RcPC polyplexes

Polyplexes were formed from RP-TAT and RcPCs **1-5** at N:P 5, and the resultant polyplex dispersion were analyzed by zeta potential and dynamic light scattering comparing to RPC **1-5** from Chapter 3.

#### 5.5.3.1 Diameter and zeta potential of RP-TAT and RcPC polyplexes

The polyplex diameters of RP-TAT, RcPCs **1-5** (~50 kDa) prepared from 2COP:TAT at 1:1 ratio and RcPC **5** at ~22 kDa with 2COP:TAT ratios are 1:1 and 1:3 were approximately 100 nm.

Zeta potentials were positive in all cases, which will allow the polyplexes to promote the internalization *via* syndecan-mediated endocytosis (**Figure 1.22**) by electrostatic interaction between the positively charged polyplexes and the negatively charged cell membrane.

#### 5.5.3.2 Extracellular stability of RP-TAT and RcPC polyplexes

The extracellular stability of the RP-TAT and RcPCs polyplexes was studied using the gel shift assay by incubating the polyplexes with polyaspartic acid (PAA). The results without PAA revealed that RP-TAT and all RcPCs were able to form stable polyplexes. However, they were unstable with PAA, indicating that RP-TAT and RcPCs polyplexes are less stable than RPCs. Thus, to use RcPCs as vectors may not be suitable *in vivo* as they would unpack and release the DNA by blood component before reaching the target cells.

### 5.5.3.3 Intracellular reduction of RP-TAT and RcPC polyplexes

In addition, GSH was used as a biological intracellular reducing agent, since GSH is present in the cytoplasm (the stability under physiological salt concentrations was studied). The polyplexes from RP-TAT and RcPCs **2-5** were stable in GSH alone (5mM) and salt solution alone (0.15 and 0.5M). However, in combination with GSH (5mM) and salt (0.15 and 0.5M), these polyplexes released DNA. However, the polyplex formed from RcPC **1** did not release DNA. These results suggested that RP-TAT and RcPCs **2-5** polyplexes are able to facilitate intracellular reduction resulting in DNA releasing for further gene expression mechanisms. Whereas, RcPC **1** although probably does undergo the disulfide bonds cleavage the high net charge on the 2COP **1** that results is still bound to the DNA by strong electrostatic interaction.

Polyplexes produced from lower molecular weight RcPC (RcPC **5** (22)) released more DNA than polyplex with higher molecular weight (RcPC **5** (45)) in the combination with GSH and NaCl. This result is indicative of the fact that the kinetics of release will be quicker with RcPC **5**(22), because shorter fragments of polycations will dissociate more rapidly from the DNA.

Polyplexes produced from RcPC at different 2COP:TAT ratios ((RcPC **5** (22, 1:1) and RcPC **5** (23, 1:3)) indicated that there is no affect of the ratio of 2COP and TAT sequences, as they are stable in GSH alone, salt alone, and released the similar amount of DNA in combination with GSH and salt.

*In summary, in comparisons between RPCs and RcPCs characteristics by DLS, zeta potential and gel shift assay, it might be expected that RcPCs will be less effective vectors*

than RPCs, because their polyplexes can be dissociated by PAA. However, the transfection efficiencies of RcPCs will be studied in Chapter 6 to compare with RPCs.

## 5.6 References

1. Ruponen, M., Honkakoski, P., Ronkko, S., Pelkonen, J., Tammi, M., and Urtili, A. (2003). Extracellular and intracellular barriers in non-viral gene delivery. *Journal of Controlled Release*, **93**, 213-217.
2. Mislick, K.A., and Baldeschwieler, J.D. (1996). Evidence for the role of proteoglycans in cation-mediated gene transfer. *Proceedings of the National Academy of Sciences of the United States of America*, **93**, 12349-12354.
3. Kopatz, I., Remy, J.S., and Behr, J.P. (2004). A model for non-viral gene delivery: through syndecan adhesion molecules and powered by actin. *Journal of Gene Medicine*, **6**, 769-776.
4. Cho, Y.W., Kim, J.D., and Park, K. (2003). Polycation gene delivery systems: escape from endosomes to cytosol. *Journal of Pharmacy and Pharmacology*, **55**, 721-734.
5. Read, M.L., Bremner, K.H., Oupicky, D., Green, N.K., Searle, P.F., and Seymour, L.W. (2003). Vectors based on reducible polycations facilitate intracellular release of nucleic acids. *Journal of Gene Medicine*, **5**, 232-245.
6. McKenzie, D.L., Smiley, E., Kwok, K.Y., and Rice, K.G. (2000). Low molecular weight disulfide cross-linking peptides as nonviral gene delivery carriers. *Bioconjugate Chemistry*, **11**, 901-909.
7. Zanta, M.A., Belguise-Valladier, P., and Behr, J.P. (1999). Gene delivery: A single nuclear localization signal peptide is sufficient to carry DNA to the cell nucleus.

- Proceedings of the National Academy of Sciences of the United States of America*, **96**, 91-96.
8. Bremner, K.H., Seymour, L.W., Logan, A., and Read, M.L. (2004). Factors influencing the ability of nuclear localization sequence peptides to enhance nonviral gene delivery. *Bioconjugate Chemistry*, **15**, 152-161.
  9. Pouton, C.W., Wagstaff, K.M., Roth, D.M., Moseley, G.W., and Jans, D.A. (2007). Targeted delivery to the nucleus. *Advanced Drug Delivery Reviews*, **59**, 698-717.
  10. Stewart, M. (2007). Molecular mechanism of the nuclear protein import cycle. *Nature Reviews Molecular Cell Biology*, **8**, 195-208.
  11. Vaysse, L., Gregory, L.G., Harbottle, R.P., Perouzel, E., Tolmachov, O., and Coutelle, C. (2006). Nuclear-targeted minicircle to enhance gene transfer with non-viral vectors *in vitro* and *in vivo*. *Journal of Gene Medicine*, **8**, 754-763.
  12. Escriou, V., Carrière, M., Scherman, D., and Wils, P. (2003). NLS bioconjugates for targeting therapeutic genes to the nucleus. *Advanced Drug Delivery Reviews*, **55**, 295-306.
  13. Brooks, H., Lebleu, B., and Vives, E. (2005). TAT peptide-mediated cellular delivery: back to basics. *Advanced Drug Delivery Reviews*, **57**, 559-577.
  14. Fonseca, S.B., Pereira, M.P., and Kelley, S.O. (2009). Recent advances in the use of cell-penetrating peptides for medical and biological applications. *Advanced Drug Delivery Reviews*, **In Press**, 1-12.
  15. Hansen, M., Kilk, K., and Langel, U. (2008). Predicting cell-penetrating peptides. *Advanced Drug Delivery Reviews*, **60**, 572-579.
  16. Torchilin, V.P. (2008). TAT peptide-mediated intracellular delivery of pharmaceutical nanocarriers. *Advanced Drug Delivery Reviews*, **60**, 548-558.

17. Wender, P.A., Galliher, W.C., Goun, E.A., Jones, L.R., and Pillow, T.H. (2008). The design of guanidinium-rich transporters and their internalization mechanisms. *Advanced Drug Delivery Reviews*, **60**, 452-472.
18. Efthymiadis, A., Briggs, L.J., and Jans, D.A. (1998). The HIV-1 TAT nuclear localization sequence confers novel nuclear import properties. *Journal of Biological Chemistry*, **273**, 1623-1628.
19. Truant, R., and Cullen, B.R. (1999). The arginine-rich domains present in human immunodeficiency virus type 1 TAT and Rev function as direct importin beta-dependent nuclear localization signals. *Molecular and Cellular Biology*, **19**, 1210-1217.
20. Nitin, N., LaConte, L., Rhee, W., and Bao, G. (2009). TATpeptide is capable of importing large nanoparticles across nuclear membrane in digitonin permeabilized cells. *Annals of Biomedical Engineering*, 1-10.
21. Manickam, D.S., and Oupicky, D. (2006). Multiblock reducible copolypeptides containing histidine-rich and nuclear localization sequences for gene delivery. *Bioconjugate Chemistry*, **17**, 1395-1403.

## **CHAPTER 6**

### **Delivery of nucleic acid using reducible *copolyations* (RcPCs) containing lysine, histidine and cysteine based sequences and TAT peptide**

# CONTENTS

List of Figures

List of Tables

## 6 DELIVERY OF NUCLEIC ACID USING REDUCIBLE COPOLYCATION (RcPC) CONTAINING LYSINE, HISTIDINE AND CYSTEINE BASED SEQUENCES AND TAT PEPTIDE

<b>6.1</b>	<b>Introduction</b>	<b>251</b>
<b>6.2</b>	<b>Objectives</b>	<b>256</b>
<b>6.3</b>	<b>Methodology</b>	<b>256</b>
<b>6.4</b>	<b>Results and discussion</b>	<b>258</b>
6.4.1	Cytotoxicity of polyplexes	258
6.4.1.1	Cytotoxicity of RP-TAT and RcPCs polyplexes	258
6.4.1.2	Cytotoxicity of RcPCs polyplexes as a function of RcPC molecular weight and 2COP:TAT ratio	261
6.4.1.2a	Cytotoxicity of RcPCs polyplexes as a function of RcPC molecular weight	261
6.4.1.2b	Cytotoxicity of RcPCs polyplexes as a function of 2COP:TAT ratio	263
6.4.2	Cell transfection of polyplexes	263
6.4.2.1	Cell transfection of RP-TAT and RcPC polyplexes based on the endosomolytic buffering: effect of CQ	265
6.4.2.2	Cell transfection of RP-TAT and RcPCs polyplexes based on intracellularly reducible property: effect of BSO/GSH-MEE	267
6.4.2.2a	Artificially increase the intracellular GSH level: effect of GSH-MEE	267
6.4.2.2b	Artificially depleting the intracellular GSH level: Effect of BSO	268
6.4.2.3	Cell transfection of RP-TAT and RcPCs polyplexes based on the combination of endosomolytic and intracellularly reducible properties	269
6.4.2.4	Cell transfection of RcPC polyplexes compared to RPCs	270



6.4.2.5	Cell transfection of RcPC polyplexes as a function of RcPC molecular weight and 2COP:TAT ratio	272
6.4.2.5a	Cell transfection of RcPC polyplexes as a function of RcPC molecular weight	272
6.4.2.5b	Cell transfection of RcPC polyplexes as a function of 2COP:TAT ratio	274
<b>6.5</b>	<b>Conclusions</b>	<b>274</b>
<b>6.6</b>	<b>References</b>	<b>277</b>

## List of Figures

Figure 6.1.	p-azido-tetrafluoro-benzyl-NLS peptide conjugate	252
Figure 6.2.	Strategy for preparation of CMVLuc-NLS	253
Figure 6.3.	psoralen-oligonucleotide-NLS peptide conjugate	254
Figure 6.4.	Schematic conjugation of succinimidyl-[4-(psoralen-8-yloxy)]-butylrate (SPB) to NLS	255
Figure 6.5.	Schematic overview of cell transfection in this chapter	257
Figure 6.6.	Cell viability following exposure to RPC <b>1-5</b> , TAT and RcPC <b>1-5</b> polyplexes at N:P 5, PLL polyplex at N:P 5, PEI polyplex at N:P 10 and cell controls	260
Figure 6.7.	Cell viability of cells transfected with RcPC <b>5</b> (45 and 22 kDa with 2COP <b>5</b> :TAT ratio 1:1), RcPC <b>5</b> (23 kDa with 2COP <b>5</b> :TAT ratio 1:3) at N:P 5, PLL polyplex at N:P 5, PEI polyplex at N:P 10 and cell controls	262
Figure 6.8.	Transfection based on CQ, GSH-MEE and BSO with RP-TAT, RcPC polyplexes <b>1-5</b> (~50 kDa) at N:P 5, PLL polyplex at N:P 5, PEI polyplex at N:P 10 and cell control	264
Figure 6.9.	Transfection of A549 cell treated with RPCs and RcPCs polyplexes without and with CQ	266
Figure 6.10.	Transfection in bEND3 and A549 of polyplexes from RPCs <b>1-5</b> (~50 kDa), RcPCs <b>1-5</b> and RP-TAT polyplexes	271
Figure 6.11.	Transfection based on CQ, GSH-MEE and BSO with RcPC <b>5</b> (45 and 22 kDa with 2COP <b>5</b> :TAT ratio 1:1), RcPC <b>5</b> (23 kDa with 2COP <b>5</b> :TAT ratio 1:3) at N:P 5, PLL polyplex at N:P 5, PEI polyplex at N:P 10 and cell control	273

## 6 DELIVERY OF NUCLEIC ACID USING REDUCIBLE COPOLYCATION (RcPC) CONTAINING LYSINE, HISTIDINE AND CYSTEINE BASED SEQUENCES AND TAT PEPTIDE

### *Abstract*

*As shown in Chapter 5 the RcPCs were synthesized via randomly oxidative polymerisation in combination of 2COPs and TAT oligopeptides. The RcPC polyplexes were characterised and it was revealed that they seemed to be suitable vectors for gene delivery in non-viral system as a result of their diameters and surface charges and the reducible nature by GSH and NaCl. However, they were unstable under simulated extracellular conditions (with PAA). In this chapter the transfection efficiencies of RcPC polyplexes were investigated and it was revealed that CQ was required to enhance the transfection of the RcPCs. In addition, using the lower molecular weight RcPCs (22 kDa) showed higher transfection level than higher molecular weight RcPCs (45 kDa) as with RPCs. The different ratio of 2COP and TAT peptides in RcPCs (1:1 and 1:3) did not affect the transfection levels. Furthermore, there is no improvement in transfection of RcPC compared to RPCs. Therefore, it may suggest that incorporation of nuclear localization signal (TAT) in this study does not improve the transfection.*

### 6.1 Introduction

Non-viral vectors are limited for transfection *in vivo* as they inefficiently transfer DNA into nucleus.<sup>[1-3]</sup> In order to improve nuclear entry of non-viral vectors, there are many strategies to couple of NLS peptide to DNA that have been developed.<sup>[4-13]</sup> For example, Ciolina and colleagues<sup>[10]</sup> developed a chemical strategy for the covalent coupling of NLS peptides (ACGAGPKKKRKV) of SV40 large T antigen to plasmid DNA. A p-azido-tetrafluorobenzyl-NLS peptide conjugate (**Figure 6.1**) was synthesized and was used to covalently associate NLS peptides to plasmid DNA by photoactivation.

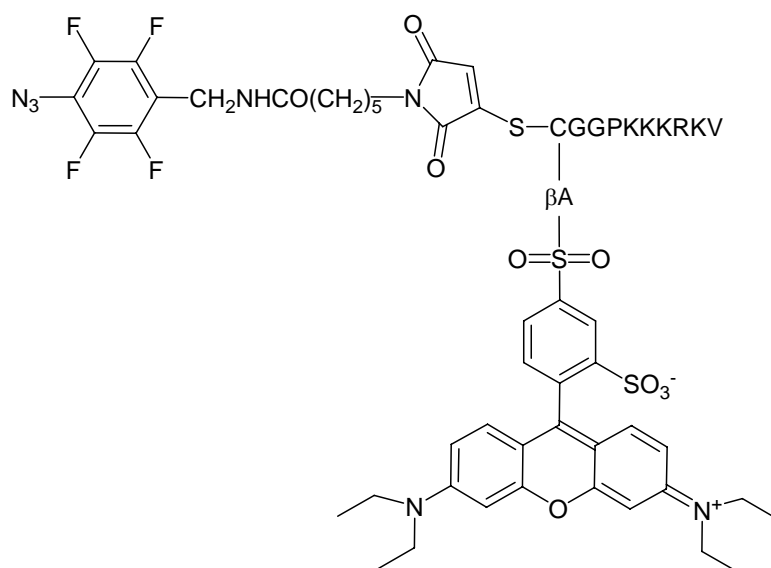


**Figure 6.1.** p-azido-tetrafluoro-benzyl-NLS peptide conjugate<sup>[10]</sup>

Zanta and colleagues<sup>[5]</sup> synthesized capped 3.3-kbp CMVLuciferase-NLS containing a signal nuclear localization signal peptide from SV40 (PKKKRKVEDPY) (**Figure 6.2**). PEI or transfectam were used to form polyplexes with CMVLuciferase-NLS. The results revealed that only a single NLS peptide per strand of DNA was required to improve the transfection efficiencies (10-1000 fold) relative to the polyplexes without NLS.

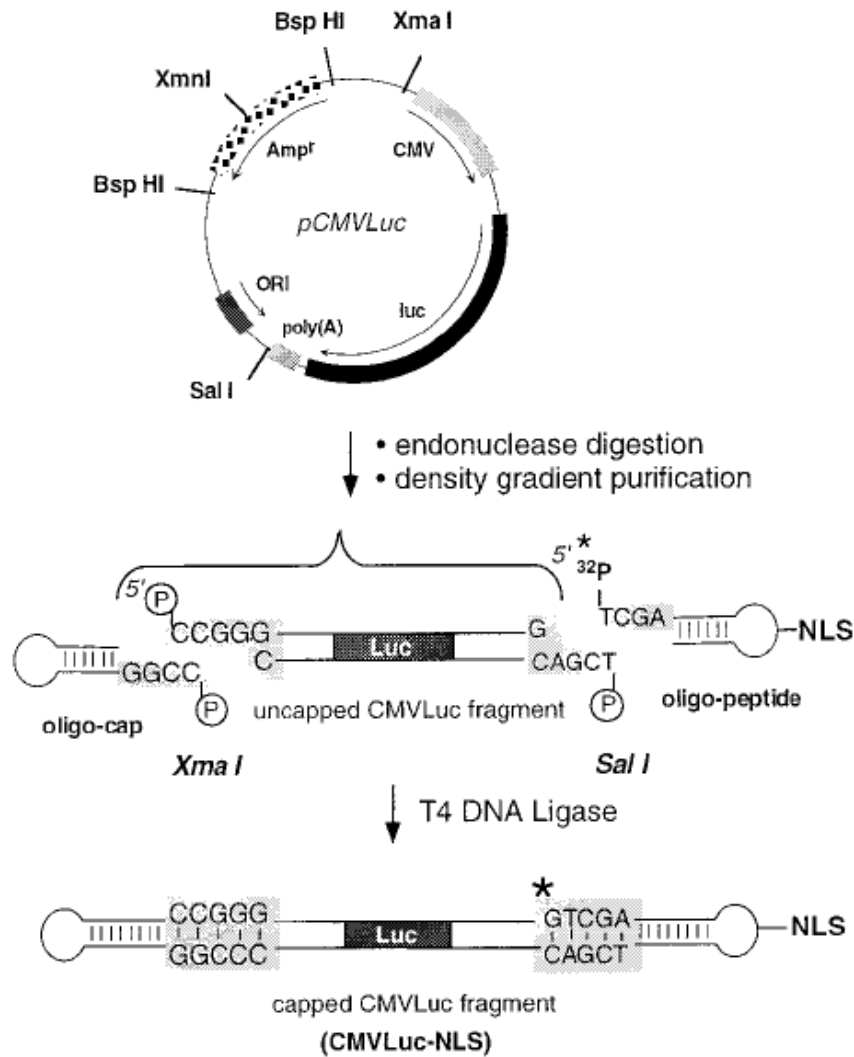
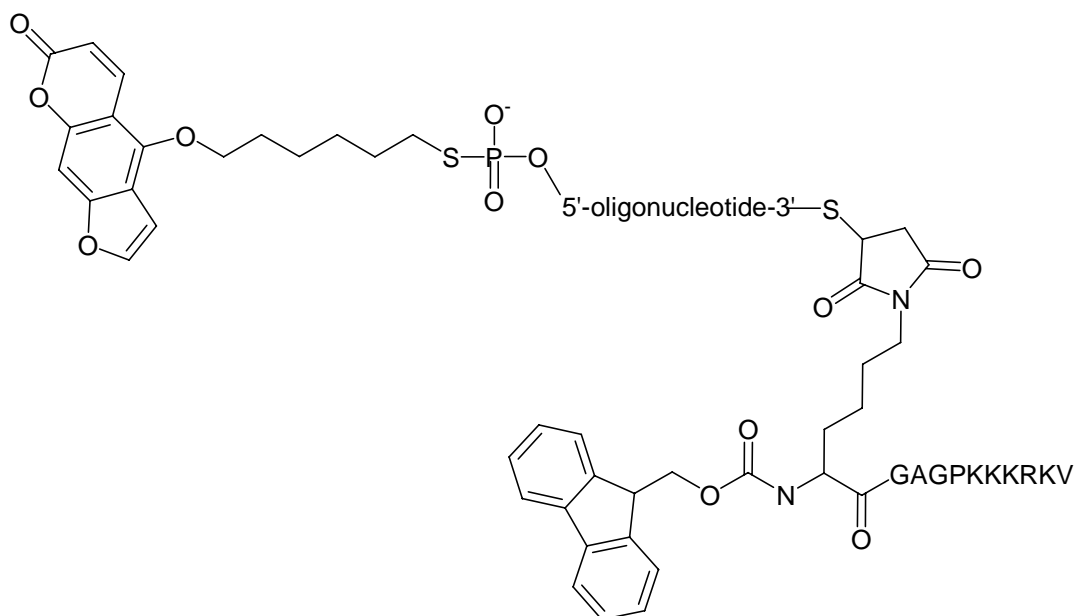


Figure 6.2. Strategy for preparation of CMVLuc-NLS<sup>[5]</sup>

However, van der Aa and colleagues<sup>[6]</sup> revealed that covalently linked NLS peptide linked to linear DNA did not enhance transfection.

Neves and colleagues<sup>[11]</sup> developed a strategy for covalent coupling of NLS peptides to plasmid DNA at a specific site by triple helix formation. A psoralen, a nucleic acid intercalating agent, was used to conjugate with NLS-peptide. A psoralen-oligonucleotide-NLS peptide conjugate was synthesized (**Figure 6.3**) and was used to covalently associate one NLS peptide to plasmid DNA by triple helix formation and photoactivation. This conjugate

interacted with the  $\alpha$ -importin which is the NLS receptor. The transfection of the plasmid DNA coupled with this conjugate indicated that there is no loss of the gene expression functionality of the plasmid. The researchers suggested that this site-specific coupling technology can be used to couple to a plasmid other ligands targeting to a specific receptor.



**Figure 6.3.** psoralen-oligonucleotide-NLS peptide conjugate<sup>[11]</sup>

The NLS (GGGPKKKRKV) was also chemically attached to psoralen – a nucleic acid-intercalating agent (**Figure 6.4**)<sup>[4]</sup> in order that the conjugate intercalated into the double strand DNA. PEI was then used to form the polyplexes with the DNA intercalated with psoralen-NLS resulting in enhancement of transfection by ~10 fold relative to PEI/DNA polyplex alone.

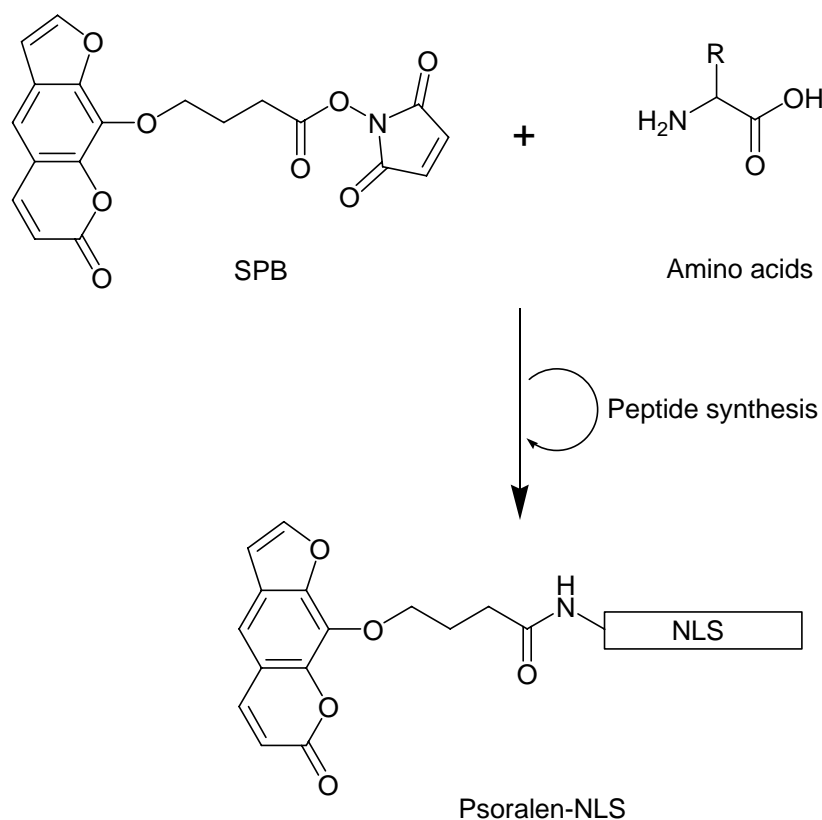


**Figure 6.4. Schematic conjugation of succinimidyl-[4-(psoralen-8-yloxy)]-butyrate (SPB) to NLS** <sup>[4]</sup>

The condensation between TAT oligomers (C(YGRKKRRQRRRG)<sub>2</sub>)<sup>[7]</sup> or TAT polymer (CQRKKRRQRRRGC)<sub>n</sub>, ~100 kDa)<sup>[8]</sup> and DNA enhanced transfection activity of DNA polyplexes and reduced cytotoxicity. However, they required chloroquine in order for the endosomal vesicles to burst.

The reducible copolypeptides<sup>[9]</sup> containing histidine-rich peptides (CKHHHKHHHKC) and nuclear localization signal peptides (CGAGPKKKRKVC) from SV40 were used as vectors in order to combine the endosomal buffering capacity and nuclear localization capability features. The transfection efficiency of the reducible copolypeptides increased when increased the content of histidine-rich peptide. However, it was still unclear as to the effect of the NLS sequence in the transfection.

## 6.2 Objectives

We have shown that the RPCs (see chapters 3 and 4) that consist of lysine, histidine and cysteine moieties are promising non-viral vectors. However, the vector transfection efficiency may be improved by incorporating the NLS peptide in order to promote DNA nuclear transport. In this chapter the cytotoxicity and transfection efficiency of RcPCs are investigated in order to compare with RPCs and see if there is an improvement in the transfection by incorporation with TAT peptide.

## 6.3 Methodology

The cell transfection of the RP-TAT and RcPCs polyplexes prepared at N:P 5 (**Figure 6.5, step 1**) were carried out based on four experiments (**Figure 6.5, step 2**) which are similar to the transfection experiments of RPCs in Chapter 4 (section 4.3).



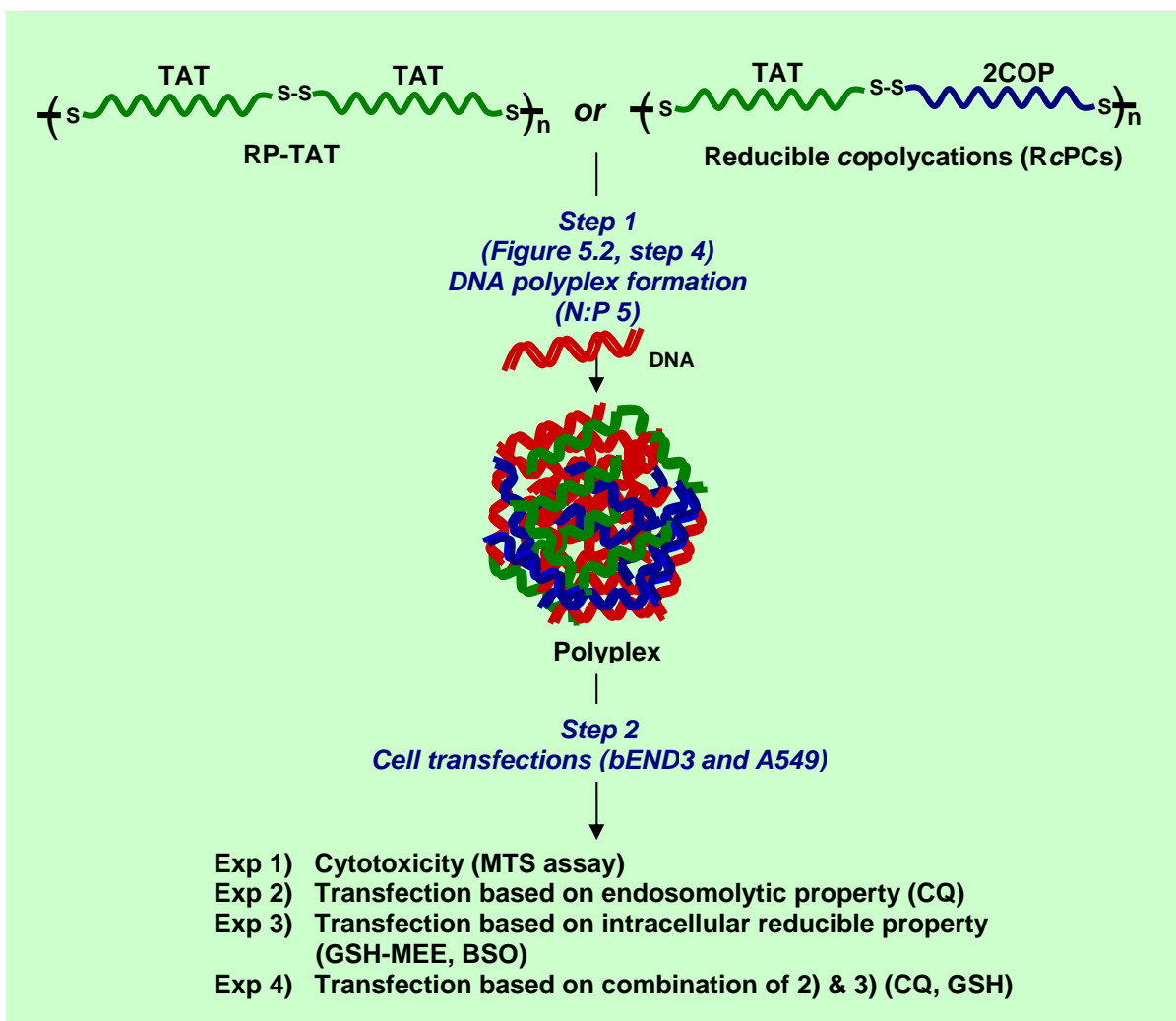


Figure 6.5. Schematic overview of cell transfection in this chapter

*Exp 1. Investigating the cytotoxicity of RP-TAT and RcPCs polyplexes:*

The cytotoxicity was investigated using the MTS assay.

*Exp 2. Investigating the endosomolytic buffering:* The transfection of

RP-TAT and RcPCs based on the endosomal buffering and endosomal escape was investigated. The transfections of polyplexes with and without CQ were investigated. Chloroquine (CQ) was added into cell lines for its ability to buffer the endosome.

*Exp 3. Investigating the intracellular reducible property:* The intracellular cleavage of the disulfide bonds in the RP-TAT and RcPCs polyplexes by GSH was studied as a function of transfection. Intracellular GSH level were boosted by adding glutathione monoethyl ester (GSH-MEE), which is cell permeable and is hydrolyzed to GSH intracellularly.<sup>[14]</sup> In addition, experiment using buthionine sulfoximine (BSO), which inhibits the synthesis of the intracellular GSH, was studied as a function of transfection.

*Exp 4. Investigating the endosomolytic buffering and intracellular reducible properties:* The transfections of polyplexes with CQ, GSH, and CQ+GSH and polyplexes alone were investigated.

## **6.4 Results and discussion**

### **6.4.1 Cytotoxicity of polyplexes (Figure 6.5, step 2, Exp1)**

#### *6.4.1.1 Cytotoxicity of RP-TAT and RcPCs polyplexes*

The cytotoxicity of RP-TAT and RcPCs polyplexes based on the effect of CQ, GSH-MEE and the combination of CQ and GSH-MEE was investigated using MTS assay. All experiments were performed as with RPCs in Chapter 4 (**Figure 4.3**). The cytotoxicity of RP-TAT and RcPC 1-5 in comparison with RPCs 1-5 are shown in **Figure 6.6**.

As can be seen in **Figure 6.6** the data demonstrated that RP-TAT and RcPCs were tolerated well by both cell lines in all cases (over 100% cell viability in most cases), and the percentage

of cell viability of cell treated with RcPCs are higher than RPCs in all cases. However, RPCs **1-5** are less toxic than PEI and PLL in both cells.

In addition, there is toxicity to cells treated with CQ and RPC polyplexes (black bars) and CQ+GSH-MEE and polyplexes (yellow bars) relative to cells treated with RPC polyplexes alone (blue bars) in most cases. However, there is none or low toxicity to cells treated with these additives (CQ, GSH-MEE and CQ+GSH-MEE) and RcPC polyplexes in bEND3. However, there is only slight toxicity to cells treated with CQ+GSH-MEE and RcPC polyplexes in A549.

The overall cytotoxicity data indicated that RP-TAT (108-140% cell viability) and RcPCs **1-5** (~86-145% cell viability) are less toxic to both cell lines and are better than PLL (79% cell viability) and PEI (69-89% cell viability) polyplexes.

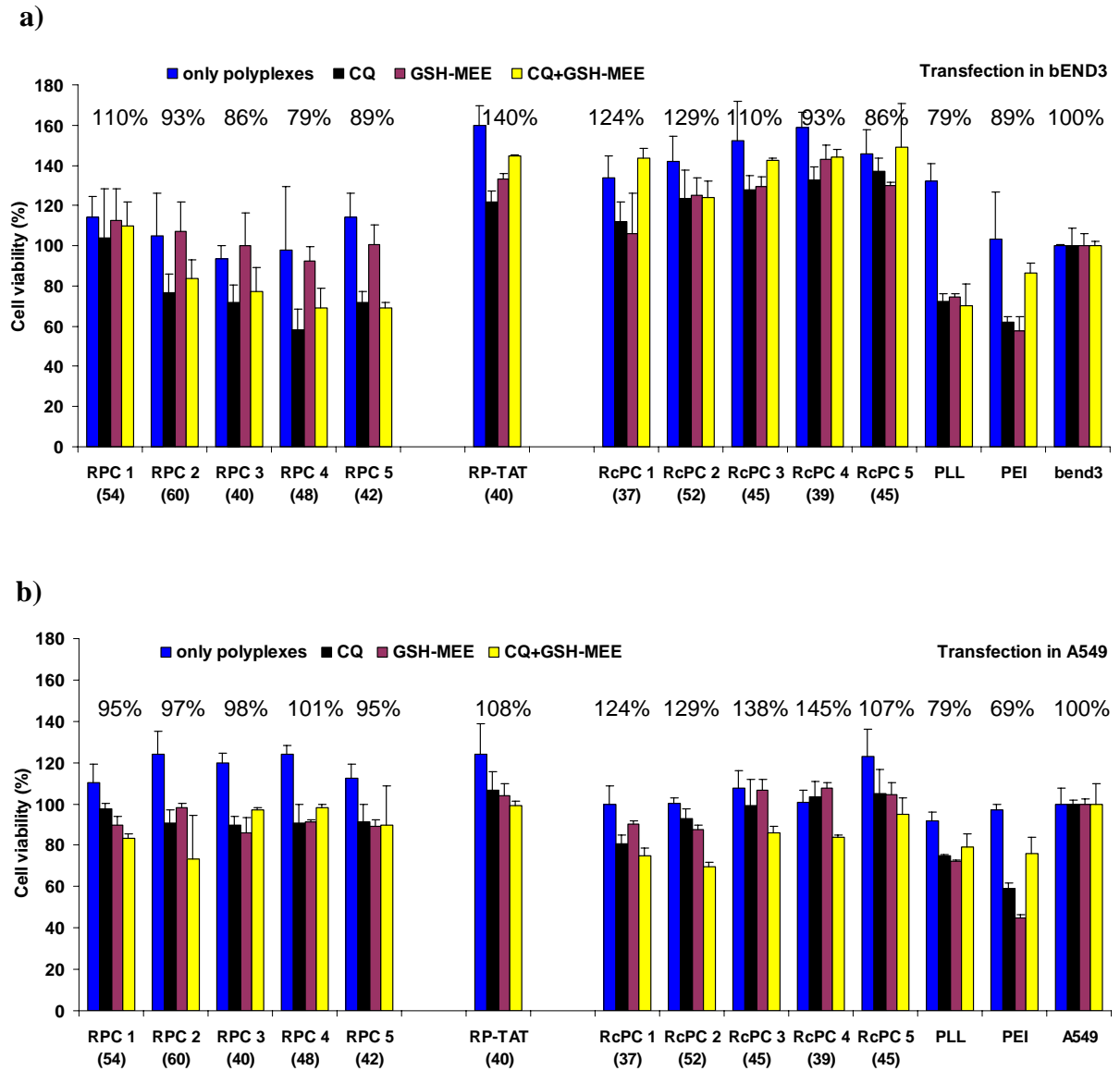


**Figure 6.6.** Cell viability following exposure to RPC 1-5 , RP-TAT and RcPC 1-5 polyplexes at N:P 5, PLL polyplex at N:P 5, PEI polyplex at N:P 10 and cell controls; (a): cell viability of transfected cells in bEND3, (b): cell viability of transfected cells in A549. Note: The percentage of cell viability shown in this diagrammed derived from the average cell viability (%) of cells treated with polyplex alone and in the combination of polyplexes and CQ, GSH-MEE and CQ+GSH-MEE in each cases

*6.4.1.2 Cytotoxicity of RcPCs polyplexes as a function of RcPC molecular weight and 2COP:TAT ratio*

6.4.1.2a Cytotoxicity of RcPCs polyplexes as a function of RcPC molecular weight

As can be seen in **Figure 6.7** there is no toxicity to cells of RcPC **5** of different molecular weights (45 and 22 kDa) for both bEND3 (**Figure 6.7a**) and A549 (**Figure 6.7b**) cells as the cell viabilities are over 100% and are better than PLL (78-81% cell viability) and PEI (77-78% cell viability) polyplexes.

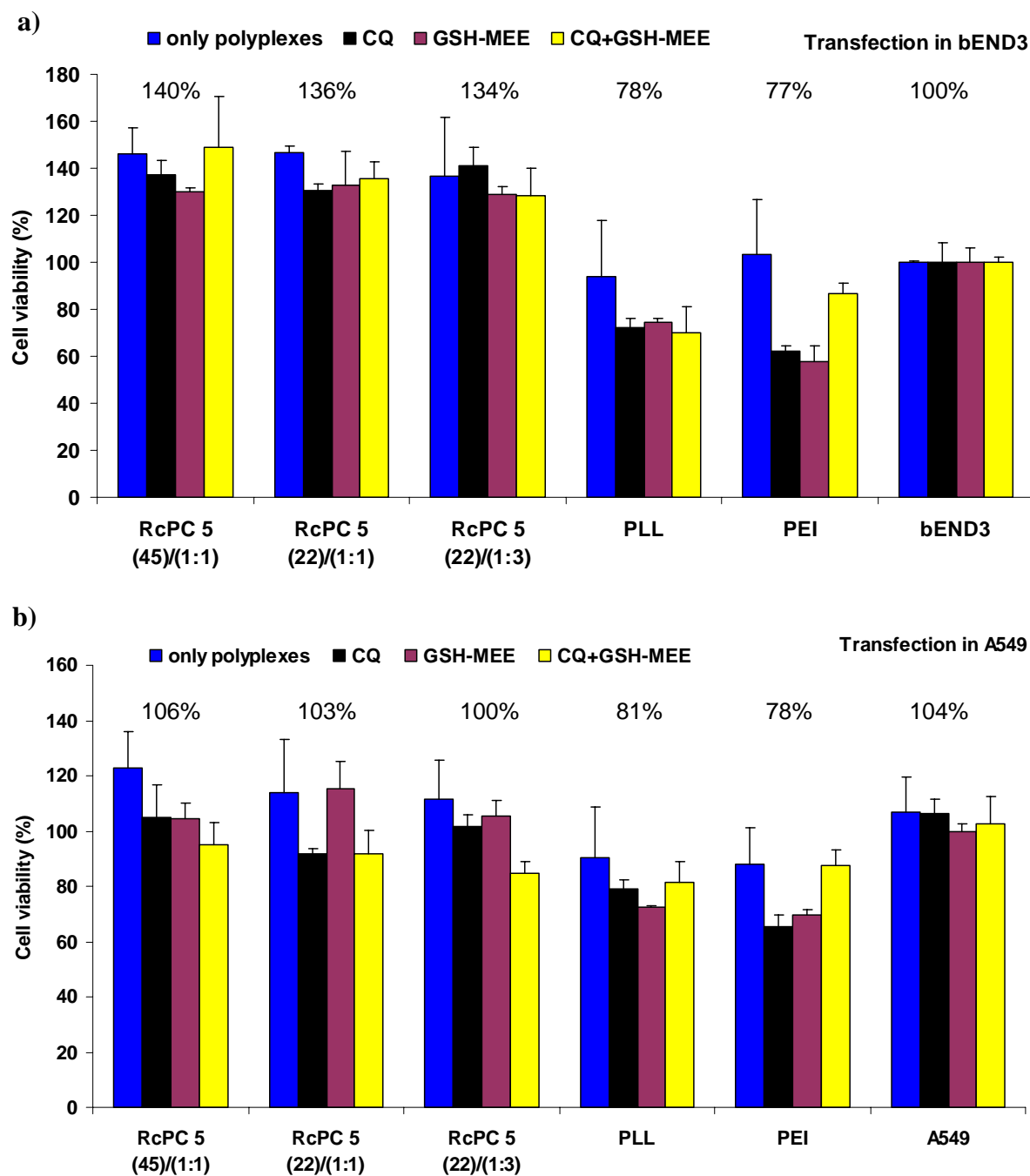


**Figure 6.7.** Cell viability of cells transfected with RcPC 5 (45 and 22 kDa with 2COP 5:TAT ratio 1:1), RcPC 5 (23 kDa with 2COP 5:TAT ratio 1:3) at N:P 5, PLL polyplex at N:P 5, PEI polyplex at N:P 10 and cell controls; (a): cell viability of transfected cells in bEND3, (b): cell viability of transfected cells in A549. Note: The percentage of cell viability shown in this diagrammed derived from the average cell viability (%) of cells treated with polyplex alone and in the combination of polyplexes and CQ, GSH-MEE and CQ+GSH-MEE in each cases

#### 6.4.1.2b Cytotoxicity of RcPCs polyplexes as a function of 2COP:TAT ratio

As can be seen in **Figure 6.7** there is no toxicity to cells of RcPC **5** (22 and 23 kDa) in different 2COP:TAT ratios (1:1 and 1:3) for both bEND3 (**Figure 6.7a**) and A549 (**Figure 6.7b**) cells as the cell viabilities are over 100% and are better than PLL and PEI polyplexes.

#### 6.4.2 Cell transfection of polyplexes (**Figure 6.5, step 2, Exp 2-4**)

The transfection efficiencies of RP-TAT and RcPCs polyplexes based on endosomolytic buffering and intracellular reduction in both cell lines were investigated. All transfection experiments were performed as outlined in Chapter 4 (**Figure 4.3**). The transfection efficiencies of RP-TAT and RcPC **1-5** based on the effect of CQ, BSO, GSH-MEE and the combination of CQ and GSH-MEE are shown in **Figure 6.8**.

The first point to note is that the overall transfection efficiency of RP-TAT is similar to RcPCs **2-5** in both cells (**Figure 6.8**). However, RP-TAT polyplexes seemed to induce higher transfection efficiency than RcPCs **1-5** in the transfection with polyplexes alone (blue bars). RcPC **1** showed the least transfection efficiency relative to other RcPCs polyplexes.

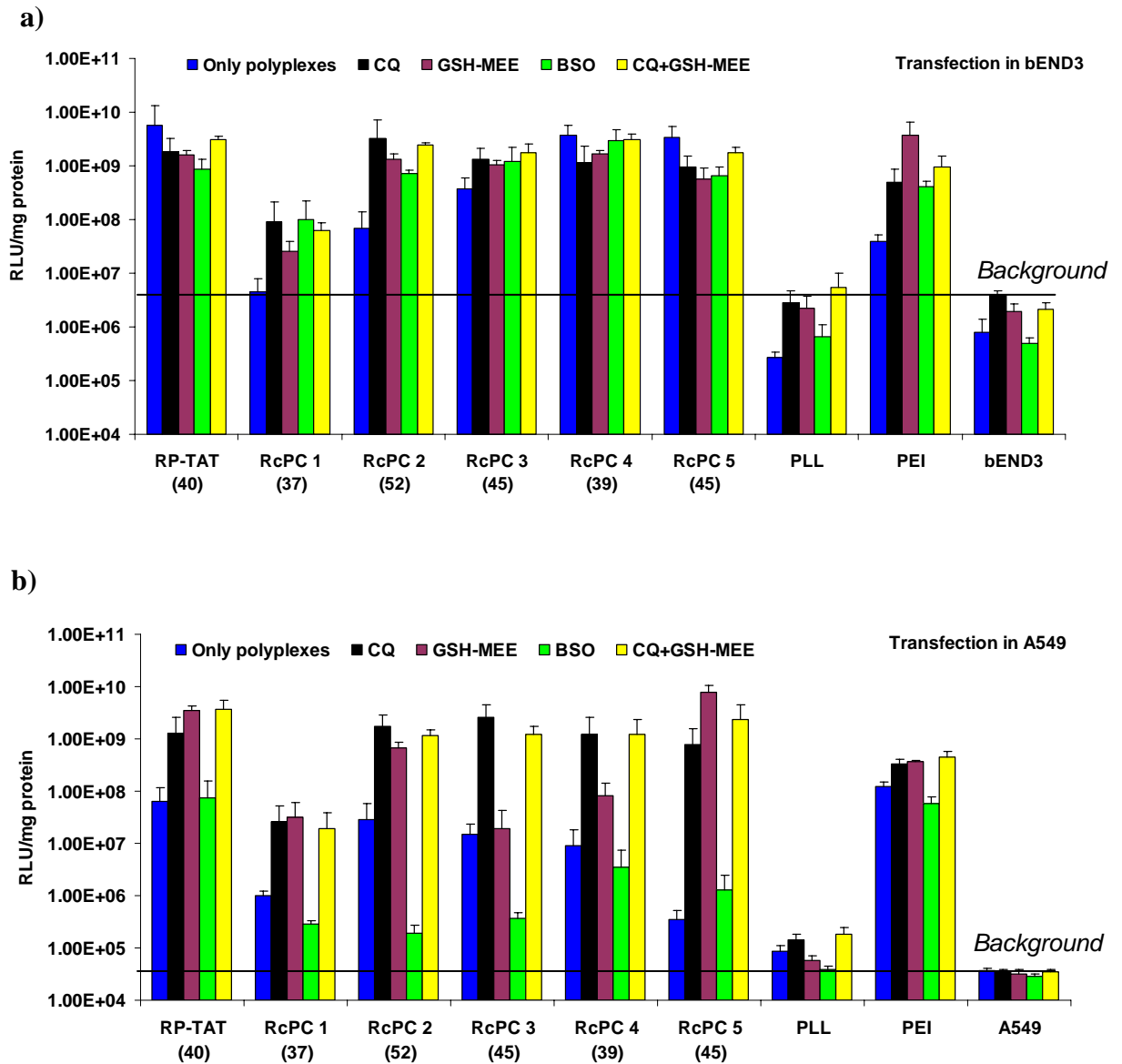


**Figure 6.8.** Transfection based on CQ, GSH-MEE and BSO with RP-TAT, RcPC polyplexes 1-5 (~50 kDa) at N:P 5, PLL polyplex at N:P 5, PEI polyplex at N:P 10 and cell control; a) transfection into bEND3 and b) transfection into A549



# **CHAPTER 7**

## **Conclusions**

# CONTENTS

List of Figures

List of Tables

## 7. CONCLUSIONS

<b>7.1</b>	<b>Conclusions</b>	<b>283</b>
7.1.1	$pK_a$ modulation of 2COPs	285
7.1.2	Diameter and zeta potential of polyplexes	285
7.1.3	Extracellular stability of polyplexes	286
7.1.4	Intracellular reduction of polyplexes	287
7.1.5	Transfection efficiency of polyplexes	288
7.1.5.1	Transfection in endothelial (bEND3) and epithelial (A549) cells	288
7.1.5.2	Transfection efficiency of RPC and RcPC polyplexes	289
7.1.5.3	Relative transfection enhancement by CQ of RPC and RcPC polyplexes	291
7.1.6	2COPs conclusion	292
7.1.7	Cross-linked RPC conclusions	292
<b>7.2</b>	<b>Limitations and future work</b>	<b>292</b>
7.2.1	Improve cell targeting	292
7.2.2	Improve nuclear localization	293
<b>7.3</b>	<b>References</b>	<b>294</b>

## List of Figures

- Figure 7.1. Disulfide bond backbone in RPC resulting in polymer chain bending compared to PLL (K<sub>20</sub>) with more rigid structure: a) PLL (K<sub>20</sub>) and b) RPC **1** (CK<sub>8</sub>C)<sub>2</sub> 285

## List of Tables

- Table 7.1. Summary of physiological and biological properties 283

## 7 CONCLUSIONS

### *Abstract*

*This chapter gives an overview of the conclusions of the experimental results presented in this thesis. Also the limitations to our research and potential future work to improve the RPC base vectors are described.*

### 7.1 Conclusions

In this thesis we have synthesized and characterised synthetic vectors by combining lysine, histidine and cysteine residues (described in Chapter 1, page 44) to provide the key features to hopefully achieve efficient gene delivery. These vectors are designed to bind DNA extracellularly (**I**), achieve cell uptake *via* endocytosis (**III**), provide a tunable endosomal release mechanism (**IV**), provide a degradable backbone in order that the DNA can be released once in the cytoplasm (**V**), and provide a nuclear localization signal (**VI**).

The summary results of the physiological and biological properties of vectors studied in this thesis are shown in **Table 7.1** and the associated text below.

**Table 7.1. Summary of physicochemical and biological properties**

Vectors	MW (kDa)	Oligopeptides	pK <sub>a</sub> of 2COPs	Polyplex diameter (nm) <sup>a</sup>	Polyplex zeta potential (mV) <sup>b</sup>	DNA released from polyplex <sup>c</sup>		Cell viability (%) <sup>d</sup>		Normalized transfection efficiency of polyplexes to PLL polyplex <sup>e</sup>		Relative transfection enhancement by CQ (%) <sup>f</sup>	
						PAA	GSH+NaCl	bEND3	A549	bEND3	A549	bEND3	A549
PLL	70	-	-	81.0 ± 0.9	11.3 ± 9.0	√	X	79	80	1.0	1.0	1049	161
PEI	25	-	-	108.7 ± 8.6	3.4 ± 0.2	√	-	83	81	147.0	1349.4	1268	271
RPC 1 (111)	111	2COP 1	10.51	132.1 ± 4.5	10.0 ± 10.9	X	X	104	88	78.0	0.3	1296	257547
RPC 2 (118)	118	2COP 2	6.20	98.3 ± 0.6	14.3 ± 9.7	X	√	102	97	1343.8	406.7	2492	722
RPC 3 (115)	115	2COP 3	6.16	99.8 ± 0.9	13.5 ± 7.2	X	√	104	108	497.9	378.4	2526	129
RPC 4 (102)	102	2COP 4	6.11	101.1 ± 2.8	5.8 ± 3.6	X	√	105	96	431.6	32.4	3316	611
RPC 5 (94)	94	2COP 5	6.09	95.5 ± 1.1	17.4 ± 11.3	X	√	101	104	1204.9	21.0	1381	717
RPC 1 (54)	54	2COP 1	10.51	99.9 ± 8.3	16.8 ± 11.0	X	X	110	95	80.6	5.9	836	12143
RPC 2 (60)	60	2COP 2	6.20	98.4 ± 0.7	10.1 ± 14.0	X	√	93	97	6892.5	2434.6	186	806
RPC 3 (40)	40	2COP 3	6.16	94.7 ± 1.5	15.5 ± 15.5	X	√	86	98	5648.7	1519.3	130	418
RPC 4 (48)	48	2COP 4	6.11	101.1 ± 2.2	5.3 ± 5.7	X	√	79	101	1633.4	166.5	32	22
RPC 5 (42)	42	2COP 5	6.09	90.7 ± 3.4	12.6 ± 12.3	X	√	89	96	4499.3	146.5	283	972
RcPC 1	37	2COP 1:TAT (1:1)	10.51	104.1 ± 1.4	13.5 ± 10.0	√	X	124	124	16.6	11.5	2055	2587
RcPC 2	52	2COP 2:TAT (1:1)	6.20	111.4 ± 2.6	8.8 ± 8.0	√	√	129	129	252.6	335.8	4889	6117
RcPC 3	45	2COP 3:TAT (1:1)	6.16	105.7 ± 3.7	17.8 ± 12.8	√	√	110	138	1390.0	173.1	360	17722
RcPC 4	39	2COP 4:TAT (1:1)	6.11	98.1 ± 3.7	10.3 ± 9.1	√	√	93	145	14177.4	107.9	29	13242
RcPC 5	45	2COP 5:TAT (1:1)	6.09	108.1 ± 1.6	11.6 ± 14.3	√	√	86	107	12717.5	4.1	28	220532
RcPC 5	22	2COP 5:TAT (1:1)	6.09	98.4 ± 0.9	12.6 ± 8.4	√	√	136	103	2715.4	40.1	112	2127
RcPC 5	23	2COP 5:TAT (1:3)	6.09	110.3 ± 1.1	12.9 ± 12.0	√	√	134	100	2593.8	36.7	178	1615
RP-TAT	40	TAT	-	95.2 ± 0.3	14.4 ± 9.3	√	√	140	108	21574.6	760.8	31	1960

<sup>a</sup> Hydrodynamic diameters of the polyplexes (N:P 5) measured by dynamic light scattering with a Zetasizer 3000 (Malvern Instruments, Worcestershire, UK)

<sup>b</sup> Zeta potential measured by with a Zetamaster (Malvern Instruments, Worcestershire, UK)

<sup>c</sup> DNA released investigated by agarose gel electrophoresis

<sup>d</sup> The percentage of cell viability derived from the average cell viability (%) of cells treated with polyplex alone and in the combination of polyplexes and CQ, GSH-MEE and CQ+GSH-MEE in each cases

<sup>e</sup> Normalized transfection efficiency of polyplexes to PLL polyplex = transfection level of polyplex/transfection level of PLL polyplex

<sup>f</sup> Relative transfection enhancement by chloroquine (%) = (transfection level of polyplex with CQ/transfection level of polyplex only)\*100

### 7.1.1 p*K*<sub>a</sub> modulation of 2COPs

We have shown that using the new strategy of increasing the mixing of the constitution of the histidine residues in the lysine residues we were able to modulate the p*K*<sub>a</sub> of 2COPs **1-5** from 10.51-6.09 (**Table 7.1, p*K*<sub>a</sub> of 2COPs**) because of the charge repulsion of subphase protons by its proximity to the protonated lysine residues. The modulation of the p*K*<sub>a</sub> of 2COPs 2-5 (p*K*<sub>a</sub> 6.20-6.09) will provide a way to modulate the buffering capacity in the early endosome (pH ~6) leading to endosomal disruption, before it develops into the late endosome where polyplexes would be degraded (vector feature **IV**) as described in the hypothesis (Chapter 1, page 48).

### 7.1.2 Diameter and zetapotential of polyplexes

Regarding to the hypothesis in Chapter 1 (page 51), the incorporation of lysine into synthetic vectors provides the strong binding of the vector to DNA *via* electrostatic interactions (Vector feature **I**). The RPCs and RcPCs in this thesis have lysine residues incorporated and not only bind strongly to the DNA, but also form polyplexes of ~100 nm (**Table 7.1, polyplex diameter**).

In addition, incorporation of lysine residues into the synthetic vectors resulted in positively charged polyplexes (**Table 7.1, polyplex zetapotential**), which further enabled them to electrostatically interact with the negatively charged cell membrane and promote the internalization into cells *via* syndecan-mediated endocytosis<sup>[1,2]</sup> (vector feature **III**) as described in the hypothesis in Chapter 1 (page 51).

### 7.1.3 Extracellular stability of polyplexes

PLL polyplexes are less stable than RPC 1 when exposed to PAA (Table 7.1, PAA). This result indicates RPC 1 binds more strongly to DNA than PLL. We hypothesized that PLL has a higher persistent length (Figure 7.1a) than RPC 1 (Figure 7.1b). This reduction in persistence length of RPC 1 is a result of the reduction in charge repulsion of the protonated lysine groups either side of the reducible disulfide bond from the cysteines, allow the s-s bond to act as a molecular hinge.

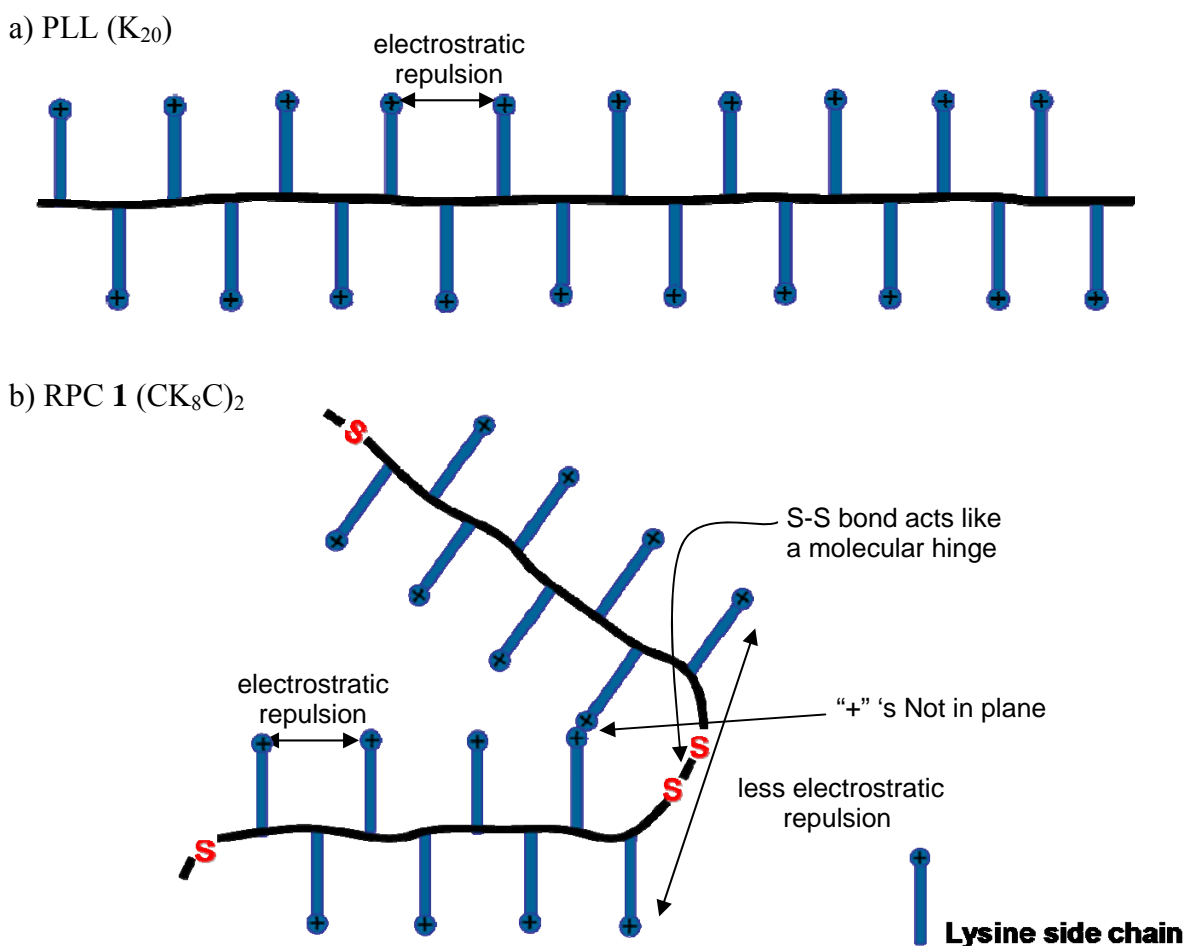


Figure 7.1. Disulfide bond backbone in RPC resulting in polymer chain bending compared to PLL ( $K_{20}$ ) with more rigid structure: a) PLL ( $K_{20}$ ) and b) RPC 1 ( $CK_8C$ )<sub>2</sub>

RPCs **2-5** have inherently more extracellular stability than other polyplexes as they did not release the DNA when exposed to PAA (**Table 7.1, PAA**). This result was a surprise as there were only 50% of the fully protonated lysine residues compared to RPC **1**, thus, the electrostatic interaction would be much weaker. However, continuing the argument around persistence length and better compaction of RPC **1** polyplexes, one can envisage that RPCs **2-5** have even shorter persistent lengths than RPC **1**, and hence compact better with DNA, and are therefore more stable. This result suggested that polyplexes formed from RPCs **2-5** are more stable extracellularly than PLL and RPC **1** polyplexes and, therefore, would be able to reach the target cells after blood stream circulation (vector feature **I**).

#### **7.1.4 Intracellular reduction and toxicity of polyplexes**

As described previously in the hypothesis (Chapter 1, page 51), the disulfide backbone in RPCs and RcPCs provides the point of cleavage of the reducible polycations by intracellular GSH leading to the DNA release in the cytoplasm (vector feature **V**). The gel shift assay of RPCs **2-5** and RcPCs **2-5** polyplexes with GSH in combination with salt revealed that they are able to be reduced and release the DNA intracellularly (**Table 7.1, GSH+NaCl**). However, treatment of polyplexes with GSH revealed no release of DNA with RPC **1** and RcPC **1**, in contrast to RPCs **2-5** and RcPCs **2-5**. Presumably, all polyplexes are undergoing disulfide bond cleavage, but the enhanced positive charge of 2COP **1** (twice as many lysine residues in RPC **1** compared to RPCs **2-5**) means the short oligopeptide fragments (2COP **1**) remain bound to the DNA, unlike 2COPs **2-5**.

In addition, all of the intracellular reducible vector systems studied here are less toxic to both cell types than the non-degradable polymers (PLL and PEI). Presumably, the RPCs and



RcPCs degrade to readily cleared fragments (2COPs) compared to the high molecular weight PLL and PEI (**Table 7.1, cell viability**).

### **7.1.5 Transfection efficiency of polyplexes**

#### *7.1.5.1 Transfection in endothelial (bEND3) and epithelial (A549) cells*

bEND3 cells have higher transfection levels than A549 cells (**Table 7.1, relative transfection efficiency of polyplexes to PLL polyplex**). The difference observed between transfection efficiencies in bEND3 (mouse brain endothelial cells) and A549 (human lung carcinoma epithelial cells) is most likely due to the different rate of cell growth *in vitro*, as endothelial cells grow faster. Change in growth rates would have affected the level of intracellular glutathione and the protein expression as described in Chapter 4 (in the transfection results with GSH-MEE/BSO). Concomitant degradation of the nuclear membrane would, therefore, have led to the release of high level of glutathione into the cytoplasm leading to more efficient release of DNA from the polyplexes to the cytoplasm resulting in higher transfection levels than in A549, and may result in the different trends of the transfection between bEND3 and A549.

The higher transfection rates of the endothelium (bEND3) cells might be a contra-indication to support the administration of the RPC polyplexes *via* intravenous injection if one was trying to treat a tumor, as the polyplexes would be internalized by blood vessels before reaching the tumor.

### 7.1.5.2 Transfection efficiency of RPC and RcPC polyplexes

In **Table 7.1** we have normalized the transfection data by dividing the PLL polyplex transfection level into all the other polyplex transfection levels. Several conclusions can be drawn from this if we consider the bEND3 cells and A549 cells both independently and then together.

bEND3 cells :

- (i) PLL polyplexes are the worst transfection agents.
- (ii) RPC **1** (111) and RPC **1** (54) have increased transfection levels over PLL (80.6 and 16.6 fold increase, respectively). Therefore, the incorporation of the disulfide bond has significantly increased the transfection efficiency.
- (iii) The histidine containing RPCs (**2-5**), both high and low molecular weight, have increased transfection efficiency over RPC **1**, ranging from 431.6 (RPC **4**) to 1343.8 (RPC **2**) for the high molecular weight materials. All of the lower molecular weight materials have even better transfection. Therefore, the incorporation of histidine moieties enhances the transfection above and beyond the introduction of the disulfide bonds.
- (iv) The lower molecular weight RPCs **2-5** have higher transfection levels than the higher molecular weight RPCs **2-5**. Therefore, molecular weight is key determinant in transfection levels. We have also shown that the diameters, surface charges and gel shift assays of polyplexes from low molecular weight RPCs **2-5** (~50 kDa) were similar to high molecular weight RPCs **2-5** (~100 kDa), but had enhanced release of DNA when treated with GSH. This result is indicative of the fact that the kinetics of DNA release is quicker with low molecular weight RPCs, presumably because shorter fragments of polycations

will dissociate more rapidly from the DNA. Therefore, the low molecular weight RPCs might induce higher transfection level than high molecular weight RPCs, and indeed this was the case.

(v) Incorporation of TAT (RcPCs **4-5**) significantly enhances the transfection of the polyplexes, whilst it is variable for RcPCs **2-3**. Thus, TAT potentially has an effect in endothelial cells (which is in contrast to A549 epithelial cells).

(vi) The cell transfections with RcPC **5** polyplexes at different 2COP:TAT ratios (1:1 and 1:3) revealed that the amount of nuclear localization signal (TAT) incorporated in the RcPCs does not affect the transfection level as similar transfection levels were determined (RcPC **5** (22 (1:1), 23 (1:3))). This result may be due to the RcPC polyplexes upon intracellular GSH reduction leading to the DNA dissociating totally from the TAT fragments, and therefore no translocation and internalization of the DNA to the nucleus. Therefore, there is no improvement in addition of TAT sequence relative to the transfection with RPC polyplexes.

A549 cells :

Similar conclusions with respect to the introduction of the disulfide bond, histidine and molecular weight can be drawn for A549 as were for bEND3 cells. However, for RcPC polyplexes the transfection levels were lower or about the same for RPCs **2-5**. Therefore, it appears that the type of cell – endothelial or epithelial – has a significant effect on the transfection levels.

### 7.1.5.3 Relative transfection enhancement by CQ of RPC and RcPC polyplexes

In **Table 7.1** the relative transfection enhancement of polyplexes by CQ are shown. Several conclusions can be drawn.

(i) We were expecting that the transfection levels of RPCs **2-5** would be less enhanced by CQ than RPC **1** because of the buffering capacity by histidine residues. However, the transfection levels of RPC **2-5** (~100 kDa) in bEND 3 enhanced by CQ were about the same or even higher than RPC **1**, which are anomalous. These results in bEND 3 are in contrast to RPC **1-5** (~100 kDa) in A549, as the transfection levels were less enhanced by CQ when incorporation of histidines (RPCs **2-5**) compared to RPC **1**. Therefore, once again, it appears that the type of cell – endothelial or epithelial – has a significant effect on the transfection levels.

(ii) The lower molecular weight RPCs **1-5** (~50 kDa) have less enhancement by CQ than the higher molecular weight RPCs **1-5** (~100 kDa) in both cells. Therefore, the lower molecular weight RPCs used in this thesis are better transfection agents than higher molecular weight RPCs.

(iii) CQ was required to enhance the transfection levels of RcPCs **1-3** compared to RPC **1-3** (~50 kDa) in bEND3. However, CQ did not affect the transfection of RcPC **4-5**. Also these results are in contrast to the transfection in A549, in which all of the RcPCs **2-5** required CQ to give better transfection levels than corresponding RPCs. Presumably, this is because the buffering capacity (proton sponge mechanism) is lower in the RcPCs.

### 7.1.6 2COPs conclusion

DNA polyplexes formed from 2COPs **1-5** at N:P 5 (Chapter 3) formed large particles (1  $\mu\text{m}$ ) over a time course of 48 hr (Chapter 3, **Table 3.7**). In general, particle diameters less than 1  $\mu\text{m}$  survive longer in the bloodstream than the larger particle if there are no interactions with blood components or macrophages.<sup>[4]</sup> Therefore, these polyplexes were not suitable for further cell transfection. As predicted the oligopeptides 2COP polyplexes were poor transfection agents relative to the RPCs (Chapter 4, **Figure 4.16**).

### 7.1.7 Cross-linked RPC conclusions

The oxidative polymerization to form *cross-linked RPCs* was also studied by oxidatively polymerising 2COPs **1-5** and 3COP **7** at 4% and 32% mole fraction of 3COP **7** (Chapter 3, section 3.4.5). The results showed termination in the growth of *cross-linked RPCs* producing low molecular weight polymers in all cases. The higher the mole fraction of 3COP used, the lower the polymer molecular weight produced. We believe the 3COP leads to the termination of the *cross-linked RPCs* during the reaction.

## 7.2 Limitations and future work

### 7.2.1 Improve cell targeting

In our primary vector design the cell targeting ligand was not attached to the vector. Therefore, these non-targeting vectors can not be used effectively in transfection *in vivo*. To improve this vector feature the targeting ligands have to be attached to the vectors as

described in Chapter 1 (Section 1.1.2.1b). The targeting ligands that have been widely used are transferrin, which specifically targets transferrin receptors that are overexpressed in rapidly dividing tissues, such as tumors,<sup>[5-13]</sup> and folic acid that specifically target folate receptors, which are also overexpressed in proliferating tissues.<sup>[13-15]</sup> In addition, various saccharide ligands such as galactose, manose, fucose, lactose as well as asialoorosomuroid and asialoglycoprotein are specifically targeting asialoglycoprotein receptors, which are abundantly expressed in hepatocytes.<sup>[12,13,16]</sup>

In addition, using endothelium (bEND3) and epithelium cell lines (A549) in the *in vitro* transfection studies indicated that the *in vivo* injection of RPC polyplexes in blood vessel would not be a suitable method for delivering genes, as the polyplexes entered into the endothelial cells. Therefore, to improve the transfection at the target sites, the administration methods have to be considered such as direct injection<sup>[17,18]</sup> and electroporation<sup>[19,20]</sup> based on formation of membrane pores induced by electric pulses into tissues.

## **7.2.2 Improve nuclear localization**

Another limitation in our studies is that the incorporation of TAT peptide in RcPCs did not improve the transfection level compared to RPCs. This result is likely to be due to the free DNA being fully released from TAT peptides after the reduction by intracellular GSH. Therefore, to improve the nuclear localization the direct covalent/non covalent attachment of NLS to DNA is a way of developing RPC based polyplexes.

There are many strategies developed to attaching the NLS to DNA as described in Chapter 6 (section 6.1). For instance, the attachment of NLS to the hair pin loop at the end of linear

DNA.<sup>[21]</sup> The intercalating agent such as psoralen<sup>[22,23]</sup> and p-azido-tetrafluoro-benzyl<sup>[24]</sup> were also chemically attached to the NLS peptide, in order that the NLS peptide is covalently attached to the DNA by photoactivation.

### 7.3 References

1. Mislick, K.A., and Baldeschwieler, J.D. (1996). Evidence for the role of proteoglycans in cation-mediated gene transfer. *Proceedings of the National Academy of Sciences of the United States of America*, **93**, 12349-12354.
2. Kopatz, I., Remy, J.S., and Behr, J.P. (2004). A model for non-viral gene delivery: through syndecan adhesion molecules and powered by actin. *Journal of Gene Medicine*, **6**, 769-776.
3. Akinc, A., Thomas, M., Klibanov, A.M., and Langer, R. (2005). Exploring polyethylenimine-mediated DNA transfection and the proton sponge hypothesis. *Journal of Gene Medicine*, **7**, 657-663.
4. Patel, H.M. (1992). Serum opsonins and liposomes - their interaction and opsonophagocytosis. *Critical Reviews in Therapeutic Drug Carrier Systems*, **9**, 39-90.
5. Dash, P.R., Read, M.L., Fisher, K.D., Howard, K.A., Wolfert, M., Oupicky, D., Subr, V., Strohalm, J., Ulbrich, K., and Seymour, L.W. (2000). Decreased binding to proteins and cells of polymeric gene delivery vectors surface modified with a multivalent hydrophilic polymer and retargeting through attachment of transferrin. *Journal of Biological Chemistry*, **275**, 3793-3802.
6. Zenke, M., Steinlein, P., Wagner, E., Cotten, M., Beug, H., and Birnstiel, M.L. (1990). Receptor-mediated endocytosis of transferrin polycation conjugates - an

- efficient way to introduce DNA into hematopoietic cells. *Proceedings of the National Academy of Sciences of the United States of America*, **87**, 3655-3659.
7. Wagner, E., Zenke, M., Cotten, M., Beug, H., and Birnstiel, M.L. (1990). Transferrin-polycation conjugates as carriers for DNA uptake into cells. *Proceedings of the National Academy of Sciences of the United States of America*, **87**, 3410-3414.
  8. Daniels, T.R., Delgado, T., Rodriguez, J.A., Helguera, G., and Penichet, M.L. (2006). The transferrin receptor part I: Biology and targeting with cytotoxic antibodies for the treatment of cancer. *Clinical Immunology*, **121**, 144-158.
  9. Daniels, T.R., Delgado, T., Helguera, G., and Penichet, M.L. (2006). The transferrin receptor part II: Targeted delivery of therapeutic agents into cancer cells. *Clinical Immunology*, **121**, 159-176.
  10. Kircheis, R., Kichler, A., Wallner, G., Kursa, M., Ogris, M., Felzmann, T., Buchberger, M., and Wagner, E. (1997). Coupling of cell-binding ligands to polyethylenimine for targeted gene delivery. *Gene Therapy*, **4**, 409-418.
  11. Ogris, M., Brunner, S., Schuller, S., Kircheis, R., and Wagner, E. (1999). PEGylated DNA/transferrin-PEI complexes: reduced interaction with blood components, extended circulation in blood and potential for systemic gene delivery. *Gene Therapy*, **6**, 595-605.
  12. Zauner, W., Ogris, M., and Wagner, E. (1998). Polylysine-based transfection systems utilizing receptor-mediated delivery. *Advanced Drug Delivery Reviews*, **30**, 97-113.
  13. Merdan, T., Kopecek, J., and Kissel, T. (2002). Prospects for cationic polymers in gene and oligonucleotide therapy against cancer. *Advanced Drug Delivery Reviews*, **54**, 715-758.



14. Wang, S., and Low, P.S. (1998). Folate-mediated targeting of antineoplastic drugs, imaging agents, and nucleic acids to cancer cells. *Journal of Controlled Release*, **53**, 39-48.
15. Lu, Y.J., and Low, P.S. (2002). Folate-mediated delivery of macromolecular anticancer therapeutic agents. *Advanced Drug Delivery Reviews*, **54**, 675-693.
16. Erbacher, P., Roche, A.C., Monsigny, M., and Midoux, P. (1996). Putative role of chloroquine in gene transfer into a human hepatoma cell line by DNA lactosylated polylysine complexes. *Experimental Cell Research*, **225**, 186-194.
17. Roy, S., Zhang, K., Roth, T., Vinogradov, S., Kao, R.S., and Kabanov, A. (1999). Reduction of fibronectin expression by intravitreal administration of antisense oligonucleotides. *Nature Biotechnology*, **17**, 476-479.
18. Nishikawa, M., Yamauchi, M., Morimoto, K., Ishida, E., Takakura, Y., and Hashida, M. (2000). Hepatocyte-targeted in vivo gene expression by intravenous injection of plasmid DNA complexed with synthetic multi-functional gene delivery system. *Gene Therapy*, **7**, 548-555.
19. Heller, R., Jaroszeski, M., Atkin, A., Moradpour, D., Gilbert, R., Wands, J., and Nicolau, C. (1996). In vivo gene electroinjection and expression in rat liver. *FEBS Letters*, **389**, 225-228.
20. Wells, J.M., Li, L.H., Sen, A., Jahreis, G.P., and Hui, S.W. (2000). Electroporation-enhanced gene delivery in mammary tumors. *Gene Therapy*, **7**, 541-547.
21. Zanta, M.A., Belguise-Valladier, P., and Behr, J.P. (1999). Gene delivery: A single nuclear localization signal peptide is sufficient to carry DNA to the cell nucleus. *Proceedings of the National Academy of Sciences of the United States of America*, **96**, 91-96.

22. Yoo, H.S., and Jeong, S.Y. (2007). Nuclear targeting of non-viral gene carriers using psoralen-nuclear localization signal (NLS) conjugates. *European Journal of Pharmaceutics and Biopharmaceutics*, **66**, 28-33.
23. Neves, C., Byk, G., Scherman, D., and Wils, P. (1999). Coupling of a targeting peptide to plasmid DNA by covalent triple helix formation. *Febs Letters*, **453**, 41-45.
24. Ciolina, C., Byk, G., Blanche, F., Thuillier, V., Scherman, D., and Wils, P. (1999). Coupling of nuclear localization signals to plasmid DNA and specific interaction of the conjugates with importin alpha. *Bioconjugate Chemistry*, **10**, 49-55.

## 7 CONCLUSIONS

### *Abstract*

*This chapter gives an overview of the conclusions of the experimental results presented in this thesis. Also the limitations to our research and potential future work to improve the RPC base vectors are described.*

### 7.1 Conclusions

In this thesis we have synthesized and characterised synthetic vectors by combining lysine, histidine and cysteine residues (described in Chapter 1, page 44) to provide the key features to hopefully achieve efficient gene delivery. These vectors are designed to bind DNA extracellularly (**I**), achieve cell uptake *via* endocytosis (**III**), provide a tunable endosomal release mechanism (**IV**), provide a degradable backbone in order that the DNA can be released once in the cytoplasm (**V**), and provide a nuclear localization signal (**VI**).

The summary results of the physiological and biological properties of vectors studied in this thesis are shown in **Table 7.1** and the associated text below.

**Table 7.1. Summary of physiological and biological properties**

Vectors	MW (kDa)	Oligopeptides	pK <sub>a</sub> of 2COPs	Polyplex diameter (nm) <sup>a</sup>	Polyplex zetapotential (mV) <sup>b</sup>	DNA released from polyplex <sup>c</sup>		Cell viability (%) <sup>d</sup>		Normalized transfection efficiency of polyplexes to PLL polyplex <sup>e</sup>		Relative transfection enhancement by CQ (%) <sup>f</sup>	
						PAA	GSH+NaCl	bEND3	A549	bEND3	A549	bEND3	A549
PLL	70	-	-	81.0 ± 0.9	11.3 ± 9.0	√	X	79	80	1.0	1.0	1049	161
PEI	25	-	-	108.7 ± 8.6	3.4 ± 0.2	√	-	83	81	147.0	1349.4	1268	271
RPC 1 (111)	111	2COP 1	10.51	132.1 ± 4.5	10.0 ± 10.9	X	X	104	88	78.0	0.3	1296	257547
RPC 2 (118)	118	2COP 2	6.20	98.3 ± 0.6	14.3 ± 9.7	X	√	102	97	1343.8	406.7	2492	722
RPC 3 (115)	115	2COP 3	6.16	99.8 ± 0.9	13.5 ± 7.2	X	√	104	108	497.9	378.4	2526	129
RPC 4 (102)	102	2COP 4	6.11	101.1 ± 2.8	5.8 ± 3.6	X	√	105	96	431.6	32.4	3316	611
RPC 5 (94)	94	2COP 5	6.09	95.5 ± 1.1	17.4 ± 11.3	X	√	101	104	1204.9	21.0	1381	717
RPC 1 (54)	54	2COP 1	10.51	99.9 ± 8.3	16.8 ± 11.0	X	X	110	95	80.6	5.9	836	12143
RPC 2 (60)	60	2COP 2	6.20	98.4 ± 0.7	10.1 ± 14.0	X	√	93	97	6892.5	2434.6	186	806
RPC 3 (40)	40	2COP 3	6.16	94.7 ± 1.5	15.5 ± 15.5	X	√	86	98	5648.7	1519.3	130	418
RPC 4 (48)	48	2COP 4	6.11	101.1 ± 2.2	5.3 ± 5.7	X	√	79	101	1633.4	166.5	32	22
RPC 5 (42)	42	2COP 5	6.09	90.7 ± 3.4	12.6 ± 12.3	X	√	89	96	4499.3	146.5	283	972
RcPC 1	37	2COP 1:TAT (1:1)	10.51	104.1 ± 1.4	13.5 ± 10.0	√	X	124	124	16.6	11.5	2055	2587
RcPC 2	52	2COP 2:TAT (1:1)	6.20	111.4 ± 2.6	8.8 ± 8.0	√	√	129	129	252.6	335.8	4889	6117
RcPC 3	45	2COP 3:TAT (1:1)	6.16	105.7 ± 3.7	17.8 ± 12.8	√	√	110	138	1390.0	173.1	360	17722
RcPC 4	39	2COP 4:TAT (1:1)	6.11	98.1 ± 3.7	10.3 ± 9.1	√	√	93	145	14177.4	107.9	29	13242
RcPC 5	45	2COP 5:TAT (1:1)	6.09	108.1 ± 1.6	11.6 ± 14.3	√	√	86	107	12717.5	4.1	28	220532
RcPC 5	22	2COP 5:TAT (1:1)	6.09	98.4 ± 0.9	12.6 ± 8.4	√	√	136	103	2715.4	40.1	112	2127
RcPC 5	23	2COP 5:TAT (1:3)	6.09	110.3 ± 1.1	12.9 ± 12.0	√	√	134	100	2593.8	36.7	178	1615
RP-TAT	40	TAT	-	95.2 ± 0.3	14.4 ± 9.3	√	√	140	108	21574.6	760.8	31	1960

<sup>a</sup> Hydrodynamic diameters of the polyplexes (N:P 5) measured by dynamic light scattering with a Zetasizer 3000 (Malvern Instruments, Worcestershire, UK)

<sup>b</sup> Zetapotential measured by with a Zetamaster (Malvern Instruments, Worcestershire, UK)

<sup>c</sup> DNA released investigated by agarose gel electrophoresis

<sup>d</sup> The percentage of cell viability derived from the average cell viability (%) of cells treated with polyplex alone and in the combination of polyplexes and CQ, GSH-MEE and CQ+GSH-MEE in each cases

<sup>e</sup> Normalized transfection efficiency of polyplexes to PLL polyplex = transfection level of polyplex/transfection level of PLL polyplex

<sup>f</sup> Relative transfection enhancement by chloroquine (%) = (transfection level of polyplex with CQ/transfection level of polyplex only)\*100

### 7.1.1 p*K*<sub>a</sub> modulation of 2COPs

We have shown that using the new strategy of increasing the mixing of the constitution of the histidine residues in the lysine residues we were able to modulate the p*K*<sub>a</sub> of 2COPs **1-5** from 10.51-6.09 (**Table 7.1, p*K*<sub>a</sub> of 2COPs**) because of the charge repulsion of subphase protons by its proximity to the protonated lysine residues. The modulation of the p*K*<sub>a</sub> of 2COPs 2-5 (p*K*<sub>a</sub> 6.20-6.09) will provide a way to modulate the buffering capacity in the early endosome (pH ~6) leading to endosomal disruption, before it develops into the late endosome where polyplexes would be degraded (vector feature **IV**) as described in the hypothesis (Chapter 1, page 48).

### 7.1.2 Diameter and zetapotential of polyplexes

Regarding to the hypothesis in Chapter 1 (page 51), the incorporation of lysine into synthetic vectors provides the strong binding of the vector to DNA *via* electrostatic interactions (Vector feature **I**). The RPCs and RcPCs in this thesis have lysine residues incorporated and not only bind strongly to the DNA, but also form polyplexes of ~100 nm (**Table 7.1, polyplex diameter**).

In addition, incorporation of lysine residues into the synthetic vectors resulted in positively charged polyplexes (**Table 7.1, polyplex zetapotential**), which further enabled them to electrostatically interact with the negatively charged cell membrane and promote the internalization into cells *via* syndecan-mediated endocytosis<sup>[1,2]</sup> (vector feature **III**) as described in the hypothesis in Chapter 1 (page 51).

### 7.1.3 Extracellular stability of polyplexes

PLL polyplexes are less stable than RPC 1 when exposed to PAA (Table 7.1, PAA). This result indicates RPC 1 binds more strongly to DNA than PLL. We hypothesized that PLL has a higher persistent length (Figure 7.1a) than RPC 1 (Figure 7.1b). This reduction in persistence length of RPC 1 is a result of the reduction in charge repulsion of the protonated lysine groups either side of the reducible disulfide bond from the cysteines, allow the s-s bond to act as a molecular hinge.

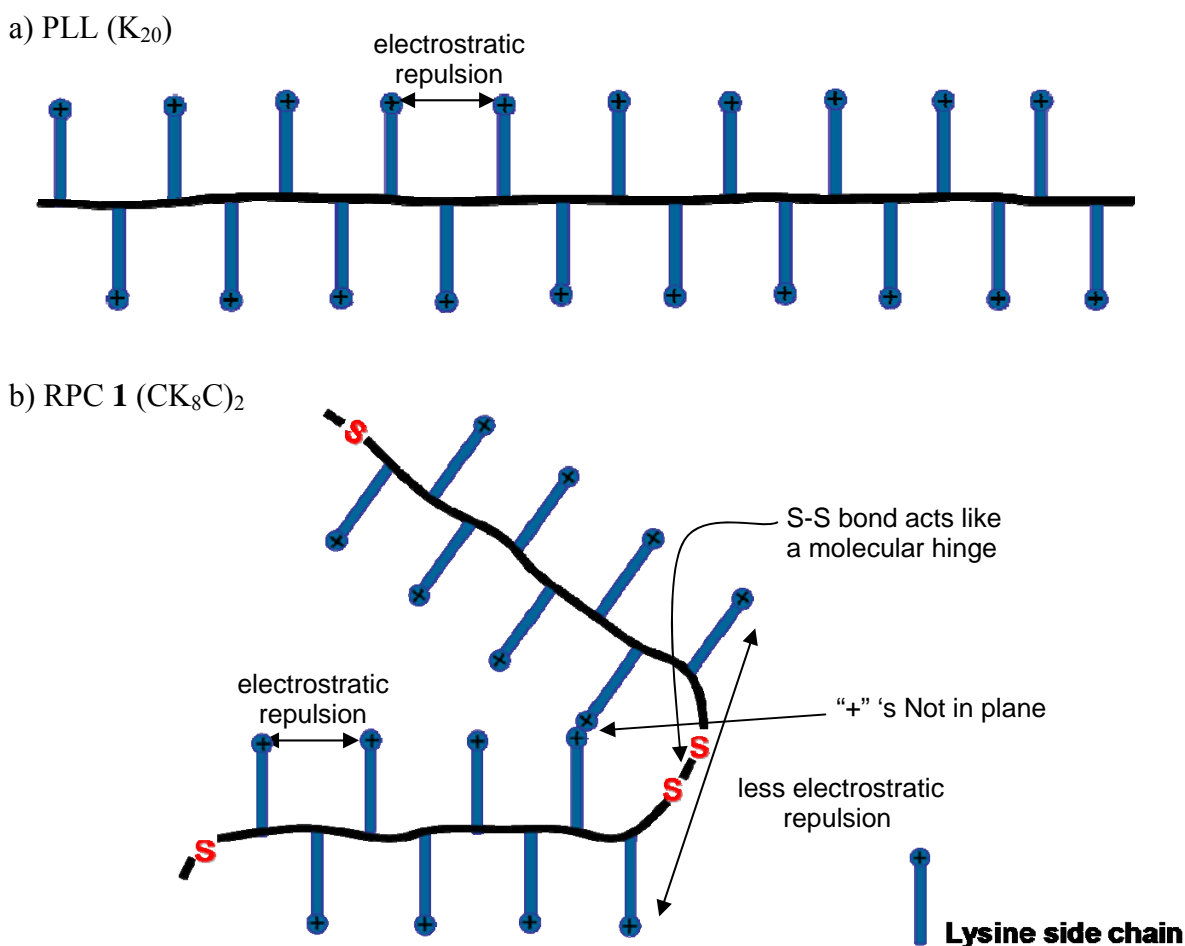


Figure 7.1. Disulfide bond backbone in RPC resulting in polymer chain bending compared to PLL ( $K_{20}$ ) with more rigid structure: a) PLL ( $K_{20}$ ) and b) RPC 1 ( $CK_8C$ )<sub>2</sub>

RPCs **2-5** have inherently more extracellular stability than other polyplexes as they did not release the DNA when exposed to PAA (**Table 7.1, PAA**). This result was a surprise as there were only 50% of the fully protonated lysine residues compared to RPC **1**, thus, the electrostatic interaction would be much weaker. However, continuing the argument around persistence length and better compaction of RPC **1** polyplexes, one can envisage that RPCs **2-5** have even shorter persistent lengths than RPC **1**, and hence compact better with DNA, and are therefore more stable. This result suggested that polyplexes formed from RPCs **2-5** are more stable extracellularly than PLL and RPC **1** polyplexes and, therefore, would be able to reach the target cells after blood stream circulation (vector feature **I**).

#### **7.1.4 Intracellular reduction and toxicity of polyplexes**

As described previously in the hypothesis (Chapter 1, page 51), the disulfide backbone in RPCs and RcPCs provides the point of cleavage of the reducible polycations by intracellular GSH leading to the DNA release in the cytoplasm (vector feature **V**). The gel shift assay of RPCs **2-5** and RcPCs **2-5** polyplexes with GSH in combination with salt revealed that they are able to be reduced and release the DNA intracellularly (**Table 7.1, GSH+NaCl**). However, treatment of polyplexes with GSH revealed no release of DNA with RPC **1** and RcPC **1**, in contrast to RPCs **2-5** and RcPCs **2-5**. Presumably, all polyplexes are undergoing disulfide bond cleavage, but the enhanced positive charge of 2COP **1** (twice as many lysine residues in RPC **1** compared to RPCs **2-5**) means the short oligopeptide fragments (2COP **1**) remain bound to the DNA, unlike 2COPs **2-5**.

In addition, all of the intracellular reducible vector systems studied here are less toxic to both cell types than the non-degradable polymers (PLL and PEI). Presumably, the RPCs and

RcPCs degrade to readily cleared fragments (2COPs) compared to the high molecular weight PLL and PEI (**Table 7.1, cell viability**).

## **7.1.5 Transfection efficiency of polyplexes**

### *7.1.5.1 Transfection in endothelial (bEND3) and epithelial (A549) cells*

bEND3 cells have higher transfection levels than A549 cells (**Table 7.1, relative transfection efficiency of polyplexes to PLL polyplex**). The difference observed between transfection efficiencies in bEND3 (mouse brain endothelial cells) and A549 (human lung carcinoma epithelial cells) is most likely due to the different rate of cell growth *in vitro*, as endothelial cells grow faster. Change in growth rates would have affected the level of intracellular glutathione and the protein expression as described in Chapter 4 (in the transfection results with GSH-MEE/BSO). Concomitant degradation of the nuclear membrane would, therefore, have led to the release of high level of glutathione into the cytoplasm leading to more efficient release of DNA from the polyplexes to the cytoplasm resulting in higher transfection levels than in A549, and may result in the different trends of the transfection between bEND3 and A549.

The higher transfection rates of the endothelium (bEND3) cells might be a contra-indication to support the administration of the RPC polyplexes *via* intravenous injection if one was trying to treat a tumor, as the polyplexes would be internalized by blood vessels before reaching the tumor.



### 7.1.5.2 Transfection efficiency of RPC and RcPC polyplexes

In **Table 7.1** we have normalized the transfection data by dividing the PLL polyplex transfection level into all the other polyplex transfection levels. Several conclusions can be drawn from this if we consider the bEND3 cells and A549 cells both independently and then together.

bEND3 cells :

- (i) PLL polyplexes are the worst transfection agents.
- (ii) RPC **1** (111) and RPC **1** (54) have increased transfection levels over PLL (80.6 and 16.6 fold increase, respectively). Therefore, the incorporation of the disulfide bond has significantly increased the transfection efficiency.
- (iii) The histidine containing RPCs (**2-5**), both high and low molecular weight, have increased transfection efficiency over RPC **1**, ranging from 431.6 (RPC **4**) to 1343.8 (RPC **2**) for the high molecular weight materials. All of the lower molecular weight materials have even better transfection. Therefore, the incorporation of histidine moieties enhances the transfection above and beyond the introduction of the disulfide bonds.
- (iv) The lower molecular weight RPCs **2-5** have higher transfection levels than the higher molecular weight RPCs **2-5**. Therefore, molecular weight is key determinant in transfection levels. We have also shown that the diameters, surface charges and gel shift assays of polyplexes from low molecular weight RPCs **2-5** (~50 kDa) were similar to high molecular weight RPCs **2-5** (~100 kDa), but had enhanced release of DNA when treated with GSH. This result is indicative of the fact that the kinetics of DNA release is quicker with low molecular weight RPCs,

presumably because shorter fragments of polycations will dissociate more rapidly from the DNA. Therefore, the low molecular weight RPCs might induce higher transfection level than high molecular weight RPCs, and indeed this was the case.

(v) Incorporation of TAT (RcPCs **4-5**) significantly enhances the transfection of the polyplexes, whilst it is variable for RcPCs **2-3**. Thus, TAT potentially has an effect in endothelial cells (which is in contrast to A549 epithelial cells).

(vi) The cell transfections with RcPC **5** polyplexes at different 2COP:TAT ratios (1:1 and 1:3) revealed that the amount of nuclear localization signal (TAT) incorporated in the RcPCs does not affect the transfection level as similar transfection levels were determined (RcPC **5** (22 (1:1), 23 (1:3))). This result may be due to the RcPC polyplexes upon intracellular GSH reduction leading to the DNA dissociating totally from the TAT fragments, and therefore no translocation and internalization of the DNA to the nucleus. Therefore, there is no improvement in addition of TAT sequence relative to the transfection with RPC polyplexes.

A549 cells :

Similar conclusions with respect to the introduction of the disulfide bond, histidine and molecular weight can be drawn for A549 as were for bEND3 cells. However, for RcPC polyplexes the transfection levels were lower or about the same for RPCs **2-5**. Therefore, it appears that the type of cell – endothelial or epithelial – has a significant effect on the transfection levels.

### 7.1.5.3 Relative transfection enhancement by CQ of RPC and RcPC polyplexes

In **Table 7.1** the relative transfection enhancement of polyplexes by CQ are shown. Several conclusions can be drawn.

(i) We were expecting that the transfection levels of RPCs **2-5** would be less enhanced by CQ than RPC **1** because of the buffering capacity by histidine residues. However, the transfection levels of RPC **2-5** (~100 kDa) in bEND 3 enhanced by CQ were about the same or even higher than RPC **1**, which are anomalous. These results in bEND 3 are in contrast to RPC **1-5** (~100 kDa) in A549, as the transfection levels were less enhanced by CQ when incorporation of histidines (RPCs **2-5**) compared to RPC **1**. Therefore, once again, it appears that the type of cell – endothelial or epithelial – has a significant effect on the transfection levels.

(ii) The lower molecular weight RPCs **1-5** (~50 kDa) have less enhancement by CQ than the higher molecular weight RPCs **1-5** (~100 kDa) in both cells. Therefore, the lower molecular weight RPCs used in this thesis are better transfection agents than higher molecular weight RPCs.

(iii) CQ was required to enhance the transfection levels of RcPCs **1-3** compared to RPC **1-3** (~50 kDa) in bEND3. However, CQ did not affect the transfection of RcPC **4-5**. Also these results are in contrast to the transfection in A549, in which all of the RcPCs **2-5** required CQ to give better transfection levels than corresponding RPCs. Presumably, this is because the buffering capacity (proton sponge mechanism) is lower in the RcPCs.

### 7.1.6 2COPs conclusion

DNA polyplexes formed from 2COPs **1-5** at N:P 5 (Chapter 3) formed large particles (1  $\mu\text{m}$ ) over a time course of 48 hr (Chapter 3, **Table 3.7**). In general, particle diameters less than 1  $\mu\text{m}$  survive longer in the bloodstream than the larger particle if there are no interactions with blood components or macrophages.<sup>[4]</sup> Therefore, these polyplexes were not suitable for further cell transfection. As predicted the oligopeptides 2COP polyplexes were poor transfection agents relative to the RPCs (Chapter 4, **Figure 4.16**).

### 7.1.7 Cross-linked RPC conclusions

The oxidative polymerization to form *cross-linked RPCs* was also studied by oxidatively polymerising 2COPs **1-5** and 3COP **7** at 4% and 32% mole fraction of 3COP **7** (Chapter 3, section 3.4.5). The results showed termination in the growth of *cross-linked RPCs* producing low molecular weight polymers in all cases. The higher the mole fraction of 3COP used, the lower the polymer molecular weight produced. We believe the 3COP leads to the termination of the *cross-linked RPCs* during the reaction.

## 7.2 Limitations and future work

### 7.2.1 Improve cell targeting

In our primary vector design the cell targeting ligand was not attached to the vector. Therefore, these non-targeting vectors can not be used effectively in transfection *in vivo*. To improve this vector feature the targeting ligands have to be attached to the vectors as

described in Chapter 1 (Section 1.1.2.1b). The targeting ligands that have been widely used are transferrin, which specifically targets transferrin receptors that are overexpressed in rapidly dividing tissues, such as tumors,<sup>[5-13]</sup> and folic acid that specifically target folate receptors, which are also overexpressed in proliferating tissues.<sup>[13-15]</sup> In addition, various saccharide ligands such as galactose, manose, fucose, lactose as well as asialoorosomucoid and asialoglycoprotein are specifically targeting asialoglycoprotein receptors, which are abundantly expressed in hepatocytes.<sup>[12,13,16]</sup>

In addition, using endothelium (bEND3) and epithelium cell lines (A549) in the *in vitro* transfection studies indicated that the *in vivo* injection of RPC polyplexes in blood vessel would not be a suitable method for delivering genes, as the polyplexes entered into the endothelial cells. Therefore, to improve the transfection at the target sites, the administration methods have to be considered such as direct injection<sup>[17,18]</sup> and electroporation<sup>[19,20]</sup> based on formation of membrane pores induced by electric pulses into tissues.

## **7.2.2 Improve nuclear localization**

Another limitation in our studies is that the incorporation of TAT peptide in RcPCs did not improve the transfection level compared to RPCs. This result is likely to be due to the free DNA being fully released from TAT peptides after the reduction by intracellular GSH. Therefore, to improve the nuclear localization the direct covalent/non covalent attachment of NLS to DNA is a way of developing RPC based polyplexes.

There are many strategies developed to attaching the NLS to DNA as described in Chapter 6 (section 6.1). For instance, the attachment of NLS to the hair pin loop at the end of linear

DNA.<sup>[21]</sup> The intercalating agent such as psoralen<sup>[22,23]</sup> and p-azido-tetrafluoro-benzyl<sup>[24]</sup> were also chemically attached to the NLS peptide, in order that the NLS peptide is covalently attached to the DNA by photoactivation.

### 7.3 References

1. Mislick, K.A., and Baldeschwieler, J.D. (1996). Evidence for the role of proteoglycans in cation-mediated gene transfer. *Proceedings of the National Academy of Sciences of the United States of America*, **93**, 12349-12354.
2. Kopatz, I., Remy, J.S., and Behr, J.P. (2004). A model for non-viral gene delivery: through syndecan adhesion molecules and powered by actin. *Journal of Gene Medicine*, **6**, 769-776.
3. Akinc, A., Thomas, M., Klibanov, A.M., and Langer, R. (2005). Exploring polyethylenimine-mediated DNA transfection and the proton sponge hypothesis. *Journal of Gene Medicine*, **7**, 657-663.
4. Patel, H.M. (1992). Serum opsonins and liposomes - their interaction and opsonophagocytosis. *Critical Reviews in Therapeutic Drug Carrier Systems*, **9**, 39-90.
5. Dash, P.R., Read, M.L., Fisher, K.D., Howard, K.A., Wolfert, M., Oupicky, D., Subr, V., Strohalm, J., Ulbrich, K., and Seymour, L.W. (2000). Decreased binding to proteins and cells of polymeric gene delivery vectors surface modified with a multivalent hydrophilic polymer and retargeting through attachment of transferrin. *Journal of Biological Chemistry*, **275**, 3793-3802.
6. Zenke, M., Steinlein, P., Wagner, E., Cotten, M., Beug, H., and Birnstiel, M.L. (1990). Receptor-mediated endocytosis of transferrin polycation conjugates - an

- efficient way to introduce DNA into hematopoietic cells. *Proceedings of the National Academy of Sciences of the United States of America*, **87**, 3655-3659.
7. Wagner, E., Zenke, M., Cotten, M., Beug, H., and Birnstiel, M.L. (1990). Transferrin-polycation conjugates as carriers for DNA uptake into cells. *Proceedings of the National Academy of Sciences of the United States of America*, **87**, 3410-3414.
  8. Daniels, T.R., Delgado, T., Rodriguez, J.A., Helguera, G., and Penichet, M.L. (2006). The transferrin receptor part I: Biology and targeting with cytotoxic antibodies for the treatment of cancer. *Clinical Immunology*, **121**, 144-158.
  9. Daniels, T.R., Delgado, T., Helguera, G., and Penichet, M.L. (2006). The transferrin receptor part II: Targeted delivery of therapeutic agents into cancer cells. *Clinical Immunology*, **121**, 159-176.
  10. Kircheis, R., Kichler, A., Wallner, G., Kursa, M., Ogris, M., Felzmann, T., Buchberger, M., and Wagner, E. (1997). Coupling of cell-binding ligands to polyethylenimine for targeted gene delivery. *Gene Therapy*, **4**, 409-418.
  11. Ogris, M., Brunner, S., Schuller, S., Kircheis, R., and Wagner, E. (1999). PEGylated DNA/transferrin-PEI complexes: reduced interaction with blood components, extended circulation in blood and potential for systemic gene delivery. *Gene Therapy*, **6**, 595-605.
  12. Zauner, W., Ogris, M., and Wagner, E. (1998). Polylysine-based transfection systems utilizing receptor-mediated delivery. *Advanced Drug Delivery Reviews*, **30**, 97-113.
  13. Merdan, T., Kopecek, J., and Kissel, T. (2002). Prospects for cationic polymers in gene and oligonucleotide therapy against cancer. *Advanced Drug Delivery Reviews*, **54**, 715-758.

14. Wang, S., and Low, P.S. (1998). Folate-mediated targeting of antineoplastic drugs, imaging agents, and nucleic acids to cancer cells. *Journal of Controlled Release*, **53**, 39-48.
15. Lu, Y.J., and Low, P.S. (2002). Folate-mediated delivery of macromolecular anticancer therapeutic agents. *Advanced Drug Delivery Reviews*, **54**, 675-693.
16. Erbacher, P., Roche, A.C., Monsigny, M., and Midoux, P. (1996). Putative role of chloroquine in gene transfer into a human hepatoma cell line by DNA lactosylated polylysine complexes. *Experimental Cell Research*, **225**, 186-194.
17. Roy, S., Zhang, K., Roth, T., Vinogradov, S., Kao, R.S., and Kabanov, A. (1999). Reduction of fibronectin expression by intravitreal administration of antisense oligonucleotides. *Nature Biotechnology*, **17**, 476-479.
18. Nishikawa, M., Yamauchi, M., Morimoto, K., Ishida, E., Takakura, Y., and Hashida, M. (2000). Hepatocyte-targeted in vivo gene expression by intravenous injection of plasmid DNA complexed with synthetic multi-functional gene delivery system. *Gene Therapy*, **7**, 548-555.
19. Heller, R., Jaroszeski, M., Atkin, A., Moradpour, D., Gilbert, R., Wands, J., and Nicolau, C. (1996). In vivo gene electroinjection and expression in rat liver. *FEBS Letters*, **389**, 225-228.
20. Wells, J.M., Li, L.H., Sen, A., Jahreis, G.P., and Hui, S.W. (2000). Electroporation-enhanced gene delivery in mammary tumors. *Gene Therapy*, **7**, 541-547.
21. Zanta, M.A., Belguise-Valladier, P., and Behr, J.P. (1999). Gene delivery: A single nuclear localization signal peptide is sufficient to carry DNA to the cell nucleus. *Proceedings of the National Academy of Sciences of the United States of America*, **96**, 91-96.



22. Yoo, H.S., and Jeong, S.Y. (2007). Nuclear targeting of non-viral gene carriers using psoralen-nuclear localization signal (NLS) conjugates. *European Journal of Pharmaceutics and Biopharmaceutics*, **66**, 28-33.
23. Neves, C., Byk, G., Scherman, D., and Wils, P. (1999). Coupling of a targeting peptide to plasmid DNA by covalent triple helix formation. *Febs Letters*, **453**, 41-45.
24. Ciolina, C., Byk, G., Blanche, F., Thuillier, V., Scherman, D., and Wils, P. (1999). Coupling of nuclear localization signals to plasmid DNA and specific interaction of the conjugates with importin alpha. *Bioconjugate Chemistry*, **10**, 49-55.

# **CHAPTER 8**

## **Appendix**

# CONTENTS

List of Figures

List of Tables

## 8 APPENDIX

<b>8.1 Preparative HPLC chromatograms of crude oligopeptides and analytical HPLC chromatograms of purified oligopeptides</b>	<b>302</b>
8.1.1 Preparative HPLC and analytical HPLC of 2COP 1	302
8.1.2 Preparative HPLC and analytical HPLC of 2COP 2	303
8.1.3 Preparative HPLC and analytical HPLC of 2COP 3	304
8.1.4 Preparative HPLC and analytical HPLC of 2COP 4	305
8.1.5 Preparative HPLC and analytical HPLC of 2COP 5	306
8.1.6 Preparative HPLC and analytical HPLC of 2COP 6	308
8.1.7 Preparative HPLC and analytical HPLC of 3COP 7	309
8.1.8 Preparative HPLC and analytical HPLC of TAT	310
<b>8.2 <sup>1</sup>H NMR of purified oligopeptides</b>	<b>311</b>
8.2.1 <sup>1</sup> H NMR of purified 2COP 1	311
8.2.2 <sup>1</sup> H NMR of purified 2COP 2	312
8.2.3 <sup>1</sup> H NMR of purified 2COP 3	313
8.2.4 <sup>1</sup> H NMR of purified 2COP 4	314
8.2.5 <sup>1</sup> H NMR of purified 2COP 5	315
8.2.6 <sup>1</sup> H NMR of purified 2COP 6	316
8.2.7 <sup>1</sup> H NMR of purified 3COP 7	317
8.2.8 <sup>1</sup> H NMR of purified TAT	318
<b>8.3 Samples of <sup>1</sup>H NMR spectra at different pH in NMR titration experiments of 2COPs</b>	<b>319</b>
<b>8.4 Samples of GPC chromatograms in oxidative polymerization experiments</b>	<b>321</b>
<b>8.5 Publication</b>	<b>323</b>

## List of Figures

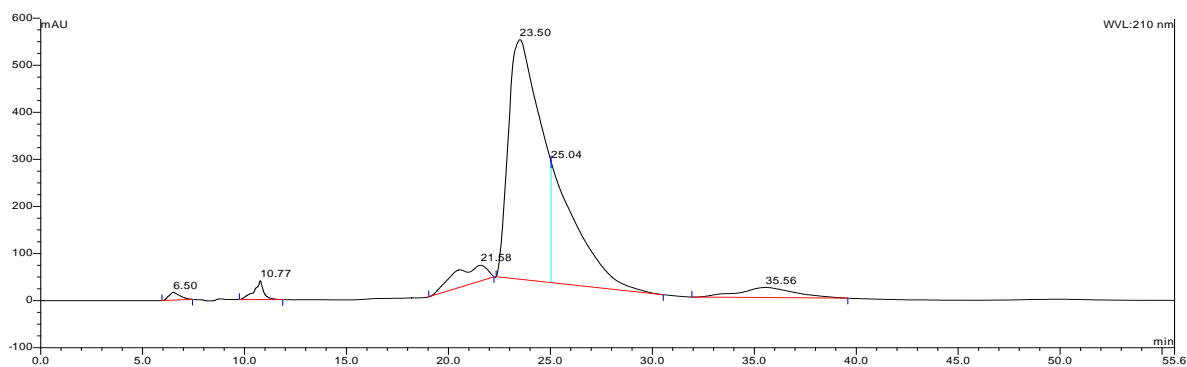
Figure 8.1.	Preparative HPLC chromatogram of crude 2COP <b>1</b>	302
Figure 8.2.	Analytical HPLC chromatogram of purified 2COP <b>1</b>	302
Figure 8.3.	Preparative HPLC chromatogram of crude 2COP <b>2</b>	303
Figure 8.4.	Analytical HPLC chromatogram of purified 2COP <b>2</b>	303
Figure 8.5.	Preparative HPLC chromatogram of crude 2COP <b>3</b>	304
Figure 8.6.	Analytical HPLC chromatogram of purified 2COP <b>3</b>	304
Figure 8.7.	Preparative HPLC chromatogram of crude 2COP <b>4</b>	305
Figure 8.8.	Analytical HPLC chromatogram of purified 2COP <b>4</b>	305
Figure 8.9.	Preparative HPLC chromatogram of crude 2COP <b>5</b>	306
Figure 8.10.	Analytical HPLC chromatogram of purified 2COP <b>5</b>	307
Figure 8.11.	Preparative HPLC chromatogram of crude 2COP <b>6</b>	308
Figure 8.12.	Analytical HPLC chromatogram of purified 2COP <b>6</b>	308
Figure 8.13.	Preparative HPLC chromatogram of crude 3COP <b>7</b>	309
Figure 8.14.	Analytical HPLC chromatogram of purified 3COP <b>7</b>	309
Figure 8.15.	Preparative HPLC chromatogram of crude TAT	310
Figure 8.16.	Analytical HPLC chromatogram of purified TAT	310
Figure 8.17.	<sup>1</sup> H NMR spectra of 2COP <b>1</b>	311
Figure 8.18.	<sup>1</sup> H NMR spectra of 2COP <b>2</b>	312
Figure 8.19.	<sup>1</sup> H NMR spectra of 2COP <b>3</b>	313
Figure 8.20.	<sup>1</sup> H NMR spectra of 2COP <b>4</b>	314
Figure 8.21.	<sup>1</sup> H NMR spectra of 2COP <b>5</b>	315
Figure 8.22.	<sup>1</sup> H NMR spectra of 2COP <b>6</b>	316
Figure 8.23.	<sup>1</sup> H NMR spectra of 3COP <b>7</b>	317
Figure 8.24.	<sup>1</sup> H NMR spectra of TAT	318
Figure 8.25.	<sup>1</sup> H NMR spectra of H <sub>e</sub> of 2COP <b>1</b> at pH 2.88, 10.37 and 12.75	319
Figure 8.26.	<sup>1</sup> H NMR spectra of H <sub>5</sub> and H <sub>6</sub> of 2COP <b>5</b> at pH 2.64, 5.84 and 7.55	319
Figure 8.27.	<sup>1</sup> H NMR spectra of H <sub>5</sub> and H <sub>6</sub> of 2COP <b>6</b> at pH 3.04, 5.54 and 7.00	320
Figure 8.28.	Comparison of the chromatogram of the oxidative polymerization of 2COP <b>1</b> at 30 mM concentration incubated at ambient for 48 hr analyzed by GPC	321

- Figure 8.29. Comparison of the chromatogram of the oxidative polymerization of 2COP **1** at 60 mM concentration incubated at ambient for 48 hr analyzed by GPC 321
- Figure 8.30. Comparison of the chromatogram of the oxidative polymerization of 2COP **1** at 18 mM concentration incubated at a) ambient and b) 40°C for 72 hr analyzed by GPC 322

## 8. APPENDIX

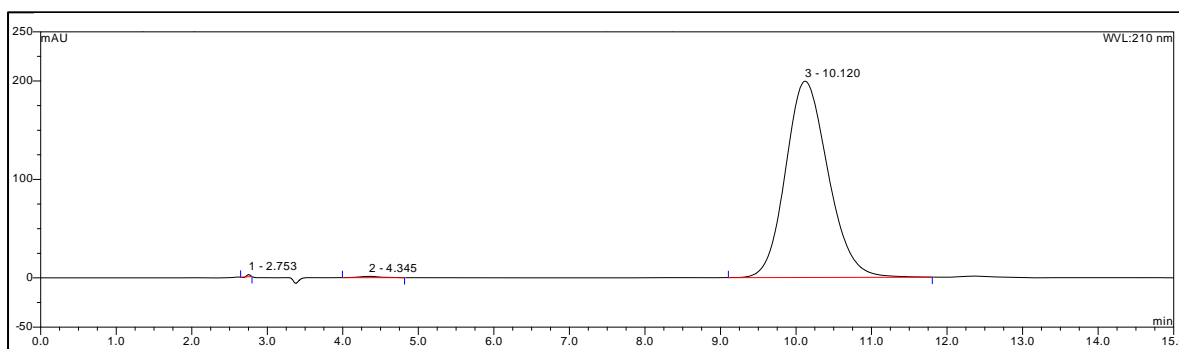
### 8.1 Preparative HPLC chromatograms of crude oligopeptides and analytical HPLC chromatograms of purified oligopeptides

#### 8.1.1 Preparative HPLC and analytical HPLC of 2COP 1



Ret.Time (min)	Area (mAU*min)	Height (mAU)	Rel.Area (%)
6.505	10.2625	16.462	0.7
10.768	21.491	39.77	1.47
21.584	72.4728	33.147	4.96
23.5	915.8373	509.08	62.65
25.035	373.135	256.823	25.53
35.561	68.6066	21.518	4.69

**Figure 8.1.** Preparative HPLC chromatogram of crude 2COP 1 with MeCN (1%) plus TFA (0.05%) as an elution solvent at 10 ml/min flow rate for 60 minutes: Preparative RP-HPLC (Phenomenex), C<sub>18</sub> with 250 mm × 21.2 mm ID and 10 μm pore size



Ret.Time (min)	Area (mAU*min)	Height (mAU)	Rel.Area (%)
2.753	0.0923	2.111	0.07
4.345	0.4416	1.347	0.34
10.12	129.9928	199.343	99.59

**Figure 8.2.** Analytical HPLC chromatogram of purified 2COP 1 with 1% of MeCN:water (60:40) plus TFA (0.05%) as an elution solvent at 10 ml/min flow rate: Analytical RP-HPLC (Phenomenex), C<sub>18</sub> with 250 mm × 4.60 mm ID and 10 μm pore size

### 8.1.2 Preparative HPLC and analytical HPLC of 2COP 2

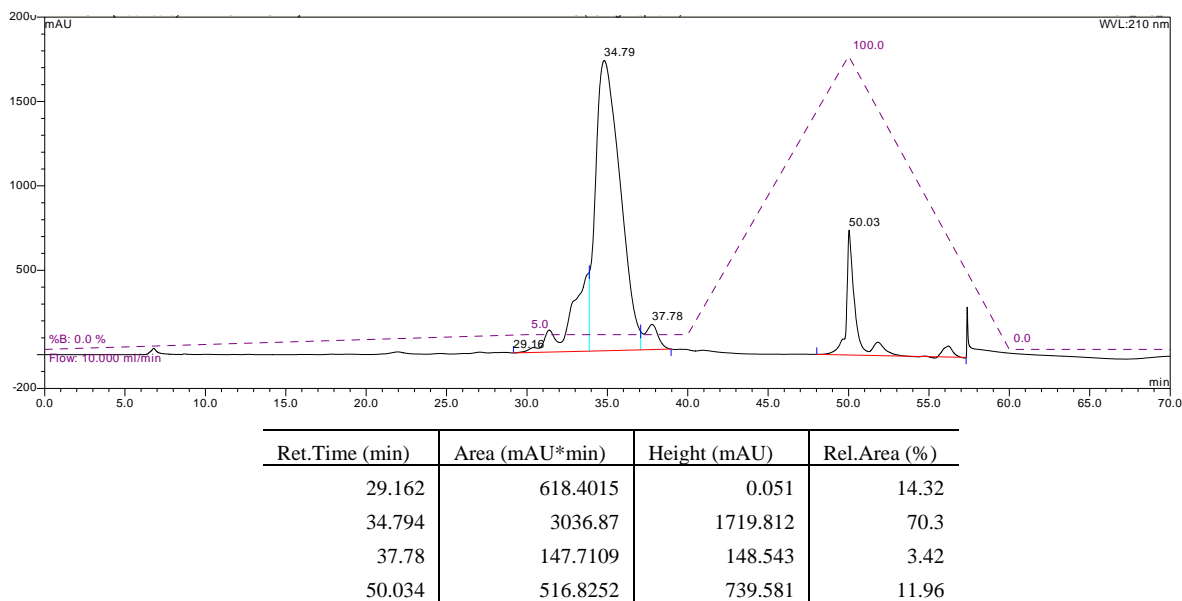


**Figure 8.3.** Preparative HPLC chromatogram of 2COP 2 with the gradient of MeCN (0-5%) plus TFA (0.05%) for the first 30 minutes, and with MeCN+TFA (5%) for further 10 minutes as an elution solvent at 10 ml/min flow rate: Preparative RP-HPLC (Phenomenex), C<sub>18</sub> with 250 mm × 21.2 mm ID and 10 μm pore size

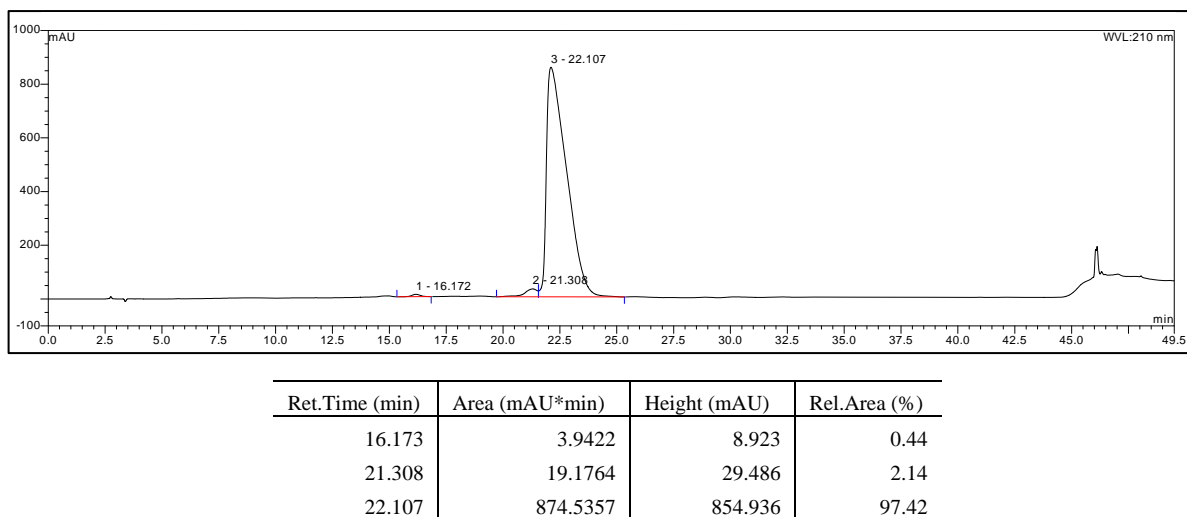
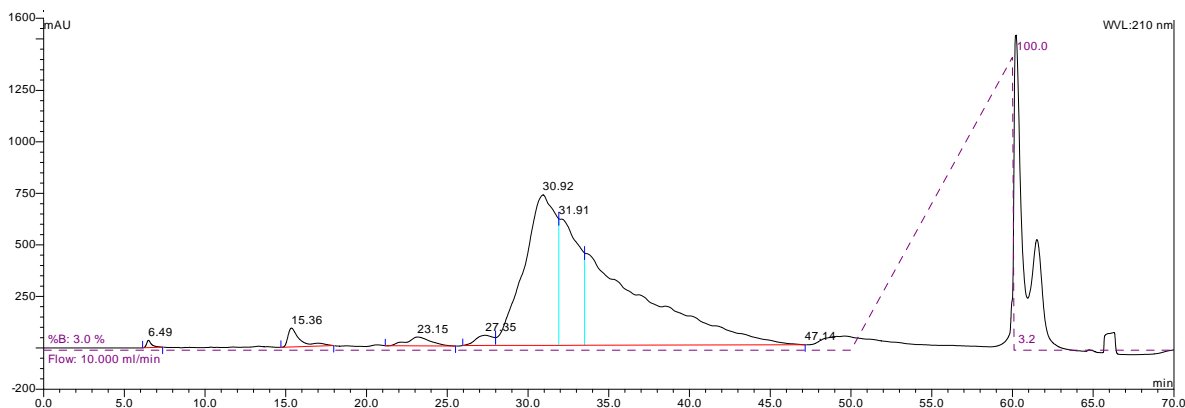


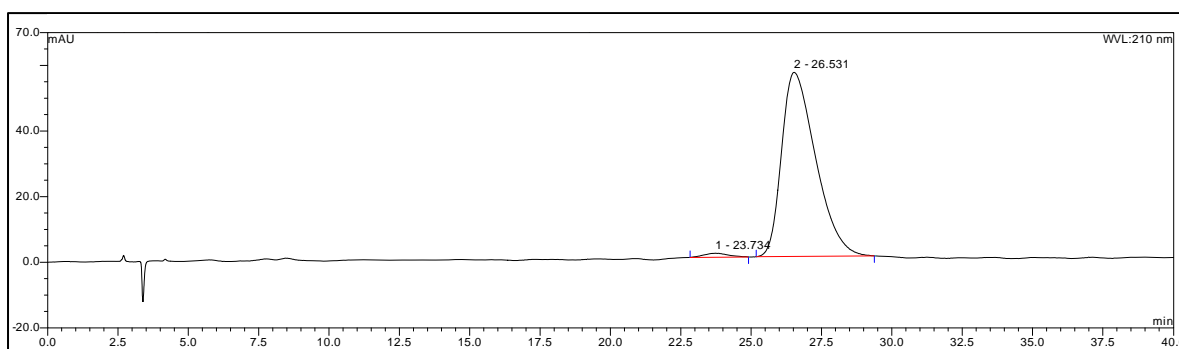
**Figure 8.4.** Analytical HPLC chromatogram of 2COP 2 with 0-5% gradient of MeCN:water (60:40) plus TFA (0.05%) as an elution solvent at 10 ml/min flow rate for 40 minutes: Analytical RP-HPLC (Phenomenex), C<sub>18</sub> with 250 mm × 4.60 mm ID and 10 μm pore size

### 8.1.3 Preparative HPLC and analytical HPLC of 2COP 3



Ret.Time (min)	Area (mAU*min)	Height (mAU)	Rel.Area (%)
6.493	12.9678	35.454	0.27
15.356	81.0607	91.457	1.68
23.147	72.938	42.955	1.51
27.355	61.993	49.589	1.28
30.919	1660.315	729.83	34.38
31.909	859.2431	613.991	17.79
47.143	2081.071	0.008	43.09

**Figure 8.5.** Preparative HPLC chromatogram of 2COP 3 with MeCN (3%) plus TFA (0.05%) as an elution solvent at 10 ml/min flow rate for 50 minutes: Preparative RP-HPLC (Phenomenex), C<sub>18</sub> with 250 mm × 21.2 mm ID and 10 μm pore size



Ret.Time (min)	Area (mAU*min)	Height (mAU)	Rel.Area (%)
23.734	1.237	1.228	1.55
26.531	78.7612	56.096	98.45

**Figure 8.6.** Analytical HPLC chromatogram of 2COP 3 with 3% of MeCN:water (60:40) plus TFA (0.05%) as an elution solvent at 10 ml/min flow rate: Analytical RP-HPLC (Phenomenex), C<sub>18</sub> with 250 mm × 4.60 mm ID and 10 μm pore size



### 8.1.4 Preparative HPLC and analytical HPLC of 2COP 4

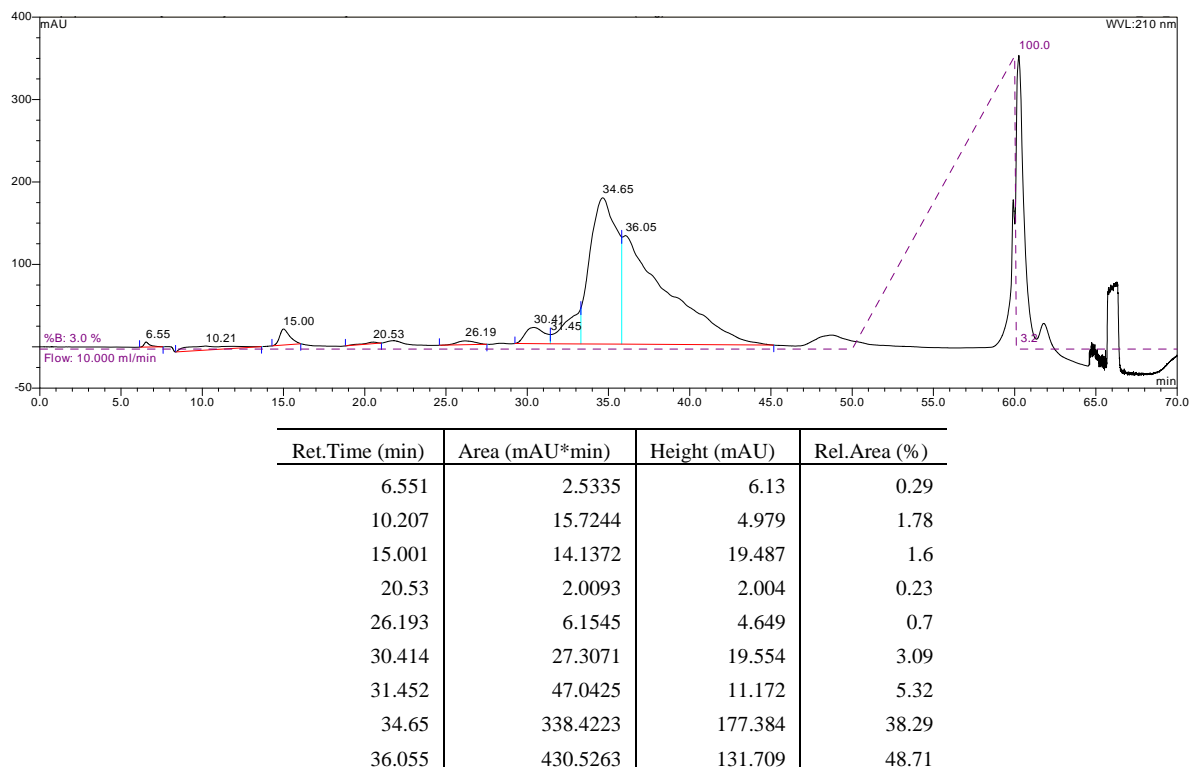


**Figure 8.7.** Preparative HPLC chromatogram of 2COP 4 with MeCN (3%) plus TFA (0.05%) as an elution solvent at 10 ml/min flow rate for 50 minutes: Preparative RP-HPLC (Phenomenex), C<sub>18</sub> with 250 mm × 21.2 mm ID and 10 μm pore size

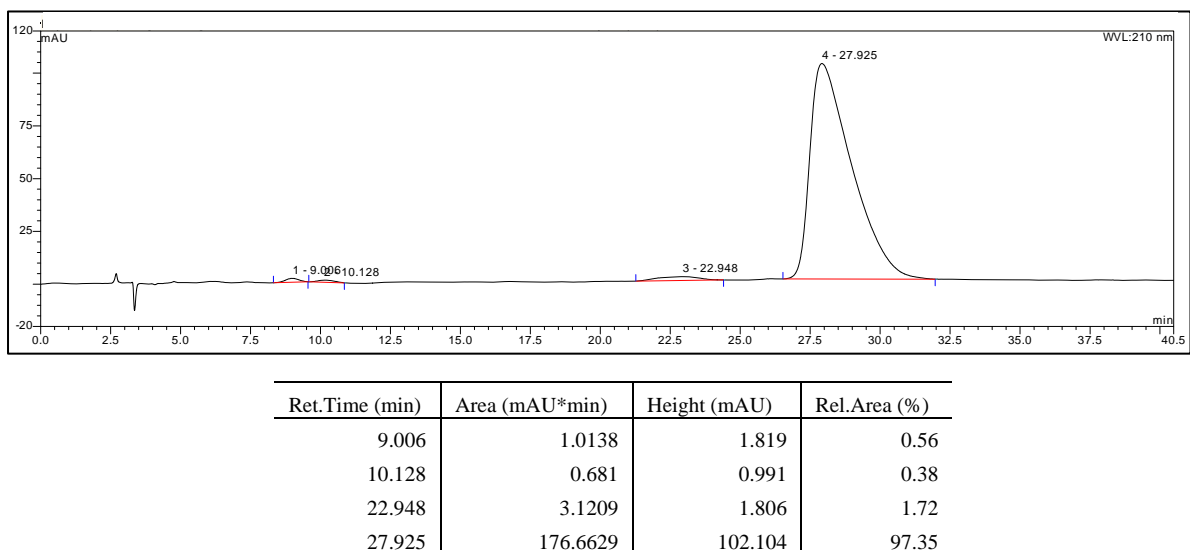


**Figure 8.8.** Analytical HPLC chromatogram of 2COP 4 with 3% of MeCN:water (60:40) plus TFA (0.05%) as an elution solvent at 10 ml/min flow rate: Analytical RP-HPLC (Phenomenex), C<sub>18</sub> with 250 mm × 4.60 mm ID and 10 μm pore size

## 8.1.5 Preparative HPLC and analytical HPLC of 2COP 5

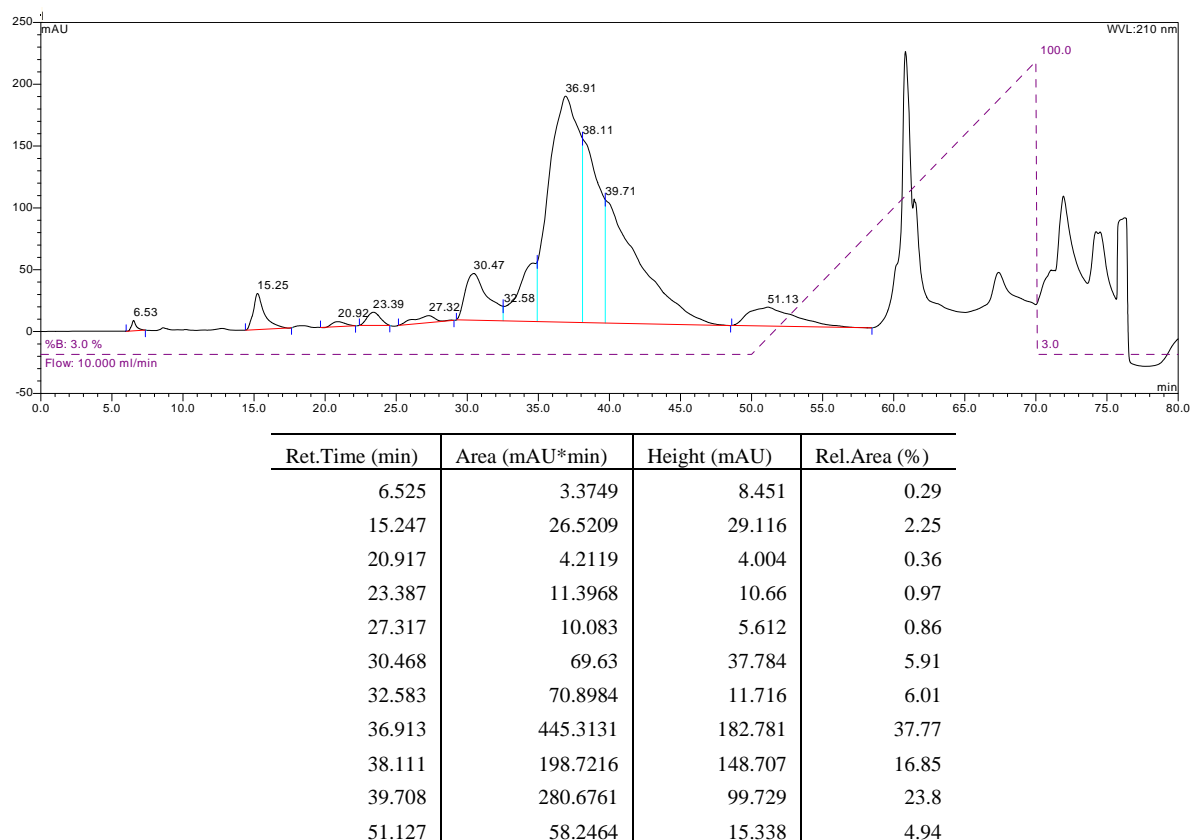
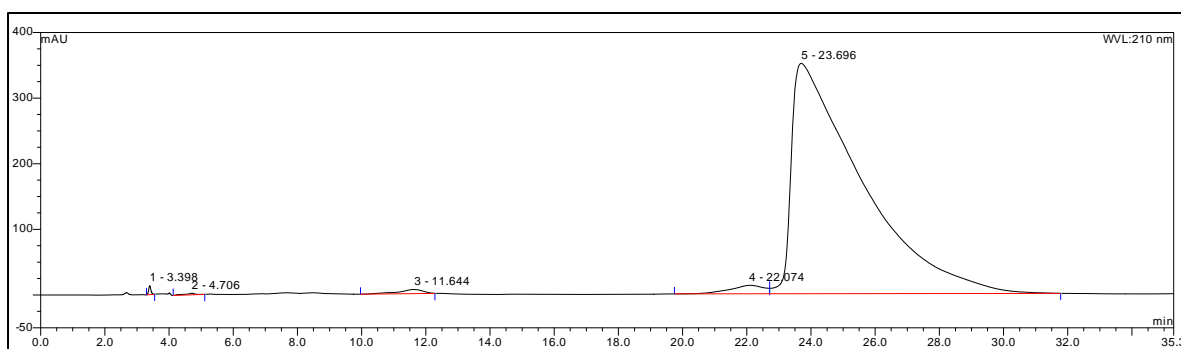


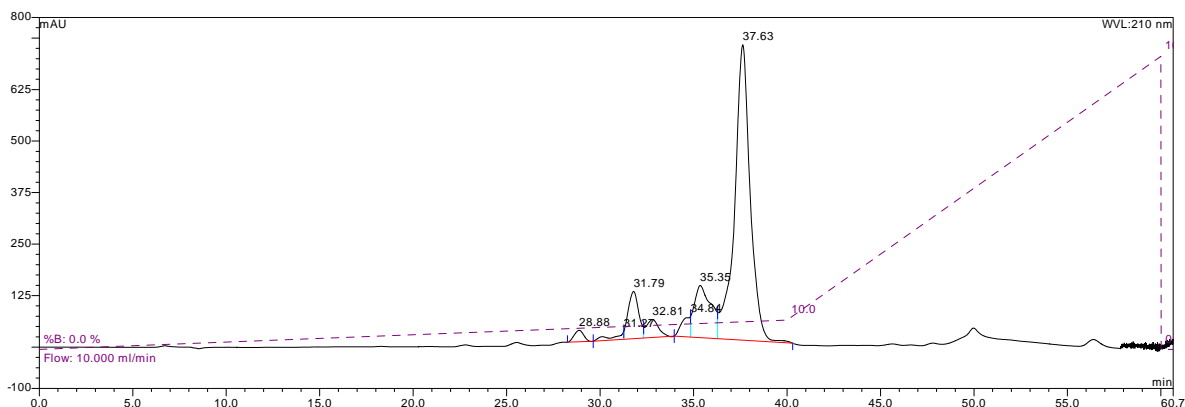
**Figure 8.9.** Preparative HPLC chromatogram of 2COP 5 with MeCN (3%) plus TFA (0.05%) as an elution solvent at 10 ml/min flow rate for 50 minutes: Preparative RP-HPLC (Phenomenex), C<sub>18</sub> with 250 mm × 21.2 mm ID and 10 μm pore size



Ret.Time (min)	Area (mAU*min)	Height (mAU)	Rel.Area (%)
3.398	1.1046	13.563	0.12
4.706	1.0048	2.424	0.11
11.645	5.5597	6.243	0.61
22.074	15.8503	12.839	1.74
23.696	885.4355	350.93	97.41

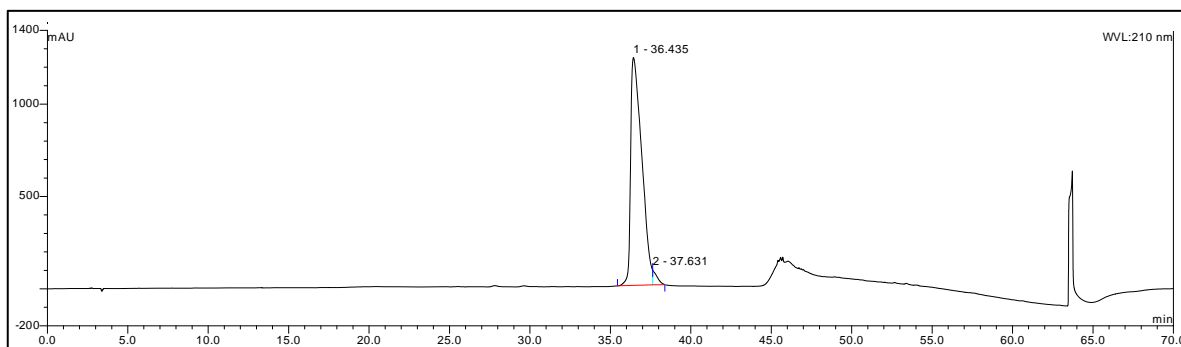
**Figure 8.10. Analytical HPLC chromatogram of 2COP 5 with 3% of MeCN:water (60:40) plus TFA (0.05%) as an elution solvent at 10 ml/min flow rate: Analytical RP-HPLC (Phenomenex), C<sub>18</sub> with 250 mm × 4.60 mm ID and 10 μm pore size**

### 8.1.6 Preparative HPLC and analytical HPLC of 2COP 6



Ret.Time (min)	Area (mAU*min)	Height (mAU)	Rel.Area (%)
28.878	16.1422	27.719	1.63
31.267	11.7999	19.283	1.19
31.793	74.5133	114.364	7.54
32.809	32.5065	43.353	3.29
34.841	26.6092	50.353	2.69
35.351	132.3657	126.6	13.39
37.631	694.6778	716.758	70.27

**Figure 8.11. Preparative HPLC chromatogram of 2COP 6 with the gradient of MeCN (0-10%) plus TFA (0.05%) as an elution solvent at 10 ml/min flow rate for 40 min: Preparative RP-HPLC (Phenomenex), C<sub>18</sub> with 250 mm × 21.2 mm ID and 10 μm pore size**



Ret.Time (min)	Area (mAU*min)	Height (mAU)	Rel.Area (%)
36.435	988.786	1234.293	97.56
37.631	24.7081	80.372	2.44

**Figure 8.12. Analytical HPLC chromatogram of 2COP 6 with 0-10% gradient of MeCN:water (60:40) plus TFA (0.05%) as an elution solvent at 10 ml/min flow rate for 40 minutes: Analytical RP-HPLC (Phenomenex), C<sub>18</sub> with 250 mm × 4.60 mm ID and 10 μm pore size**

### 8.1.7 Preparative HPLC and analytical HPLC of 3COP 7

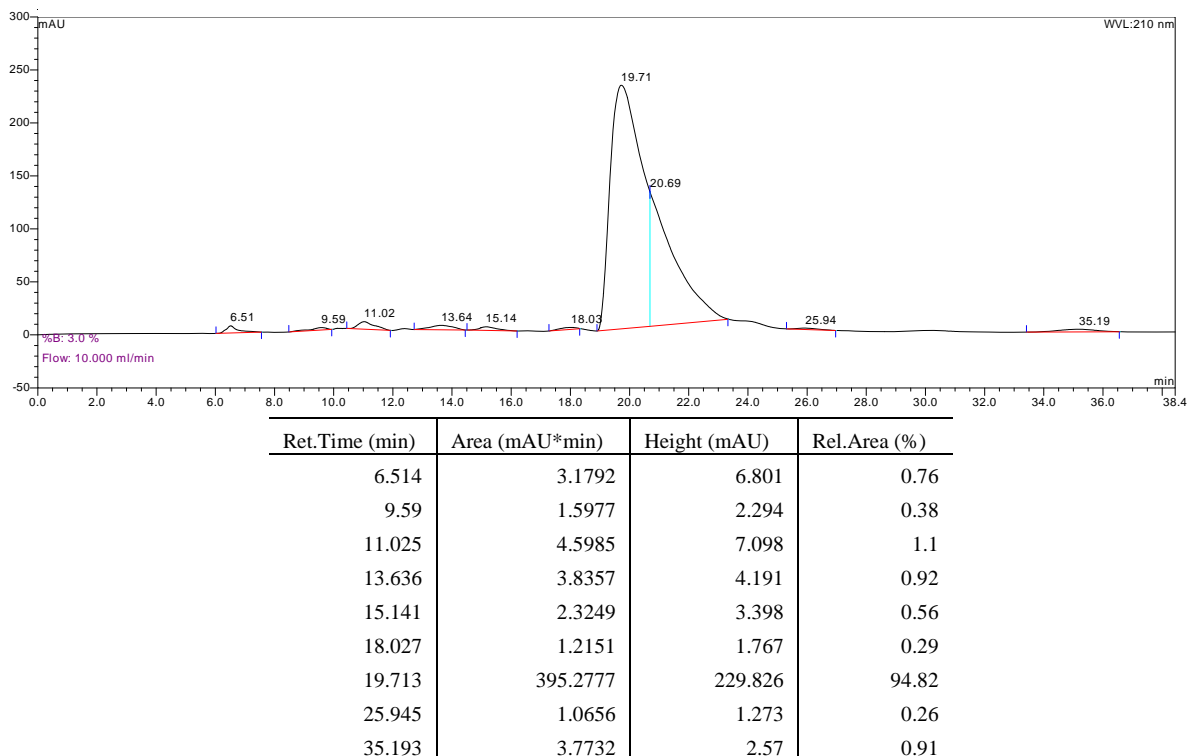


**Figure 8.13. Preparative HPLC chromatogram of 3COP 7 with MeCN (3%) plus TFA (0.05%) as an elution solvent at 10 ml/min flow rate for 50 minutes: Preparative RP-HPLC (Phenomenex), C<sub>18</sub> with 250 mm × 21.2 mm ID and 10 μm pore size**

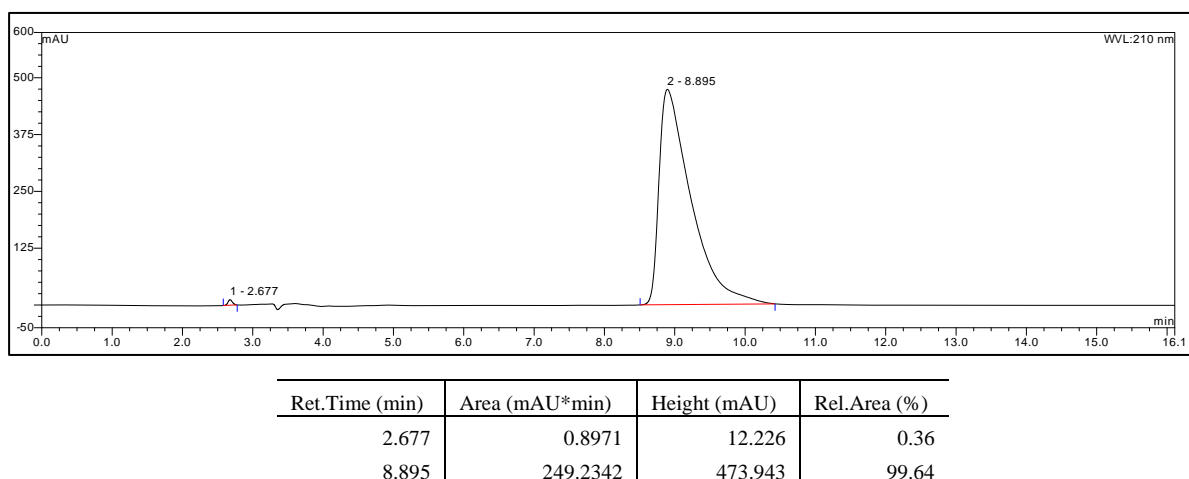
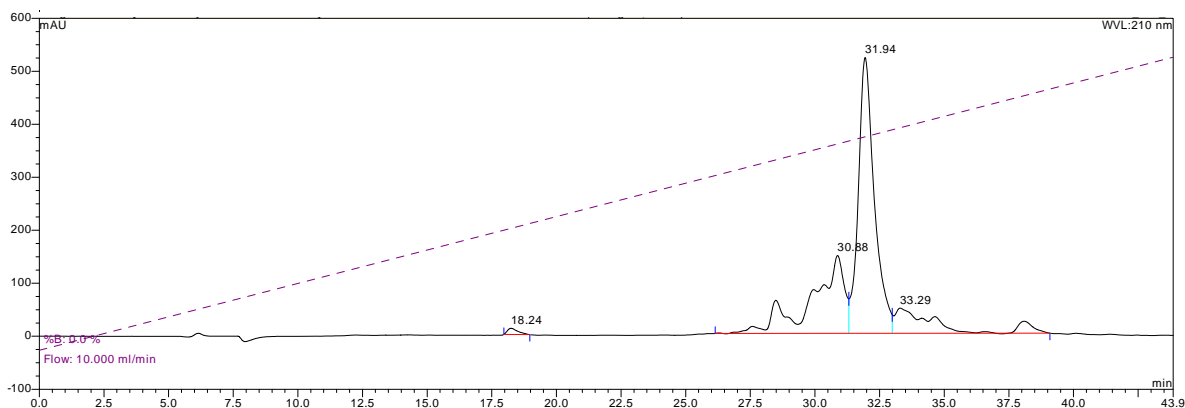


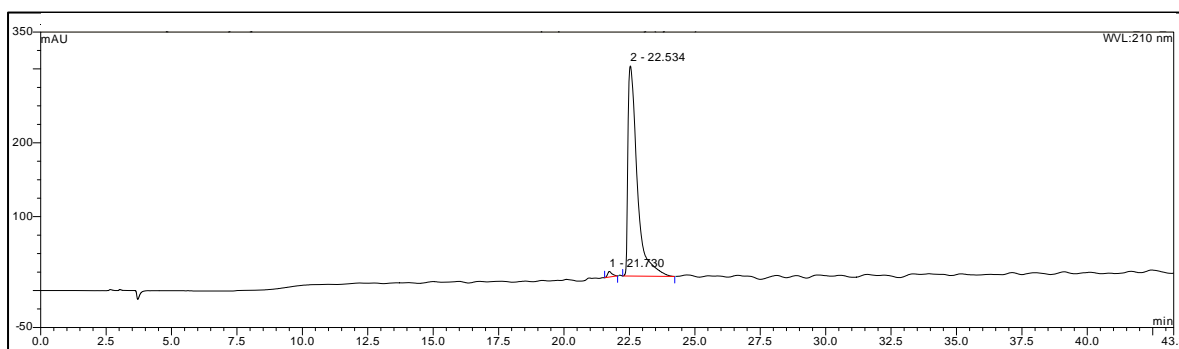
**Figure 8.14. Analytical HPLC chromatogram of 3COP 7 with 3% of MeCN:water (60:40) plus TFA (0.05%) as an elution solvent at 10 ml/min flow rate: Analytical RP-HPLC (Phenomenex), C<sub>18</sub> with 250 mm × 4.60 mm ID and 10 μm pore size**

### 8.1.8 Preparative HPLC and analytical HPLC of TAT



Ret.Time (min)	Area (mAU*min)	Height (mAU)	Rel.Area (%)
18.243	5.4387	11.66	0.8
30.876	212.0514	146.898	31.21
31.94	375.2773	520.296	55.23
33.288	86.6549	47.511	12.75

**Figure 8.15. Preparative HPLC chromatogram of TAT with the gradient of MeCN (0-20%) plus TFA (0.05%) as an elution solvent at 10 ml/min flow rate for 60 min: Preparative RP-HPLC (Phenomenex), C<sub>18</sub> with 250 mm × 21.2 mm ID and 10 μm pore size**



Ret.Time (min)	Area (mAU*min)	Height (mAU)	Rel.Area (%)
21.73	1.5041	7.601	1.27
22.534	116.876	284.337	98.73

**Figure 8.16. Analytical HPLC chromatogram of TAT with 0-20% gradient of MeCN:water (60:40) plus TFA (0.05%) as an elution solvent at 10 ml/min flow rate for 40 minutes: Analytical RP-HPLC (Phenomenex), C<sub>18</sub> with 250 mm × 4.60 mm ID and 10 μm pore size**

## 8.2 $^1\text{H}$ NMR of purified oligopeptides

### 8.2.1 $^1\text{H}$ NMR of purified 2COP 1

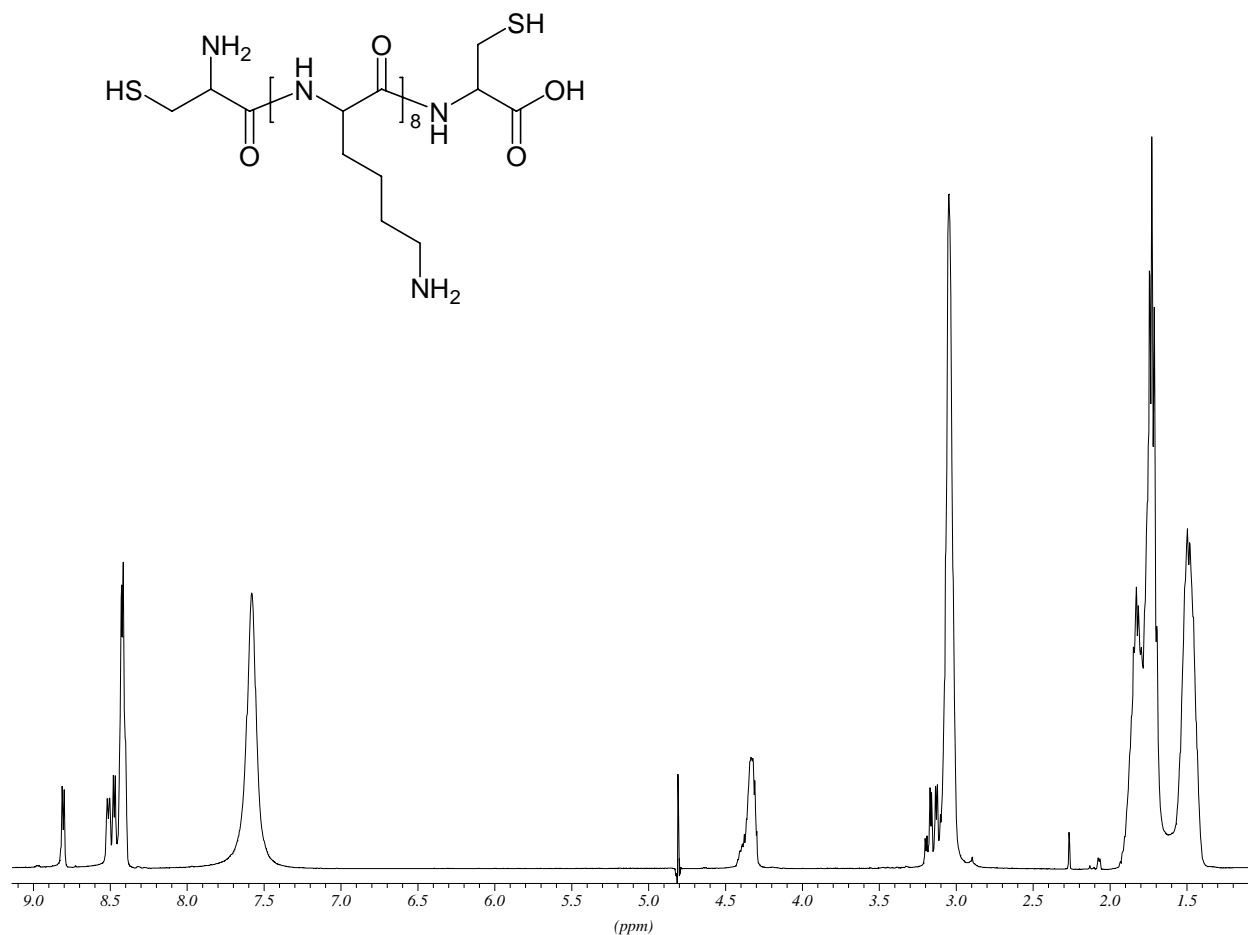


**Figure 8.17.**  $^1\text{H}$  NMR spectra of 2COP 1

$^1\text{H}$  NMR  $\delta$  (ppm) ( $\text{D}_2\text{O}:\text{H}_2\text{O} = 1:9$ ): 4.61 (t,  $J = 5.23\text{Hz}$ , 1H, -CO-CH-N-), 4.36-4.24 (m, 9H, -CO-CH-N-), 2.98 (t,  $J = 6.99\text{ Hz}$ , 20H, CH-C<sub>3</sub>H<sub>6</sub>-CH<sub>2</sub>-NH<sub>2</sub>, -CH<sub>2</sub>-SH), 1.79-1.66 (m, 32H, CH-CH<sub>2</sub>-CH<sub>2</sub>-CH<sub>2</sub>-CH<sub>2</sub>-NH<sub>2</sub>, CH-CH<sub>2</sub>-CH<sub>2</sub>-CH<sub>2</sub>-CH<sub>2</sub>-NH<sub>2</sub>), 1.45-1.42 (m, 16H, CH-CH<sub>2</sub>-CH<sub>2</sub>-CH<sub>2</sub>-CH<sub>2</sub>-NH<sub>2</sub>)

## 8.2.2 $^1\text{H}$ NMR of purified 2COP 2

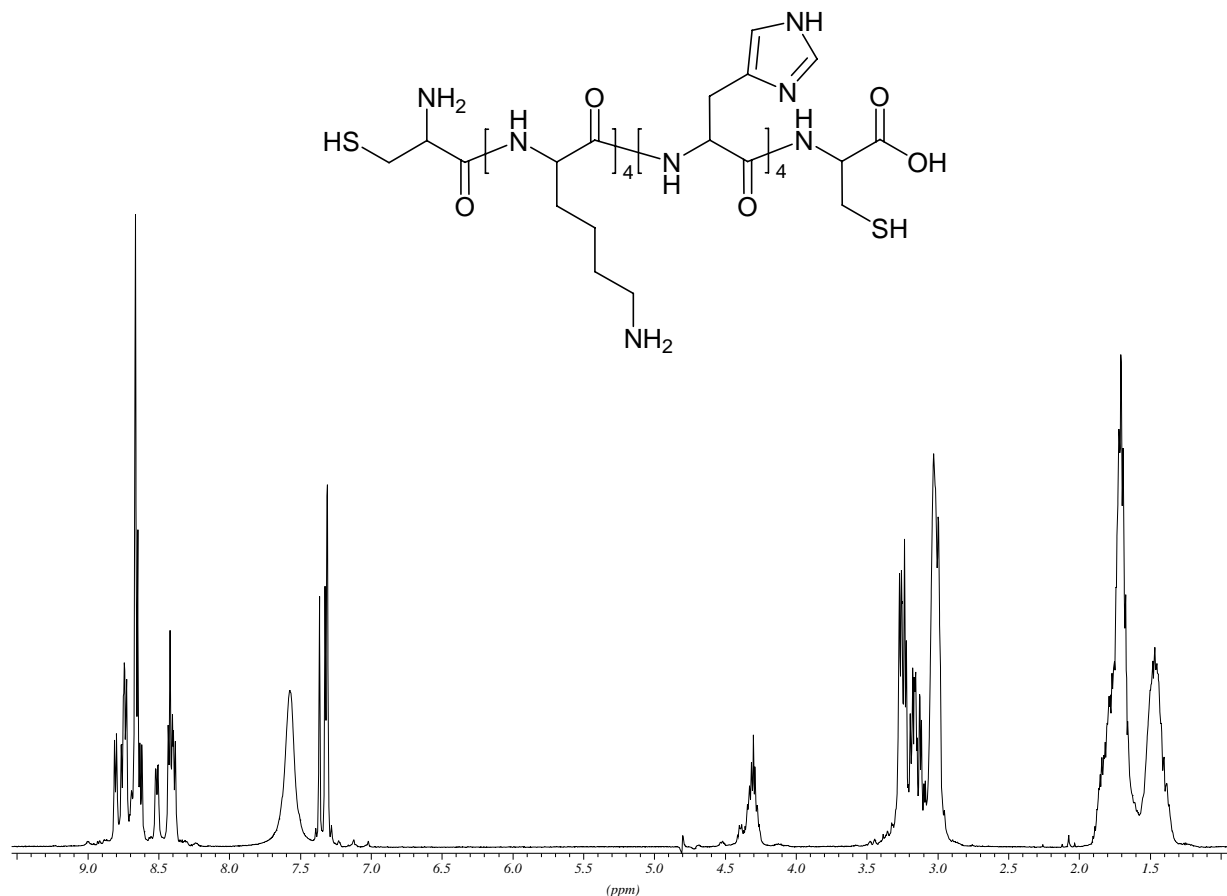


**Figure 8.18.**  $^1\text{H}$  NMR spectra of 2COP 2

$^1\text{H}$  NMR  $\delta$  (ppm) ( $\text{D}_2\text{O}:\text{H}_2\text{O} = 1:9$ ): 8.63-8.61 (m, 4H, Im,  $-\text{N}=\text{C}\underline{\text{H}}-\text{NH}-$ ), 7.32-7.27 (m, 4H, Im,  $-\text{C}-\text{CH}-\text{N}-$ ), 4.69-4.63 (m, 4H,  $-\text{CO}-\text{C}\underline{\text{H}}-\text{N}-$ ), 4.54 (t, 1H,  $J = 5.73$  Hz,  $-\text{CO}-\text{C}\underline{\text{H}}-\text{N}-$ ), 4.35 (t,  $J = 5.73$  Hz, 1H,  $-\text{CO}-\text{C}\underline{\text{H}}-\text{N}-$ ), 4.33-4.21 (m, 4H,  $-\text{CO}-\text{C}\underline{\text{H}}-\text{N}-$ ), 3.21-3.10 (m, 10H,  $-\text{NH}-\text{CH}-\text{C}\underline{\text{H}}_2-$ ,  $-\text{C}\underline{\text{H}}_2-\text{SH}$ ), 3.07-2.92 (m, 10H,  $\text{CH}-\text{C}_3\text{H}_6$ ,  $\text{C}\underline{\text{H}}_2-\text{NH}_2$ ,  $-\text{C}\underline{\text{H}}_2-\text{SH}$ ), 1.74-1.66 (m, 16H,  $\text{CH}-\text{C}\underline{\text{H}}_2-\text{CH}_2-\text{CH}_2-\text{CH}_2-\text{NH}_2$ ,  $\text{CH}-\text{CH}_2-\text{CH}_2-\text{C}\underline{\text{H}}_2-\text{CH}_2-\text{NH}_2$ ), 1.45-1.38 (m, 8H,  $\text{CH}-\text{CH}_2-\text{C}\underline{\text{H}}_2-\text{CH}_2-\text{CH}_2-\text{NH}_2$ )



### 8.2.3 $^1\text{H}$ NMR of purified 2COP 3

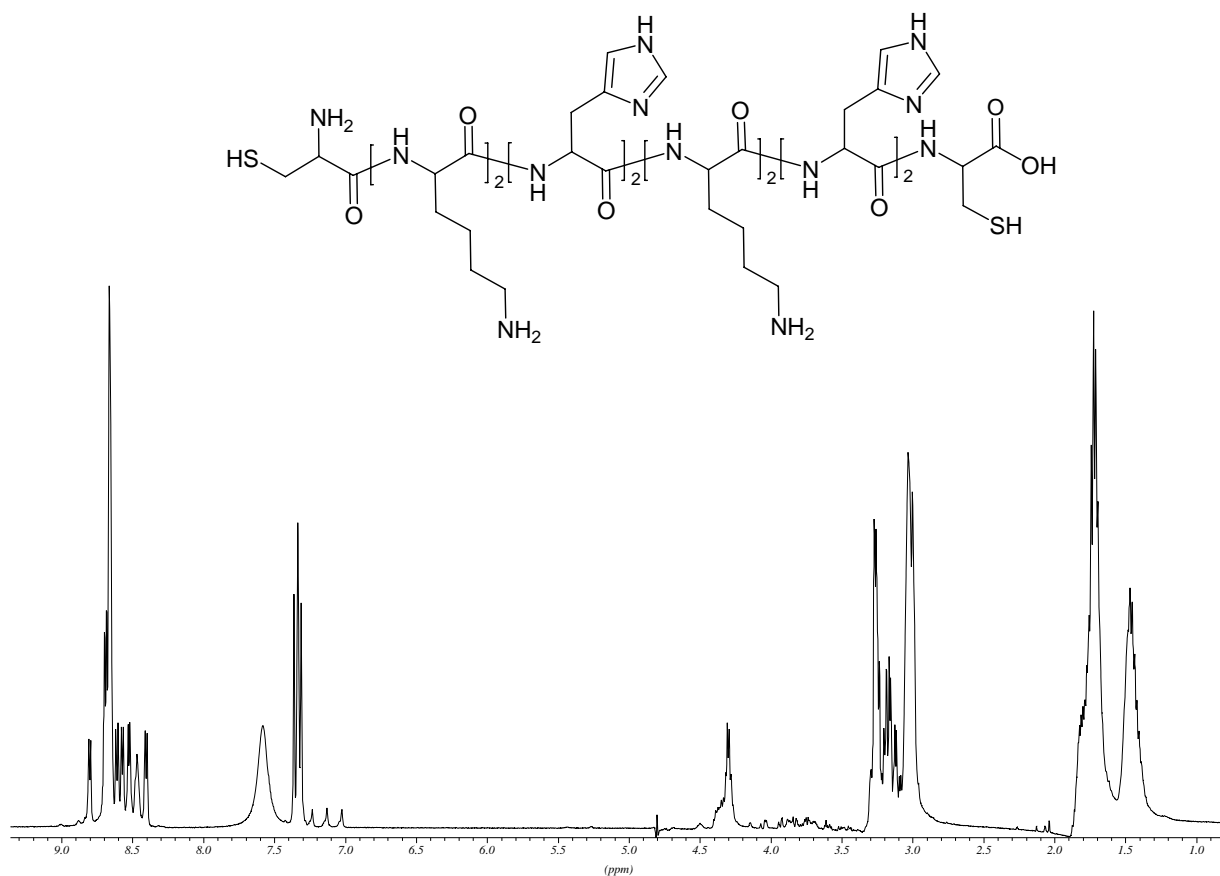


**Figure 8.19.**  $^1\text{H}$  NMR spectra of 2COP 3

$^1\text{H}$  NMR  $\delta$  (ppm) ( $\text{D}_2\text{O}:\text{H}_2\text{O} = 1:9$ ): 8.63-8.62 (m, 4H, Im,  $-\text{N}=\text{CH}-\text{NH}-$ ), 7.31-7.26 (m, 4H, Im,  $-\text{C}-\text{CH}-\text{N}-$ ), 4.67-4.64 (m, 4H,  $-\text{CO}-\text{CH}-\text{N}-$ ), 4.49 (t, 1H,  $J = 5.59$  Hz,  $-\text{CO}-\text{CH}-\text{N}-$ ), 4.34-4.21 (m, 5H,  $-\text{CO}-\text{CH}-\text{N}-$ ), 3.25-3.10 (m, 10H,  $-\text{NH}-\text{CH}-\text{CH}_2-$ ,  $-\text{CH}_2-\text{SH}$ ), 3.08-2.89 (m, 10H,  $\text{CH}-\text{C}_3\text{H}_6-\text{CH}_2-\text{NH}_2$ ,  $-\text{CH}_2-\text{SH}$ ), 1.77-1.65 (m, 16H,  $\text{CH}-\text{CH}_2-\text{CH}_2-\text{CH}_2-\text{CH}_2-\text{NH}_2$ ,  $\text{CH}-\text{CH}_2-\text{CH}_2-\text{CH}_2-\text{CH}_2-\text{NH}_2$ ), 1.45-1.35 (m, 8H,  $\text{CH}-\text{CH}_2-\text{CH}_2-\text{CH}_2-\text{CH}_2-\text{NH}_2$ )

## 8.2.4 $^1\text{H}$ NMR of purified 2COP 4

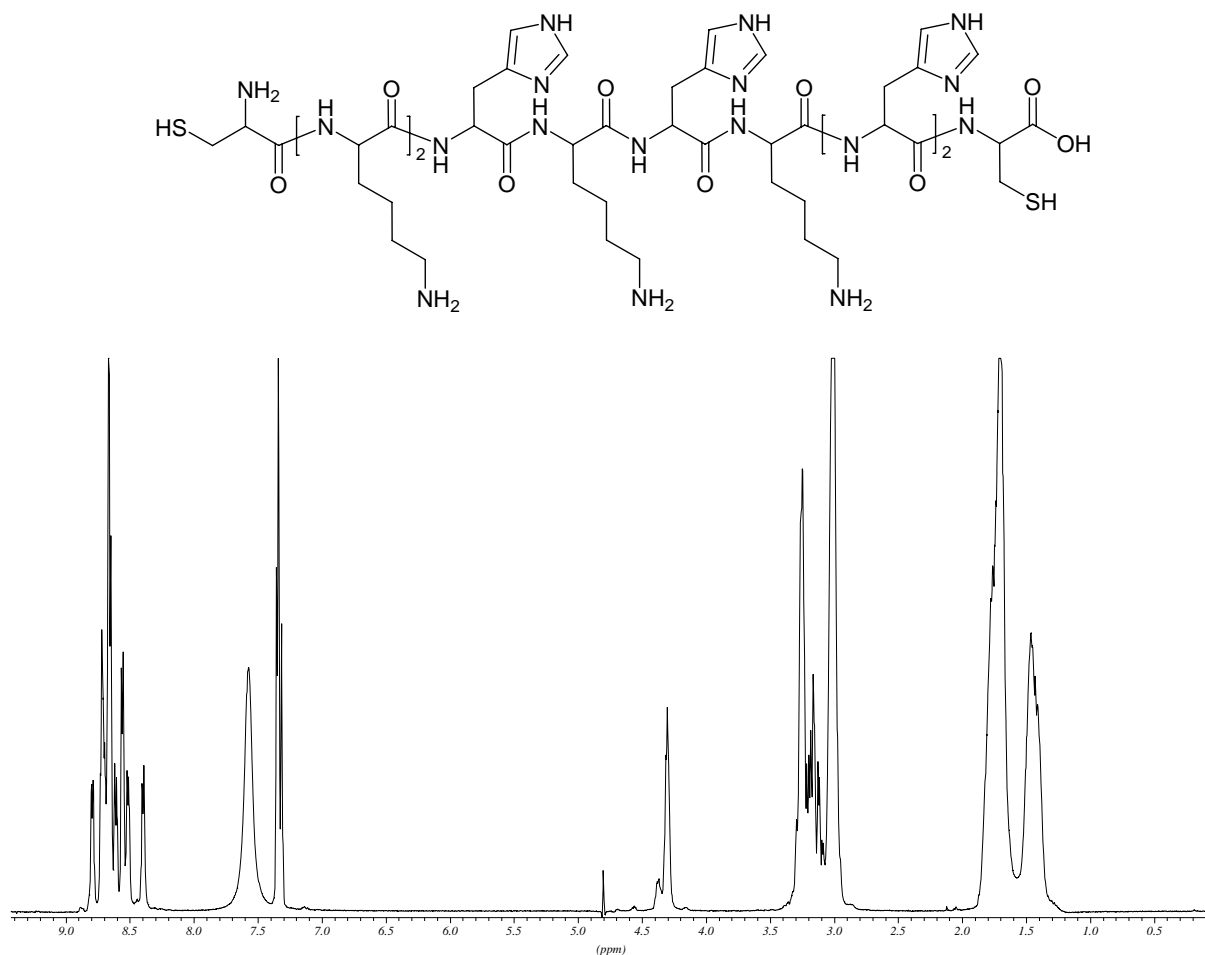


**Figure 8.20.**  $^1\text{H}$  NMR spectra of 2COP 4

$^1\text{H}$  NMR  $\delta$  (ppm) ( $\text{D}_2\text{O}:\text{H}_2\text{O} = 1:9$ ): 8.64-8.62 (m, 4H, im,  $-\text{N}=\text{CH}-\text{NH}-$ ), 7.32-7.28 (m, 4H, im,  $-\text{C}-\text{CH}-\text{N}-$ ), 4.69-4.63 (m, 4H,  $-\text{CO}-\text{CH}-\text{N}-$ ), 4.53 (t, 1H,  $J = 5.66$  Hz,  $-\text{CO}-\text{CH}-\text{N}-$ ), 4.35 (m, 1H,  $-\text{CO}-\text{CH}-\text{N}-$ ), 4.33-4.27 (m, 4H,  $-\text{CO}-\text{CH}-\text{N}-$ ), 3.26-3.03 (m, 10H,  $-\text{NH}-\text{CH}-\text{CH}_2-$ ,  $-\text{CH}_2-\text{SH}$ ), 2.98-2.90 (m, 10H,  $\text{CH}-\text{C}_3\text{H}_6-\text{CH}_2-\text{NH}_2$ ,  $-\text{CH}_2-\text{SH}$ ), 1.76-1.65 (m, 32H,  $\text{CH}-\text{CH}_2-\text{CH}_2-\text{CH}_2-\text{CH}_2-\text{NH}_2$ ,  $\text{CH}-\text{CH}_2-\text{CH}_2-\text{CH}_2-\text{CH}_2-\text{NH}_2$ ), 1.43-1.35 (m, 8H,  $\text{CH}-\text{CH}_2-\text{CH}_2-\text{CH}_2-\text{CH}_2-\text{NH}_2$ )

## 8.2.5 $^1\text{H}$ NMR of purified 2COP 5

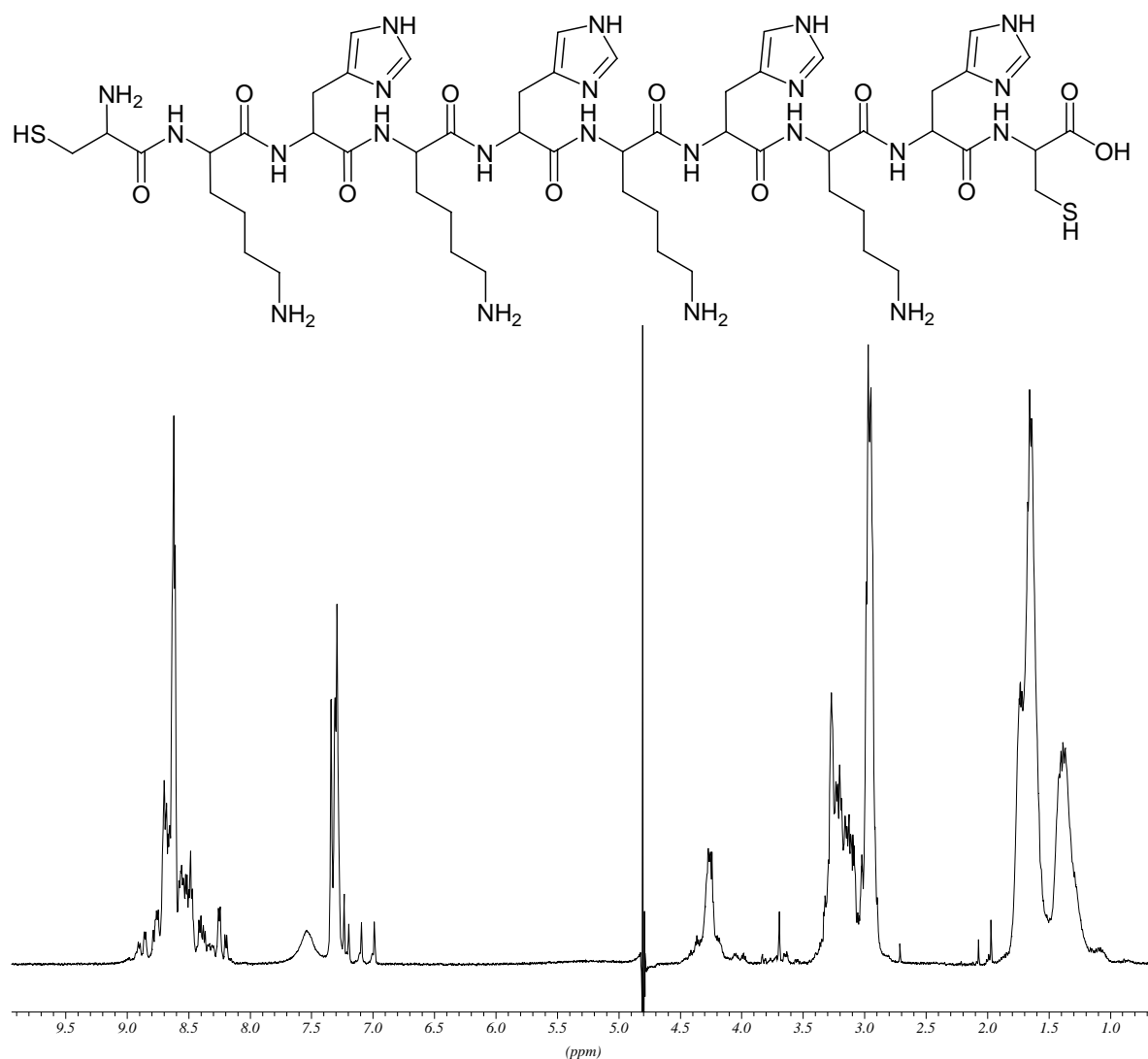


**Figure 8.21.**  $^1\text{H}$  NMR spectra of 2COP 5

$^1\text{H}$  NMR  $\delta$  (ppm) ( $\text{D}_2\text{O}:\text{H}_2\text{O} = 1:9$ ): 8.64-8.63 (m, 4H, Im,  $-\text{N}=\text{CH}-\text{NH}-$ ), 7.34-7.30 (m, 4H, Im,  $-\text{C}-\text{CH}-\text{N}-$ ), 4.69-4.63 (m, 4H,  $-\text{CO}-\text{CH}-\text{N}-$ ), 4.55 (t, 1H,  $J = 5.62$  Hz,  $-\text{CO}-\text{CH}-\text{N}-$ ), 4.33-4.24 (m, 5H,  $-\text{CO}-\text{CH}-\text{N}-$ ), 3.22-3.07 (m, 10H,  $-\text{NH}-\text{CH}-\text{CH}_2-$ ,  $-\text{CH}_2-\text{SH}$ ), 3.01-2.94 (m, 10 H,  $\text{CH}-\text{C}_3\text{H}_6-\text{CH}_2-\text{NH}_2$ ,  $-\text{CH}_2-\text{SH}$ ), 1.74-1.64 (m, 16H,  $-\text{CH}-\text{CH}_2-\text{CH}_2-\text{CH}_2-\text{NH}_2$ ,  $-\text{CH}-\text{CH}_2-\text{CH}_2-\text{CH}_2-\text{CH}_2-\text{NH}_2$ ), 1.45-1.38 (m, 8H,  $-\text{CH}-\text{CH}_2-\text{CH}_2-\text{CH}_2-\text{CH}_2-\text{NH}_2$ )

## 8.2.6 $^1\text{H}$ NMR of purified 2COP 6

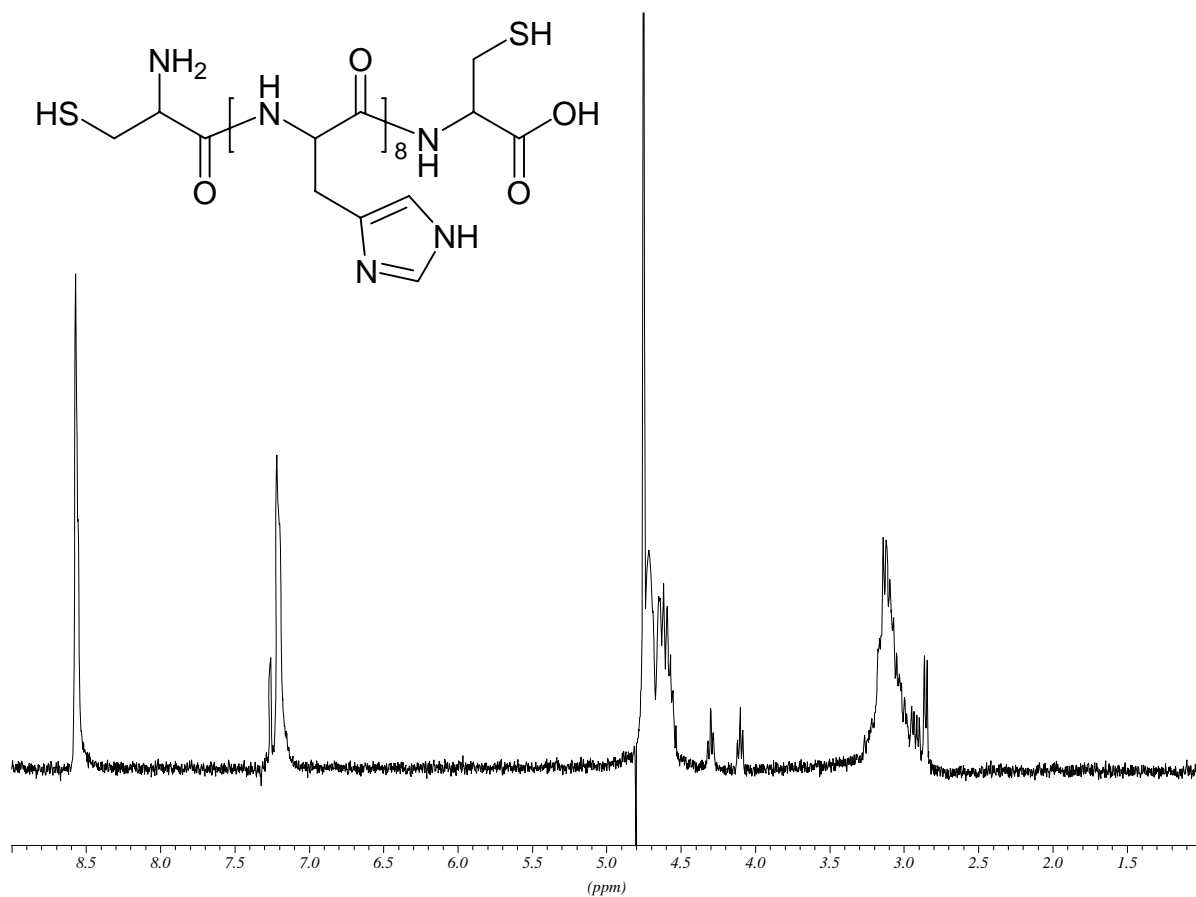
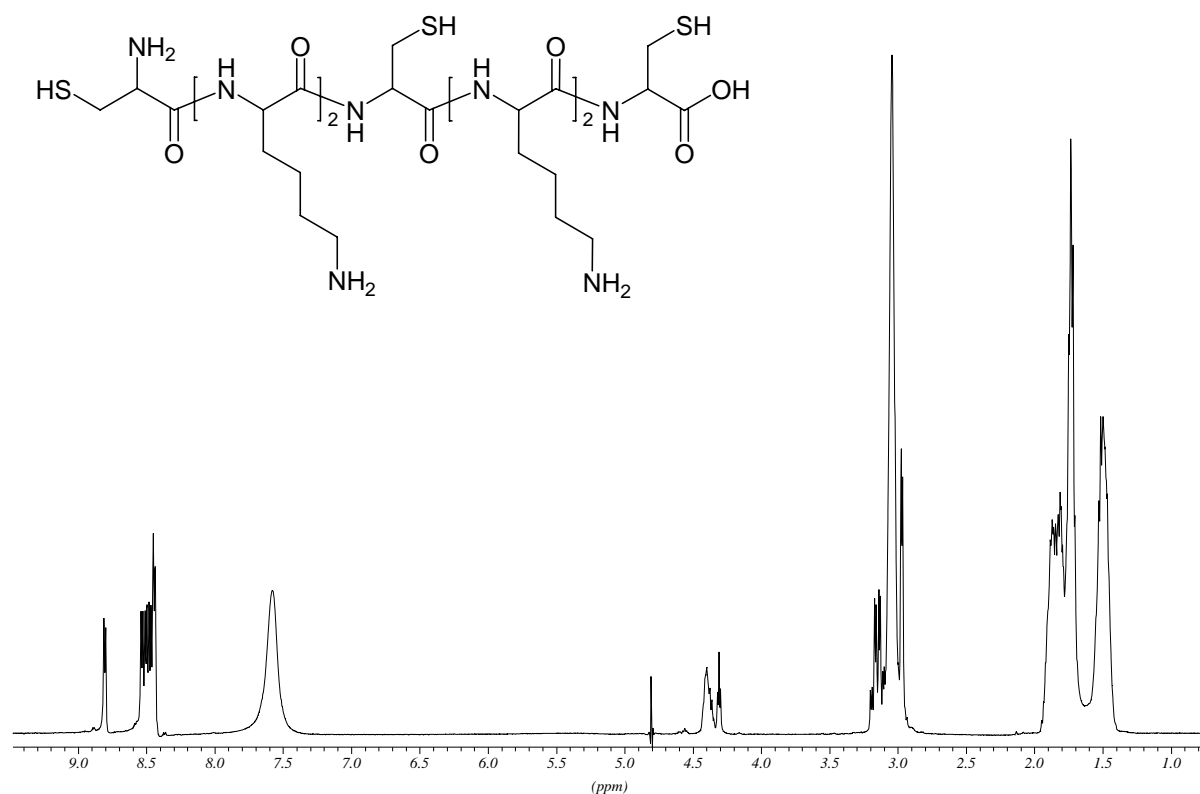


Figure 8.22.  $^1\text{H}$  NMR spectra of 2COP 6

$^1\text{H}$  NMR  $\delta$  (ppm) ( $\text{D}_2\text{O}$ ): 8.64-8.63 (m, 8H, Im,  $-\text{N}=\text{CH}-\text{NH}-$ ), 7.28-7.26 (m, 8H, Im,  $-\text{C}-\text{CH}-\text{N}-$ ), 4.73-4.63 (m, 8H,  $-\text{CO}-\text{CH}-\text{N}-$ ), 4.45 (t, 1H,  $J = 5.38$  Hz,  $-\text{CO}-\text{CH}-\text{N}-$ ), 4.17 (t,  $J = 5.37$  Hz, 1H,  $-\text{CO}-\text{CH}-\text{N}-$ ), 3.00-2.84 (m, 20H,  $-\text{NH}-\text{CH}-\text{CH}_2-$ ,  $-\text{CH}_2-\text{SH}$ )

## 8.2.7 $^1\text{H}$ NMR of purified 3COP 7



**Figure 8.23.**  $^1\text{H}$  NMR spectra of 3COP 7

$^1\text{H}$  NMR  $\delta$  (ppm) ( $\text{D}_2\text{O}:\text{H}_2\text{O} = 1:9$ ): 4.54-4.49 (m, 2H, -CO-CH<sub>2</sub>-N-), 4.36-4.31 (m, 4H, -CO-CH<sub>2</sub>-N-), 3.13-2.90 (m, 14H, CH-C<sub>3</sub>H<sub>6</sub>-CH<sub>2</sub>-NH<sub>2</sub>, -CH<sub>2</sub>-SH), 1.81-1.66 (m, 16H, CH-CH<sub>2</sub>-CH<sub>2</sub>-CH<sub>2</sub>-CH<sub>2</sub>-NH<sub>2</sub>, CH-CH<sub>2</sub>-CH<sub>2</sub>-CH<sub>2</sub>-CH<sub>2</sub>-NH<sub>2</sub>), 1.45-1.42 (m, 8H, CH-CH<sub>2</sub>-CH<sub>2</sub>-CH<sub>2</sub>-CH<sub>2</sub>-NH)

## 8.2.8 $^1\text{H}$ NMR of purified TAT

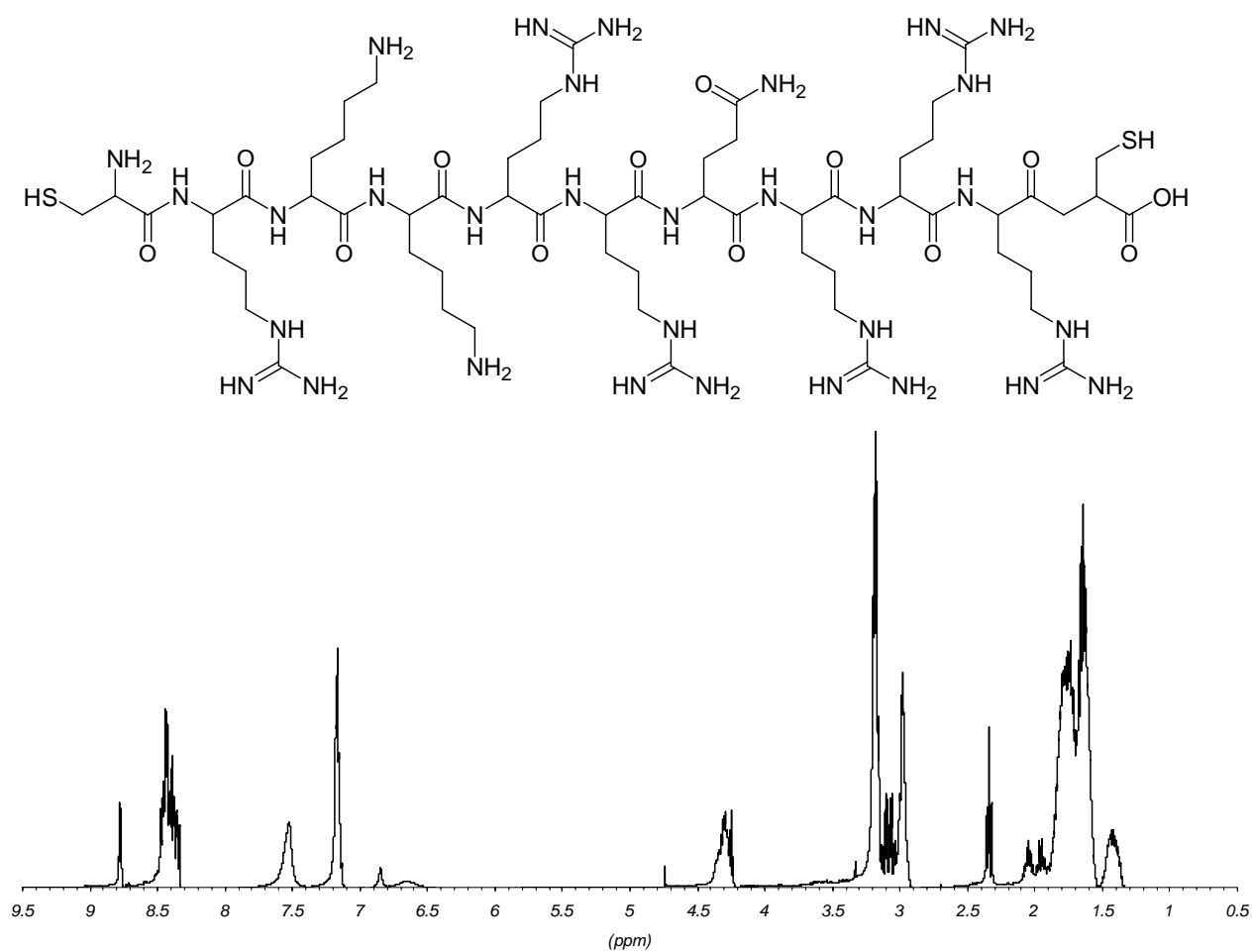


**Figure 8.24.**  $^1\text{H}$  NMR spectra of TAT

$^1\text{H}$  NMR  $\delta$  (ppm) ( $\text{D}_2\text{O}:\text{H}_2\text{O}=1:9$ ): 8.78 (d,  $J = 6.41$  Hz, 1H,  $-\text{CH}-\text{CO}-\text{NH}-$ ), 8.48 (m, 9H,  $-\text{CH}-\text{CO}-\text{NH}-$ ), 7.52 (m, 4H,  $-\text{CH}-\text{CH}_2-\text{CH}_2-\text{CH}_2-\text{NH}_2$ ), 7.18-7.16 (m, 6H,  $-\text{CH}-\text{CH}_2-\text{CH}_2-\text{CH}_2-\text{NH}-\text{CNH}-\text{NH}_2$ ,  $-\text{N}-\text{CH}-\text{CH}_2-\text{NH}_2$ ), 4.34-4.24 (m, 4H,  $-\text{CO}-\text{CH}-\text{N}-$ ), 3.20-3.16 (m, 12H,  $-\text{CH}-\text{CH}_2-\text{CH}_2-\text{CH}_2-\text{NH}-\text{CNH}-\text{NH}_2$ ), 3.10 (dq, 2H,  $J = 17.42$  Hz, 5.50 Hz,  $-\text{N}-\text{CH}-\text{CH}_2-\text{SH}$ ), 3.04-2.98 (m, 6H,  $-\text{CH}-\text{CH}_2-\text{CH}_2-\text{CH}_2-\text{CH}_2-\text{NH}_2$ ,  $-\text{N}-\text{CH}-\text{CH}_2-\text{SH}$ ), 2.34 (t,  $J = 8.14$  Hz, 2H,  $-\text{CH}-\text{CH}_2-\text{CH}_2-\text{CO}-\text{NH}_2$ ), 2.06-1.92 (m, 2H,  $-\text{CH}-\text{CH}_2-\text{CH}_2-\text{CO}-\text{NH}_2$ ), 1.82-1.61 (m, 32H,  $\text{CH}-\text{CH}_2-\text{CH}_2-\text{CH}_2-\text{CH}_2-\text{NH}_2$ ,  $-\text{CH}-\text{CH}_2-\text{CH}_2-\text{CH}_2-\text{NH}-\text{CNH}-\text{NH}_2$ ), 1.44-1.36 (m, 4H,  $\text{CH}-\text{CH}_2-\text{CH}_2-\text{CH}_2-\text{CH}_2-\text{NH}_2$ )

### 8.3 Samples of $^1\text{H}$ NMR spectra at different pH in NMR titration experiments of 2COPs

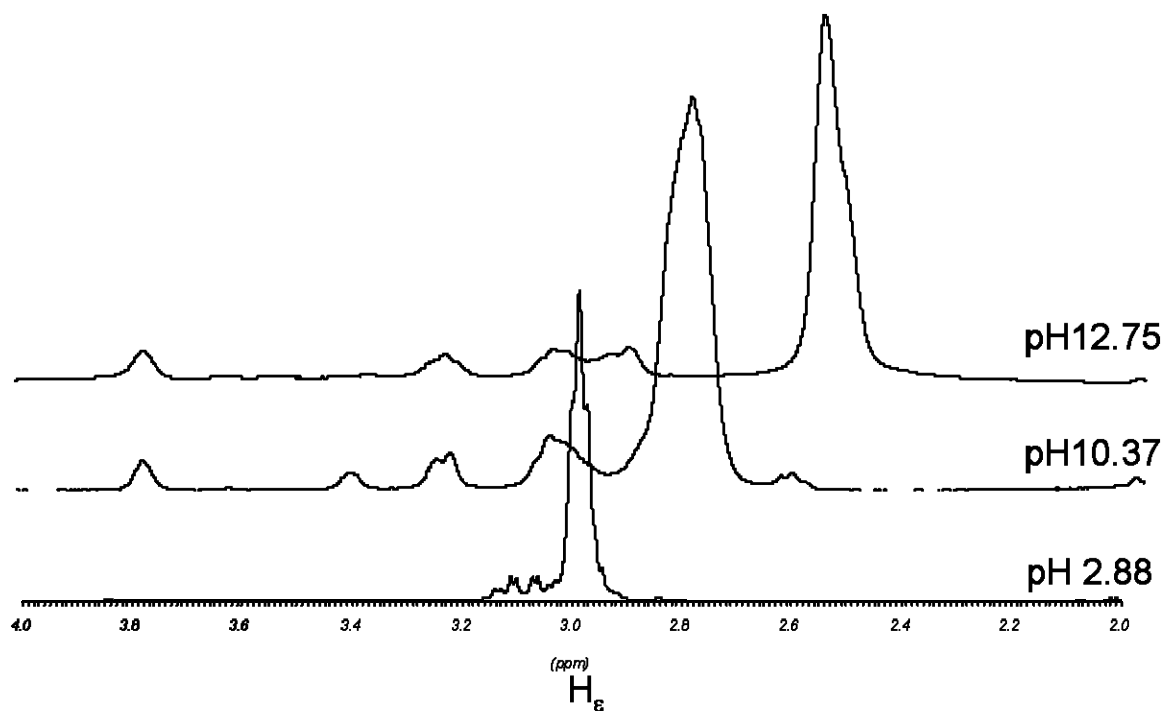


Figure 8.25.  $^1\text{H}$  NMR spectra of  $\text{H}_\epsilon$  of 2COP 1 at pH 2.88, 10.37 and 12.75

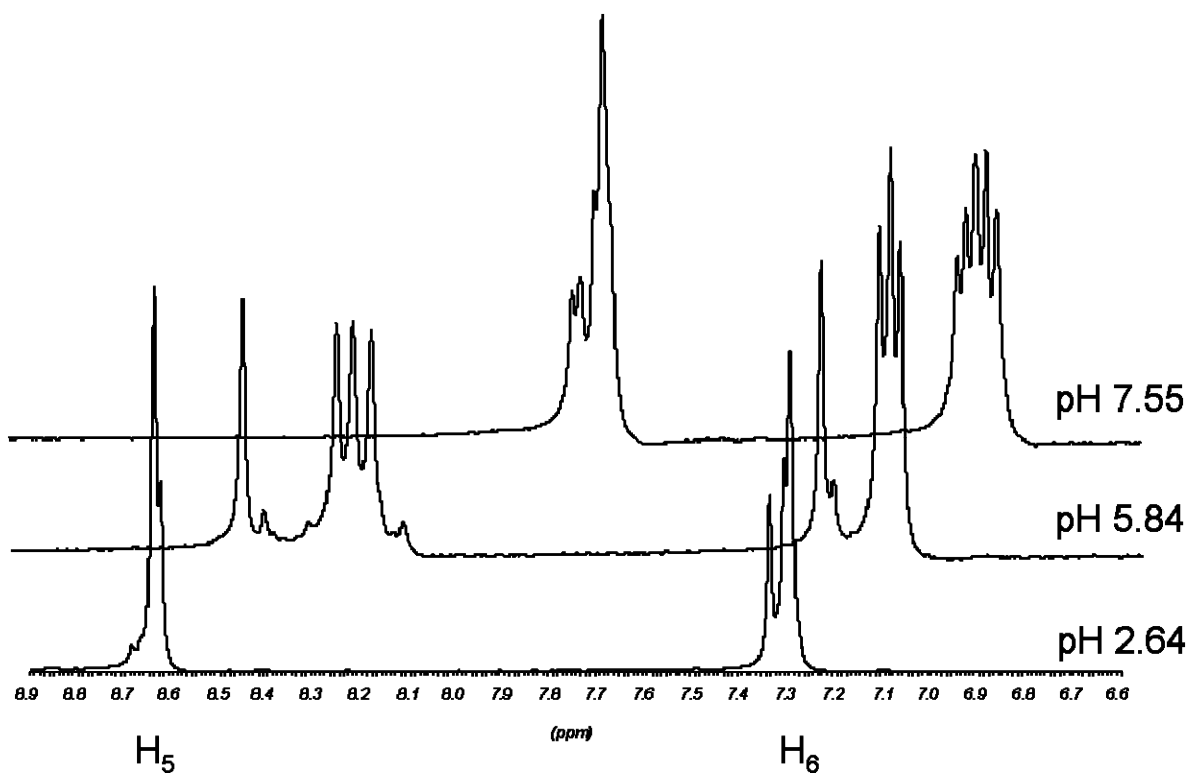


Figure 8.26.  $^1\text{H}$  NMR spectra of  $\text{H}_5$  and  $\text{H}_6$  of 2COP 5 at pH 2.64, 5.84 and 7.55

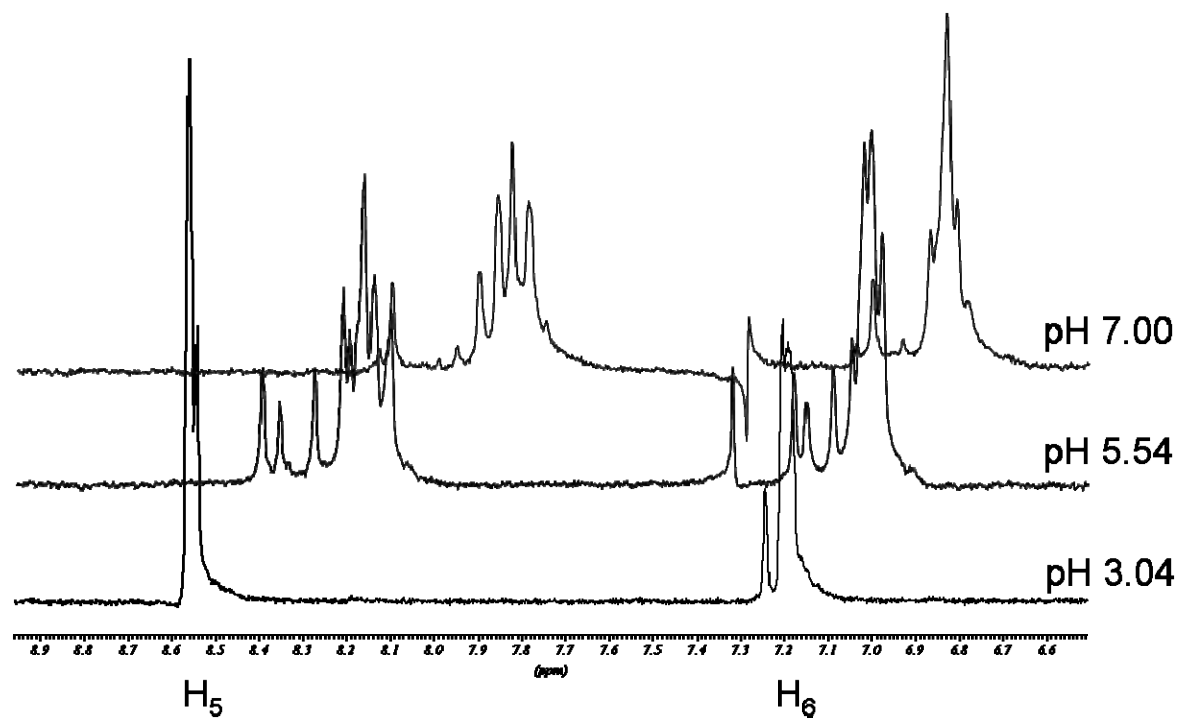
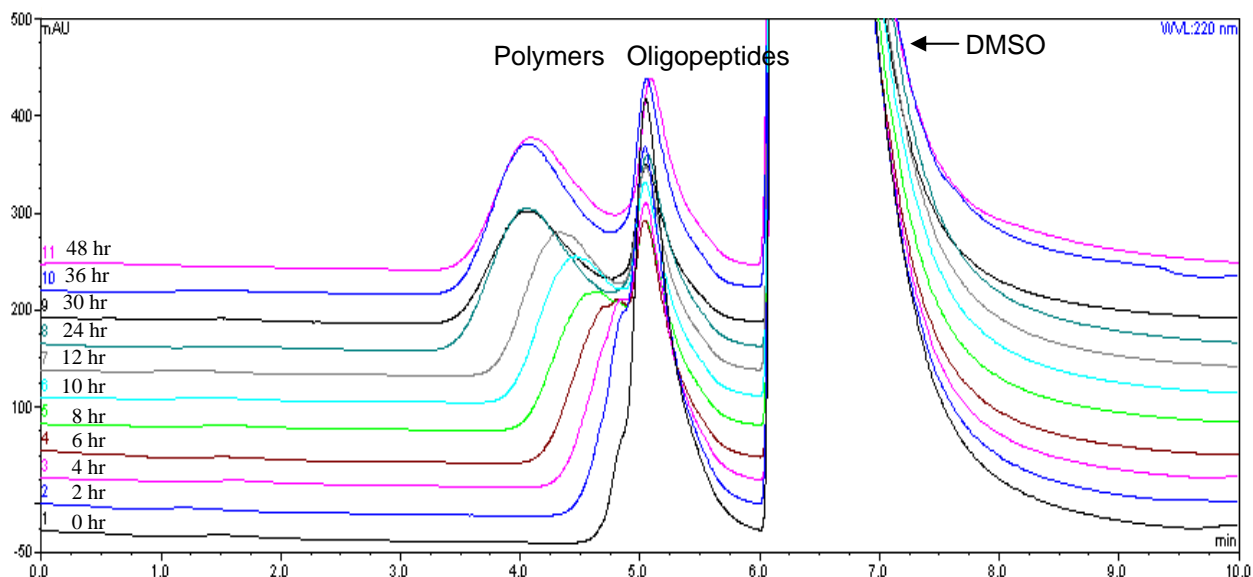


Figure 8.27.  $^1\text{H}$  NMR spectra of  $\text{H}_5$  and  $\text{H}_6$  of 2COP 6 at pH 3.04, 5.54 and 7.00



## 8.4 Samples of GPC chromatograms in oxidative polymerization experiments



**Figure 8.28.** Comparison of the chromatogram of the oxidative polymerization of 2COP 1 at 30 mM concentration incubated at ambient for 48 hr analyzed by GPC

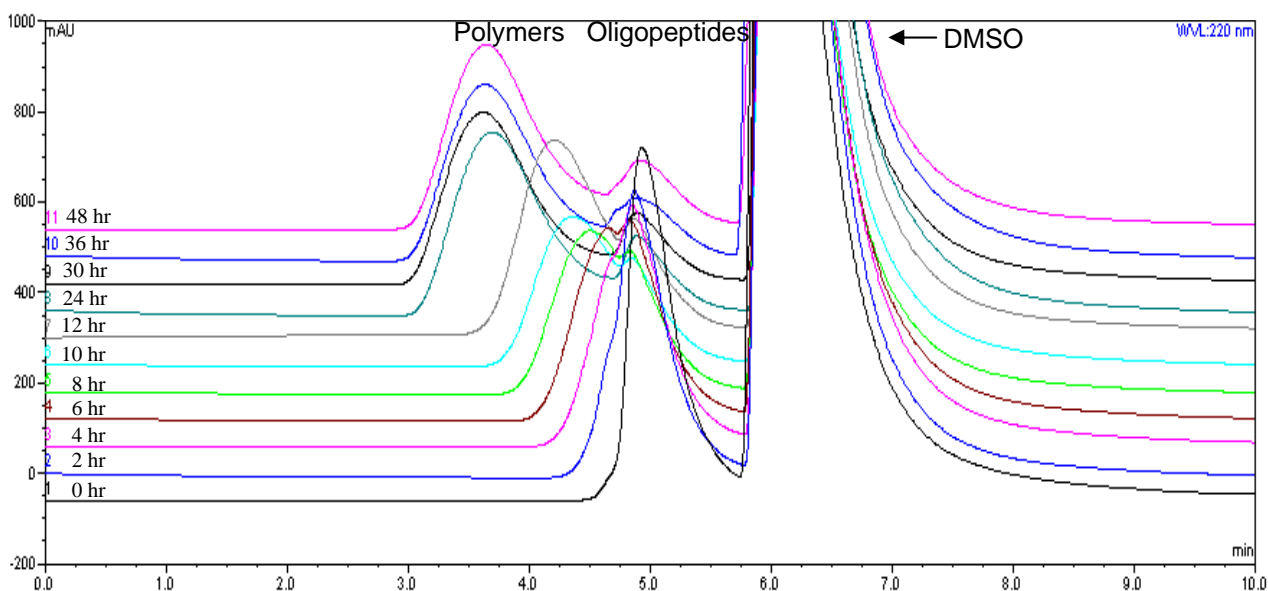
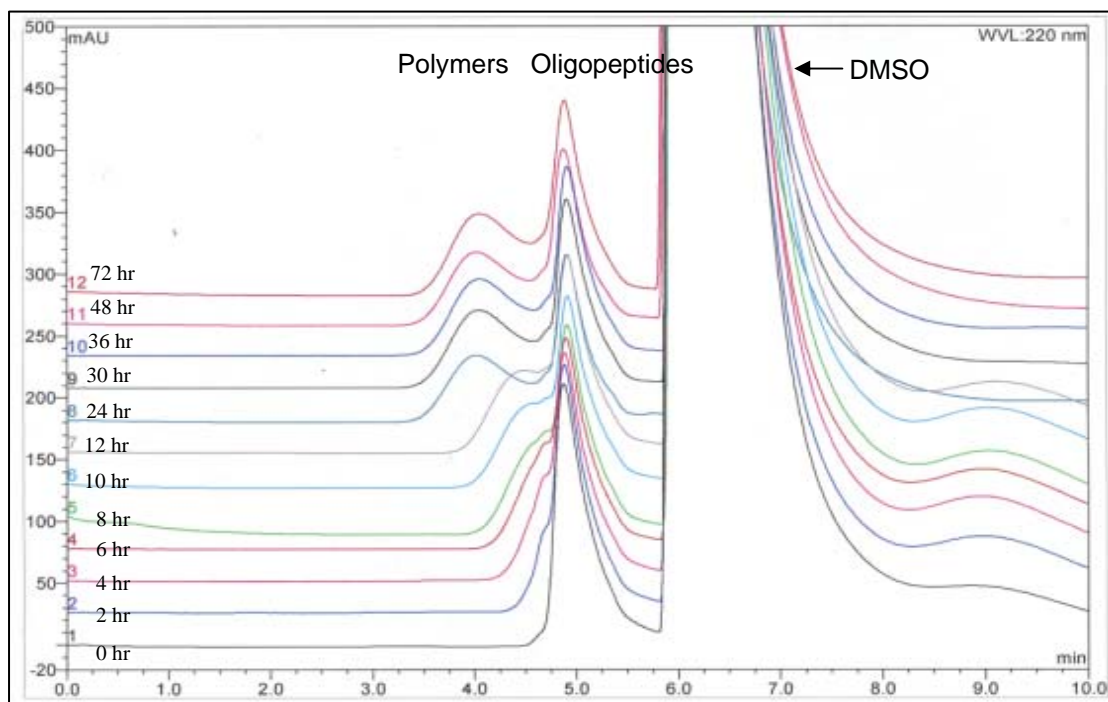


**Figure 8.29.** Comparison of the chromatogram of the oxidative polymerization of 2COP 1 at 60 mM concentration incubated at ambient for 48 hr analyzed by GPC

a)



b)

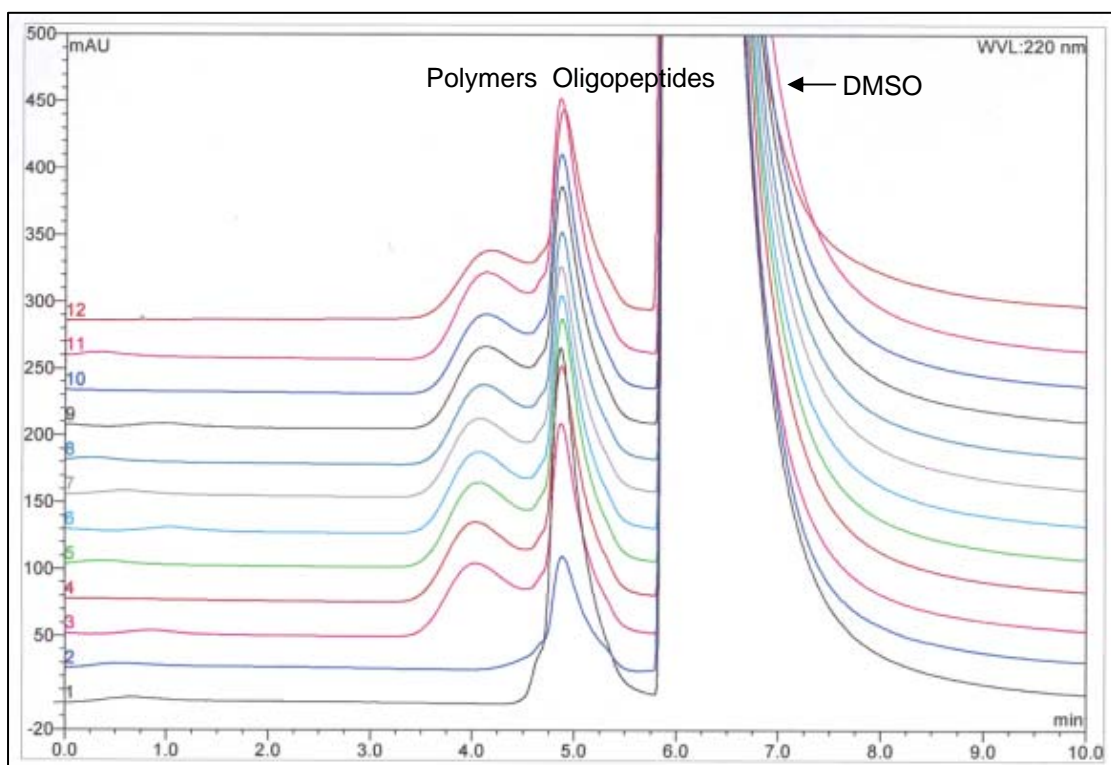


Figure 8.30. Comparison of the chromatogram of the oxidative polymerization of 2COP 1 at 18 mM concentration incubated at a) ambient and b) 40°C for 72 hr analyzed by GPC

## 8.5 Publication

Nasanit, R., Iqbal, P., Soliman, M., Spencer, N., Allen, S., Davies, M.C., Briggs, S.S., Seymour, L.W., Preece, J.A., and Alexander, C. (2008). Combination dual responsive polypeptide vectors for enhanced gene delivery. *Molecular Biosystems*, **4**, 741-745.